Retinal Pigment Epithelial Detachment

Differential Diagnosis and Therapy

Maria Andreea Gamulescu
Horst Helbig
Joachim Wachtlin
Editors

Springer

Retinal Pigment Epithelial Detachment

Maria Andreea Gamulescu • Horst Helbig
Joachim Wachtlin
Editors

Retinal Pigment Epithelial Detachment

Differential Diagnosis and Therapy

Springer

Editors
Maria Andreea Gamulescu
Department of Ophthalmology
University Hospital
Regensburg
Germany

Horst Helbig
Department of Ophthalmology
University Hospital
Regensburg
Germany

Joachim Wachtlin
Department of Ophthalmology
Sankt Gertrauden Hospital
Berlin
Germany

ISBN 978-3-319-56131-8 ISBN 978-3-319-56133-2 (eBook)
DOI 10.1007/978-3-319-56133-2

Library of Congress Control Number: 2017943110

Printed on acid-free paper

This Springer imprint is published by Springer Nature
The registered company is Springer International Publishing AG
The registered company address is: Gewerbestrasse 11, 6330 Cham, Switzerland

Contents

Abbreviations

AFVD	Adult-onset foveomacular vitelliform dystrophy
AMD	Age-related macular degeneration
AREDS	Age-Related Eye Disease Study
BM	Bruch's membrane
BR	Blue reflectance
BVN	Branching vascular network
C3NeF	C3 nephritic factor
CAIs	Carbonic anhydrase inhibitors
CAPT	Complications of Age-Related Macular Degeneration Prevention Trial
CC	Choriocapillaris
CFH	Complement factor H
CFP	Color fundus photography
CMT	Central macular thickness
CNV	Choroidal neovascularization
CSCR	Central serous chorioretinopathy
cSLO	Confocal scanning laser ophthalmoscope or ophthalmoscopy
DMPL	Diode micropulse laser
EDI SD-OCT	Enhanced depth imaging spectral domain optical coherence tomography
FA	Fluorescein angiography
FAF	Fundus autofluorescence
GA	Geographic atrophy
GCL	Ganglion cell layer
GR	Green reflectance
ICG	Indocyanine green
ICGA	Indocyanine green angiography
INL	Inner nuclear layer
IPL	Inner plexiform layer
IR	Infrared imaging
IRBP	Interphotoreceptor matrix retinoid-binding protein

IRN	Intraretinal neovascularization
LGH	Late geographic hyperfluorescence
MC	Multi-color spectral-imaging
MCGN	Mesangiocapillary glomerulonephritis
MMPs	Matrix metalloproteases
MPGN	Membranoproliferative glomerulonephritis
NFL	Nerve fiber layer
NIA	Near-infrared autofluorescence
NIR	Near-infrared reflectance
OCT	Optical coherence tomography
OCTA	Optical coherence tomography-angiography
OLM	Outer limiting membrane
ONL	Outer nuclear layer
OPL	Outer plexiform layer
PCV	Polypoidal choroidal vasculopathy
PDT	Photodynamic therapy
PED	Pigment epithelial detachment
PEDF	Pigment epithelium-derived factor
RAP	Retinal angiomatous proliferation
RD	Retinal detachment
RPD	Reticular pseudodrusen
RPE	Retinal pigment epithelium
rtPA	Recombinant tissue plasminogen activator
SD-OCT	Spectral domain optical coherence tomography
SNPs	Single-nucleotide polymorphisms
SRF	Subretinal fluid
SRI	Spectral reflectance imaging
SRN	Subretinal neovascularization
SRT	Selective retina therapy
SW-FAF	Short-wavelength fundus autofluorescence
TD-OCT	Time-domain optical coherence tomography
TGF-β	Transforming growth factor-β
TIMP3	Tissue inhibitor of metalloproteases-3
TTT	Transpupillary thermotherapy
UEHT	University Eye Hospital Tuebingen
VEGF	Vascular endothelial growth factor
VEGF-A	Vascular endothelial growth factor-A
VKH	Vogt Koyanagi Harada disease
vPED	Vascularized pigment epithelial detachment

Chapter 1
Anatomy and Pathophysiology of Retinal Pigment Epithelial Detachment

Olaf Strauß

1.1 Introduction

The retinal pigment epithelium (RPE) is a monolayer of pigmented cells localized between the photoreceptors and the blood vessels of the choroid. Being the most important interaction partner with the photoreceptors in visual function, any change in RPE function leads to photoreceptor degeneration. The structural integrity and function of the tissue complex "photoreceptor-RPE-choroid" is dependent on close spatial interaction of those cells. This is achieved on one hand by the interphotoreceptor matrix which forms a matrix between RPE and photoreceptors. On the other hand, Bruch's membrane forms another interface between RPE and choroid. These interfaces enable free exchange of nutrients, oxygen, and bioactive molecules such as growth factors or cytokines between the cells and layers of the photoreceptor-RPE-choroid complex. The adhesion between the layers is ensured by the elimination of extracellular fluid by the RPE towards the choroid as well as by the maintenance of the protein composition of the extracellular matrix. Pathogenesis of retinal pigment epithelial detachment (PED), however, is not yet fully clarified; different concepts try to explain the development of PED under different circumstances. The most widely accepted concept is that RPE detachment can be caused by a reduced fluid flow through an ageing Bruch's membrane or by a passive inflow of water caused by changes in osmolarity of the extracellular matrix, e.g., in age-related macular degeneration or degenerative PED. Idiopathic PED (e.g., in central serous chorioretinopathy) is thought to result from choroidal dysfunction and increased permeability of choroidal vessels, possibly due to overactivation of mineralocorticoid receptors in the choroidal endothelial cells. Local inflammation or ischemia can also lead to hyperpermeability of choroidal vessels and thereby to inflammatory/ischemic PED.

O. Strauß
Experimental Ophthalmology, Department of Ophthalmology, Charite University Medicine Berlin, Campus Virchow Clinic, Augustenburger Platz 1, Berlin 13353, Germany
e-mail: olaf.strauss@charite.de

M.A. Gamulescu et al. (eds.), *Retinal Pigment Epithelial Detachment*,
DOI 10.1007/978-3-319-56133-2_1

1.2 The Retinal Pigment Epithelium: Interface Between Blood and Photoreceptors

The retinal pigment epithelium (RPE) is a pigmented monolayer localized between the light-sensitive outer segments of the photoreceptors and the blood supply by the fenestrated endothelium of the choriocapillaris [1, 2] (Fig. 1.1). According to its location, the RPE serves as an interface between the photoreceptors and the body system, interacting with both the photoreceptors and the choriocapillaris. This interaction requires a tight morphological connection between the neighboring tissues,

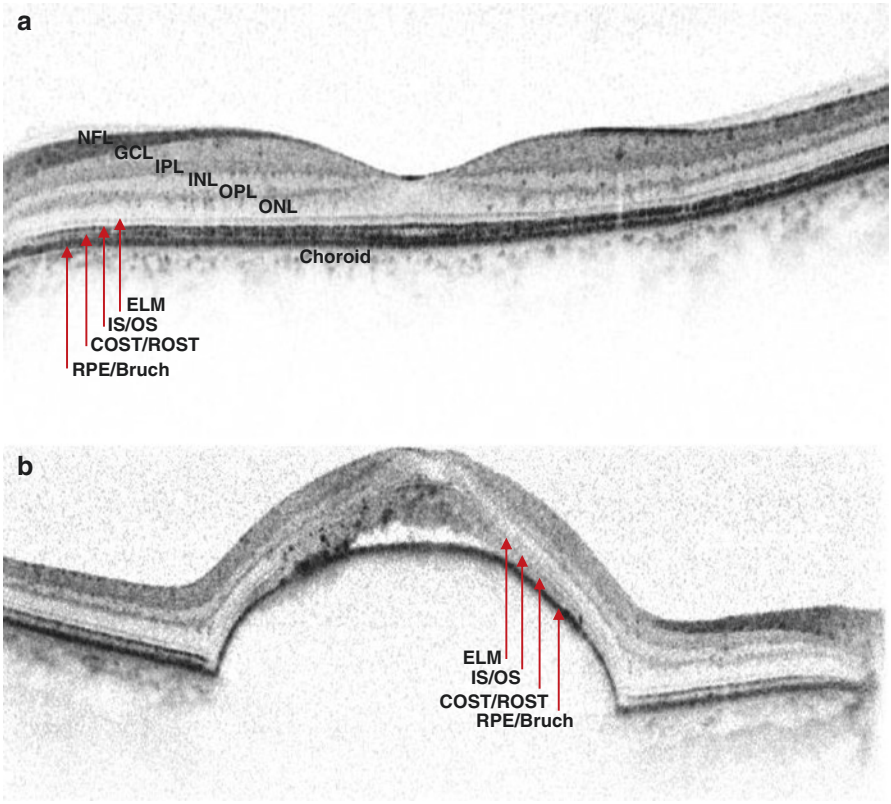

Fig. 1.1 The retinal pigment epithelium and the retina in optical coherence tomography (OCT). (**a**) OCT section of a healthy retina. The reflective bands correlate with the different layers of the retina from the nerve fiber layer to the choroid. (**b**) OCT section of a retina with retinal pigment epithelial detachment (PED). (*NFL* nerve fiber layer, *GCL* ganglion cell layer, *IPL* inner plexiform layer, *INL* inner nuclear layer, *OPL* outer plexiform layer, *ONL* outer nuclear layer, *OLM* outer limiting membrane, *IS/OS* transition between photoreceptor inner and outer segments, *COST/ROST* area in which photoreceptor (cones/rods) outer segments and RPE apical microvilli overlap, *RPE/Bruch* array of RPE's basolateral membrane and Bruch's membrane)

which is enabled by highly organized extracellular matrices. On the photoreceptor side, the subretinal space is filled by the interphotoreceptor matrix which changes its structure between light and dark [3–7]. These structural changes mainly include the spatial distribution of the interphotoreceptor matrix retinoid-binding protein (IRBP) between light and dark. On the choroidal side, Bruch's membrane represents a multilayered complex matrix, which enables the regulated exchange of nutrients and signaling molecules such as growth factors or immune cytokines between the RPE and the choroid [8, 9].

1.3 Function of the RPE

The main function of the RPE is to be a close interaction partner for the light-sensitive photoreceptors [1, 2] (Fig. 1.2). Early in evolution already, development of light-sensitive organs started with a combination between pigmented and light-sensitive cells. This way, the RPE becomes part of the visual process: absorption of light energy, re-isomerization of all-trans retinal in the visual cycle, renewal of the light-sensitive photoreceptor outer segments, and spatial K^+ buffering [1, 2]. All these functions need to be carefully coordinated between the neighboring tissues. Since the RPE is interacting with its adjacent tissues via specialized extracellular matrices, this coordination has to occur by using diffusible factors. For that purpose, the RPE can be considered as a secretory epithelium, which secretes a large variety of cytokines and growth factors [1, 2]. For example, the RPE secretes onto the photoreceptor side the pigment epithelium-derived factor (PEDF) known to function as both neuroprotective and antiangiogenic factor [10–12]. In cell culture, ATP is secreted to the same side and may coordinate the phagocytosis of the photoreceptor outer segments [13]. In interaction with the choroidal side, the

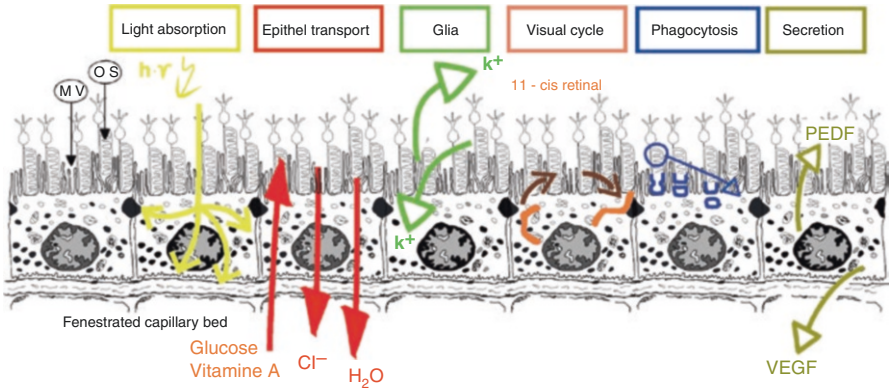

Fig. 1.2 Summary of RPE functions to interact with photoreceptors (From: Strauss 2005, Physiol. Rev. [2])

RPE actively establishes the immune privilege of the eye and ensures the supply of nutrients and oxygen to the photoreceptors [1, 2, 14, 15]. Therefore, the RPE secretes the vascular endothelial growth factor (VEGF-A) to the blood side to stabilize the fenestrated architecture of the choriocapillaris [16, 17]. In the healthy eye, the RPE also secretes immune regulatory factors such as complement inhibitory factors or interleukins [18–20].

1.4 Mechanisms of Adherence Between RPE and Photoreceptors in Health and Disease

1.4.1 Basic Mechanisms in Health

The tight spatial interaction between the photoreceptors and the RPE is maintained by an active transepithelial transport of water from the photoreceptor to the choroidal side [21–23] (Fig. 1.3). Driven by intraocular pressure, water from the vitreous body accumulates in the retina. Furthermore, large amounts of water are produced by the metabolic activity of retinal neurons [23]. Müller cells in the inner and the RPE in the outer retina achieve the reduction and control of extracellular volume. With a transportation rate of approximately 11 μL/cm^2/h, RPE water transport is quite high [22]. Since the RPE is a functional tight epithelium, this transport occurs almost completely by the transcellular transportation route. It is driven by a transepithelial transport of Cl^- from the photoreceptor (apical) to the choroidal (basolateral) side of the RPE [24]. By ATP-hydrolysis, the apically localized Na^+/K^+-ATPase energizes this transport by removing Na^+ from the intracellular space in exchange with K^+ which is pumped into the subretinal space against the concentration gradient [25, 26] (Fig. 1.3a). K^+ recycles back into the RPE through apical potassium channels [21]. The net transport results in a gradient for Na^+ across the apical membrane of the RPE, which is directed into the RPE cells. Indeed, the active transport activity of Na^+/K^+-ATPase produces a mechanic adhesion force between the RPE and the neuronal retina, which is lost after specific inhibition of the Na^+/K^+-ATPase [27]. The gradient for Na^+ is then used for a secondary active transport of Cl^- across the apical membrane by the $Na^+/2Cl^-/K^+$-cotransporter [24, 28, 29] (Fig. 1.3b). RPE cells are known to display comparatively high intracellular Cl^- concentration. The basolateral membrane displays a high Cl^- conductance which is provided by different types of Cl channels in the basolateral membrane [30]. Through these Cl channels, intracellular Cl^- leaves the RPE cells across the basolateral membrane towards the choroid. This creates a net transport of Cl^- from the photoreceptor to the choroidal side, which results in a basolaterally negative transepithelial potential. The transepithelial flux of Cl^- osmotically drives water across the RPE through the water channels aquaporin 1 and 4 that are expressed on both the apical and the basolateral membrane of the RPE [31, 32] (Fig. 1.3c).

The metabolic activity of the retinal neurons also leads to the production of lactate, which accumulates in the subretinal space in large concentrations [2, 33], and is also removed from there by the RPE [33]. This requires a tight regulation of intracellular pH [21] coupled to the transepithelial transport of ions and water. pH

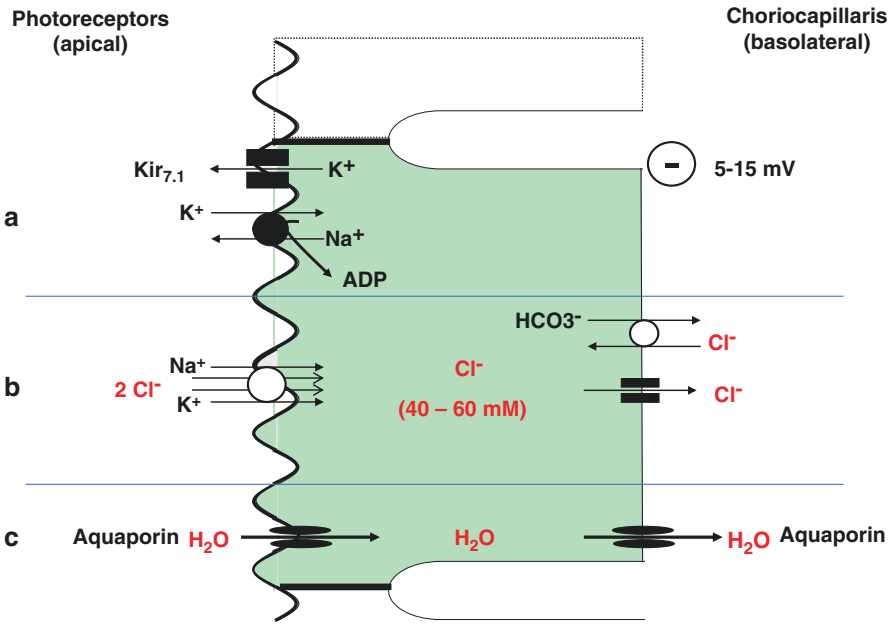

Fig. 1.3 Simplified model of transepithelial water transport by the RPE. Water transport is driven by a transepithelial transport of Cl^- which osmotically drives passive transport of water resulting in a basolateral negative potential. (**a**) Primary active transport of Na^+ energizes the transepithelial transport: Na^+/K^+-ATPase hydrolyzes ATP to transport Na^+ against concentration gradients out of the cell in exchange with a transport of K^+ into the cell. K^+ recycles back into subretinal space through Kir7.1 K^+ channels. (**b**) Na^+ gradient established by Na^+/K^+-ATPase drives secondary active transport by the $Na^+/2Cl^-/K^+$-cotransporter which takes up Na^+, K^+, and Cl^- from subretinal space into the RPE across the apical membrane. Since Na^+ and K^+ are transported back into the subretinal space by activity of Kir7.1 and Na^+/K^+-ATPase, Cl^- accumulates in the RPE leading to high intracellular Cl^- concentrations. At the basolateral side, Cl^- leaves the cell through various Cl channels to the blood stream. This net flux of Cl^- across basolateral membrane is partly counterbalanced by the activity of the Cl^-/HCO_3^--cotransporter which transports HCO_3^- for pH regulation into the RPE cell. (**c**) Route of water across the RPE through the aquaporin water channels

regulation occurs by bicarbonate transport across the apical and the basolateral membrane. Across the basolateral membrane, bicarbonate is removed from intracellular space of the RPE cells in exchange with Cl^- by the activity of the Cl^-/HCO_3^--exchanger [34] (Fig. 1.3b). Since this transport results in an uptake of Cl^- back into the RPE intracellular space, it reduces the net outward flux of Cl^- and thus the transepithelial transport of water [2, 21–23].

1.4.2 Transepithelial Transport in Disease

In general, the RPE can quickly adapt to the requirements of transepithelial water transport. For example, it has been shown that increasing light intensity results in a transient increase of extracellular volume in the retinal layers, that is quickly reduced by increased transport activity of the RPE [21, 22]. Furthermore, transepithelial

transport can be pharmacologically stimulated to reduce pathologically increased extracellular volume, i.e., macular edema [35]. The pharmacologic intervention is based on the fact that normal pH regulation reduces the transepithelial net transport for Cl^- and water via bicarbonate extrusion from subretinal space. The application of carbonic anhydrase inhibitors leads to a reduction in bicarbonate production and, therefore, in less bicarbonate transport [36]. Subsequently, the reduced bicarbonate transport out of the RPE cell results in a reduced Cl^- uptake and this in turn increases the efficiency of Cl^- efflux and the net transport of water across the RPE.

1.5 Causes Leading to RPE Detachment

1.5.1 Changes in Bruch's Membrane and in Sub-pigment-Epithelial Space

Changes in Bruch's membrane are the major cause for RPE detachment in the elderly. Age-related changes of Bruch's membrane are known for a long time and have also been discussed to represent a major cause for age-related macular degeneration [1, 9, 37], see also chapter 3 (PED in AMD).

As indicated above, Bruch's membrane has to fulfill a large variety of functions such as being an interface between the RPE and the blood stream in the choroid. First of all, Bruch's membrane has to be permeable enough to permit the exchange of water or hydrophilic factors, such as growth factors, between the RPE and the choroid. Its composition based on extracellular matrix proteins moreover ensures an environment that maintains structure and function of both the RPE and the endothelium of the choriocapillaris [9]. The main effect of age-dependent changes in Bruch's membrane is the reduction of the hydraulic conductivity or the ability to conduct water [38].

There are two patho-mechanisms which are discussed to cause the beforementioned structural changes in Bruch's membrane resulting in reduced hydraulic conductivity. One is the altered/modified control of the homeostasis of extracellular matrix proteins [39–41] and thereby osmolarity in the sub-pigment-epithelial space (44). The extracellular matrix in general and also Bruch's membrane undergo a constant rearrangement in structure and protein composition. The leading enzymes for this process are the matrix metalloproteases (MMPs) [39]. These enzymes disintegrate the structure of Bruch's membrane to enable a functional restructuration. On the other side, the stability of Bruch's membrane is maintained by inhibitors of the MMPs. One of the most important inhibitors of MMPs is the tissue inhibitor of metalloproteases-3 (TIMP3) which is secreted by the RPE [42]. Reduced secretion or inhibitory capacity of TIMP3 causes, e.g., Sorsby's fundus dystrophy [42]. John Marshall's group found that the activity of MMPs is reduced in Bruch's membrane of eyes from elderly people [38, 39, 43, 44]. As a consequence, Bruch's membrane suffers structural changes: an increase in thickness and collagen-crosslinking [9].

The second cause for the decrease in the hydraulic conductivity of Bruch's membrane is an accumulation of lipids. Curcio and Johnson found that in the aged Bruch's membrane there is an increasing number of highly structured lipid bodies or droplets [45]. The origin of these lipids is not clear though. The authors think that the highly organized structure points to an organized transportation process rather than a simple uptake by diffusion. Two theories are discussed. One is that these lipid bodies are produced by the RPE under a situation of metabolic stress [45]. The other theory is that the lipid bodies stem from the plasma and that they are accumulated by a comparable process as it happens in arterial sclerosis. So far, no data exists that would proof one of these hypotheses.

The reduction in hydraulic conductivity has three major consequences:

- Water which has been transported at rather high transportation rates by the RPE from the vitreous space to the sub-RPE space cannot pass Bruch's membrane and further into the blood stream. The water, then, will inevitably accumulate between RPE and Bruch's membrane. This effect alone should be sufficient to cause RPE detachment [8, 37], namely degenerative PED. At the same time, changes in extracellular matrix components in the sub-RPE space are thought to lead to a higher osmolarity with subsequent inflow of water from the choriocapillaris along a concentration gradient (44), further increasing the amount of "trapped" water.
- Oxygen can no longer diffuse freely across Bruch's membrane, creating a hypoxic environment in the RPE and outer retinal layers. It is believed that this could be one of the initial steps leading to increased secretion of VEGF and ultimately to choroidal neovascularization [8, 37], which in turn can cause PED by exsudation into the sub-RPE space.
- Factors required for communication between the RPE and the endothelium of the choriocapillaris or the immune system cannot be freely exchanged. Thus the interaction between the RPE and the endothelium or the immune system is altered [8, 18]. It is not clear in which way this leads to RPE detachment; however, it is discussed that local inflammatory processes due to reduced inhibitory control of the immune system might possibly cause fluid accumulation by increased permeability of the choriocapillaris and thereby RPE detachment. Indeed, in the etiology of age-related macular degeneration, the loss of immune inhibitory activity by the RPE in association with a reduced exchange of immune regulatory factors through Bruch's membrane was found to play a major role [8, 18, 46].

1.5.2 Changes in Choroid and Choriocapillaris

While the age-related changes in Bruch's membrane and its increased hydrophobicity in the elderly are widely accepted as pathophysiologic cause of degenerative PED, the causes leading to non-degenerative PED are much less elucidated.

In idiopathic, inflammatory and ischemic PED, clinical observation seems to imply that water is mainly derived from the choroid and the choriocapillaris, as the fluorescein dye fills the PEDs exuding from the choroid. In this pathophysiologic concept, increased permeability of the choroidal vessels is implied, caused by breakdown of the blood ocular barrier by, e.g., inflammation (inflammatory PED) [47] or endovascular damage by malignant hypertension or eclampsia (ischemic PED) [48]. However, patients presenting with these type of PED are rare and this concept still has to be substantiated. See also chapter 9 (PED in systemic disease).

In contrast to this, pathophysiology of idiopathic PED like in central serous chorioretinopathy (CSCR) is better understood. Here, overactivation of mineralocorticoid receptors by corticoids in the choroidal vessels is thought to lead to hyperpermeability. This concept would fit the widespread belief that this illness is triggered by increased exogenous and endogenous glucocorticoid levels [49]. Also, it would explain the potential beneficial effect of mineralocorticoid antagonists [50]. See also chapter 8 (PED in CSCR).

In these non-degenerative PED, water would have to be pressed by high hydrostatic pressure from the choroid to the sub-RPE room where it could accumulate. However, hydrostatic pressure in the choroid seems to be somewhat lower than in the vitreous body, rendering this rather unlikely. Another explanation might be an increased osmolarity in the sub-RPE space as previously described for age-related PED. Again, the underlying pathophysiologic process is unknown.

1.6 The Effect of RPE Detachment: Mesenchymal Transdifferentiation of the RPE

Both the structural changes in Bruch's membrane and the detachment of the RPE have severe consequences for the structural integrity of the photoreceptor-RPE-choroid complex. The main effect is the establishment of a diffusion barrier for an exchange of molecules between these tissues. First of all, the supply of nutrients and oxygen is disturbed, resulting in metabolic stress for both the photoreceptors and the RPE [9, 51]. Since the RPE's function is required for photoreceptor function and structural integrity, the reduced RPE function would impair photoreceptor function and ultimately lead to loss of vision [2]. As already discussed above for the changes in Bruch's membrane, the inability to exchange signaling molecules has severe effects on the stability of the choriocapillaris and the photoreceptors [52–54]. Driven by hypoxia, but also by the changes in the extracellular matrix, the VEGF-A production can increase leading to choroidal neovascularization. The reduced inhibition of the immune system further supports these changes triggering local inflammation [55–57].

On the other hand, RPE detachment can set off severe changes in RPE differentiation. The changed environment forces the RPE to increase its secretory activity [58, 59]. As an example, RPE cells isolated from choroidal neovascular membranes maintain a higher VEGF-A secretion in cell culture even over several passages [58, 59]. The

mechanic stress resulting from fluid accumulation between RPE and Bruch's membrane leads to a loss of the RPE's epithelial barrier function. Hence, a further transdifferentiation of the RPE occurs towards a mesenchymal phenotype [60–62]. These transdifferentiated cells do not form an epithelium any longer. They now show secretion of growth factors known in scar formation as well as the ability to migrate. A key factor in this mesenchymal transdifferentiation is the transforming growth factor-β (TGF-β). TGF-β promotes the transdifferentiation of RPE cells and can also be secreted in an autocrine way by the RPE itself and promote formation of fibrovascular lesions [60, 61, 63–65]. These effects seem to be linked to Bruch's membrane disruption, as laser coagulation leads to an increase in TGF-β production [66].

1.7 Summary

The cause and at the same time the consequence of RPE detachment are the generation of a diffusion barrier between the RPE and the choriocapillaris. Bruch's membrane seems to play a prominent role—at least in degenerative PED, where structural changes lead to a reduction in hydraulic conductivity with increasing age of individuals. In the first instance, the supply of oxygen and nutrients is reduced, which decreases the metabolic function of the RPE and secondarily the photoreceptor function. This changes establish a pro-angiogenic and pro-inflammatory environment. Finally, the reduced exchange of signaling molecules between the neighboring tissues leads to inflammation, drusen formation and to choroidal neovascularization. As a second severe effect, the RPE can undergo an increased TGF-β production and a transdifferentiation into a mesenchymal phenotype under mechanical stress, leading to scarring and further thickening of the diffusion barrier. The postulated hyperpermeability of the choroid and choriocapillaris—in idiopathic, inflammatory and ischemic PED—and especially the trigger leading to this, still has to be proven.

References

1. Sparrow JR, Hicks D, Hamel CP. The retinal pigment epithelium in health and disease. Curr Mol Med. 2010;10:802–23.
2. Strauss O. The retinal pigment epithelium in visual function. Physiol Rev. 2005;85:845–81. doi:10.1152/physrev.00021.2004.
3. Carter-Dawson L, Burroughs M. Interphotoreceptor retinoid-binding protein (IRBP) and opsin in the rds mutant mouse: EM immunocytochemical analysis. Prog Clin Biol Res. 1989;314:291–300.
4. Hageman GS, Johnson LV. Structure, composition and function of the retinal interphotoreceptor matrix. Prog Retin Eye Res. 1991;10:207–49.
5. Hodson S, Armstrong I, Wigham C. Regulation of the retinal interphotoreceptor matrix Na by the retinal pigment epithelium during the light response. Experientia. 1994;50:438–41.
6. Hollyfield JG. Hyaluronan and the functional organization of the interphotoreceptor matrix. Invest Ophthalmol Vis Sci. 1999;40:2767–9.

7. Uehara F, Matthes MT, Yasumura D, LaVail MM. Light-evoked changes in the interphotoreceptor matrix. Science. 1990;248:1633–6.
8. Bird AC. Bruch's membrane change with age. Br J Ophthalmol. 1992;76:166–8.
9. Booij JC, Baas DC, Beisekeeva J, Gorgels TG, Bergen AA. The dynamic nature of Bruch's membrane. Prog Retin Eye Res. 2010;29:1–18. doi:10.1016/j.preteyeres.2009.08.003.
10. Cao W, Tombran-Tink J, Chen W, Mrazek D, Elias R, McGinnis JF. Pigment epithelium-derived factor protects cultured retinal neurons against hydrogen peroxide-induced cell death. J Neurosci Res. 1999;57:789–800.
11. Dawson DW, Volpert OV, Gillis P, Crawford SE, Xu H, Benedict W, Bouck NP. Pigment epithelium-derived factor: a potent inhibitor of angiogenesis. Science. 1999;285:245–8.
12. King GL, Suzuma K. Pigment-epithelium-derived factor—a key coordinator of retinal neuronal and vascular functions. N Engl J Med. 2000;342:349–51.
13. Mitchell CH. Release of ATP by a human retinal pigment epithelial cell line: potential for autocrine stimulation through subretinal space. J Physiol. 2001;534:193–202.
14. Wolfensberger TJ, Tufail A. Systemic disorders associated with detachment of the neurosensory retina and retinal pigment epithelium. Curr Opin Ophthalmol. 2000;11:455–61.
15. Ishida K, Panjwani N, Cao Z, Streilein JW. Participation of pigment epithelium in ocular immune privilege. 3. Epithelia cultured from iris, ciliary body, and retina suppress T-cell activation by partially non-overlapping mechanisms. Ocul Immunol Inflamm. 2003;11:91–105.
16. Frank RN. Growth factors in age-related macular degeneration: pathogenic and therapeutic implications. Ophthalmic Res. 1997;29:341–53.
17. Strauss O, Heimann H, Foerster MH, Agostini H, Hansen LL, Rosenthal R. Activation of L-type Ca2+ channels is necessary for growth factor-dependent stimulation of VEGF secretion by RPE cells. Invest Ophthalmol Vis Sci. 2003;44:e-abstract 3926.
18. Sparrow JR, Ueda K, Zhou J. Complement dysregulation in AMD: RPE-Bruch's membrane-choroid. Mol Aspects Med. 2012;33:436–45. doi:10.1016/j.mam.2012.03.007.
19. Holtkamp GM, de Vos AF, Kijlstra A, Peek R. Expression of multiple forms of IL-1 receptor antagonist (IL-1ra) by human retinal pigment epithelial cells: identification of a new IL-1ra exon. Eur J Immunol. 1999;29:215–24.
20. Liversidge J, McKay D, Mullen G, Forrester JV. Retinal pigment epithelial cells modulate lymphocyte function at the blood-retina barrier by autocrine PGE2 and membrane-bound mechanisms. Cell Immunol. 1993;149:315–30.
21. Hughes BA, Gallemore RP, Miller SS. Transport mechanisms in the retinal pigment epithelium. In: Marmor MF, Wolfensberger TJ, editors. The retinal pigment epithelium. New York: Oxford University Press; 1998. p. 103–34.
22. Gallemore RP, Hughes BA, Miller SS. Retinal pigment epithelial transport mechansisms and their contribution to the electroretinogram. Prog Retin Eye Res. 1997;16:509–66.
23. Strauss O. Transport mechanisms of the retinal pigment epithelium to maintain visual function. Heat Mass Transf. 2014;50:303–13.
24. Hu JG, Gallemore RP, Bok D, Frambach DA. Chloride transport in cultured fetal human retinal pigment epithelium. Exp Eye Res. 1996;62:443–8.
25. Quinn RH, Miller SS. Ion transport mechanisms in native human retinal pigment epithelium. Invest Ophthalmol Vis Sci. 1992;33:3513–27.
26. Hu JG, Gallemore RP, Bok D, Lee AY, Frambach DA. Localization of NaK ATPase on cultured human retinal pigment epithelium. Invest Ophthalmol Vis Sci. 1994;35:3582–8.
27. Frambach DA, Roy CE, Valentine JL, Weiter JJ. Precocious retinal adhesion is affected by furosemide and ouabain. Curr Eye Res. 1989;8:553–6.
28. Joseph DP, Miller SS. Apical and basal membrane ion transport mechanisms in bovine retinal pigment epithelium. J Physiol. 1991;435:439–63.
29. Quinn RH, Quong JN, Miller SS. Adrenergic receptor activated ion transport in human fetal retinal pigment epithelium. Invest Ophthalmol Vis Sci. 2001;42:255–64.
30. Wimmers S, Karl MO, Strauss O. Ion channels in the RPE. Prog Retin Eye Res. 2007;26:263–301. doi:10.1016/j.preteyeres.2006.12.002.

31. Stamer WD, Bok D, Hu J, Jaffe GJ, McKay BS. Aquaporin-1 channels in human retinal pigment epithelium: role in transepithelial water movement. Invest Ophthalmol Vis Sci. 2003;44:2803–8.
32. Hamann S. Molecular mechanisms of water transport in the eye. Int Rev Cytol. 2002; 215:395–431.
33. Hamann S, la Cour M, Lui GM, Bundgaard M, Zeuthen T. Transport of protons and lactate in cultured human fetal retinal pigment epithelial cells. Pflugers Arch. 2000;440:84–92.
34. Lin H, Miller SS. pHi-dependent Cl-HCO3 exchange at the basolateral membrane of frog retinal pigment epithelium. Am J Physiol. 1994;266:C935–45.
35. Marmor MF. Mechanisms of fluid accumulation in retinal edema. Doc Ophthalmol. 1999;97:239–49.
36. Marmor MF. Control of subretinal fluid: experimental and clinical studies. Eye (Lond). 1990;4(Pt 2):340–4. doi:10.1038/eye.1990.46.
37. Guymer R, Luthert P, Bird A. Changes in Bruch's membrane and related structures with age. Prog Retin Eye Res. 1999;18:59–90.
38. Starita C, Hussain AA, Marshall J. Decreasing hydraulic conductivity of Bruch's membrane: relevance to photoreceptor survival and lipofuscinoses. Am J Med Genet. 1995;57:235–7. doi:10.1002/ajmg.1320570224.
39. Hussain AA, Lee Y, Zhang JJ, Marshall J. Disturbed matrix metalloproteinase activity of Bruch's membrane in age-related macular degeneration. Invest Ophthalmol Vis Sci. 2011;52: 4459–66. doi:10.1167/iovs.10-6678.
40. Itoh Y, Kimoto K, Imaizumi M, Nakatsuka K. Inhibition of RhoA/Rho-kinase pathway suppresses the expression of type I collagen induced by TGF-beta2 in human retinal pigment epithelial cells. Exp Eye Res. 2007;84:464–72. doi:10.1016/j.exer.2006.10.017.
41. Ahir A, Guo L, Hussain AA, Marshall J. Expression of metalloproteinases from human retinal pigment epithelial cells and their effects on the hydraulic conductivity of Bruch's membrane. Invest Ophthalmol Vis Sci. 2002;43:458–65.
42. Qi JH, Ebrahem Q, Moore N, Murphy G, Claesson-Welsh L, Bond M, Baker A, Anand-Apte B. A novel function for tissue inhibitor of metalloproteinases-3 (TIMP3): inhibition of angiogenesis by blockage of VEGF binding to VEGF receptor-2. Nat Med. 2003;9: 407–15.
43. Bird AC, Marshall J. Retinal pigment epithelial detachments in the elderly. Trans Ophthalmol Soc U K. 1986;105(Pt 6):674–82.
44. Kumar A, El-Osta A, Hussain AA, Marshall J. Increased sequestration of matrix metalloproteinases in ageing human Bruch's membrane: implications for ECM turnover. Invest Ophthalmol Vis Sci. 2010;51:2664–70. doi:10.1167/iovs.09-4195.
45. Curcio CA, Johnson M, Rudolf M, Huang JD. The oil spill in ageing Bruch membrane. Br J Ophthalmol. 2011;95:1638–45. doi:10.1136/bjophthalmol-2011-300344.
46. Kirchhof B, Sorgente N. Pathogenesis of proliferative vitreoretinopathy. Modulation of retinal pigment epithelial cell functions by vitreous and macrophages. Dev Ophthalmol. 1989; 16:1–53.
47. Green K1, Paterson CA, Cheeks L, Slagle T, Jay WM, Aziz MZ. Ocular blood flow and vascular permeability in endotoxin-induced inflammation. Ophthalmic Res 1990;22:287–94.
48. Starita C1, Hussain AA, Patmore A, Marshall J. Localization of the site of major resistance to fluid transport in Bruch's membrane. Invest Ophthalmol Vis Sci 1997;38:762–7.
49. Zhao M1, Célérier I, Bousquet E, Jeanny JC, Jonet L, Savoldelli M, Offret O, Curan A, Farman N, Jaisser F, Behar-Cohen F. Mineralocorticoid receptor is involved in rat and human ocular chorioretinopathy. J Clin Invest 2012;122:2672–9.
50. Bousquet E1, Beydoun T, Zhao M, Hassan L, Offret O, Behar-Cohen F. Mineralocorticoid receptor antagonism in the treatment of chronic central serous chorioretinopathy. A pilot study. Retina 2013;33:2096–102.
51. Stefansson E, Geirsdottir A, Sigurdsson H. Metabolic physiology in age related macular degeneration. Prog Retin Eye Res. 2011;30:72–80. doi:10.1016/j.preteyeres.2010.09.003.

52. Kliffen M, Sharma HS, Mooy CM, Kerkvliet S, de Jong PT. Increased expression of angiogenic growth factors in age-related maculopathy. Br J Ophthalmol. 1997;81:154–62.
53. Mousa SA, Lorelli W, Campochiaro PA. Role of hypoxia and extracellular matrix-integrin binding in the modulation of angiogenic growth factors secretion by retinal pigmented epithelial cells. J Cell Biochem. 1999;74:135–43.
54. Reddy VM, Zamora RL, Kaplan HJ. Distribution of growth factors in subfoveal neovascular membranes in age-related macular degeneration and presumed ocular histoplasmosis syndrome. Am J Ophthalmol. 1995;120:291–301.
55. Bhutto I, Lutty G. Understanding age-related macular degeneration (AMD): relationships between the photoreceptor/retinal pigment epithelium/Bruch's membrane/choriocapillaris complex. Mol Aspects Med. 2012;33:295–317. doi:10.1016/j.mam.2012.04.005.
56. Jasielska M, Semkova I, Shi X, Schmidt K, Karagiannis D, Kokkinou D, Mackiewicz J, Kociok N, Joussen AM. Differential role of tumor necrosis factor (TNF)-alpha receptors in the development of choroidal neovascularization. Invest Ophthalmol Vis Sci. 2010;51:3874–83. doi:10.1167/iovs.09-5003.
57. Oh H, Takagi H, Takagi C, Suzuma K, Otani A, Ishida K, Matsumura M, Ogura Y, Honda Y. The potential angiogenic role of macrophages in the formation of choroidal neovascular membranes. Invest Ophthalmol Vis Sci. 1999;40:1891–8.
58. Schlunck G, Martin G, Agostini HT, Camatta G, Hansen LL. Cultivation of retinal pigment epithelial cells from human choroidal neovascular membranes in age related macular degeneration. Exp Eye Res. 2002;74:571–6.
59. Rosenthal R, Heimann H, Agostini H, Martin G, Hansen LL, Strauss O. Ca2+ channels in retinal pigment epithelial cells regulate vascular endothelial growth factor secretion rates in health and disease. Mol Vis. 2007;13:443–56.
60. Baldwin AK, Cain SA, Lennon R, Godwin A, Merry CL, Kielty CM. Epithelial-mesenchymal status influences how cells deposit fibrillin microfibrils. J Cell Sci. 2014;127:158–71. doi:10.1242/jcs.134270.
61. Chen X, Xiao W, Wang W, Luo L, Ye S, Liu Y. The complex interplay between ERK1/2, TGFbeta/Smad, and Jagged/Notch signaling pathways in the regulation of epithelial-mesenchymal transition in retinal pigment epithelium cells. PLoS One. 2014;9:e96365. doi:10.1371/journal.pone.0096365.
62. Saika S, Yamanaka O, Flanders KC, Okada Y, Miyamoto T, Sumioka T, Shirai K, Kitano A, Miyazaki K, Tanaka S, Ikeda K. Epithelial-mesenchymal transition as a therapeutic target for prevention of ocular tissue fibrosis. Endocr Metab Immune Disord Drug Targets. 2008;8:69–76.
63. Hoerster R, Muether PS, Vierkotten S, Hermann MM, Kirchhof B, Fauser S. Upregulation of TGF-ss1 in experimental proliferative vitreoretinopathy is accompanied by epithelial to mesenchymal transition. Graefes Arch Clin Exp Ophthalmol. 2014;252:11–6. doi:10.1007/s00417-013-2377-5.
64. Lee J, Moon HJ, Lee JM, Joo CK. Smad3 regulates Rho signaling via NET1 in the transforming growth factor-beta-induced epithelial-mesenchymal transition of human retinal pigment epithelial cells. J Biol Chem. 2010;285:26618–27. doi:10.1074/jbc.M109.073155.
65. Saika S, Yamanaka O, Okada Y, Tanaka S, Miyamoto T, Sumioka T, Kitano A, Shirai K, Ikeda K. TGF beta in fibroproliferative diseases in the eye. Front Biosci (Schol Ed). 2009;1:376–90.
66. Matsumoto M, Yoshimura N, Honda Y. Increased production of transforming growth factor-beta 2 from cultured human retinal pigment epithelial cells by photocoagulation. Invest Ophthalmol Vis Sci. 1994;35:4245–52.

Chapter 2
Imaging in Retinal Pigment Epithelial Detachment

Seleman Bedar and Ulrich Kellner

2.1 Introduction

Retinal imaging is critical in the evaluation of patients with PED. For many years, retinal specialist could only use ophthalmoscopy, fundus photography, and fluorescein angiography (FA) as imaging tools in retinal diseases. In recent years, there have been major advances in digital imaging systems that enhance the evaluation of patients with retinal diseases, such as indocyanine green angiography (ICGA), infrared imaging (IR), fundus autofluorescence (FAF), multi-color spectral-imaging (MC), optical coherence tomography (OCT), and OCT-angiography (OCTA). These advancements have improved our understanding of various retinal diseases including PED. The following chapter reviews retinal imaging techniques used in patients with PED and highlights benefits and limitations of each imaging technique. It is important to emphasize that all of the following imaging tools do not replace a careful ophthalmoscopy but work as an addition.

S. Bedar
AugenZentrum Siegburg, MVZ ADTC Siegburg GmbH,
Europaplatz 3, 53721 Siegburg, Germany
e-mail: selemanbedar@me.com

U. Kellner (✉)
Retina Science, 53225 Bonn, Germany
e-mail: kellneru@retinascience.de

M.A. Gamulescu et al. (eds.), *Retinal Pigment Epithelial Detachment*,
DOI 10.1007/978-3-319-56133-2_2

2.2 Angiography

2.2.1 Fluorescein Angiography

FA is an imaging modality to depict retinal and choroidal circulation after intravenous injection of fluorescein dye. It is used to visualize dynamic processes in the retinal and choroidal blood system. It is the leading imaging tool for the diagnosis of many vascular and exudative retinal or choroidal disorders. Fluorescein dye is well tolerated in most patients, but FA is an invasive procedure with possible side effects, including transient nausea, vomiting, and rarely anaphylaxis. The incidence of mild side effects is about 8%, moderate side effects occur in 1–2%, and severe side effects like anaphylaxis are rare. Fluorescein dye is eliminated through the kidney, so it has to be used with caution in patients with impaired renal function. Examination takes about 5–10 min and in special cases eventually longer. Through the introduction of the noninvasive OCT, especially the high-definition spectral domain OCT (SD-OCT), FA has lost its importance as follow-up technique in patients with exudative macular diseases. Here, it is only used when new findings are present or in cases where visual acuity and clinical and OCT findings don't match.

The typical early presentation of serous / predominantly serous PED in FA is a disc-shaped hypofluorescence in the region of the RPE detachment with delayed ring-like hyperfluorescence and progressive pooling beginning from the rim of the PED, which is sharply demarcated, and increasing until the late phase (Figs. 2.1e–f (left images), and 2.4e–g (left images)). This classic pattern of FA in PED can have additional special features depending on the cause of PED. Serous PEDs in patients with AMD are often related to CNV, most frequently occult CNVs, resulting in "vascularized" or "fibrovascular" PEDs) (Figs. 2.2, 2.3, 2.4, 2.5 and 2.6). In these cases early, irregular progressive leakage, suggestive of occult CNV is seen either in one specific location at the rim of the PED or allover it, filling it out completely. A "notch" in the PED is a very high indicator for an occult CNV beneath the RPE (Fig. 2.2e-g (right images) and 2.6d-e). Rarely, a serous PED is associated with classic CNV. CNVs are often seen at the border of the PED (Fig. 2.2, 2.6) and seldom within the RPE detachment (Figs. 2.3 and 2.5).

2.2.2 Indocyanine Green Angiography

ICG is a fluorescein dye which enables specific analysis of the choroidal circulation. Like FA, it is also administered intravenously but in contrast to FA it is eliminated through the liver. ICG contains sodium iodide and therefore should be avoided in patients with iodide intolerance. For many retinal diseases, it is considered to be a secondary imaging test, but it can be very helpful in some cases of PED. It takes 10–20 min to perform an examination because the late phase of ICGA occurs later compared to FA. It is one of the most important imaging techniques in patients with idiopathic polypoidal choroidal

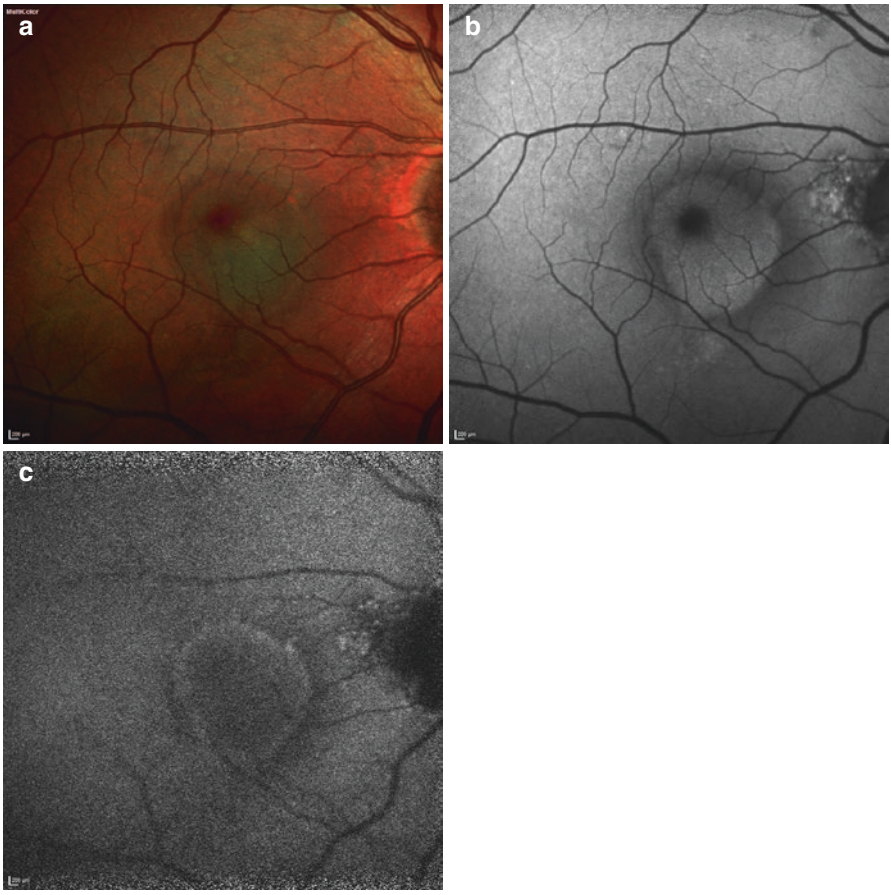

Fig. 2.1 Serous PED (61 year old female patient) (**a**) MultiColor image delineates the PED with a mild greenish area in the lower part of the PED (**b**) FAF image with a slightly increased FAF signal within the PED and a darker area delineating the rim of the PED due to relative blockage caused by subretinal fluid. (**c**) NIA image with increased intensity at the border of the PED but blockage of the usually high NIA intensity in the foveal area (**d**) NIR (left) & SD-OCT image showing a central elevation with fluid beneath the RPE and subretinal fluid next to the PED. There is denser material beneath the RPE, the choroidal layers are blocked due to the high elevation. (**e**) FA (left) & ICGA (right) at 33 sec: Both show early hypofluorescence. (**f**) FA (left) & ICGA (right) at 5.41 min: FA shows late staining at the border of the PED area while ICGA shows persistent hypofluorescence of the PED. As seen in the other images, the lesion extends irregularly at the lower end of the PED. The parapapillary lesions are not connected with the PED

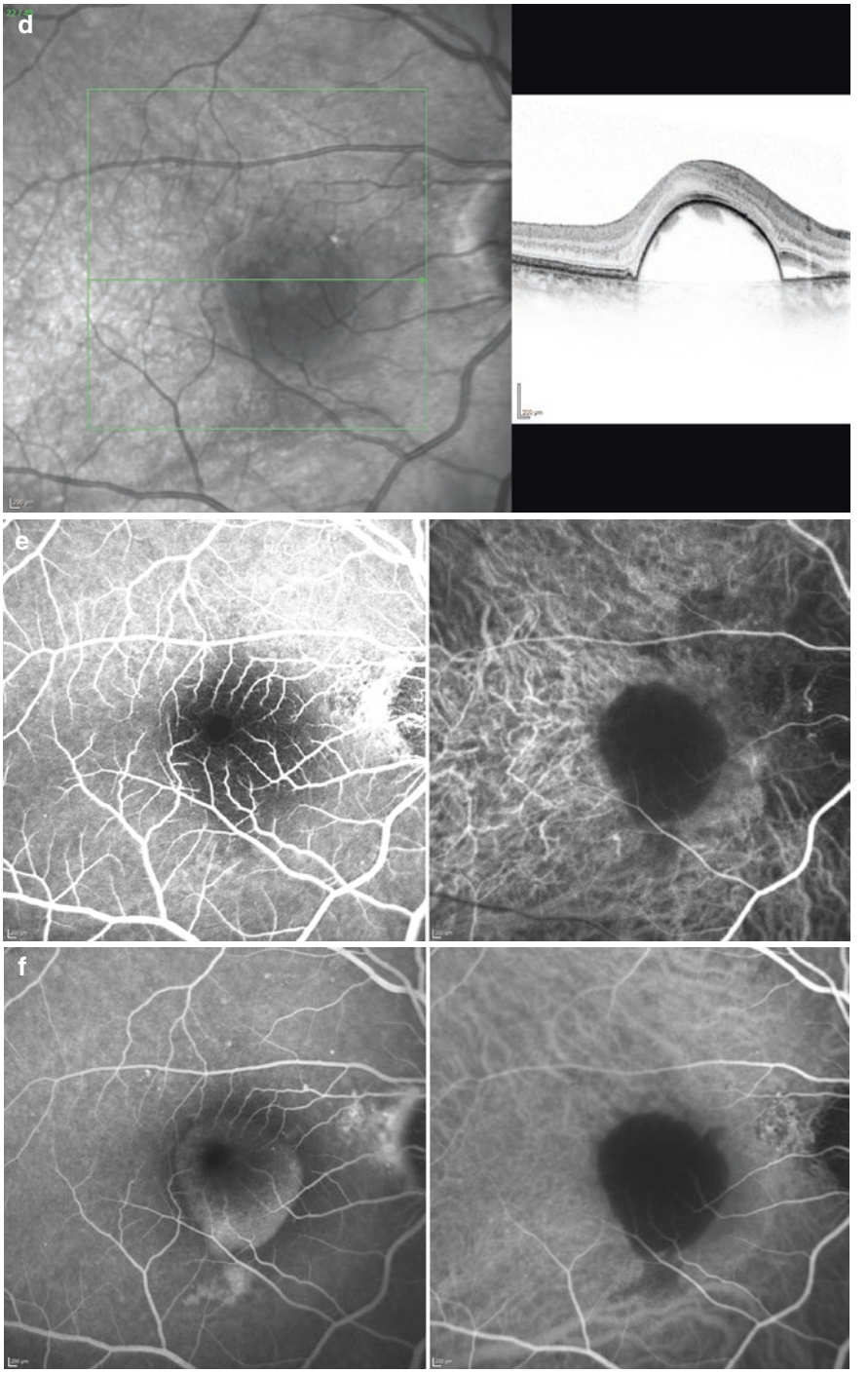

Fig. 2.1 (continued)

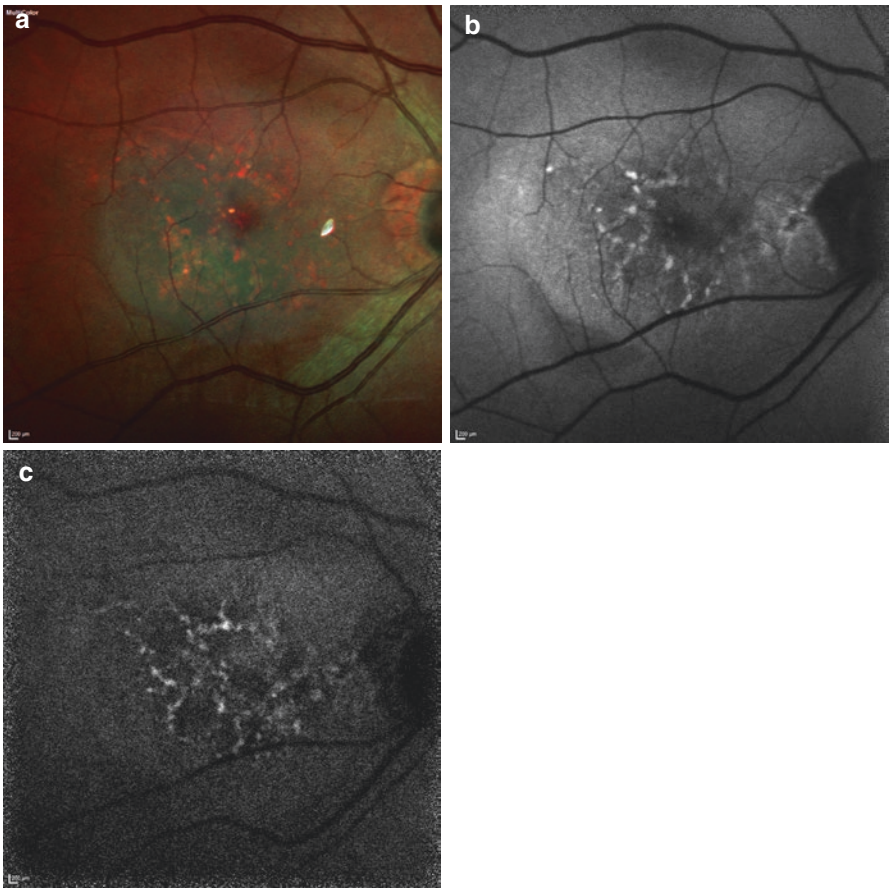

Fig. 2.2 Vascularized PED with prominent serous portion (75 year old male patient) (**a**) MultiColor image presenting a central greenish elevation with multiple red spots (**b**) FAF image with decreased FAF intensity at the lower PED border and increased and decreased FAF within the PED (**c**) NIA image with multiple areas of increased NIA within the PED (**d**) NIR (left) & SD-OCT image presenting a huge PED with dark intraretinal spots corresponding to the red spots in MultiColor and the spots of increased FAF and NIA material. The content of the PED is predominantly serous (hyporeflective). Subretinal fluid as well as a thickening of the sub-RPE-complex suggestive of CNV is present on the nasal side. The choroidal layers cannot be visualized due to the high elevation of the PED. (**e**) FA (left) & ICGA (right) at 59 sec: Early hypofluorescence within the PED (**f**) FA (left) & ICGA (right) at 3.24 min: FA shows variable fluorescence within the PED and temporal staining. ICGA shows hypofluorescence. (**g**) FA (left) & ICGA (right) at 9.33 min: There is limited change to the previous image. However, in all angiography images, some irregularities are evident between PED and optic nerve head, in the region where the CNV was suspected in SD-OCT.

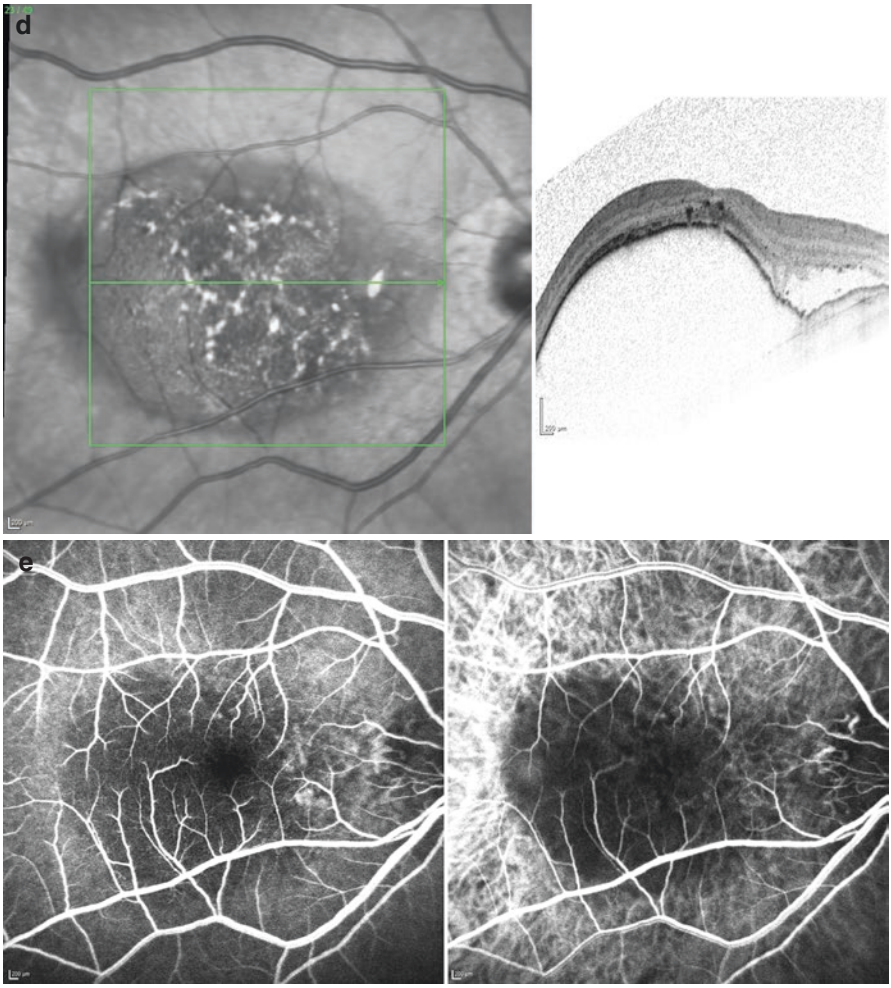

Fig. 2.2 (continued)

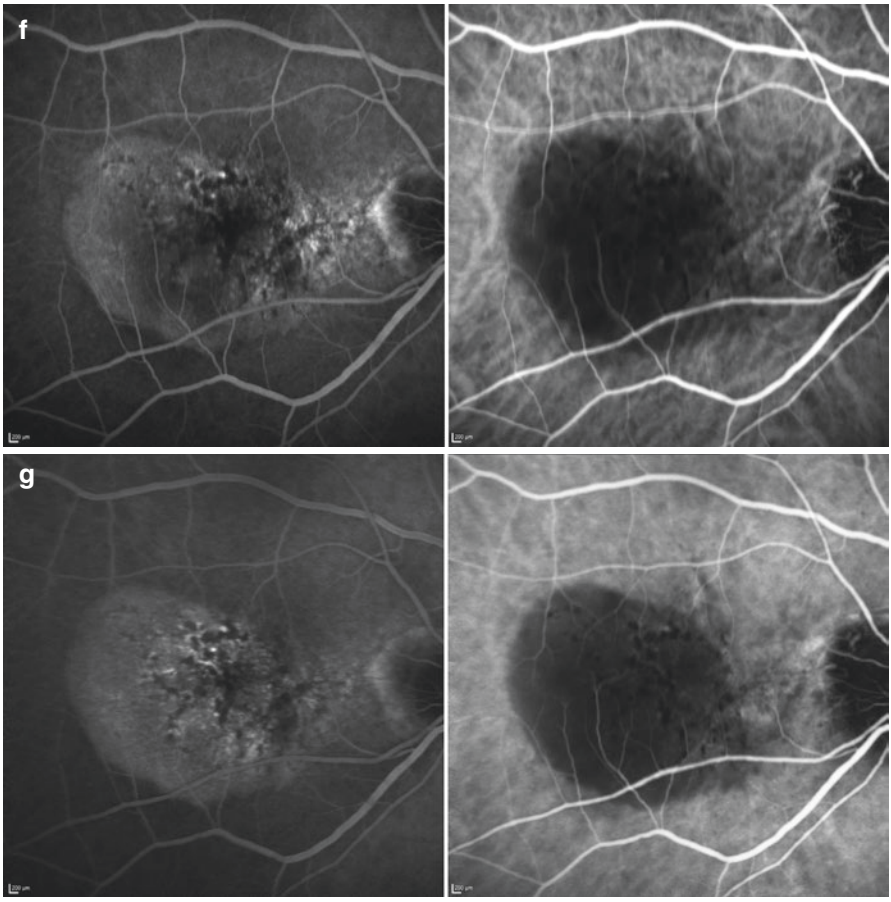

Fig. 2.2 (continued)

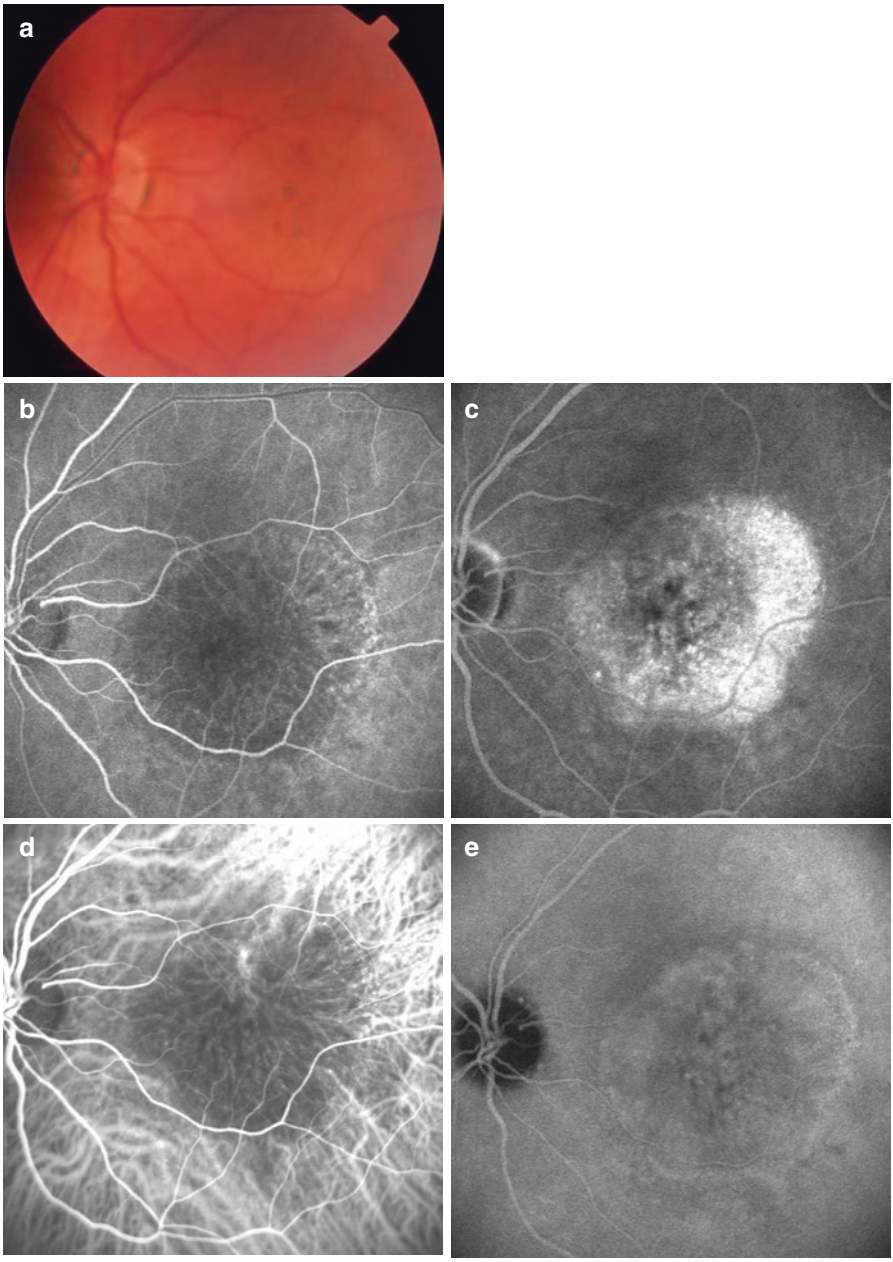

Fig. 2.3 Fibrovascular PED. (**a**) Fundus picture showing disc-shaped PED with slight pigment clumping (**b**) FA early frame showing fine vascular network, the stippled hyperfluorescence increasing to the late frame (**c**) with slight leakage in the temporal part of the PED. (**d**) ICGA early frame depicting the feeder vessel of the fibrovascular network, (**e**) ICGA late frame showing plaque formation. (**f**) Another patient: NIR (left) and SD-OCT image showing an irregular PED with shallow slopes and middle-reflective material beneath the RPE (fibrovascular material).

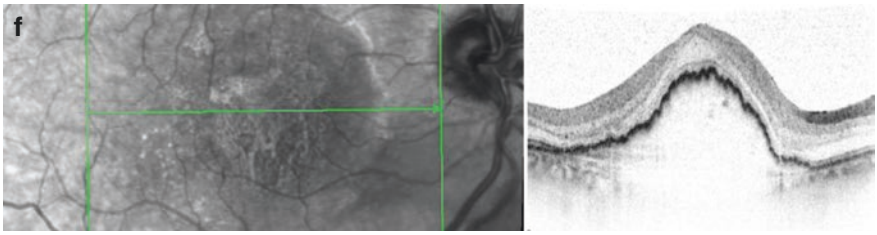

Fig. 2.3 (continued)

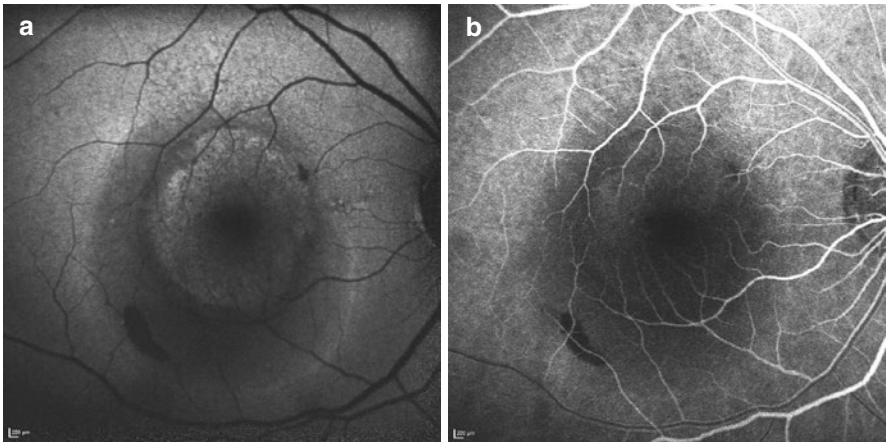

Fig. 2.4 PED with temporal retinal pigment epithelium rip. (**a**) FAF prior to RPE rip: classic signs of PED with an increased FAF within the PED, a darker area delineating the PED and a ring of increased FAF at the border of the subretinal fluid. Small subretinal hemorrhage at the lower temporal border of the PED (**b**), (**c**) FA at 33 sec and 7.28 min prior to RPE rip with central hypofluorescence within the PED and increasing mild stippled hyperfluorescence in the superior part of the PED in the late frame. (**d**) NIR (left) & SD-OCT image prior to RPE rip. NIR delineates the area of PED and subretinal fluid. The SD-OCT shows double elevated PED with subretinal fluid between the elevations as well as peripheral. (**e**) MultiColor image with a macular elevation indicated by the green color and an irregular red area corresponding to the increased near-infrared reflectance in the area with retracted RPE. (**f**) FAF after tearing of RPE showing an increased FAF in the area with retracted RPE and a markedly decreased FAF temporal in the area of absent RPE. (**g**), (**h**) FA at 1.06 and 7.05 min min after RPE rip with blockage in the area of the retracted RPE and hyperfluorecence in the area of the rip. Hyperfluorescent spots are visible at the nasal border of the PED. (**i**) NIR (left) & SD-OCT image. NIR shows increased reflectance from the retracted RPE and the folds of the RPE. SD-OCT shows a central fibrovascular PED with an absence of RPE at the temporal border of the PED in the area with subretinal fluid.

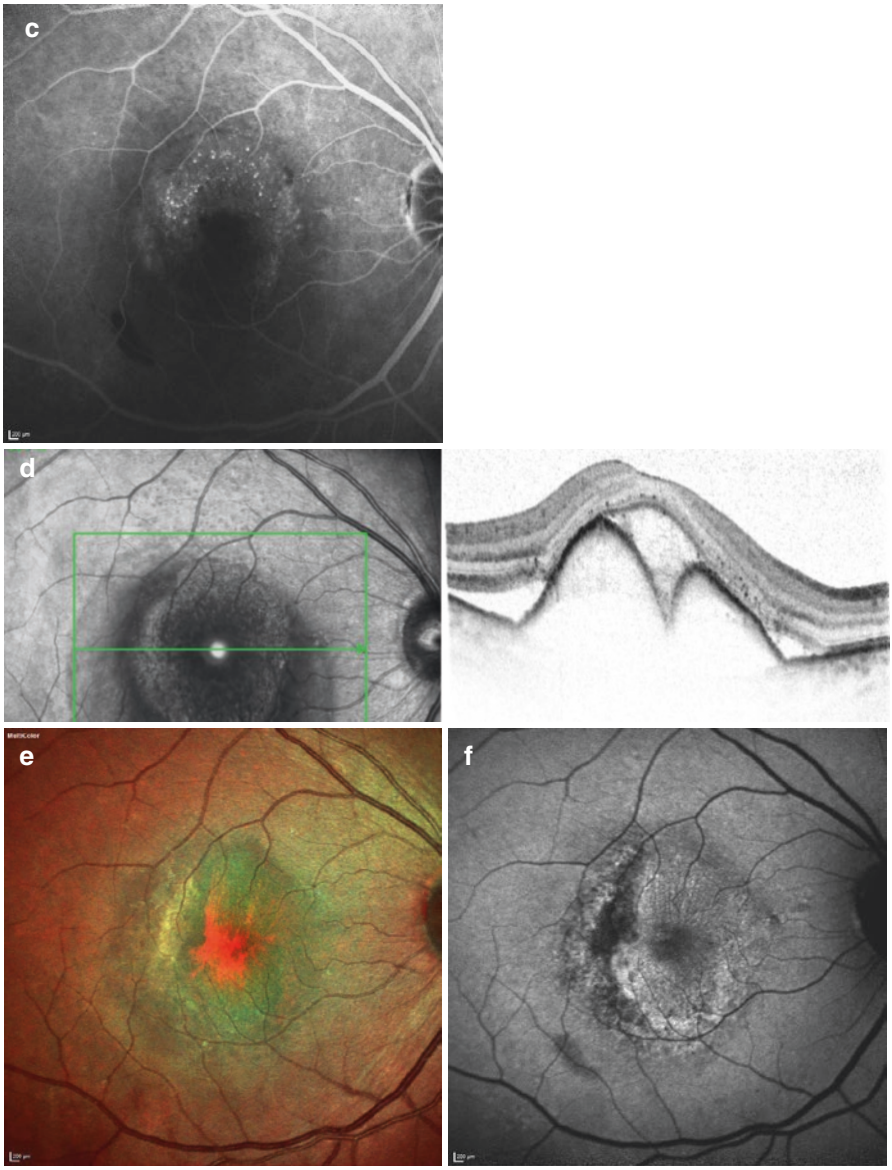

Fig. 2.4 (continued)

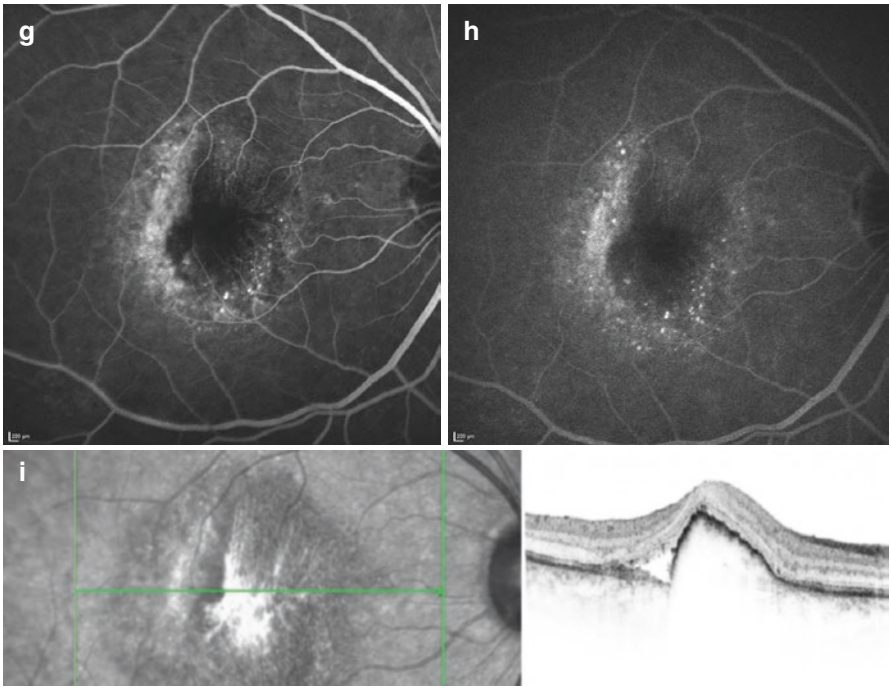

Fig. 2.4 (continued)

vasculopathy (PCV) or retinal angiomatous proliferation (RAP), which are both causes for developing PED. It also helps to identify the "feeder vessel" in choroidal neovascularization.

As a general rule in ICGA, a serous PED appears hypofluorescent in the early *and* late phase due to the blockade-effect of the subretinal fluid accumulation and the higher affinity of the dye to plasma proteins, preventing extravasation of the dye (Figs. 2.1e–g, 2.3e–f, and 2.4d–e). Depending on the cause of the PED, some additional signs can be seen:

PCV: ICGA can demonstrate vascular ectasies, which are most likely located temporal to the optic disc (Fig. 2.4d–e). Since FA masks ectasies due to extravasation of the dye, ICGA is superior to FA in PCV imaging.

RAP: ICGA can help in distinguishing retinal from choroidal vascular pathologies and is used as an additional imaging technique to demonstrate retinochoroidal anastomoses.

Occult CNV: ICGA can show variable results in occult CNV. It can lead to hyperfluorescence in the middle and late phase. As mentioned above, it may help to identify "feeder vessels."

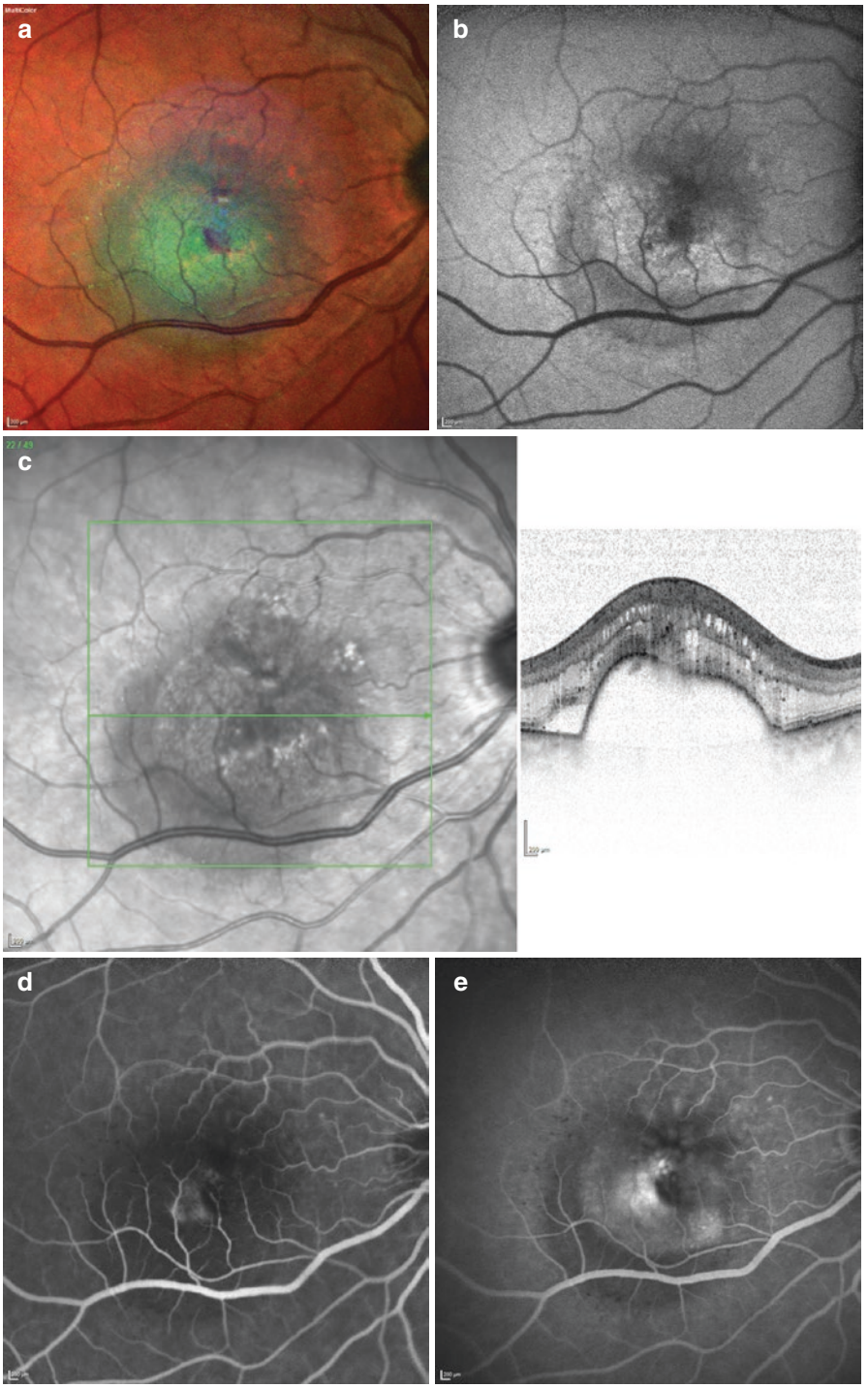
a
b
c
d
e

In all three diseases (PCV/RAP/occult CNV), the so-called "hot spots" may be seen. Hot spots are small localized hyperfluorescences in the middle and late phase of ICGA (Fig. 2.1f). They are usually smaller than one optic disc diameter.

2.2.3 Angiography Summary

Angiography Pros:

- Best technique for visualization of leakage (FA)
- Distinction of CNV and different types of CNV
- Long-standing experience as imaging techniques
- Valuable in making the correct initial diagnosis in retinal diseases
- Best techniques for the evaluation of central AND peripheral retinal (FA) and choroidal (ICGA) circulation

Angiography Cons:

- Invasive procedure with possible side effects
- Time-consuming (ICG more than FA)

2.3 Spectral Domain Optical Coherence Tomography

SD-OCT is a noninvasive imaging technique which uses reflected light to produce detailed images of ophthalmic structures resulting in three-dimensional anatomic information about retinal layers, RPE and choroid. Nowadays, it is the most commonly used imaging technique in retinology. "Spectral domain" OCT (SD-OCT) is the latest generation of OCTs and works much faster and gives more detailed images compared to the first generation of OCT, which was called "time domain" OCT. Modern devices combine SD-OCT with confocal scanning laser ophthalmoscope (cSLO) (Spectralis HRA/OCT, Heidelberg Engineering). They use simultaneous recording of both techniques, which allows comparison of cross-sectional OCT findings to fundus images. In recent years, SD-OCT has mostly replaced FA

Fig. 2.5 Mixed hemorrhagic and serous PED in exudative AMD (74 year old female patient) (**a**) MultiColor image with a PED visualized in green with two red hemorrhagic spots inside the PED (**b**) FAF image with blockage in the areas of the hemorrhages, increased FAF intensity centrally surrounded by decreased autofluorescence in the region of subretinal fluid (**c**) NIR (left) & SD-OCT image demonstrating serous PED with accompanying marked intra- and subretinal fluid (**d**) FA at 54 sec with early staining indicating a paracentral CNV. (**e**) FA at 5.58 min demonstrating a CNV with leakage, late pooling in the PED and cystoid macular edema. Notice the notch at border of the PED. This could also be well a RAP lesion (see chapter 5). For final diagnosis, a ICGA should be performed.

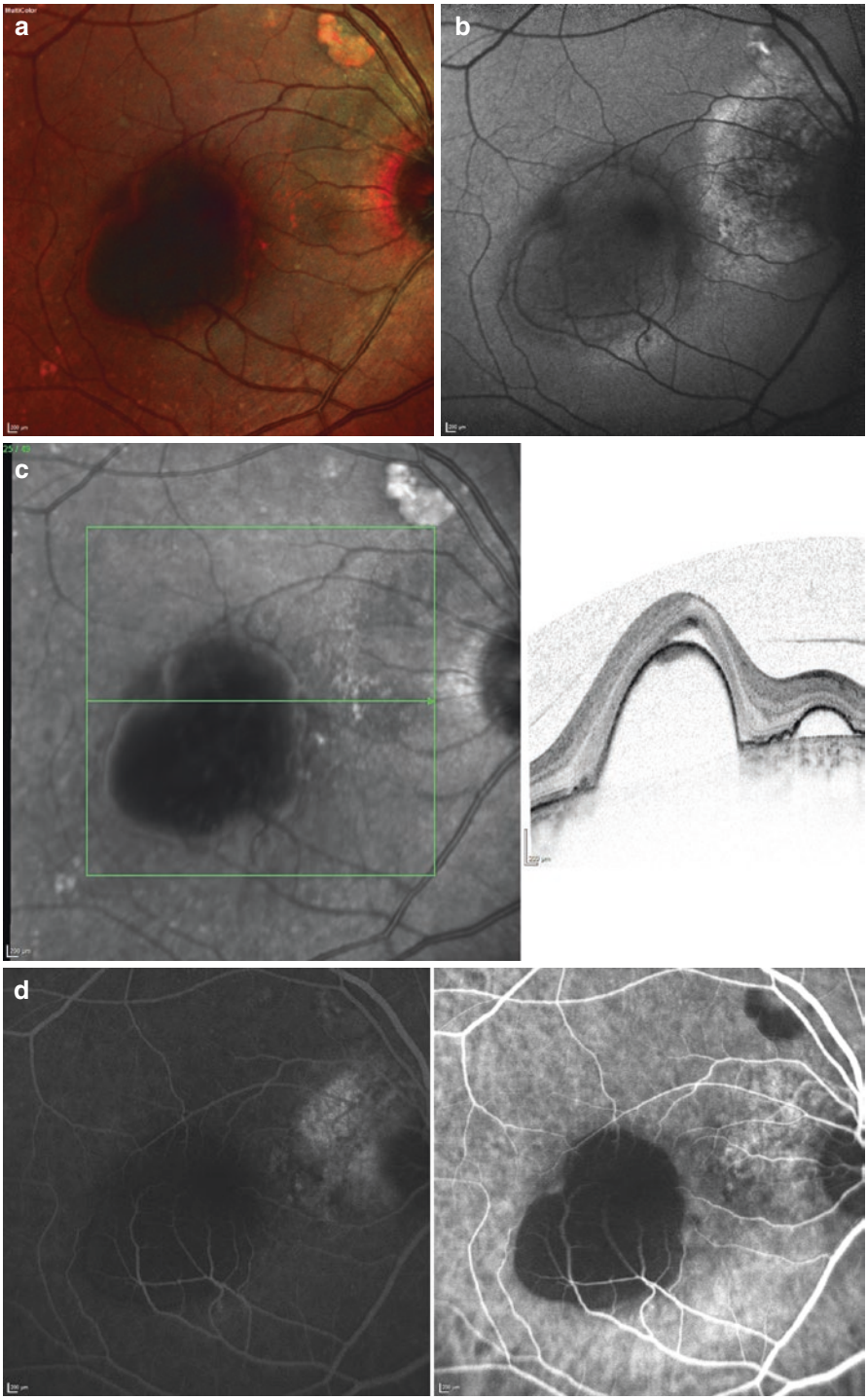
a
b
c
d

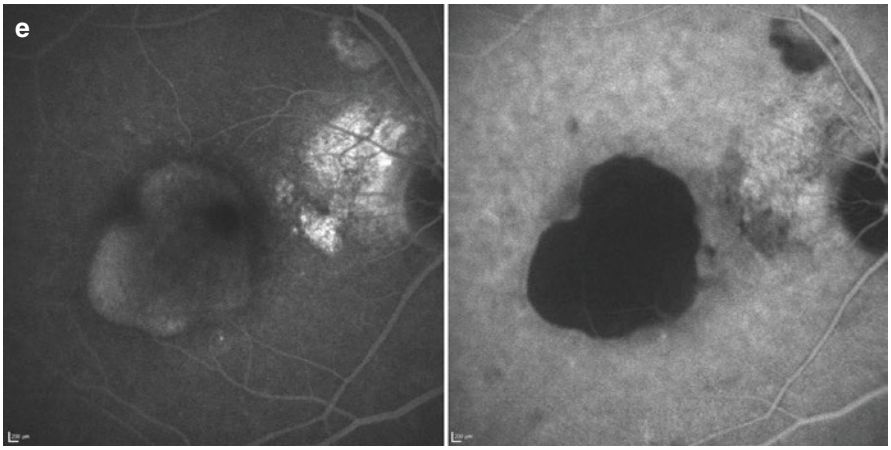

Fig. 2.6 (continued)

as standard technique for follow-up examination and monitoring therapeutic success of patients with exudative macular disorders (e.g., anti-VEGF therapy in AMD or diabetic/vascular edema). Limitations of SD-OCT include the impossibility to visualize active leakage in CNV.

SD-OCT oftentimes makes it possible to distinguish between different types of PED (serous/fibrovascular/drusenoid/hemorrhagic/mixed types). All of them have the detachment of RPE basement membrane and RPE from the remaining Bruch membrane in common. However, differences exist concerning the inner reflectivity and the morphology at the PED border:

Serous PED shows a sharp and steep border on OCT tomographic images (Figs. 2.1d, 2.3d, 2.4c, and 2.5c). They tend to have a "bubble like" appearance in OCT with smooth curved surface and lower reflectivity inside the "bubble." Depending on the content of the serous fluid, reflectivity can vary from very low to low. Completely serous PEDs in which no CNV can be demonstrated in either technique are very unusual, especially in AMD. One possible pathomechanism for serous PEDs are CNVs, which often can be

Fig. 2.6 Serous PED in PCV (74 year old female patient) (**a**) MultiColor image shows a dark red area with well-defined borders corresponding to a hemorrhagic PED. In addition peripapillary lesions are present. (**b**) FAF image with a decreased FAF signal due to blockage in the PED. Peripapillar region with increased FAF intensity indicate an area with previous subretinal fluid . (**c**) NIR (left) & SD-OCT image presenting a prominent central serous PED and a smaller serous PED in the peripapillar region. Subretinal fluid is visible above the central PED. (**d**) FA (left) & ICGA (right) at 1.22 min: Both show early hypofluorescence within the large PED, which is more clearly seen in the ICGA. Early hyperfluorescence is present in the peripapillary area, where ICGA identifies several hyperfluorescent spots. (**e**) FA (left) & ICGA (right) at 10.19 min: FA shows late staining of the PED area and increased peripapillary hyperfluorescence. ICGA shows hypofluorescence within the large PED and staining in the peripapillary region. A notch is visible at the superior temporal border of the PED

visualized only by ICGA. This leads to a mixed type of PED with serous and fibrovascular parts, called vascularized PED (Fig. 2.5c). Sometimes, the vascularized part of the PED is visualized in OCT as a "second" smaller and irregular PED with medium internal reflectivity, adjacent to the main serous PED.

Fibrovascular PED show a flat border, which oftentimes precludes exact localization of PED rim, and a bumpy or wavy surface. Internal reflectivity is medium high and irregular (Fig. 2.2c).

Drusenoid PEDs are formed by confluent soft drusen in the macular region. They are moderately reflective structures underneath the RPE band (Fig. 2.7c).

Hemorrhagic PEDs show an average to high internal reflectivity and mostly a smooth surface, with sub- or intraretinal hemorrhage in addition to the RPE detachment (Fig. 2.6c). Hemorrhages can lead to low reflectivity of the underlying choriocapillaris. A pathognomonic sign in cases of PCV are hemorrhagic PEDs presenting with a blood level in their lower part (Fig. 2.8).

PED types can change over the time of the disease and should not be classified just based on the SD-OCT. Fundoscopic and angiographic examination is always mandatory.

2.3.1 SD-OCT Summary

SD-OCT-Pros:

- Best technique for detailed anatomic information of the posterior pole
- Fast and noninvasive
- Gold standard for follow-up examinations of patients with exudative disorders (e.g., PED)
- Very useful in differentiation of PED subtypes

SD-OCT-Cons:

- No visualizing of active leakage
- Inferior in specific diagnosing retinal and choroidal vascular disease
- Difficulties in myopic patients
- Reduced resolution in imaging of peripheral retinal structures (only possible in wide-angle mode)

Fig. 2.7 Drusenoid PED (78 year old male patient) (**a**) MultiColor image with multiple soft confluent drusen (**b**) FAF with variably increased FAF intensity corresponding to the drusen (**c**) NIR (left) & SD-OCT image with multiple moderate dense deposits beneath the RPE forming a PED (**d**) FA at 48 sec shows mild staining of the drusen (**e**) FA at 3.53 min: shows mild staining without any change during the course of the FA

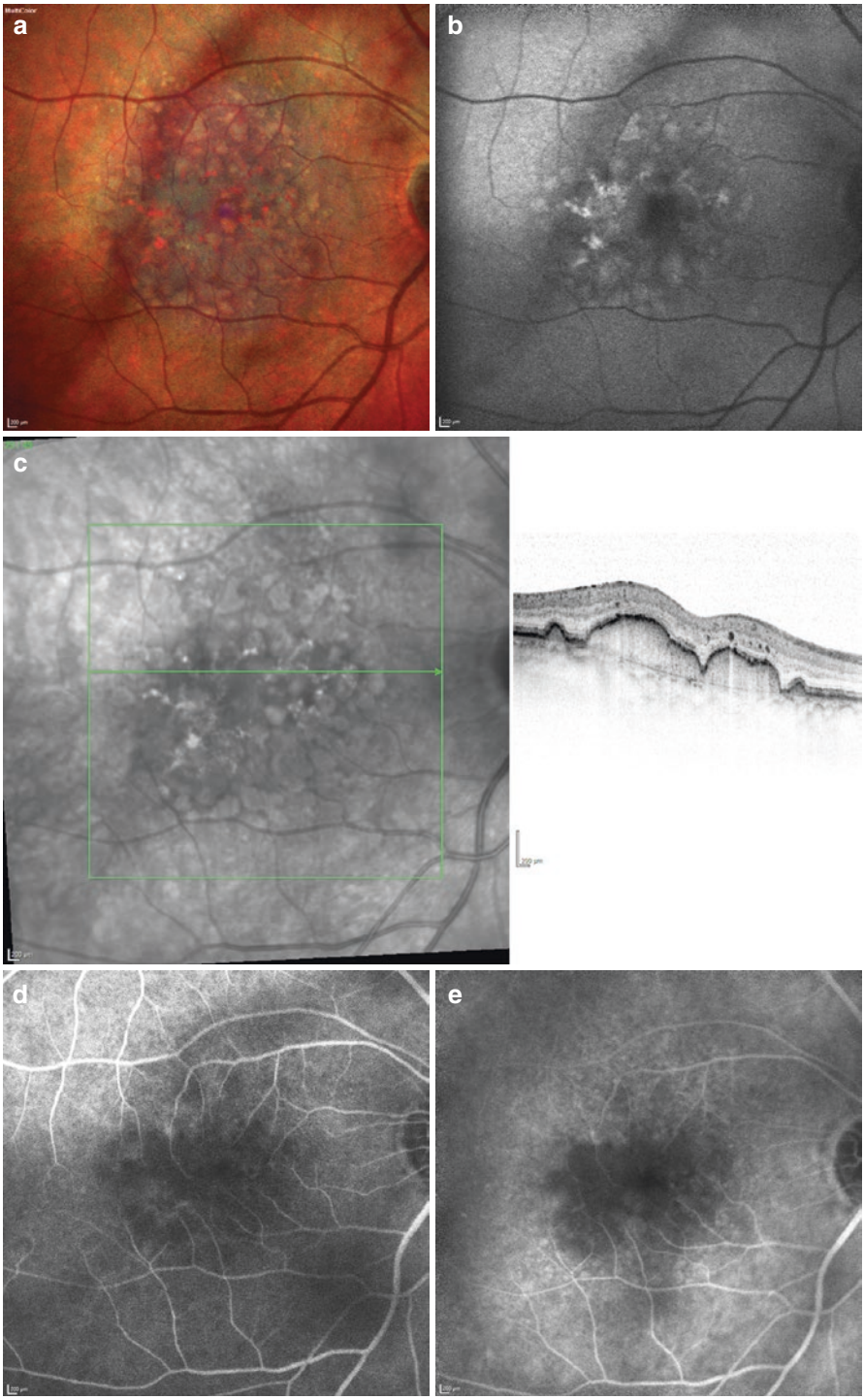
a
b
c
d
e

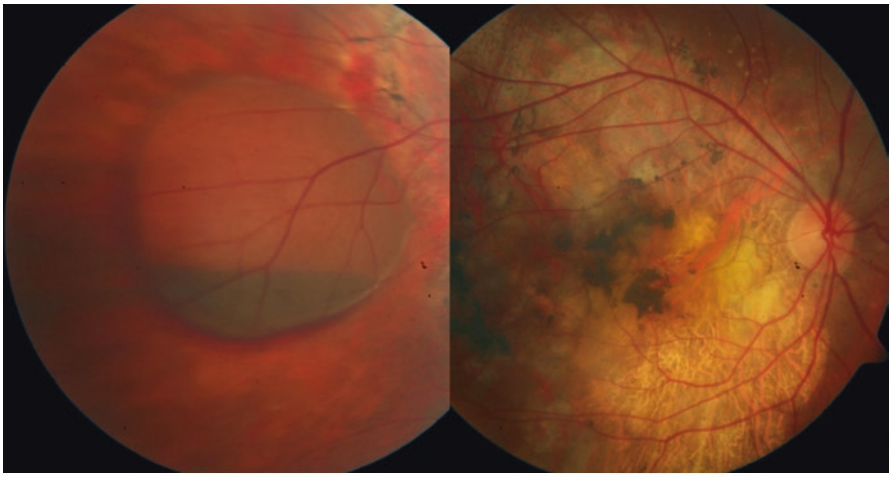

Fig. 2.8 Chronic stage of PCV in the right eye of a patient with extensive submacular scarring and prominent hemorrhagic PED temporal to the macula with pathognomonic blood level in its lower part (image courtesy of M.A. Gamulescu)

2.4 OCT-Angiography

OCTA is one of the newest techniques in retinal imaging modalities. It uses motion contrast to compare the decorrelation signal between sequential OCT B-scans taken at the same cross-section in order to visualize retinal and choroidal vasculature. This concludes that areas of motion appear white and vice versa (e.g., vascular blood flow appears white and tissue or static hemorrhages or serous leakage are dark). Advantages compared to standard FA and ICGA are that it is faster, noninvasive, and that it does not require the use of intravenous dye. It helps to visualize retinal and choroidal capillary vasculature in real time, which could be used to detect early disease activity in diabetic retinopathy, vascular diseases, or AMD. Disadvantages include the inability to view leakage, increased potential for artifacts, problems with correct segmentation of layers, and limited field of view. Further studies are needed to determine if OCTA can be established as an important imaging modality in PED.

2.4.1 OCTA Summary

OCTA-Pros:

– Noninvasive and fast tool to visualize retinal and choroidal vasculature even in miosis

– Three-dimensional imaging technique
– Segmentation in several layers of retinal and choroidal vasculature

OCTA-Cons:

– Limited field of view
– Lack of experience
– Segmentation accuracy limited
– Inability of detecting leakage
– Increased potential for artifacts, especially in PED and in highly myopic patients

2.5 Autofluorescence

2.5.1 Fundus Autofluorescence

FAF uses the distribution of lipofuscin in the RPE cells as a parameter for assessing RPE structure. It is a noninvasive procedure which reflects the metabolic state of the RPE. FAF has its highest efficiency obtained with short-wavelength fundus autofluorescence (SW-FAF) from 480 to 540 nm. In normal eyes, FAF is known to be of low intensity with a reduced signal in the foveal area, due to the absorption of luteal pigment. In numerous retinal diseases, morphological abnormalities can be detected by FAF before they become visible on ophthalmoscopy (e.g., retinitis pigmentosa, chloroquin retinal toxicity, geographic atrophy). It has therefore been widely used in the diagnosis of non-exudative retinal diseases. For example, pathological FAF at the borders of atrophic lesions in dry AMD is of key importance to predict the development of the disease. Modern FAF systems use confocal scanning laser ophthalmoscope (cSLO) and combine it with spectral domain optical coherence tomography (SD-OCT) (e.g., Spectralis HRA/OCT, Heidelberg Engineering, Heidelberg, Germany).

FAF imaging in eyes with PED shows variable FAF phenomena: Depending on the composition of subpigment epithelial fluid, the FAF signal over the lesion can be increased, decreased, or unchanged. The majority of PEDs show an increased FAF signal over the lesion, surrounded by a well-defined less autofluorescent halo delineating the entire border of the lesion (Figs. 2.1c and 2.3b). PEDs with decreased FAF signal over the lesion can correspond to areas of RPE atrophy or fibrovascular scarring (Figs. 2.2b and 2.4b). Rarely, PEDs show cartwheel pattern with hyperpigmented radial lines and a diminished FAF signal between those lines. This FAF pattern is highly indicative of drusenoid PEDs (Fig. 2.7b). Some PEDs show changing FAF phenomena over time: Starting with decreased FAF signal early after development of PED and developing an increased FAF signal after months of persistent PED, due to changes in the composition of the subretinal fluid.

2.5.2 *Near-Infrared Autofluorescence*

Near-infrared autofluorescence (NIA) uses the distribution of melanin in the RPE cells to assess RPE structure. Melanin granula are mainly located in the foveal area with decreasing intensity paracentral. The quantity of melanin granula towards the periphery is constant. Melanin is an effective absorber of light and has therefore a protective effect on RPE cells. NIA uses a different excitation wavelength compared to FAF (787 nm). In contrast to FAF, NIA in normal eyes shows the highest intensity under the fovea with a decrease towards the border of the macular and is then unchanged towards the periphery. Its usage is similar to FAF, which includes hereditary and non-exudative macular disorders. NIA in PED shows a reduced signal due to blockage of the normally centrally high intensity of NIA (Fig. 2.3c). The border of PED can often be visualized in NIA with an increased intensity (Figs. 2.1c and 2.3c).

2.5.3 *Autofluorescence Summary*

Autofluorescence Pros:

- Noninvasive fast way to demonstrate certain retinal and/or choroidal pathologies
- Very useful in hereditary disorders
- Complementing techniques for different issues

Autofluorescence Cons:

- Heterogeneous signs in PED
- No leakage visualization
- No differentiation of PED types

2.6 Spectral Reflectance Imaging

Spectral reflectance imaging (SRI) are noninvasive techniques using different wavelengths to evaluate the retina and choroid by measuring the unfiltered reflected light. Different wavelengths are reflected from different structures and therefore reveal information about different retinal and choroidal structures.

2.6.1 *Blue Reflectance*

Blue reflectance (BR) uses a wavelength of 486 nm. This technique is useful for visualizing pathologies of the retinal surface, e.g., epiretinal membranes or nerve fiber layer defects (Fig. 2.2a1).

2.6.2 Green Reflectance

Green reflectance (GR) uses a wavelength of 518 nm. This technique is also useful for visualizing pathologies of the retinal surface, but in contrast to BR it penetrates deeper in the retina and in addition gives more information about intraretinal structures (Fig. 2.2a2).

2.6.3 Near-Infrared Reflectance

Near-infrared reflectance (NIR) uses a wavelength of 810 nm. This technique is very comfortable for the patient due to lowest glare and allows examination in uncooperative patients and media opacities. NIR penetrates mostly through the retina and provides detailed information about the border between retina and RPE as well as the choroid. NIR shows the circumference of PED most clearly (Fig. 2.2a3).

2.6.4 Multi-Color Scanning Laser Imaging

Multi-color scanning laser imaging uses a combination of the before mentioned wavelengths to create a multi-color image. Compared to fundus photography it shows retinal pathologies with more detail.

Marked PEDs appear green in MC due to the relative blockage of the near-infrared wavelength which is very useful in PED imaging (Figs. 2.1a, 2.2a, 2.3a, 2.5a, 2.6a, and 2.9a). It is therefore a superior imaging tool in PED imaging compared to fundus photography. In addition, the combination of wavelengths in the MC image allows a better definition of lesion borders.

2.6.5 Spectral Reflectance Imaging Summary

SRI-Pros

- More detailed imaging of retinal diseases compared to fundus photography
- Imaging through pupil in miosis
- Possible simultaneous SD-OCT
- Characteristic green color in PED

SRI-Cons:

- More operator dependent than fundus photography
- No leakage visualization

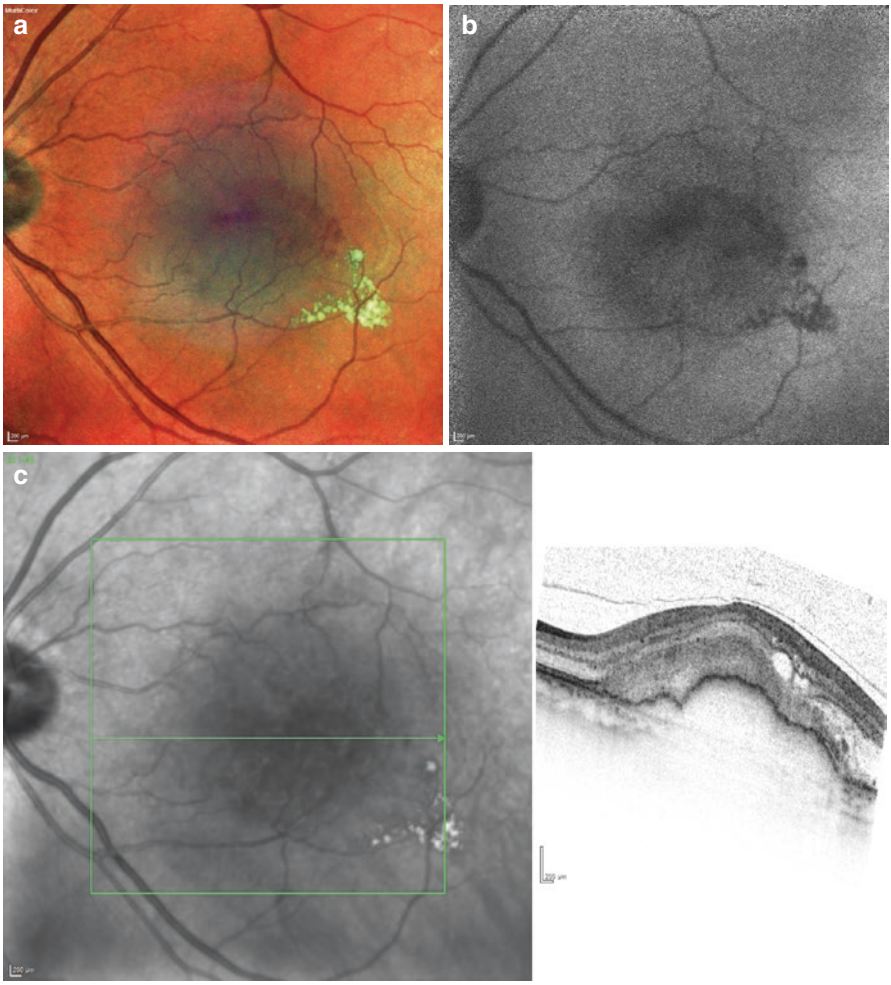

Fig. 2.9 Hemorrhagic PED in exudative AMD (78 year old female patient) (**a**) MultiColor image with a central intraretinal hemorrhagic lesion surrounded by a circular detachment indicated by the greenish color. In addition exudates temporal of the macula are visible. (**b**) FAF image with a decreased FAF intensity due to blockage in the area of PED and exudates (**c**) NIR (left) & SD-OCT image with PED detachment and massive subretinal material centrally and intra- and subretinal fluid temporally (**d**) FA at 25 sec shows blockage by the PED and the exudates (**e**) FA at 1.01 min develops a hyperfluorescence in the temporal lower part of the PED. (**f**) FA at 6:41 min shows progressive hyperfluorescence indicating a CNV and staining in the PED except for the blockage by the hemorrhage and the exudates

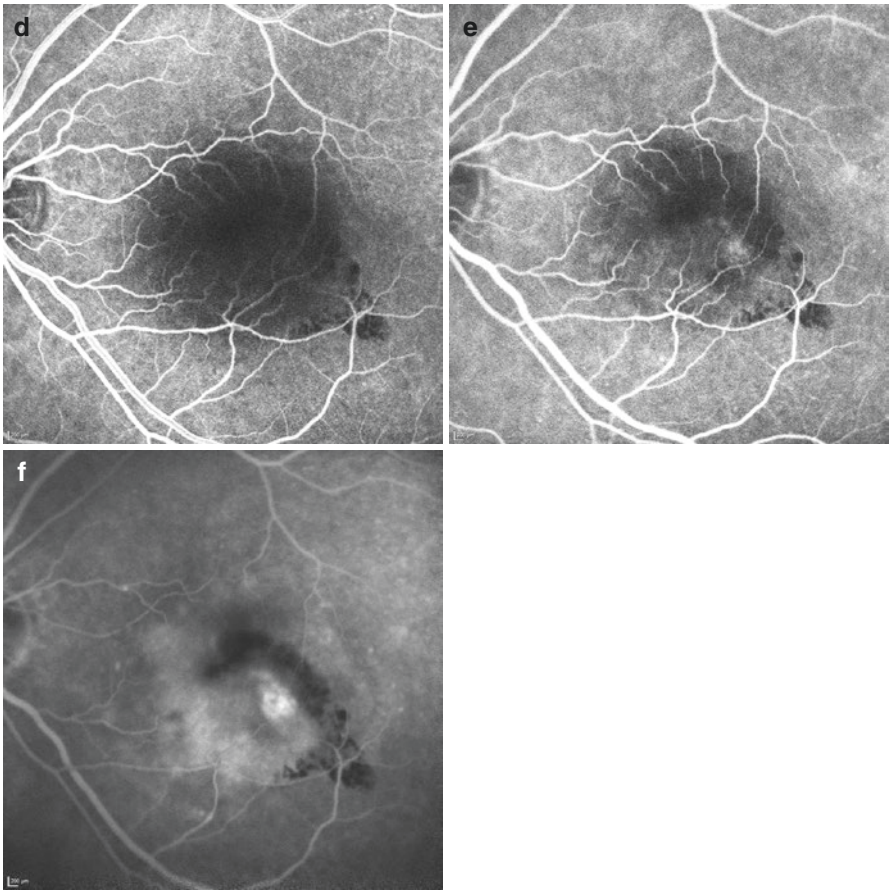

Fig. 2.9 (continued)

2.7 Summary

Different imaging techniques are available to evaluate different features of PED. Usually, the combination of some but not all of these methods is required to distinguish different forms of PED and for the follow-up during treatment. SD-OCT is the most important and widespread imaging technique, which is a fast and noninvasive tool to differentiate PED subtypes and for follow-up examinations of exudative disorders. FA and ICGA are used to detect and localize CNVs and are important techniques in diagnosing PEDs related to PCV and RAP. FAF, NIA, and SRI are complementing techniques in PED diagnostic. OCTA is a new imaging modality, which is not established yet in the diagnostic of PED patients.

Chapter 3
Retinal Pigment Epithelial Detachment in Age-Related Macular Degeneration

Albrecht Lommatzsch

3.1 Introduction

Age-related macular degeneration (AMD) is the most common cause of blindness defined by law, in the western world, its late stages having a reported frequency of 12% [1]. It is a complex disease of the central retina with a prevalence of 30% in the population aged over 80 years.

Demographic developments and extended life expectancy in modern industrialized nations potentiate the problem for the future. AMD is a metabolic disorder of the photoreceptors and the retinal pigment epithelium (RPE) with accumulation of lipofuscin granules in the retinal pigment epithelial cells and increased deposits in Bruch's membrane (drusen). In addition to age, it is also assumed to be caused by a genetic disposition and by environmental factors [2].

On the basis of existing pathogenetic concepts, AMD is subdivided into an early form and late forms. In late AMD, a distinction is made between the atrophic and the exudative type.

In patients with exudative AMD, choroidal neovascularization (CNV) extends under and through the RPE. The characteristic clinical signs of this type of AMD are lipid deposits, subretinal hemorrhage, and accumulation of intraretinal and subretinal fluid [3, 4]. Pigment epithelial detachment (PED) can occur and is differentiated into serous, vascularized, and fibrovascular PED. In PED, the pigment epithelium detaches from the remaining layers of Bruch's membrane along with its basal membrane [5]. The characteristic clinical sign is a prominent lesion, usually round. It has

A. Lommatzsch
Department of Ophthalmology, St. Franziskus Hospital, Hohenzollernring 74, 48145 Muenster, Germany

Department of Ophthalmology, University of Duisburg-Essen, Hufelandstraße 55, 45147 Essen, Germany
e-mail: albrecht.lommatzsch@web.de

M.A. Gamulescu et al. (eds.), *Retinal Pigment Epithelial Detachment*,
DOI 10.1007/978-3-319-56133-2_3

proved useful in the past to regard PED as a special type of occult neovascularization, as this morphological subgroup of occult CNV differs from the other late forms of AMD with associated CNV in terms of the natural course of the disease and the response to various treatment methods [5, 6].

Possible prognostic factors for treatment success can be identified using modern diagnostic methods such as spectral domain (SD) OCT imaging and OCT-angiography. A tear in the RPE is a feared complication in patients with PED (see Chapter 7), as extensive subretinal hemorrhage can occur along with severe deterioration of vision.

In early forms of AMD, large confluent drusen can result in the so-called drusenoid PED (see Chapter 4). A CNV cannot be demonstrated in these patients by angiography or on OCT scan.

In connection with exudative AMD, the occurrence of PED may also be associated with retinal angiomatous proliferation (see Chapter 5), or polypoidal choroidal vasculopathy (see Chapter 6).

3.2 Epidemiology

Around 30–50 million people throughout the world suffer from AMD, of which approximately 10–15% have neovascular AMD [7, 8]. In Germany, the numbers amount to 270,000–485,000, with an additional 35,000–50,000 new cases occurring each year [8, 9]. The risk of developing exudative AMD increases with age. While 0.5–1.0% of 60-year-olds are affected, the prevalence of exudative AMD increases to 10–15% among 85- to 90-year-olds [8]. The second eye may also be affected by neovascular AMD, with a risk of 12% within a year and 27% within 4 years [10]. PED occurs as a specific morphological manifestation in around 10% of all patients with exudative AMD [5, 6]. With the currently increasing use of high-resolution, three-dimensional imaging, an even higher proportion of PED in AMD patients can be assumed.

3.3 Pathogenesis

Histologically, in PED, the RPE detaches from the inner collagen fiber layer of Bruch's membrane along with its basal membrane.

As this process is often associated with choroidal neovascularization (CNV), a disc-shaped scar may subsequently arise in the long term. In serous or drusenoid PED, RPE and photoreceptor cells may die by apoptosis with consecutive formation of an atrophic area [11–13].

As shown in studies using electron microscopy and light microscopy, Bruch's membrane becomes thicker in connection with AMD [13]. Increasing thickness can be observed even during the normal aging process of the RPE and Bruch's membrane [14]. However, the authors of this study found high individual fluctuation in the

parameters studied and suggested that around half of the increase in thickness was due to natural aging, and the other half to factors such as genetic disposition and environmental factors [15, 16]. The increase in thickness of Bruch's membrane is associated with a reorganization of the layered structures of Bruch's membrane (see also Chapter 1). While there are five clearly separate layers in young people, these clear layers become less distinct with increasing age, and increased deposits of membrane particles and particles of a higher density are observed, as are increased links between structures [15]. These structural changes are associated with a change in the biochemical composition and the physical and physiological characteristics of Bruch's membrane [14]. In the course of these changes, diffuse (basal laminar and linear drusen) or localized deposits (soft drusen) may occur as signs of early AMD [17].

Central ideas about pathogenesis are derived from the theory of the reduced hydraulic conductivity of Bruch's membrane, increasingly acting as a hydrophobic barrier. This is caused by a multitude of factors: progressive lipid deposits and collagen cross-linking as well as a change in the composition of tissue-degrading enzymes and their inhibitors. On the basis of this, the association between neovascularization and unaltered RPE pump activity can lead to the formation of PED as part of exudative AMD.

In addition to collagen cross-linking, calcification of Bruch's membrane may occur, beginning in the elastic layer [18]. This study extrapolated that the hydraulic conductivity of Bruch's membrane is reduced by the sum of the age-related changes to the extent that passage would theoretically no longer be possible by the age of 130 years.

Furthermore, the so-called integrins on the surface of RPE cells and laminin play a decisive role in the formation of PED as adhesion proteins between the basal membrane of the RPE cell layer and the inner collagen layer of Bruch's membrane. In addition to age-related changes in the expression of various integrin subunits in RPE cells, the correct alignment of the integrin subunits is also crucial for the strength of adhesion [19]. An altered integrin expression pattern of the RPE may also be an early risk factor for PED formation. Decreased expression and abnormal alignment of integrin subunits may also explain problems with reattachment of the RPE after the PED has flattened. In addition, the amount of laminin in the retina changes with age [20], with laminin 5 being particularly important for RPE adhesion.

It was originally assumed that the serous secretion that forms a PED originates from a permeable choriocapillaris or from abnormal ingrowth of blood vessels [21]. If the PED is associated with a CNV or a retinal angiomatous proliferation and growth through the RPE, these unstable irregular vessels may be the cause of the accumulation of fluid under the RPE. However, a PED is not necessarily associated with a CNV [22]. The flow of fluid from the vitreous cavity through the retina towards the choroid is physiologically determined by the net transport of ions by the RPE and the barrier function of the RPE [23]. Experiments with isolated RPE layers in dogs showed that even a high hydrostatic pressure gradient cannot change the flow of fluid through an intact RPE against this gradient. The pump action of the

RPE may thus conceivably be strong enough to detach the RPE by fluid accumulation from Bruch's membrane underneath it, which becomes increasingly hydrophobic with age [24] (see also Chapter 1). The fluid under the PED in exudative AMD must therefore originate both from permeable blood vessels and from RPE cells although the exact share of each cannot be determined.

3.4 Clinical Examination

The characteristic clinical signs of PED include a typical prominent lesion, usually round, at the posterior pole. Indirect stereoscopic ophthalmoscopy is an effective method to evaluate the lesion. Subretinal fluid can often also be seen. Small marginal subretinal hemorrhages can also be observed in red-free light, indicating an associated CNV. In connection with exudative AMD, the clinical signs of PED also include drusen, pigment epithelial displacement, and atrophic spots.

Extensive subretinal hemorrhaging in patients known to have AMD is often caused by a tear in the RPE [25]. Isolated sub-pigment epithelial hemorrhages from a CNV may also show the clinical signs of PED, but these PED are more darkly colored.

The characteristic clinical signs of retinal angiomatous proliferation (RAP) with PED are small intraretinal hemorrhages associated with the PED. There are typically vessels converging on the center of the PED that do not alter their caliber and grow into deeper layers of the retina in the center as far as the RPE. Due to the high degree of bilaterality of RAP, it is important to carry out a thorough examination of the second eye to detect early stages of RAP (Fig. 3.1) [26]. See also Chapter 5.

Typical clinical signs of PCV are multiple lesions such as subretinal hemorrhages in several places, drusen, PE proliferation, and not infrequently several small and larger PEDs. In most cases, the PED is found in the papillomacular region (Fig. 3.2) [27]. See also Chapter 6.

3.5 Imaging

Fluorescein and indocyanine green angiography as well as SD-OCT imaging can be used to detect pathological changes in AMD and its differential diagnoses reliably in three dimensions. A vascularized PED is typically seen in the early phase of angiography as a hypofluorescent, usually round lesion. If there is an associated occult CNV, this stains early on, usually as a marginal "notch," most clearly visible in indocyanine green angiography. In contrast, the serous part of the PED shows considerably delayed hyperfluorescence in fluorescein angiography and only begins to stain in the late frames, while it remains hypofluorescent throughout the whole course of indocyanine

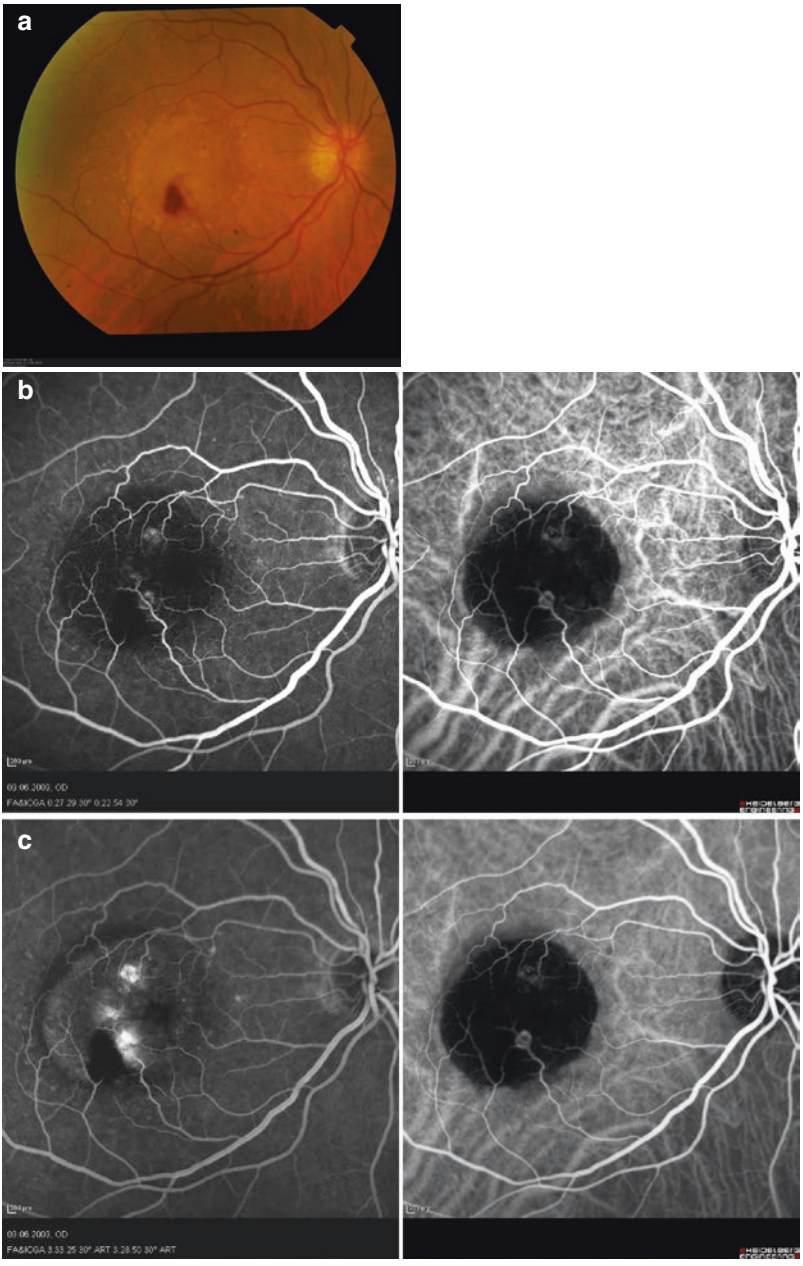

Fig. 3.1 RAP. (**a**) PED associated to a RAP-lesion with central intraretinal hemorrhage (**b**) FA and ICG angiography of the middle phase with typical hypofluorescence of the PED and hyperfluorescent staining of the retinal proliferative complexes (**c**) increasing fluorescein flow in the FA and even better imaging of RAP in the ICG uptake (**d**) SD-OCT image with illustration of PED and the retinal angiomatous complex centrally above the PED

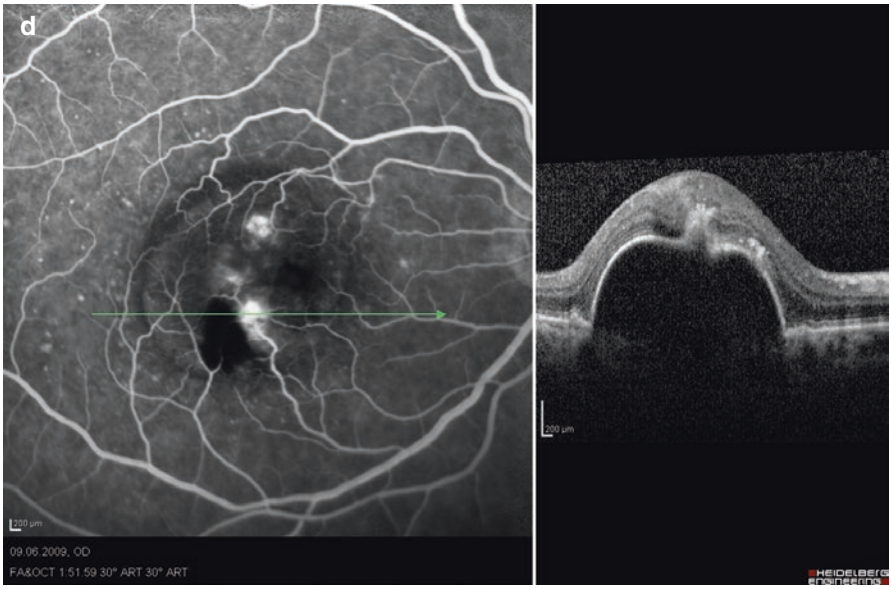

Fig. 3.1 (continued)

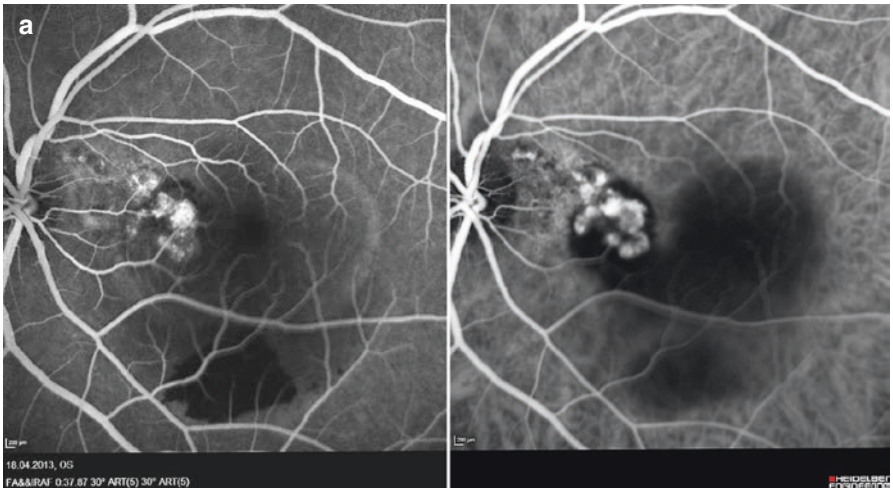

Fig. 3.2 PCV. FA und ICG imaging in early and late phase (**a**, **b**) with typical cluster-like changes in the choroid and an associated PED. SD-OCT imaging (**c**) with the typical domeshaped and middle-reflective PED representing the polypoidal lesion (*left*) adjacent to a serous PED (*right*) and subretinal fluid

Fig. 3.2 (continued)

green angiography (see also Sect. 3.7). A fibrovascular PED would show stippled hyperfluorescence increasing in the late frames with only minimal leakage.

Classification of PED in AMD is not always clear-cut in the literature. It is based on angiographic findings and is thus subdivided into the following [28, 29]: drusenoid PED, serous PED, vascularized PED and fibrovascular PED.

3.6 Drusenoid PED

Soft drusen are dynamic, i.e., they may regress in size or may become larger and coalesce. On funduscopy, yellowish-grayish disc-shaped changes are observed, some of which are marked by isolated secondary pigmentary alterations (Fig. 3.3). If several drusen become confluent over a larger area (>1000 µm), this may lead to

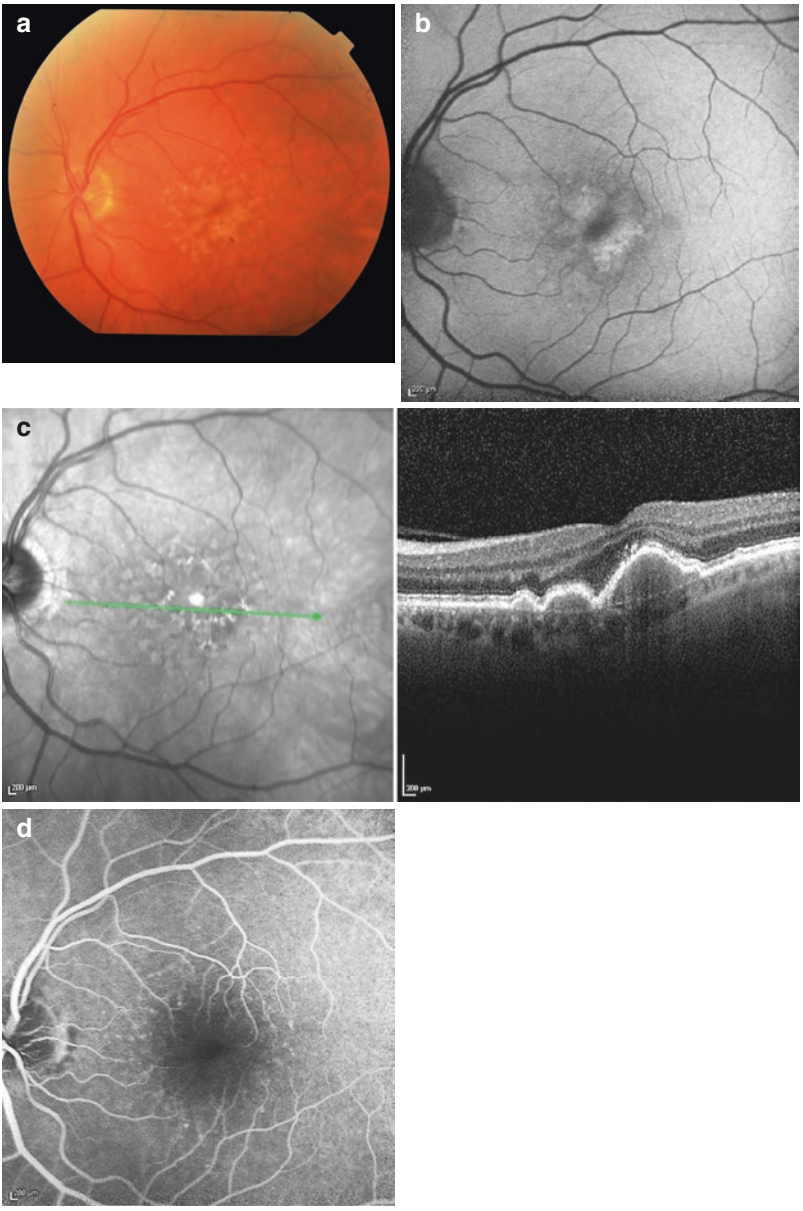

Fig. 3.3 Drusenoid PED. (**a**) Fundus image of a drusenoid PED with confluent drusen perifoveolar (**b**) Fundus autofluorescence (FAF) with increased FAF in the PED as a sign of lipofuscin accumulation (**c**) SD-OCT—image in the central section without intraretinal or subretinal fluid (**d**) FA, middle phase, PED shows only slight and hardly dicscernible fluorescein accumulation

clinically visible drusenoid PED. The increased barrier function of these confluent deposits and at the same time a disturbance in the pump action of the RPE may also result in hybrid forms with serous PED components [5, 29, 30]. Drusenoid PED shows only slightly increasing hyperfluorescence on fluorescein angiography and remains hypofluorescent on indocyanine green angiography. OCT shows typical dome-shaped appearance with medium internal reflectivity. See Chapter 4.

3.7 Serous PED

Purely serous PED formally consists of a detachment of the RPE without detectable CNV. Clinically, it is clearly visible on funduscopy as a detachment of the RPE and thickening of the macula. The presence of soft drusen is associated with a heightened risk of progression of AMD. In terms of the diagnosis, an attempt should be made to rule out CNV using fluorescein and indocyanine green angiography. On fluorescein angiography, due to the fluorescein slowly accumulating in the PED from the edge, a typical ring-shaped hyperfluorescence is observed, which increases in intensity in the course of time and may eventually fill out the entire PED in the form of a disc, but does not show any leaking. On OCT, a clearly defined, steep and usually smoothly delimited echo-free PED and, depending on the height of the fluid cushion, shading of the choriocapillaris are seen. Purely serous PED is fairly uncommon in patients with AMD. Usually, no intraretinal fluid can be seen; occasionally there is a thin subretinal film of fluid at the edge and at the apex of the PED (Fig. 3.4). As long as an active CNV cannot be detected, no treatment option is available. Particularly if there is an intraretinal edema, however, a thorough examination should always be performed again to detect an accompanying CNV and to rule our RAP lesions (see also Chapter 5), as this would have consequences for the choice of treatment [28]. In purely serous PED associated CNV can also develop in 25–30% of cases, therefore, close monitoring control should always be performed [31, 32].

3.8 Vascularized and Fibrovascular PED

If the PED is partially or completely filled with fibrovascular material, it is referred to as a vascularized or fibrovascular PED, respectively. Vascularized or fibrovascular PEDs are considerably more common than the aforementioned purely serous PEDs. Due to the presence of a CNV, they are classified as occult CNV. The CNV grows underneath the RPE (occult = hidden) and thus results in the detachment of the RPE from Bruch's membrane. On fluorescein angiography, fibrovascular PED demonstrates a slow and partly dotted hyperfluorescence and leakage in the late phase (Fig. 3.5, and Chap. 2 Fig. 2.3). ICG angiography may enhance visualization of CNV associated with PED in

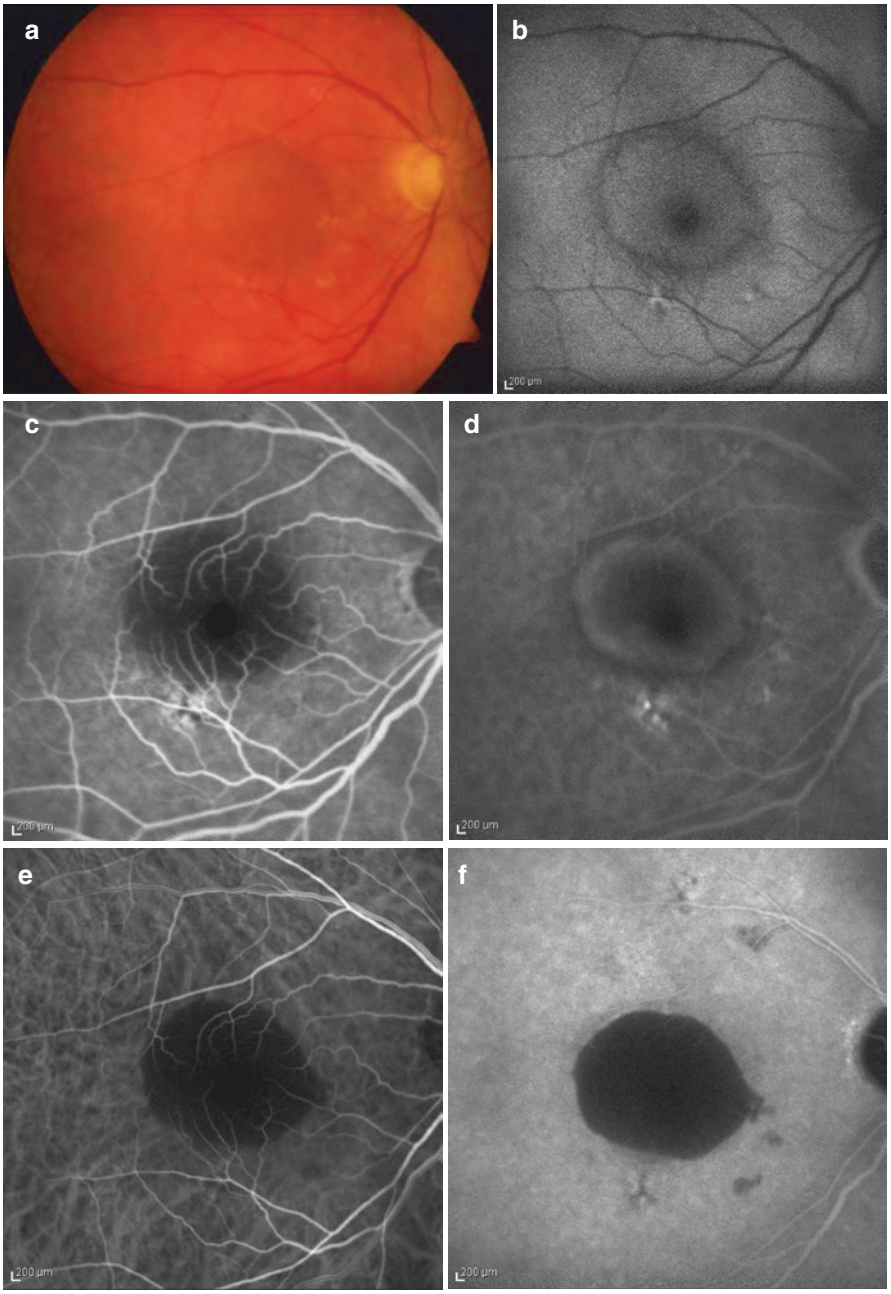

Fig. 3.4 Serous PED. (**a**) Dome-shaped PED in macular region, surrounded by some small drusen. (**b**) FAF showing increased autofluorescence throughout the PED with hypo-autofluorescence in the foveal region and at the margin. (**c**), (**d**) FA early and late frame depicting the initial hypofluorescence of the PED with slow and ringlike filling from the margin. (**e**), (**f**) ICGA early and late frame: hypofluorescence troughout the whole examination. No sign of CNV can be detected. (**g**) SD-OCT showing purely serous PED with steep borders and only a slight film of subretinal fluid at the apex

Fig. 3.4 (continued)

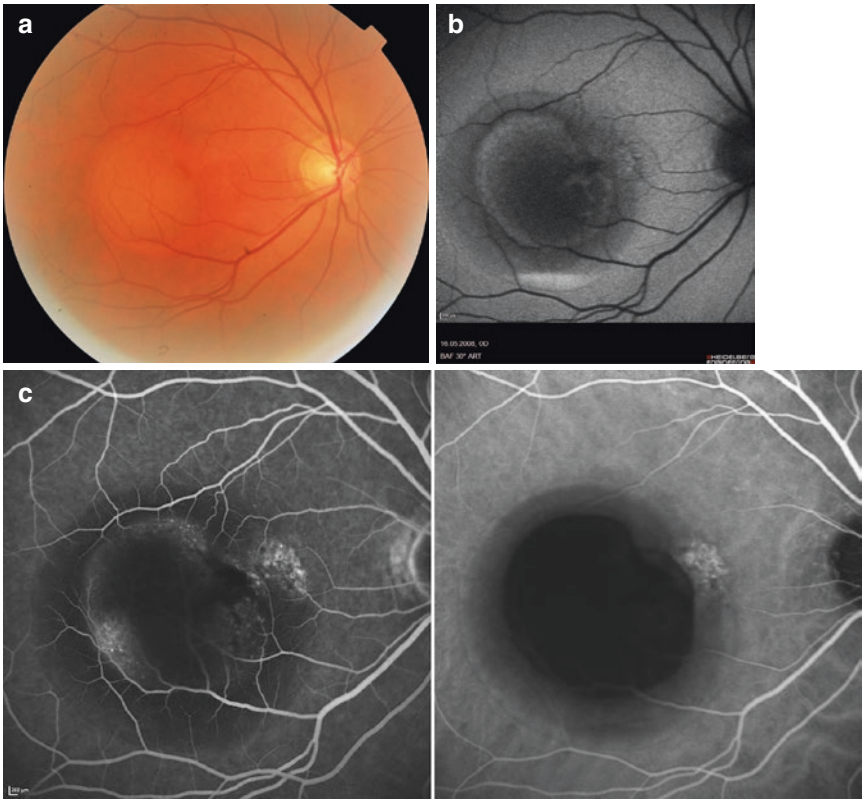

Fig. 3.5 Vascularized PED. (**a**) Fundus image with a central circular PED and peripheral single drusen (**b**) FAF recording with typical increased FAF (**c**) FA with hypofluorescent PED in the middle phase and a marginal hyperfluorescence as an indication for an occult CNV, right ICGA with typical hypofluorescence (**d**) SD-OCT image subretinal fluid because of CNV is shown

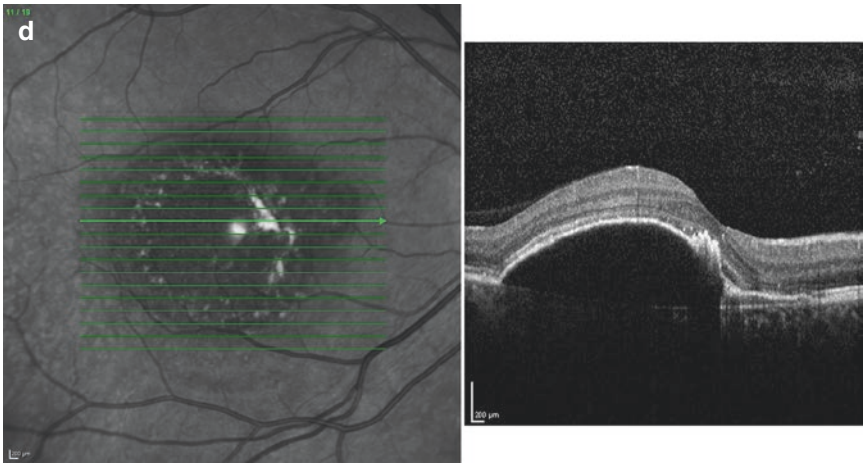

Fig. 3.5 (continued)

AMD, sometimes showing the feeder vessel of the CNV in the early frames and a plaque-like hyperfluorescence in the late frames.

Especially the differentiation of occult CNV associated with PED from RAP and PCV is easiest using indocyanine green angiography (ICGA). In RAP, the intraretinal proliferation can usually be seen as a hyperfluorescent dot ("hot spot") in the area of the CNV. PCV is typically characterized by distended cluster-shaped choroidal hyperfluorescent vessels [26, 33] (see also Chapters 5 and 6).

Cross-sectional imaging using SD-OCT allows the height of a PED to be visualized and quantified. In addition, as in exudative AMD, intraretinal and subretinal fluid and hemorrhages can generally be visualized. Visualization of the sub-pigment epithelial space results in very different findings. Hyperreflective layers under the pigment epithelium are interpreted as fibrosis and are associated with the risk of an RPE tear [34] (See also Chapter 7).

SD-OCT imaging is the diagnostic basis for assessing the course of disease during treatment regardless of the particular subtype of PED and repeat treatment protocol. It is based on the general activity criteria of CNV in patients with AMD.

The surface of the PED may also take very different forms on OCT. A smooth, stretched, dome-shaped surface should be distinguished from a wavy, multi-lobed surface with one or more peaks, for example, as this too affects the risk of a tear in the RPE. It was found that the risk for an RPE tear is highest in high, dome-shaped PED with a smooth surface [35] (see Chapter 7).

Modern OCT-angiography (OCTA) is hoped to provide further insight into the pathogenetic concept and better visualization of the sub-pigment epithelial space. At present, exact and defined segmentation of the PED is still the methodologically limiting factor, and it has not yet been definitively clarified which segmentation line allows the best interpretation (Fig. 3.6, Fig. 3.7).

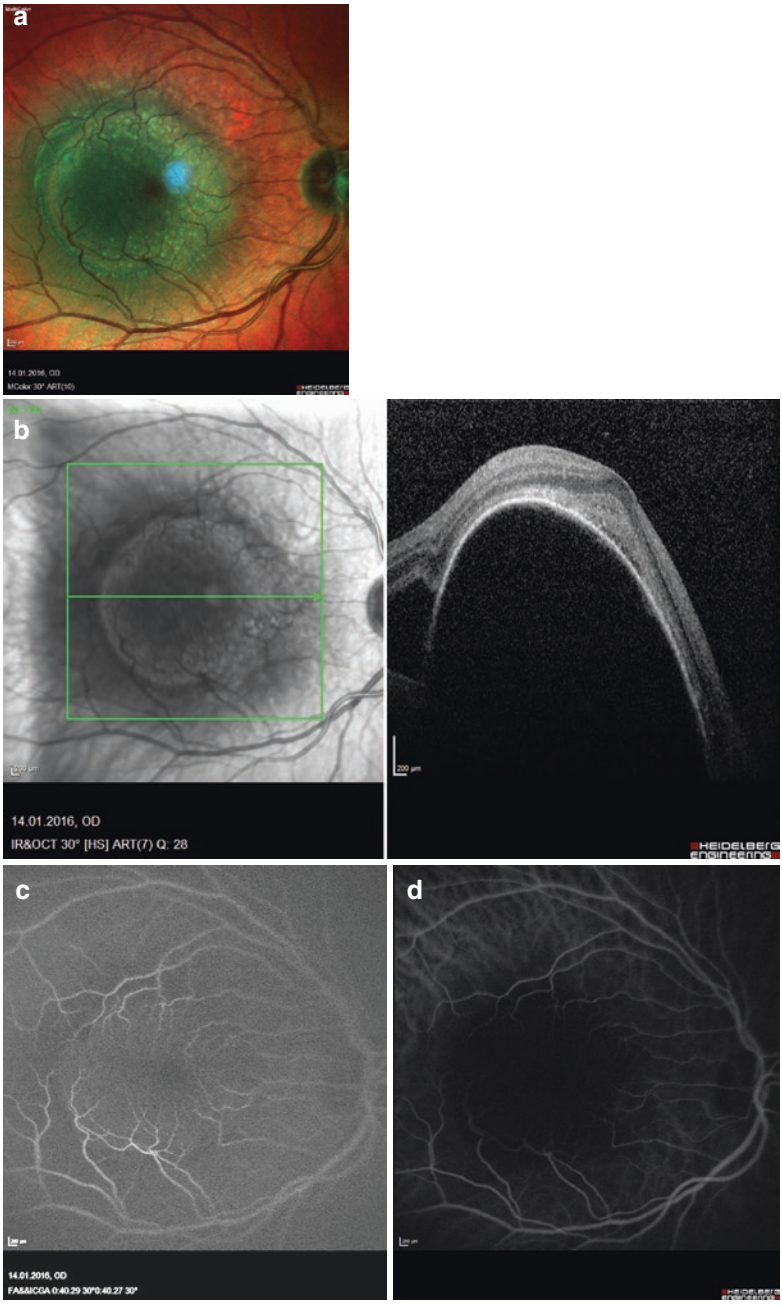

Fig. 3.6 Vascularized PED associated with age-related macular degeneration in a 72-year-old patient: (**a**) Multicolor image; (**b**) OCT; (**c**) and (**d**) early phase FA and ICGA; (**e**) and (**f**) late phase FA and ICGA; (**g**) en face OCTA image using sub-pigment epithelial segmentation shown in B-Scan (**h**) *Asterisk*: notch seen in late phase FA and ICGA as well as in en face OCTA. *Multiplication symbol*: flow artifacts in sub-pigment epithelial space as seen in en face OCTA

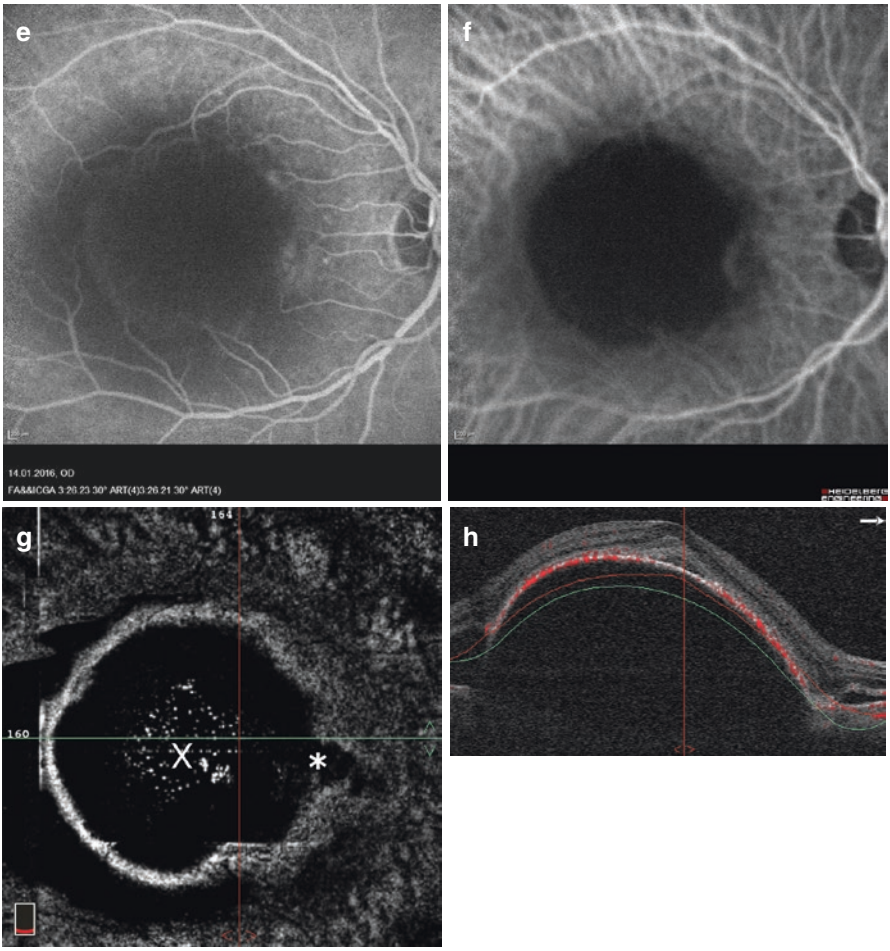

Fig. 3.6 (continued)

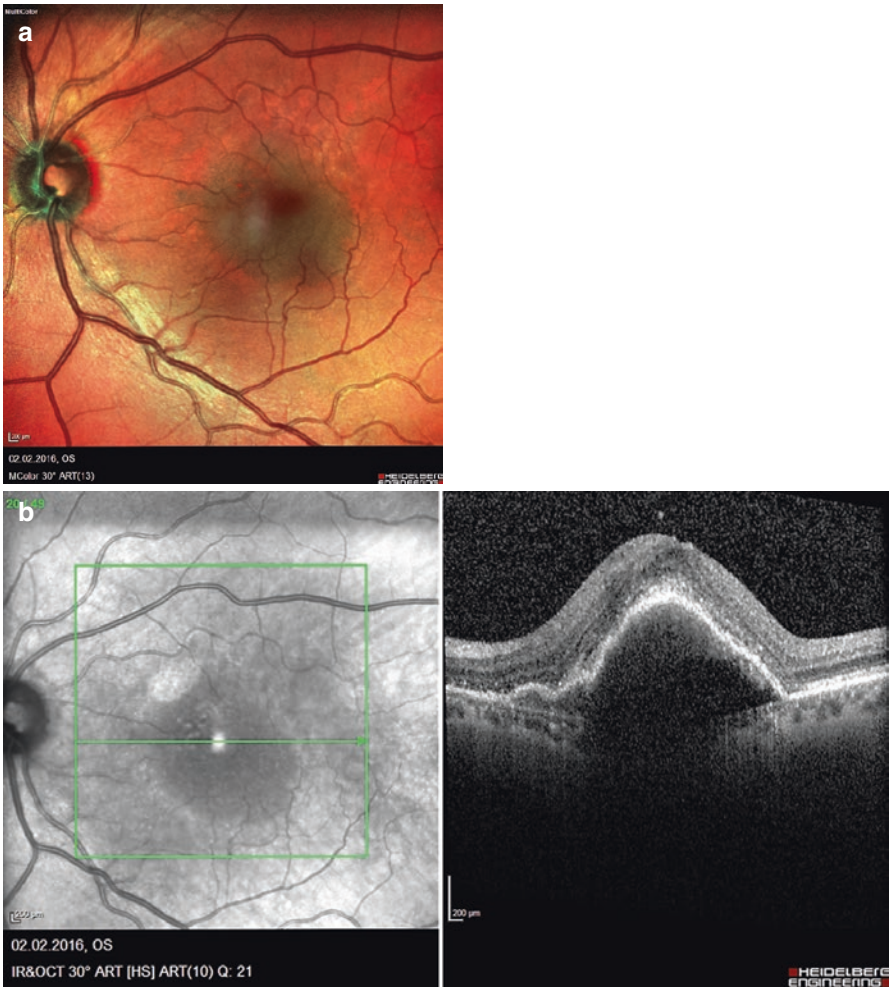

Fig. 3.7 Pigment epithelial detachment associated with age-related macular degeneration in a 74-year-old patient: (**a**) Multicolor image; (**b**) OCT; (**c**) and (**d**) early phase FA and ICGA; (**e**) and (**f**) late phase FA and ICGA; (**g**) Optovue Avanti en face OCTA image using sub-pigment epithelial segmentation shown in B-Scan (**h**); (**i**) Zeiss Angioplex en face OCTA image using sub-pigment epithelial segmentation shown in B-Scan (**j**); (**k**) Optovue Avanti en face OCTA image using choroid capillaris segmentation shown in B-Scan (**l**); (**m**) Zeiss Angioplex en face OCTA image using choroid capillaris segmentation shown in B-Scan (**n**); *Asterisk*: CNV seen in late phase FA and ICGA as well as in en face OCTA

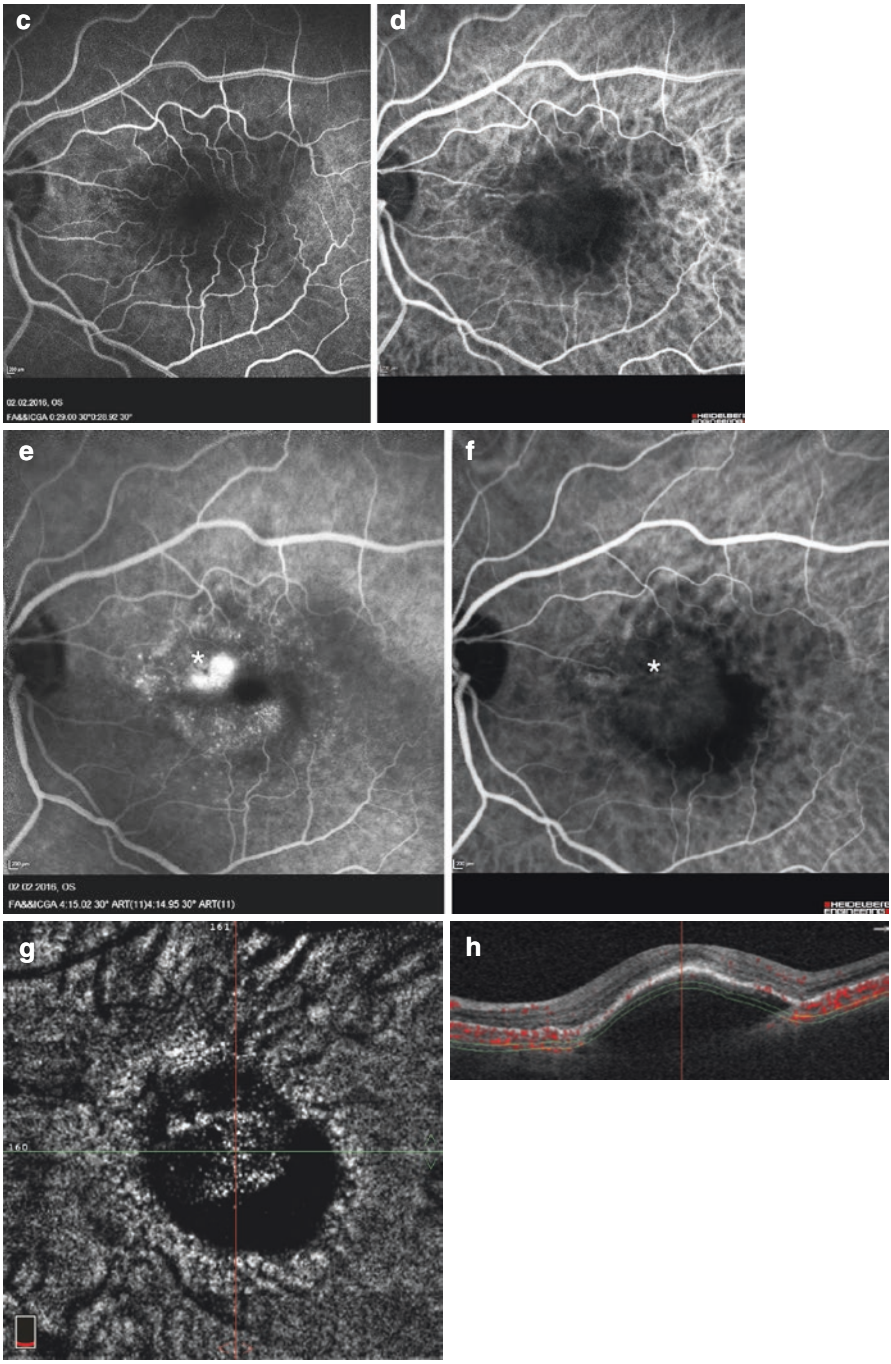

Fig. 3.7 (continued)

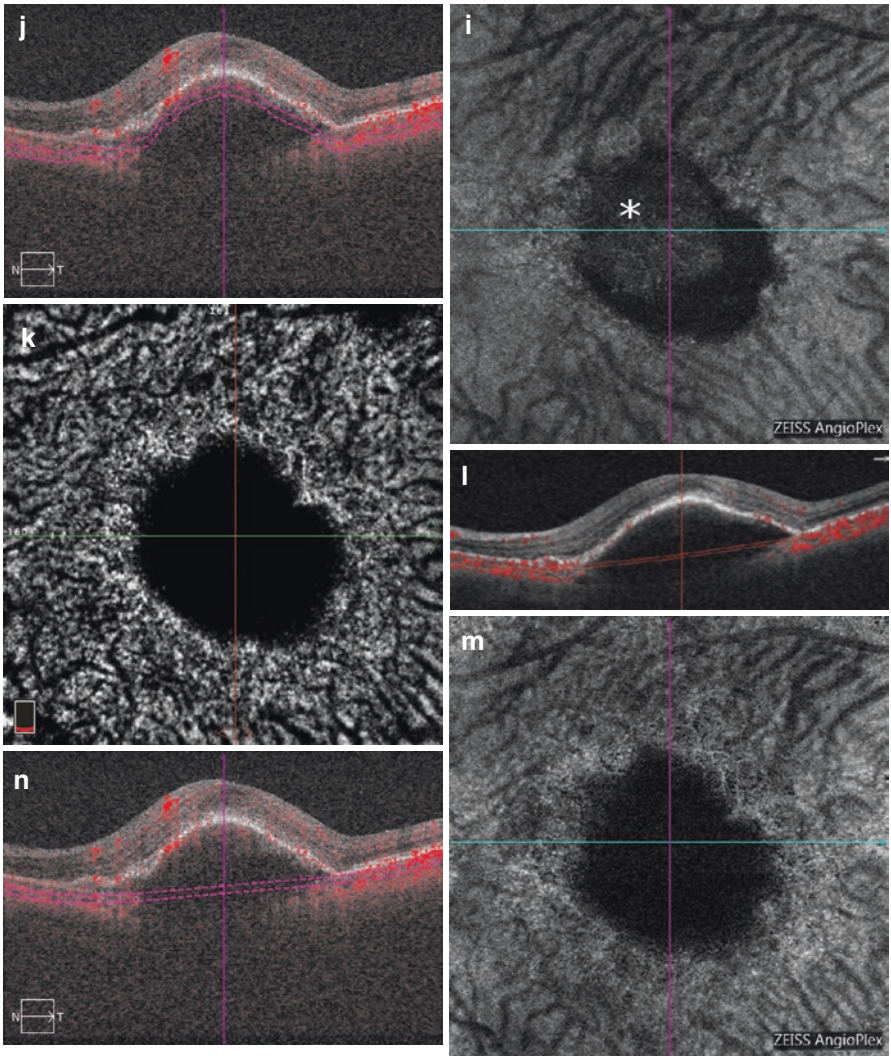

Fig. 3.7 (continued)

3.9 Natural Course

Decline in visual acuity is a common outcome, with or without progression to advanced forms of AMD [36]. In the natural course of the disease, after detachment of RPE, the supply to the photoreceptors deteriorates. This is followed by apoptosis of the sensory and RPE cells with the formation of an atrophic area or a disc-formed scar. The detachment of the pigment epithelium can also lead to a rupture of the pigment epithelium, with an often dramatic and acute deterioration of visual acuity. The risk of an RPE tear in the natural course of the disease is given as 10–12%, depending on publication cited [4, 6], see also chapter 7. An RPE tear with massive subretinal hemorrhage is a feared complication. In a few cases, with spontaneous cicatrization of the causal CNV, the PED may disappear completely and visual acuity may improve at a functional level (Fig. 3.8).

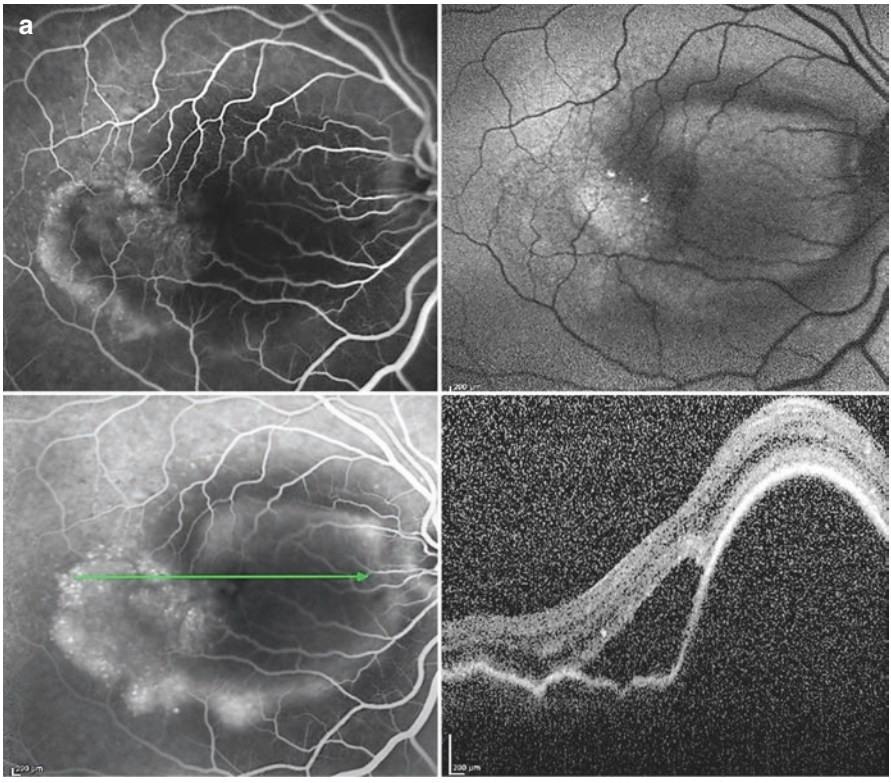

Fig. 3.8 RPE tear. (**a**) Large vascularized PED with subretinal fluid in SD-OCT image and decrease of visual acuity. Therefore, decision for anti-VEGF therapy was made. (**b**) FA and SD-OCT 4 weeks after the third injection show a large RPE tear with a long tear edge of rolled RPE (*arrow*) (**c**) the result has further worsened 3 months later by cicatricial contractions. The RPE-free area still increased (*star*)

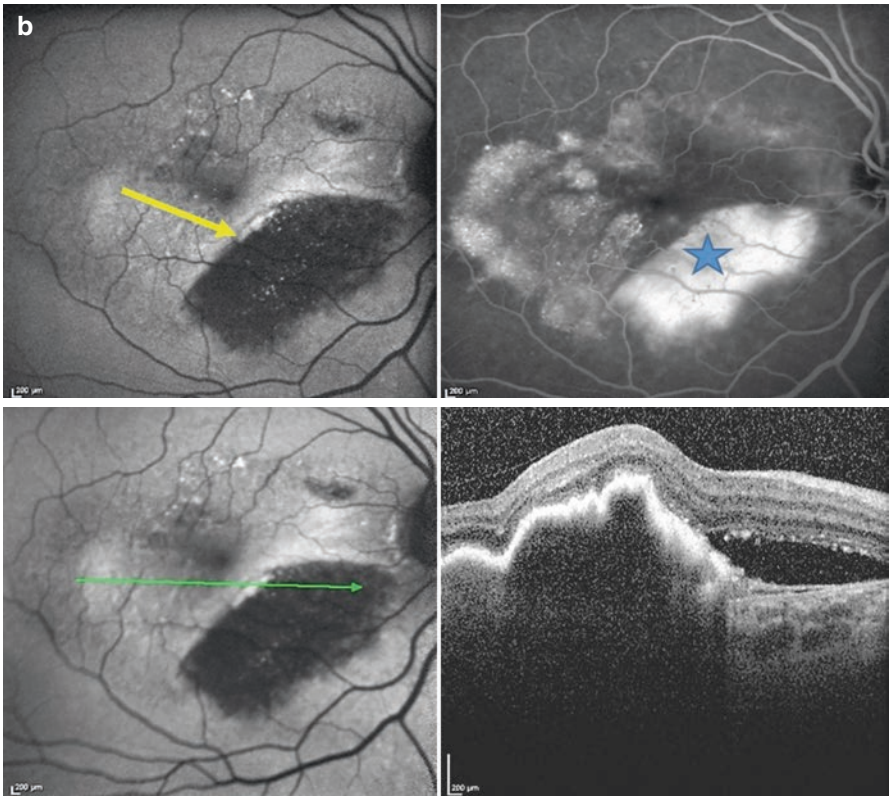

Fig. 3.8 (continued)

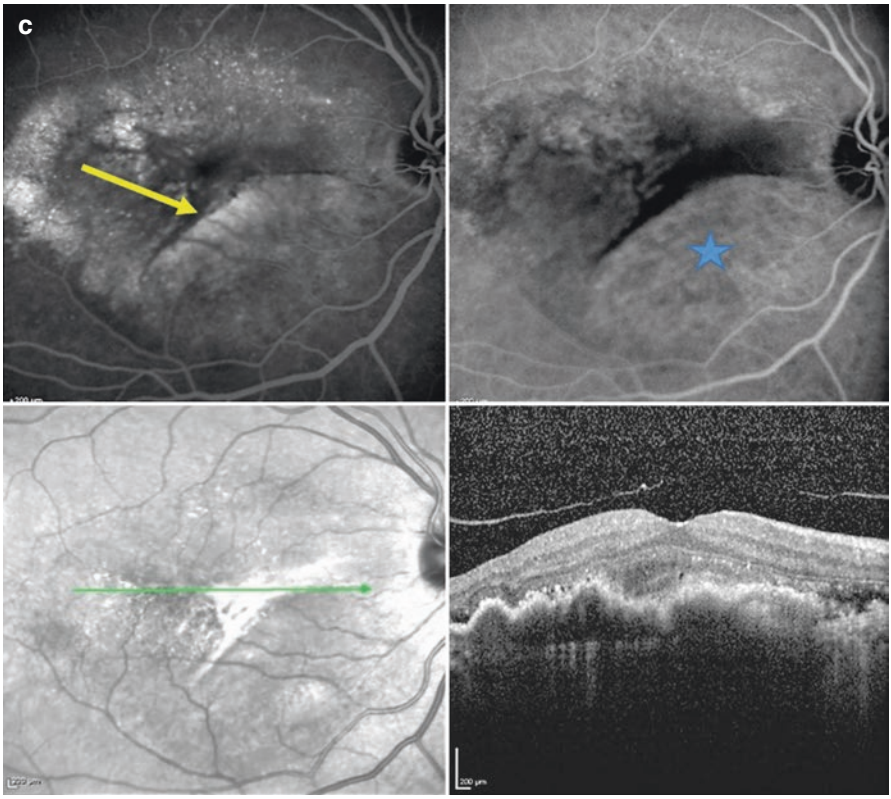

Fig. 3.8 (continued)

3.10 Therapy

The causes of AMD cannot as yet be treated. In early stages of the disease, it was shown by the Age-Related Eye Disease Study (AREDS) that daily oral administration of antioxidative vitamins and zinc reduces progression to a late stage of AMD [37]. Moreover, observations suggest that omega-3 fatty acids and carotenoids such as lutein and zeaxanthin may also play a role in the prevention of AMD. This assumption was not confirmed in the AREDS 2 Study.

Standard treatment for exudative AMD is currently intravitreal administration of anti-vascular endothelial growth factor (VEGF) drugs. The approved drugs are aflibercept (Eylea) and ranibizumab (Lucentis). Bevacizumab (Avastin) is an off-label drug with comparable efficacy and safety.

Patients with vascularized or fibrovascular PED in connection with AMD are treated in the same way. Nevertheless, regular check-up examinations must be carried out on an ongoing basis. In view of the risk of a RPE tear during treatment (Fig. 3.8), not every PED should be regarded as a sign of activity. Without intraretinal or

subretinal fluid, a PED—especially the purely serous subtype—can initially merely be monitored [38, 39]. Small subretinal accumulations of fluid at the edge of the PED may remain stable for years, and central visual acuity may not necessarily deteriorate.

In contrast, central intraretinal cystoid spaces should always be regarded as an indication for treatment. Due to these particular features, a repeat treatment protocol based on PRN criteria is certainly superior to the "treat and extend" protocol.

The choice of treatment is more complex after an RPE tear. There are indications in the literature that continued treatment after an RPE tear, even one including the fovea, shows better results over the long term than a discontinuation of treatment. Studies using fundus autofluorescence (FAF) have shown that an RPE-free area with lost FAF recovered FAF years later with continued treatment and the microperimetric responses may also recover. This suggests a possible form of regeneration of the RPE [40] (see also chapter 7).

In patients with extensive subretinal or sub-pigment epithelial hemorrhage with or without RPE tear, anti-VEGF therapy is not successful. In these patients, a short-term surgical intervention is the only treatment option. The choice of surgical procedure depends on the extent of hemorrhage, the visual acuity in the patient's second eye, and the general condition of the patient. In patients with extensive subretinal hemorrhages within the major vascular arcades, vitrectomy in combination with subretinal application of recombinant tissue plasminogen activator (rtPA) with or without bevacizumab administration combined with a gas tamponade has proved to be successful [41].

In treatment-resistant patients with a PED, ICGA should be carried out to rule out PCV. In patients with PCV and PED, a combination of anti-VEGF therapy and photodynamic treatment with verteporfin has proved to be more effective than monotherapy with anti-VEGF inhibitors. In addition, thermal laser ± anti-VEGF might be an option in extrafoveal located polyps (see chapter 6).

3.11 Differential Diagnosis

PEDs may occur in connection with a variety of ocular—and less frequently in primarily non-ocular—diseases. PED most commonly occurs in connection with AMD. Knowledge of possible differential diagnoses is important for the prognosis and helps in choosing the form of treatment and the individual counseling and care for the patient.

The main differential diagnosis is central serous chorioretinopathy (CSCR). Much more often than clinically visible, an associated PED is observed on the SD-OCT image, which may be very small beneath the typical neurosensory detachment. This PED, which varies considerably in size, is the "leaking point" often visible on FA. In terms of differential diagnosis, a classic CSCR with PED lacks the drusen that are typical for AMD. However, especially in older patients, some SD-OCT findings may not allow clear differentiation. The main differential diagnoses of PED are summarized in Table 3.1.

Table 3.1 Main differential diagnoses of PED

Differential diagnosis
Central serous chorioretinopathy (CSCR)
Choroidal hemangioma
Sub-pigment epithelial hemorrhage
Choroidal osteoma
Choroidal melanoma
Choroidal nevus
Inflammatory diseases
Metastases

3.12 Summary

AMD is the most common cause of PED in the elderly. Apart from drusenoid PED, there are three main exudative PED forms that can be differentiated: serous, vascularized and fibrovascular PED. Overlapping features and other causes of PED (RAP, PCV, chronic CSCR) may complicate the difinite diagnosis. However, a clear differentiation between the PED forms can help in counseling of the patient and in choice of therapy.

References

1. Bressler NM, Bressler SB. Preventative ophthalmology. Age-related macular degeneration. Ophthalmology. 1995;102:1206–11.
2. Bird AC, Bressler NM, Bressler SB, et al. An international classification and grading system for age-related maculopathy and age-related macular degeneration. The International ARM Epidemiological Study Group. Surv Ophthalmol. 1995;39:367–74.
3. Green WR, Enger C. Age-related macular degeneration histopathologic studies. The 1992 Lorenz E. Zimmerman Lecture. Ophthalmology. 1993;100:1519–35.
4. Pauleikhoff D, Loffert D, Spital G, et al. Pigment epithelial detachment in the elderly. Clinical differentiation, natural course and pathogenetic implications. Graefes Arch Clin Exp Ophthalmol. 2002;240:533–8.
5. Bird AC, Marshall J. Retinal pigment epithelial detachments in the elderly. Trans Ophthalmol Soc U K. 1986;105(Pt 6):674–82.
6. Casswell AG, Kohen D, Bird AC. Retinal pigment epithelial detachments in the elderly: classification and outcome. Br J Ophthalmol. 1985;69:397–403.
7. Ambati J, Ambati BK, Yoo SH, Ianchulev S, Adamis AP. Age-related macular degeneration: etiology, pathogenesis, and therapeutic strategies. Surv Ophthalmol. 2003;48:257–93.
8. Schrader WF. [Age-related macular degeneration: a socioeconomic time bomb in our aging society]. Ophthalmologe. 2006;103:742–8.
9. Pauleikhoff D, Scheider A, Wiedmann P, et al. Neovascular age-related macular degeneration in Germany. Encroachment on the quality of life and the financial implications. Ophthalmologe. 2009;106(3):242–51. doi:10.1007/s00347-008-1797-9.
10. Wong TY, Chakravarthy U, Klein R, et al. The natural history and prognosis of neovascular age-related macular degeneration: a systematic review of the literature and meta-analysis. Ophthalmology. 2008;115:116–26.
11. Arroyo JG, Yang L, Bula D, Chen DF. Photoreceptor apoptosis in human retinal detachment. Am J Ophthalmol. 2005;139:605–10.

12. Chang CJ, Lai WW, Edward DP, Tso MO. Apoptotic photoreceptor cell death after traumatic retinal detachment in humans. Arch Ophthalmol. 1995;113:880–6.
13. Green WR, Key III. SN. Senile macular degeneration: a histopathologic study. Trans Am Ophthalmol Soc. 1977;75:180–254.
14. Okubo A, Rosa Jr RH, Bunce CV, et al. The relationships of age changes in retinal pigment epithelium and Bruch's membrane. Invest Ophthalmol Vis Sci. 1999;40:443–9.
15. Bairati Jr A, Orzalesi N. The ultrastructure of the pigment epithelium and of the photoreceptor-pigment epithelium junction in the human retina. J Ultrastruct Res. 1963;41:484–96.
16. Nakaizumi Y, Hogan MJ, Feeney L. The ultrastructure of Bruch's membrane. 3. The macular area of the human eye. Arch Ophthalmol. 1964;72:395–400.
17. Lommatzsch A, Hermans P, Muller KD, et al. Are low inflammatory reactions involved in exudative age-related macular degeneration? Morphological and immunhistochemical analysis of AMD associated with basal deposits. Graefes Arch Clin Exp Ophthalmol. 2008;246:803–10.
18. Davis WL, Jones RG, Hagler HK. An electron microscopic histochemical and analytical X-ray microprobe study of calcification in Bruch's membrane from human eyes. J Histochem Cytochem. 1981;29:601–8.
19. Guymer R, Luthert P, Bird A. Changes in Bruch's membrane and related structures with age. Prog Retin Eye Res. 1999;18:59–90.
20. Kunze A, Abari E, Semkova I, Paulsson M, Hartmann U. Deposition of nidogens and other basement membrane proteins in the young and aging mouse retina. Ophthalmic Res. 2010;43:108–12.
21. Gass JD. Pathogenesis of tears of the retinal pigment epithelium. Br J Ophthalmol. 1984;68:513–9.
22. Barondes MJ, Pagliarini S, Chisholm IH, Hamilton AM, Bird AC. Controlled trial of laser photocoagulation of pigment epithelial detachments in the elderly: 4 year review. Br J Ophthalmol. 1992;76:5–7.
23. Strauss O. The retinal pigment epithelium in visual function. Physiol Rev. 2005;85:845–81.
24. Bird AC. Doyne Lecture. Pathogenesis of retinal pigment epithelial detachment in the elderly; the relevance of Bruch's membrane change. Eye (Lond). 1991;5(Pt 1):1–12.
25. Mouallem A, Sarraf D, Chen X, et al. Double retinal pigment epithelium tears in neovascular age-related macular degeneration. Retina. 2016;36:2197–204.
26. Yannuzzi LA, Negrao S, Iida T, et al. Retinal angiomatous proliferation in age-related macular degeneration. Retina. 2001;21:416–34.
27. Yannuzzi LA, Sorenson J, Spaide RF, Lipson B. Idiopathic polypoidal choroidal vasculopathy (IPCV). Retina. 1990;10:1–8.
28. Gamulescu MA, Helbig H, Wachtlin J. [Differential diagnosis and therapy of pigment epithelial detachment]. Ophthalmologe. 2014;111:79–90; quiz 91–2.
29. Hartnett ME, Weiter JJ, Garsd A, Jalkh AE. Classification of retinal pigment epithelial detachments associated with drusen. Graefes Arch Clin Exp Ophthalmol. 1992;230:11–9.
30. Zayit-Soudry S, Moroz I, Loewenstein A. Retinal pigment epithelial detachment. Surv Ophthalmol. 2007;52:227–43.
31. Pauleikhoff D, Koch JM. Prevalence of age-related macular degeneration. Curr Opin Ophthalmol. 1995;6:51–6.
32. Baumal CR, Reichel E, Duker JS, Wong J, Puliafito CA. Indocyanine green hyperfluorescence associated with serous retinal pigment epithelial detachment in age-related macular degeneration. Ophthalmology. 1997;104:761–9.
33. Yannuzzi LA, Wong DW, Sforzolini BS, et al. Polypoidal choroidal vasculopathy and neovascularized age-related macular degeneration. Arch Ophthalmol. 1999;117:1503–10.
34. Spaide RF. Enhanced depth imaging optical coherence tomography of retinal pigment epithelial detachment in age-related macular degeneration. Am J Ophthalmol. 2009;147:644–52.
35. Lehmann B, Heimes B, Gutfleisch M, et al. [Serous vascularized pigment epithelial detachment in exudative AMD. Morphological typing and risk of tears in the RPE]. Ophthalmologe. 2015;112:49–56.

36. Cukras C, Agron E, Klein ML, et al. Natural history of drusenoid pigment epithelial detachment in age-related macular degeneration: age-related eye disease study report no. 28. Ophthalmology. 2010;117:489–99.
37. Age-Related Eye Disease Study Research Group. A randomized, placebo-controlled, clinical trial of high-dose supplementation with vitamins C and E and beta carotene for age-related cataract and vision loss: AREDS report no. 9. Arch Ophthalmol. 2001;119:1439–52.
38. Chan CK, Lin SG. Retinal pigment epithelial tear after ranibizumab therapy for subfoveal fibrovascular pigment epithelial detachment. Eur J Ophthalmol. 2007;17:674–6.
39. Chan CK, Meyer CH, Gross JG, et al. Retinal pigment epithelial tears after intravitreal bevacizumab injection for neovascular age-related macular degeneration. Retina. 2007;27:541–51.
40. Bartels S, Barrelmann A, Book B, et al. [Tear in retinal pigment epithelium under anti-VEGF therapy for exudative age-related macular degeneration : function recovery under intensive therapy]. Ophthalmologe. 2014;111:460–4.
41. Hillenkamp J, Surguch V, Framme C, Gabel VP, Sachs HG. Management of submacular hemorrhage with intravitreal versus subretinal injection of recombinant tissue plasminogen activator. Graefes Arch Clin Exp Ophthalmol. 2010;248:5–11.

Chapter 4
Drusenoid Retinal Pigment Epithelial Detachment

Monika Fleckenstein, Arno Philipp Göbel, Steffen Schmitz-Valckenberg, and Frank Gerhard Holz

4.1 Introduction

Drusenoid pigment epithelial detachments (PED) are most commonly associated with age-related macular degeneration (AMD) and primarily represent a feature of the non-neovascular stage. However, discrimination between drusenoid, serous, or vascularized PED is challenging albeit of high relevance since the clinical management and the course of disease differs.

4.2 Classification and Definition

Drusen are deposits of extracellular debris located between the basal lamina of the retinal pigment epithelium and the inner collagenous layer of Bruch's membrane [1, 2]. They have a complex composition including lipids, carbohydrates, zinc, and a plethora of different proteins, including apolipoproteins [3–9].

Drusen may present as clusters and become confluent over time ("confluent drusen"). Large confluent drusen may form clinically evident "drusenoid PED" without underlying choroidal neovascularization (CNV) [10, 11].

Funduscopically, drusen appear as yellowish nodular lesions located at the posterior pole of the eye. Previous classifications of AMD have included the following qualities of drusen: drusen size (e.g., large vs. small), character (e.g., soft vs. hard), location, number, and area [12–14].

M. Fleckenstein, M.D. (✉) • A.P. Göbel, M.D.
S. Schmitz-Valckenberg, M.D., F.E.B.O. • F.G. Holz, M.D.
Department of Ophthalmology, University of Bonn, Ernst-Abbe-Str. 2, 53127 Bonn, Germany
e-mail: monika.Fleckenstein@ukb.uni-bonn.de; arnog@uni-bonn.de;
steffen.schmitz-valckenberg@ukb.uni-bonn.de; frank.holz@ukb.uni-bonn.de

M.A. Gamulescu et al. (eds.), *Retinal Pigment Epithelial Detachment*,
DOI 10.1007/978-3-319-56133-2_4

A recently published AMD classification by Ferris et al. stresses the relevance of drusen size in the context of AMD, particularly with regard to the prognostic relevance for progression to late-stage disease. Hereby, small drusen (≤63 μm) are considered as normal aging changes and should be differentiated from early AMD [15]. Medium size drusen (>63 and ≤125 μm) without associated pigment abnormalities represent early AMD, while large drusen (>125 μm) and/or any AMD-related pigmentary abnormality (i.e., any definite hyper- or hypopigmentary abnormalities associated with medium or large drusen) represent intermediate AMD [15].

In the Age-Related Eye Disease Study (AREDS), a drusenoid PED was defined as a fairly well-circumscribed, shallow elevation of the retinal pigment epithelium formed by a confluence of soft drusen, often located in the central macula [16]. There is no established size criterion to distinguish large drusen from drusenoid PEDs. However, the AREDS defined a large druse as measuring at least 125 μm and a drusenoid PED as measuring at least 350 μm in the narrowest diameter [16, 17]. Historically, drusenoid PED has been distinguished from other PEDs, such as fibrovascular PEDs and hemorrhagic PEDs, by clinical appearance, fluorescein angiography (FA), histopathology, and a better short-term visual prognosis [16].

Although drusenoid PEDs are most commonly associated with AMD, various other retinal diseases may be associated with drusenoid PEDs, including Malattia Leventinese, cuticular drusen, and maculopathy associated with membranoproliferative glomerulonephritis (MPGN) type II. Also, they can overlay choroidal nevi [17].

4.3 Epidemiology

Not many data exists concerning epidemiology of drusenoid PED. In the AREDS study, of the 4757 participants, 387 had a drusenoid PED in at least one eye at some point in the study with 68 of them having drusenoid PED in both eyes at some point during the study [16].

4.4 Pathogenesis

Enlargement with subsequent confluence of soft drusen may result in drusenoid PED (Fig. 4.1). These soft drusen probably enlarge by the imbibition of fluid and material which the RPE may have been unable to traffic out of the retina if the lipid nature of membranous debris creates a hydrophobic barrier in Bruch's membrane [10, 18].

Sarks and co-workers stated that it may also be possible that fluid enters drusen at an earlier stage because histologically, the shape of the separated globules or fragments inside the drusen often suggests they would "fit together like a puzzle" and because the basement membrane is sometimes found to be folded into the drusen [10]. Furthermore, they found that the larger soft drusen were and the more fluid was present within them, the more rapidly the drusen developed and

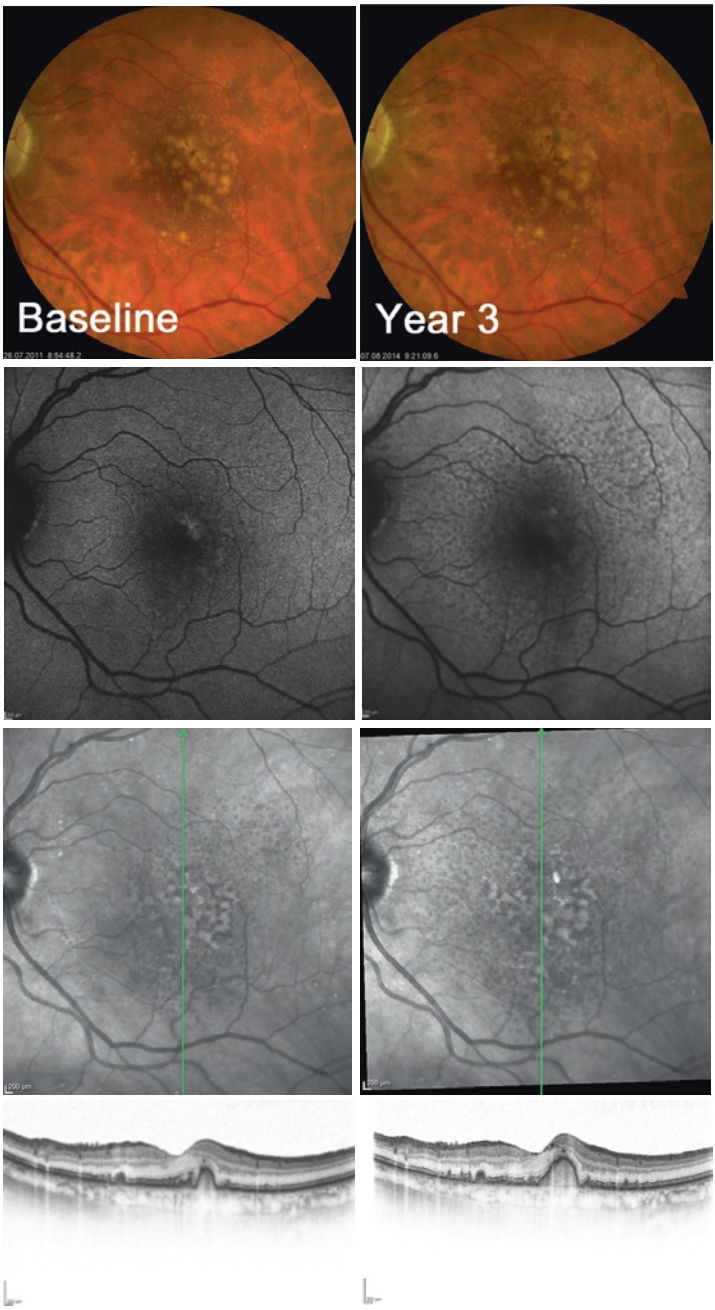

Fig. 4.1 Enlargement of soft drusen over time producing a drusenoid pigment epithelium detachment. Images (from *left* to *right*: color fundus photography, fundus autofluorescence [FAF], infrared reflectance with corresponding spectral domain optical coherence tomography [SD-OCT]) were taken at baseline (*upper row*) and at 3-year follow-up (*lower row*). On color fundus photography, there is an increase in the number and extent of drusen over time. The FAF images show irregular signals (normal, increased, decreased) in the area of drusen. On SD-OCT, the parafoveally located drusen increase in size over time

faded, more often leading to corresponding geographic atrophy than CNV [10]. These clinicopathological observations suggest that larger size and higher fluid content of drusenoid PEDs may both be predictors of their evolution towards RPE atrophy [17].

4.5 Clinical Examination

4.5.1 Stereoscopic Funduscopy

The well-circumscribed yellow or yellow-white elevations of the drusenoid PED typically present with a speckled or stellate pattern of brown or gray pigmentation on their surface (Figs. 4.2, 4.3, and 4.4). This central lesion is frequently surrounded by large soft drusen (Figs. 4.2, 4.3, 4.4, and 4.5).

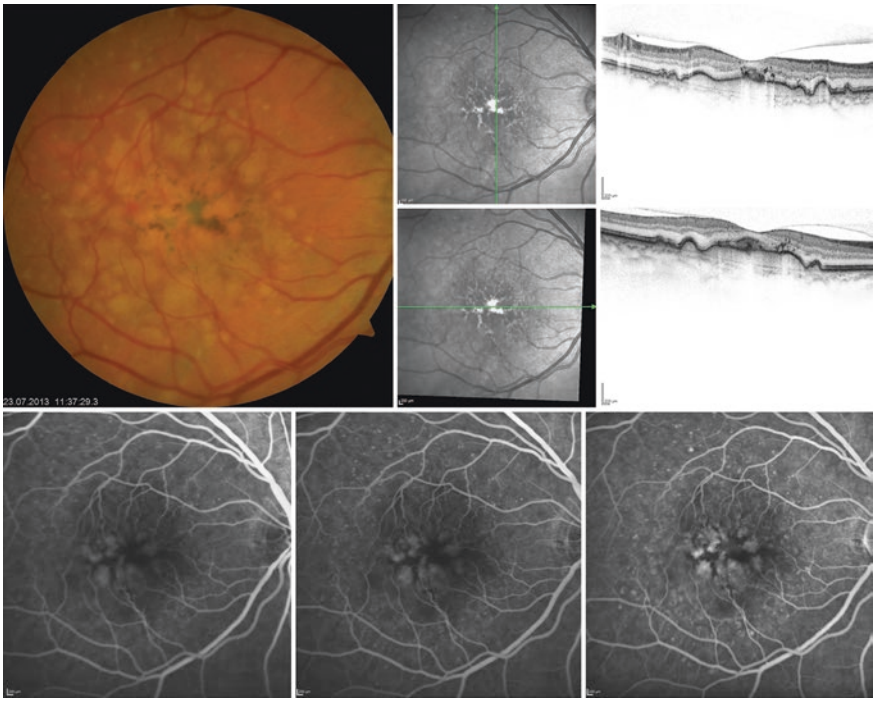

Fig. 4.2 Color fundus photography and spectral-domain imaging show a central drusenoid pigment epithelium detachment surrounded by soft drusen (*upper image panel*) fluorescein angiography in drusenoid pigment epithelium detachment (*lower row* from *left* to *right*: fluorescein angiography 0.39, 2.07, 5.02 min, respectively). The drusen show faint but progredient hyperfluorescence. However, there is no clear leakage. The centrally decreased fluorescence signal is due to blocking effects of overlaying star-shaped pigment alterations (*upper image panel*)

Fig. 4.3 Progression of a drusenoid pigment epithelium detachment to geographic atrophy with disappearance of drusen material. At baseline (*upper row*), there is a large drusenoid pigment epithelium detachment with hyperpigmentary changes on top of the central lesion ("pigment clumping"). FAF imaging shows an irregular signal with areas of increased (corresponding to hyperpigmentary changes) and decreased FAF. On SD-OCT, there is a large elevation of the retinal pigment epithelium band and the retinal layers. After 3 years (*lower row*), an area of atrophy at the former location of the drusenoid pigment epithelium detachment has developed, corresponding to a well-demarcated area of decreased FAF signal. On SD-OCT imaging, drusen material has disappeared and increased reflectance of the choriocapillaris can be seen in this area

Fig. 4.4 Progression of a drusenoid pigment epithelium detachment to geographic atrophy on top of the drusen material. At baseline (*upper row*), there is a large drusenoid pigment epithelium detachment with overlying hyperpigmentation that correlates with increased signals in FAF imaging. On SD-OCT imaging, there are focal spots on top of the drusenoid PED correlating with pigment clumping. After 3 years (*lower row*), a large area of geographic atrophy has developed, corresponding to a well-demarcated decreased FAF signal. On SD-OCT, the drusen material is still present. Loss of outer retinal layers and the sharply demarcated signal enhancement within the drusen indicates that there is RPE atrophy on top of the drusen material

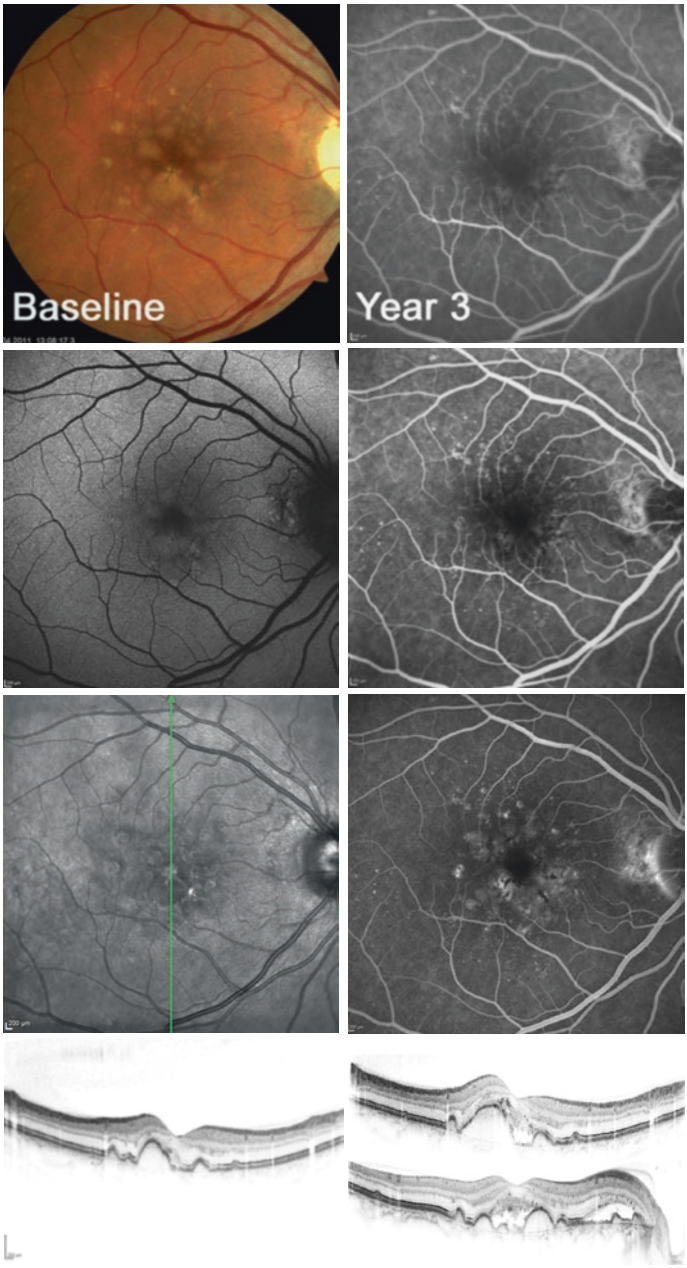

Fig. 4.5 Development of choroidal neovascularization (CNV) in an eye with drusenoid pigment epithelium detachment. At baseline (*left column*), there is a relatively small drusenoid PED. After 3 years (*right column*), fluorescein angiography (from *top* to *bottom*: 0.32, 1.05, and 13.50 min, respectively) reveals a leakage adjacent to the optic disc indicative for peripapillary CNV. On SD-OCT, drusenoid pigment epithelium detachment has increased (*upper image, vertical scan*) and there is subretinal fluid in the center as well as adjacent to the optic disc (*lower image, horizontal scan*) that was both interpreted to be associated with peripapillary CNV. The patient therefore received anti-VEGF treatment

4.6 Imaging

4.6.1 Optical Coherence Tomography

On optical coherence tomography (OCT) imaging, drusenoid PEDs usually show a smooth contour of the detached hyperreflective RPE band (Figs. 4.1, 4.2, 4.3, 4.4, and 4.5) that may have an undulating appearance [17] (Figs. 4.2 and 4.4). Hyperreflective signals atop the drusenoid PED with posterior signal shadowing are frequently found and correspond to pigment clumping (Figs. 4.1, 4.3, and 4.4).

The material beneath the retinal pigment epithelium band typically has a rather homogeneous appearance with increased reflectivity to variable extent. Drusenoid PEDs are not typically associated with overlying subretinal or intraretinal fluid. Roquet and co-workers found that the presence of sub- or intraretinal fluid and the increase in material hyporeflectivity under the retinal pigment epithelium band were associated with CNV [19]. However, the presence of a hyporeflective area between the neurosensory retina and the retinal pigment epithelium band does not necessarily indicate an associated CNV [17]: especially in-between drusenoid PEDs the appearance of subretinal fluid may merely indicate that the cluster of coalescent drusen produces mechanical strain to the outer retinal layers that locally pulls the sensory retina away from its normal position [20].

In recent studies, spectral-domain (SD) OCT imaging has allowed for detection of subtle changes in the area and volume of drusenoid PEDs [21–24]. Quantitative SD-OCT imaging of drusenoid PEDs therefore appears to be useful for identifying the natural history of disease progression and as a clinical tool for monitoring eyes with AMD in clinical trials [21].

4.6.2 Fundus Autofluorescence Imaging

The fundus autofluorescence (FAF) signal in drusenoid PEDs is variable [25]. Drusenoid PEDs frequently exhibit a mild increased FAF signal (Fig. 4.1) with a surrounding halo with decreased FAF. However, the FAF signal associated with the PED lesion may also be normal or decreased [17]. Focal spots with increased FAF appear to correlate with hyperpigmentation (Fig. 4.3), circumscribed areas with a decreased FAF signal usually correspond to RPE atrophy (Fig. 4.4). It has been speculated that different FAF changes may indicate different stages of drusen evolution that may appear similar by clinical examination [26].

4.6.3 Fluorescein Angiography

Interpretation of FA to differentiate drusenoid PED from a vascularized PED or classic CNV may be challenging although the latter exhibit more intense late staining or frank leakage [11, 19]. In drusenoid PED, there is faint but progredient hyperfluorescence in FA. This staining has to be differentiated from leakage from classic CNV that would show a well-demarcated hyperfluorescence in the early phase of FA and leakage in the late phase (Fig. 4.2). The combination of FA with OCT imaging is often helpful for the differential diagnosis, but also to diagnose adjacent or newly formed CNV (Fig. 4.5).

Focal hypo- and hyperfluorescent signals associated with the PED lesion may represent blocking effects of overlying pigment alterations or window defects in areas of RPE atrophy, respectively [17] (Figs. 4.2 and 4.4).

4.6.4 Indocyanine Green Angiography

With indocyanine green angiography (ICGA) using a confocal scanning laser ophthalmoscope system, the content of the drusenoid PED will block the fluorescence emitted from the underlying choroidal vasculature and, therefore, the PED will appear as a homogeneous hypofluorescent lesion during the early phase and remain hypofluorescent throughout the transit [17]. While in vascularized PEDs ICG angiography may demonstrate a hyperfluorescent "hot spot" at the border or within the PED confirming the presence of CNV, in drusenoid PEDs such signals are absent [19].

4.7 Natural History

The natural history of eyes with drusenoid PED is characterized by a high rate of progression to both geographic atrophy (Figs. 4.3 and 4.4) and neovascular AMD (Fig. 4.5) [16, 19].

Roquet and co-workers analyzed 61 eyes of 32 patients with drusenoid PED that were followed for an average of 4.6 years (range 1–17 years) [19]. Three different natural outcomes were identified: persistence of drusenoid PED (38%), development of geographic atrophy (49%), and CNV (13%). Based on Kaplan Meier survival analysis, drusenoid PED had a 50% chance of developing geographic atrophy after 7 years. If the drusenoid PED was greater than two disc diameters or was associated with metamorphopsia at initial presentation, progression to atrophy or ingrowth of CNV occurred after 2 years ($p < 0.01$) [19].

In the context of AREDS, a total of 311 eyes (from 255 participants) with drusenoid PED were followed for a median follow-up time of 8 years subsequent to the initial detection of a drusenoid PED [16]. Of the 282 eyes that did not have advanced AMD at baseline, advanced AMD developed within 5 years in 119 eyes (42% in total, 19% progressing to central geographic atrophy, and 23% progressing to neovascular AMD). In the remaining eyes that did not develop advanced AMD (n = 163), progressive fundus changes, typified by the development of calcified drusen and pigmentary changes, were detected [16]. Visual decline was prominent among study eyes, with approximately 40% of all eyes decreasing in visual acuity by ≥15 letters at 5-year follow-up. Mean visual acuity decreased from 76 letters (approximately 20/30) at baseline to 61 letters (approximately 20/60) at 5 years. Five-year decreases in mean visual acuity averaged 26 letters for eyes progressing to advanced AMD and 8 letters for non-progressing eyes [16]. This study further underlined that a decline of visual acuity is a common outcome in drusenoid PED, with or without progression to advanced forms of AMD [16].

Recently, SD-OCT imaging was used to identify morphologic features of drusenoid PED lesions that correlate to future disease progression [21–24].

Quyang and co-workers reported that the presence of hyperreflective foci overlying the drusen, a heterogeneous internal reflectivity of drusenoid lesions, or choroidal thickness directly below drusenoid lesions less than 135 μm at baseline increased the risk of local atrophy developing over the ensuing months [22]. Furthermore, the migrated hyperreflective foci and the change of internal reflectivity of drusenoid lesions from homogeneous to heterogeneous during the study period were predictive of atrophy development by the last follow-up [22].

Clemens and co-workers have evaluated a morphology score for drusenoid PED regarding predictability of a decline in retinal function beyond best-corrected visual acuity. The drusenoid PED morphology score consisted of five parameters: hyperreflective spots in infrared reflectance imaging, lesion diameter, lesion height, presence of vitelliform-like material in the subretinal space or subretinal fluid, and integrity of the ellipsoid zone in SD-OCT.

4.8 Therapeutic Intervention

There is no proven treatment for drusenoid PEDs. If there is no evidence for an associated CNV, treatment with anti-VEGF is not indicated.

Laser photocoagulation has been shown to induce regression of soft drusen and drusenoid PEDs [27–37]. However, the Choroidal Neovascularization Prevention Trial revealed that in patients with unilateral CNV, laser treatment to the fellow-eyes with large drusen increased the short-term incidence of CNV [34]. In the Complications of Age-Related Macular Degeneration Prevention Trial (CAPT), low-intensity laser treatment did not induce a clinically significant benefit for vision

in eyes of patients with bilateral large drusen [38]. Though, more recently, Guymer and co-workers demonstrated that a single unilateral application of nanosecond laser to the macula produced bilateral improvements in macula appearance *and* function [39]. The same group reported that nanosecond laser resolved drusen independently of retinal damage and improved Bruch membrane structure [40]. However, so far evidence is lacking to demonstrate an effect on progression of AMD.

Since CNV may develop over time, patients with drusenoid PED should be examined regularly [11]. If CNV develops, anti-VEGF therapy is recommended (Fig. 4.5). Patients should be instructed to regularly perform Amsler grid testing and immediately return if metamorphopsia or a change in already existing metamorphopsia is perceived.

4.9 Differential Diagnosis of Drusenoid PED

Vitelliform lesions represent an important differential diagnosis of drusenoid PED (Fig. 4.6). The term "vitelliform" is nonspecific, referring to a round, yellowish lesion that looks like an egg yolk (Fig. 4.7). Vitelliform lesions show intense hyperautofluorescence on FAF (Figs. 4.6 and 4.7) and hypofluorescence in the early phase on FA (Fig. 4.6), corresponding to the hyperreflective vitelliform material between the neurosensory retina and RPE on SD-OCT. Funduscopic differentiation between vitelliform lesions and drusenoid PED might be challenging. However, multimodal imaging allows for differentiation in most cases: On FAF imaging, the vitelliform lesion is sharply demarcated and shows an intense increased signal while in drusenoid PED, the signal is more irregular (Fig. 4.6). Vitelliform lesions and drusen are not located in the same anatomic compartment. SD-OCT imaging in drusenoid PED shows an elevated RPE band at the border of the lesion, while in vitelliform lesions, the RPE band appears to stay at the original level and only the neurosensory retina is elevated (Fig. 4.6).

Vitelliform lesions may be seen in a broad range of macular conditions, such as adult-onset foveomacular vitelliform dystrophy (AFVD), Best vitelliform macular dystrophy, mitochondrial retinal dystrophy associated with the m.3243A>G mutation, vitreofoveal traction, acute vitelliform polymorphous exudative maculopathy, and paraneoplastic vitelliform retinopathy [41]. Within this group of conditions, AFVD represents the most probable differential diagnosis to drusenoid PED. AFVD is characterized by subretinal vitelliform macular lesions and is usually diagnosed after the age of 40. Patients are usually slightly younger than patients presenting with drusenoid PED. Similarly to the course of drusenoid PED, the vitelliform lesions gradually increase and then decrease in size over the years, and may leave an area of atrophic outer retina and retinal pigment epithelium (Fig. 4.7). This process is accompanied by a loss of visual acuity.

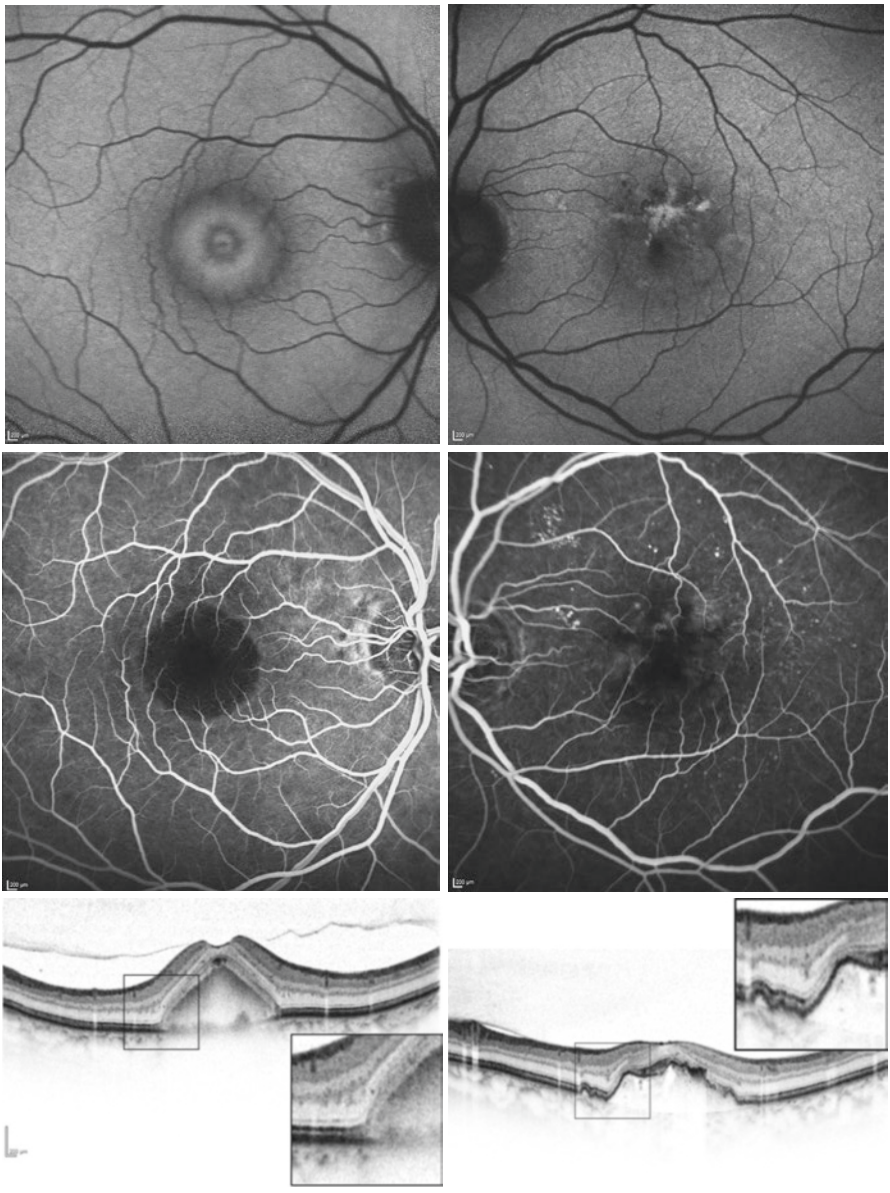

Fig. 4.6 Differentiation between vitelliform lesions and drusenoid pigment epithelium detachment. On FAF imaging, the vitelliform lesion shows an increased signal that is sharply demarcated (*upper left image*). In drusenoid PED, the FAF signal is more irregular (*upper left image*). In the early phase of fluorescein angiography, there is blockage by the vitelliform lesion resulting in a sharply circumscribed hypofluorescent signal (*middle left image*), while the blockage of fluorescence by the drusenoid PED is diffuse (*middle right image*). Vitelliform lesions and drusen are not located in the same anatomic compartment: drusenoid PED elevates the RPE as shown in SD-OCT imaging (*lower right image*), while in vitelliform lesions, the RPE band appears to stay at the former level and only the neurosensory retina is elevated (*lower left image*)

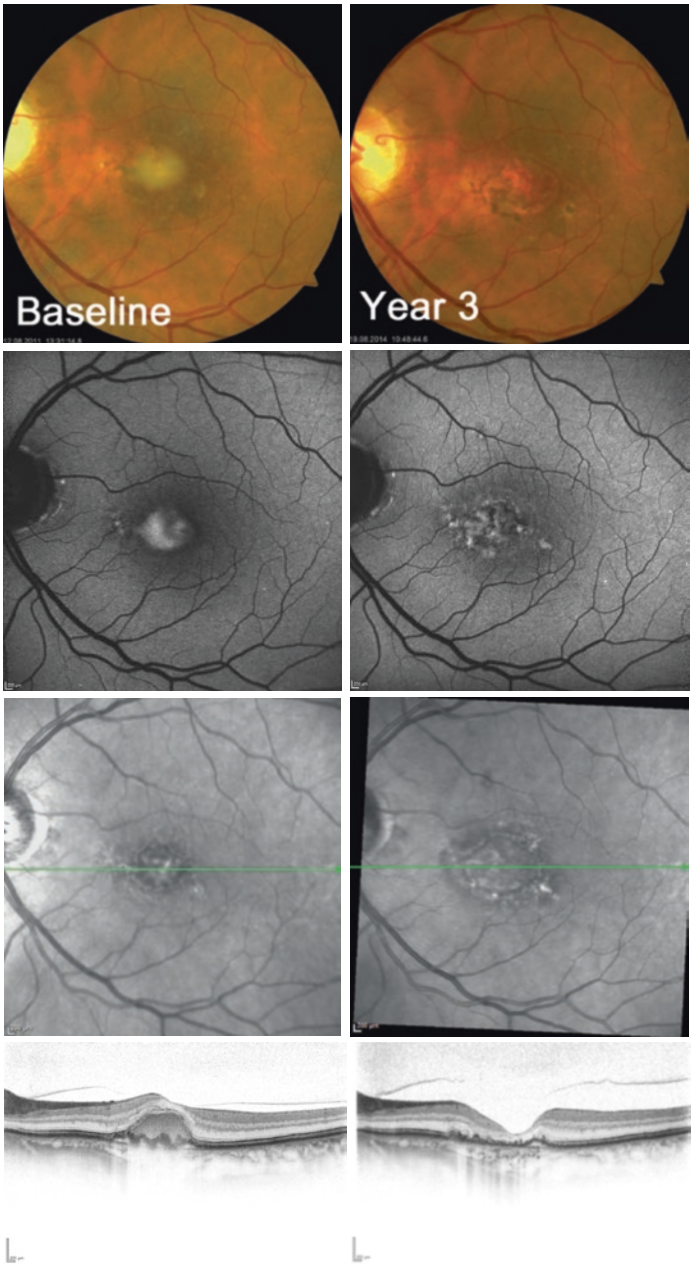

Fig. 4.7 Progression of a vitelliform lesion to atrophy. At baseline (*left column*), there is a round yellowish lesion on funduscopy. The FAF signal is intensely increased in the area of the vitelliform lesion. SD-OCT imaging shows the material that elevates the neurosensory retina and which is located above small dome-shaped lesions that represent soft drusen. After 3 years (*right column*), the vitelliform lesion and the drusen have disappeared. On FAF imaging, there is an irregular signal with increased and decreased FAF indicating progression to atrophy. On SD-OCT imaging, there is loss of the vitelliform material and of the outer retinal layers

4.10 Summary

Drusenoid PED in AMD results from confluence of soft drusen. So far, there is no proven treatment available. Geographic atrophy and CNV may develop in the course of the disease. Therefore, patients should be monitored on a regular basis. Detection/exclusion of CNV may be challenging in dusenoid PED; hence, a multimodal imaging approach is needed. Only if CNV is detected, anti-VEGF therapy is indicated.

References

1. Green WR, Enger C. Age-related macular degeneration histopathologic studies. The 1992 Lorenz E. Zimmerman Lecture. Ophthalmology. 1993;100(10):1519–35.
2. Sarks SH. Council Lecture. Drusen and their relationship to senile macular degeneration. Aust J Ophthalmol. 1980;8(2):117–30.
3. Anderson DH, Ozaki S, Nealon M, et al. Local cellular sources of apolipoprotein E in the human retina and retinal pigmented epithelium: implications for the process of drusen formation. Am J Ophthalmol. 2001;131(6):767–81.
4. Crabb JW, Miyagi M, Gu X, et al. Drusen proteome analysis: an approach to the etiology of age-related macular degeneration. Proc Natl Acad Sci U S A. 2002;99(23):14682–7.
5. Lengyel I, Flinn JM, Peto T, et al. High concentration of zinc in sub-retinal pigment epithelial deposits. Exp Eye Res. 2007;84(4):772–80.
6. Li CM, Chung BH, Presley JB, et al. Lipoprotein-like particles and cholesteryl esters in human Bruch's membrane: initial characterization. Invest Ophthalmol Vis Sci. 2005;46(7):2576–86.
7. Malek G, Li CM, Guidry C, Medeiros NE, Curcio CA. Apolipoprotein B in cholesterol-containing drusen and basal deposits of human eyes with age-related maculopathy. Am J Pathol. 2003;162(2):413–25.
8. Mullins RF, Russell SR, Anderson DH, Hageman GS. Drusen associated with aging and age-related macular degeneration contain proteins common to extracellular deposits associated with atherosclerosis, elastosis, amyloidosis, and dense deposit disease. FASEB J. 2000;14(7):835–46.
9. Mullins RF, Hageman GS. Human ocular drusen possess novel core domains with a distinct carbohydrate composition. J Histochem Cytochem. 1999;47(12):1533–40.
10. Sarks JP, Sarks SH, Killingsworth MC. Evolution of soft drusen in age-related macular degeneration. Eye (Lond). 1994;8(Pt 3):269–83.
11. Gamulescu MA, Helbig H, Wachtlin J. [Differential diagnosis and therapy of pigment epithelial detachment]. Ophthalmologe. 2014;111(1):79–90; quiz 91–2.
12. Bird AC, Bressler NM, Bressler SB, et al. An international classification and grading system for age-related maculopathy and age-related macular degeneration. The International ARM Epidemiological Study Group. Surv Ophthalmol. 1995;39(5):367–74.
13. Ferris FL, Davis MD, Clemons TE, et al. A simplified severity scale for age-related macular degeneration: AREDS Report No. 18. Arch Ophthalmol. 2005;123(11):1570–4.
14. Seddon JM, Sharma S, Adelman RA. Evaluation of the clinical age-related maculopathy staging system. Ophthalmology. 2006;113(2):260–6.
15. Ferris III FL, Wilkinson CP, Bird A, et al. Clinical classification of age-related macular degeneration. Ophthalmology. 2013;120(4):844–51.
16. Cukras C, Agron E, Klein ML, et al. Natural history of drusenoid pigment epithelial detachment in age-related macular degeneration: age-related eye disease study report no. 28. Ophthalmology. 2010;117(3):489–99.

17. Mrejen S, Sarraf D, Mukkamala SK, Freund KB. Multimodal imaging of pigment epithelial detachment: a guide to evaluation. Retina. 2013;33(9):1735–62.
18. Bird A. Pathogenesis of retinal pigment epithelial detachment in the elderly: the relevance of Bruch's membrane change. Eye (Lond). 1991;5(Doyne Lecture):1–12.
19. Roquet W, Roudot-Thoraval F, Coscas G, Soubrane G. Clinical features of drusenoid pigment epithelial detachment in age related macular degeneration. Br J Ophthalmol. 2004;88(5):638–42.
20. Sikorski BL, Bukowska D, Kaluzny JJ, Szkulmowski M, Kowalczyk A, Wojtkowski M. Drusen with accompanying fluid underneath the sensory retina. Ophthalmology. 2011;118(1):82–92. doi: 10.1016/j.ophtha.2010.04.017.
21. Alexandre de Amorim Garcia Filho C, Yehoshua Z, Gregori G, Farah ME, Feuer W, Rosenfeld PJ. Spectral-domain optical coherence tomography imaging of drusenoid pigment epithelial detachments. Retina. 2013;33(8):1558–66.
22. Ouyang Y, Heussen FM, Hariri A, Keane PA, Sadda SR. Optical coherence tomography-based observation of the natural history of drusenoid lesion in eyes with dry age-related macular degeneration. Ophthalmology. 2013;120(12):2656–65.
23. Framme C, Wolf S, Wolf-Schnurrbusch U. Small dense particles in the retina observable by spectral-domain optical coherence tomography in age-related macular degeneration. Invest Ophthalmol Vis Sci. 2010;51(11):5965–9.
24. Clemens CR, Alten F, Heiduschka P, Eter N. Morphology score as a marker of retinal function in drusenoid pigment epithelial detachment. Retina. 2015;35:1351–9.
25. Karadimas P, Bouzas EA. Fundus autofluorescence imaging in serous and drusenoid pigment epithelial detachments associated with age-related macular degeneration. Am J Ophthalmol. 2005;140(6):1163–5.
26. Gobel AP, Fleckenstein M, Heeren TF, Holz FG, Schmitz-Valckenberg S. In-vivo mapping of drusen by fundus autofluorescence and spectral-domain optical coherence tomography imaging. Graefes Arch Clin Exp Ophthalmol. 2016;254:59–67.
27. Cleasby GW, Nakanishi AS, Norris JL. Prophylactic photocoagulation of the fellow eye in exudative senile maculopathy. A preliminary report. Mod Probl Ophthalmol. 1979;20:141–7.
28. Wetzig PC. Treatment of drusen-related aging macular degeneration by photocoagulation. Trans Am Ophthalmol Soc. 1988;86:276–90.
29. Sigelman J. Foveal drusen resorption one year after perifoveal laser photocoagulation. Ophthalmology. 1991;98(9):1379–83.
30. Figueroa MS, Regueras A, Bertrand J. Laser photocoagulation to treat macular soft drusen in age-related macular degeneration. Retina. 1994;14(5):391–6.
31. Frennesson IC, Nilsson SE. Laser photocoagulation of soft drusen in early age-related maculopathy (ARM). The one-year results of a prospective, randomised trial. Eur J Ophthalmol. 1996;6(3):307–14.
32. Sarks SH, Arnold JJ, Sarks JP, Gilles MC, Walter CJ. Prophylactic perifoveal laser treatment of soft drusen. Aust N Z J Ophthalmol. 1996;24(1):15–26.
33. Guymer RH, Gross-Jendroska M, Owens SL, Bird AC, Fitzke FW. Laser treatment in subjects with high-risk clinical features of age-related macular degeneration. Posterior pole appearance and retinal function. Arch Ophthalmol. 1997;115(5):595–603.
34. Laser treatment in eyes with large drusen. Short-term effects seen in a pilot randomized clinical trial. Choroidal Neovascularization Prevention Trial Research Group. Ophthalmology. 1998;105(1):11–23.
35. Olk RJ, Friberg TR, Stickney KL, et al. Therapeutic benefits of infrared (810-nm) diode laser macular grid photocoagulation in prophylactic treatment of nonexudative age-related macular degeneration: two-year results of a randomized pilot study. Ophthalmology. 1999;106(11):2082–90.
36. Rodanant N, Friberg TR, Cheng L, et al. Predictors of drusen reduction after subthreshold infrared (810 nm) diode laser macular grid photocoagulation for nonexudative age-related macular degeneration. Am J Ophthalmol. 2002;134(4):577–85.

37. Little HL, Showman JM, Brown BW. A pilot randomized controlled study on the effect of laser photocoagulation of confluent soft macular drusen. Ophthalmology. 1997;104(4):623–31.
38. Group CoA-RMDPTR. Laser treatment in patients with bilateral large drusen: the complications of age-related macular degeneration prevention trial. Ophthalmology. 2006;113(11):1974–86.
39. Guymer RH, Brassington KH, Dimitrov P, et al. Nanosecond-laser application in intermediate AMD: 12-month results of fundus appearance and macular function. Clin Experiment Ophthalmol. 2014;42(5):466–79.
40. Jobling AI, Guymer RH, Vessey KA, et al. Nanosecond laser therapy reverses pathologic and molecular changes in age-related macular degeneration without retinal damage. FASEB J. 2015;29(2):696–710.
41. Saksens NT, Fleckenstein M, Schmitz-Valckenberg S, et al. Macular dystrophies mimicking age-related macular degeneration. Prog Retin Eye Res. 2014;39:23–57.

Chapter 5
Retinal Pigment Epithelial Detachment in Retinal Angiomatous Proliferation

Maria Andreea Gamulescu

5.1 Introduction

Retinal angiomatous proliferation (RAP) is a distinct subtype of age-related macular degeneration (AMD) with specific features in fundoscopy and imaging. Still, there is controversy about the origin of these lesions, namely, retinal or choroidal vasculature. Pigment epithelial detachment (PED) and retino-choroidal anastomosis can develop over time and are the hallmark of late-stage disease. Although many names have been proposed for this entity, their common feature is the intraretinal vascular proliferation and exudation and therefore, the term "RAP" is widely accepted.

5.2 Epidemiology

RAP lesions are found in 10–29% of all newly diagnosed neovascular AMD cases in Caucasians [1–5], especially in patients diagnosed with occult choroidal neovascularization (CNV) [2, 6]. The percentages increase up to 34% when using videoangiography and the combination of fluorescein and indocyanine green angiography (FA and ICGA) [4, 5]. In South Korean and in Japanese populations, the incidence is lower, 11% and 4.5%, respectively [7, 8]. In African patients, RAP seems to be very rare, and no incidence numbers have been published up to now. This difference between ethnic groups is thought to arise from differences in genetic factors, and in food or in melanin content of the RPE cells, among others. Overall, RAP patients are older (mean 79 years) than the typical patients with exudative AMD (mean 72 years) [9].

M.A. Gamulescu
Department Ophthalmology, University Hospital, Regensburg, Germany
e-mail: gamulescu@eye-regensburg.de

M.A. Gamulescu et al. (eds.), *Retinal Pigment Epithelial Detachment*,
DOI 10.1007/978-3-319-56133-2_5

5.3 Pathogenesis

As mentioned above, pathogenesis of RAP is not yet completely clarified. In 1992, Hartnett et al. first described a "retinal vascular abnormality": a feeding retinal arteriole dipping towards the retinal pigment epithelium (RPE) and forming an angiomatous lesion in the outer retina with sub-RPE-component [9] presuming a retinal origin. Almost 10 years later, in 2001, Yannuzzi et al. [10] presented a possible evolution of the lesion (then termed "retinal angiomatous proliferation," RAP) from an initial intraretinal neovascularization (IRN) with compensatory telangiectatic proliferation of deep retinal capillaries ("stage 1") to a "stage 2" with subretinal neovascularization (SRN) and retinal–retinal anastomosis to a final "stage 3" with PED and sub-RPE-neovascularization (Fig. 5.1, left). Gass et al. on the other hand postulated a five-stage evolution originating from a small sub-RPE neovascularization (stage 1) which extends to the deep retinal capillaries (stage 2), leading to the formation of "piggy-back" subretinal neovascularization on top of a developing PED (stages 3 and 4) and finally to a disciform scar with chorioretinal anastomosis (stage 5) [46] (Fig. 5.1, middle).

Different OCT studies support either the retinal [11] or the choroidal [12] origin of RAP lesions or both [13], while the rare histologic studies on surgically excised RAP lesions rather tend to support the retinal origin [14, 15]. In those studies, only

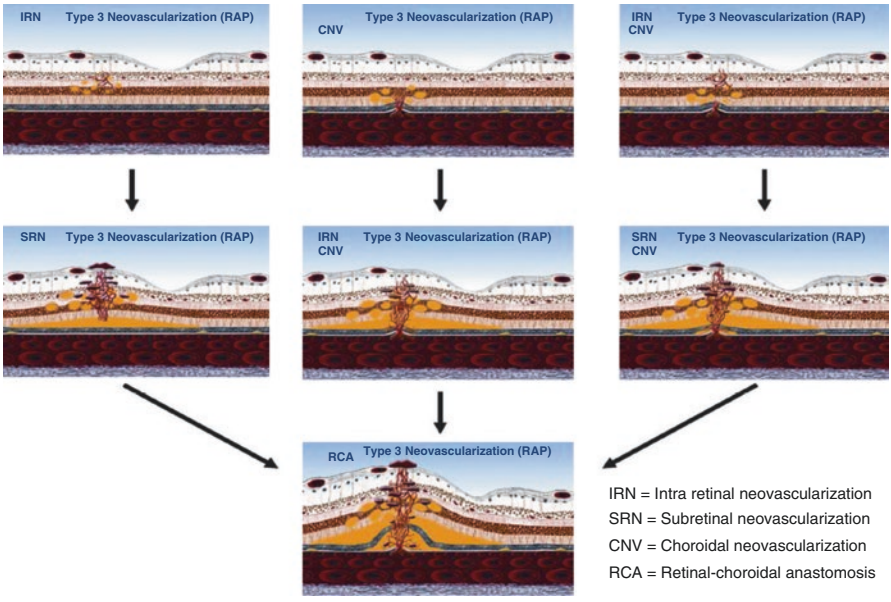

Fig. 5.1 Schematic diagram of three theories for the development of RAP lesions or type 3 neovascularization [20] *Left column*, initial focal retinal proliferation and progression; *center column*, initial focal choroidal proliferation and progression; *right column*, focal retinal proliferation with simultaneous choroidal proliferation

subretinal neovascularization but no "true" CNV (which is at least in part located in the choroid) could be demonstrated. However, existing subretinal or choroidal parts of the lesion may have been ripped off during surgery. There is only one paper correlating fundus and angiography findings 4 months before to histological serial sections of the whole globe in a patient with RAP [16]. Here, neovascular intraretinal angiomatous complex without the presence of subretinal pigment epithelial neovascularization could be demonstrated. Likewise, animal models of transgenic mice with overexpression of VEGF in the retina show development of intra- and subretinal CNV without invasion of blood vessels from the choroid, thereby demonstrating that formation of intraretinal neovascularization with growth towards the subretinal space—as found in RAP lesions—is indeed possible [17, 18].

Irrespective of the origin of the lesion, the common feature of RAP lesions is the leakage during intraretinal proliferation of vessels, leading to accumulation of intraretinal cystoid spaces. Freund et al. therefore proposed a new, more descriptive term of "type 3 neovascularization" for RAP lesions—expanding Gass' classic definition of type 1 (sub-RPE, occult) and type 2 (subretinal, classic) neovascularization—and emphasizing the intraretinal nature of the lesion [19, 20] (Fig. 5.1, right).

Newer publications focus on the comorbidity of RAP lesions and reticular pseudodrusen (RPD): described as a yellowish interlacing network of oval or round lesions of 125–250 μm, seen best on blue-light or red-free fundus photography and infrared images [21, 22] (see Fig. 5.13), RPD are located in the subretinal space and thought to be a distinctive feature of AMD with a high risk (twice the risk as compared to indistinct soft drusen) of progression to late-stage AMD: incidence of geographic atrophy 21% vs. 9% and exudative AMD 20% vs. 10%, respectively [23]. There seems to be a strong association of RPD and RAP lesions as compared to non-RAP exudative AMD: Ueda-Arakawa et al. found RPD in 83% of eyes with RAP in Japanese AMD patients—and only 9% in typical AMD and 2% in PCV [24]. Other publications in Asian and Caucasian patients found percentages of 45–70.3% eyes with RPD in RAP-AMD patients [26–29], at the same time pointing out that RPD are predominantly found in the superior outer macula and therefore might be missed on conventional 20° × 20° central imaging [28]. However, despite the apparently clear association between RPD and RAP, because of their different fundus localizations, the pathogenetic relationship (be it increased intraretinal VEGF-levels because of RPD leading to a thickened Bruch's membrane, or choroidal ischemia leading to deposition of RPD) is not clear yet.

5.4 Clinical Examination

Clinical examination is extremely important and can already hint to the underlying pathology: patients with RAP lesions normally are older than the typical exudative AMD patient [9]. Hallmarks of the disease are small, feather-like intraretinal hemorrhages at the end of a parafoveal capillary. Because of the intraretinal location of

the neovascular complex, RAP lesions exhibit more intraretinal edema (cystoid spaces) and consequently more hard exudates than choroidal neovascularizations (Figs. 5.2, 5.4a, 5.5a, and 5.6a). These features seen on fundoscopy, together with specific OCT findings like serous PED in combination with prominent intraretinal cystoid spaces (Fig. 5.3), should always prompt the examiner to suspect RAP and to initiate further specific imaging ([3]; see Sect 5.5 below).

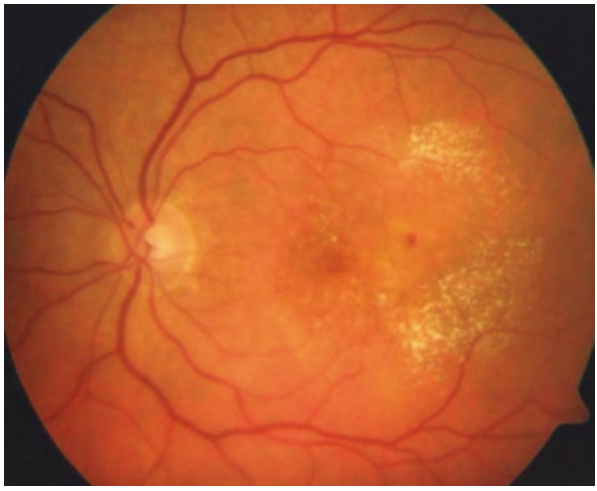

Fig. 5.2 Typical clinical appearance of a RAP lesion: paracentral intraretinal small hemorrhage at the end of a capillary with surrounding ring of hard exudates and accompanying retinal thickening and edema

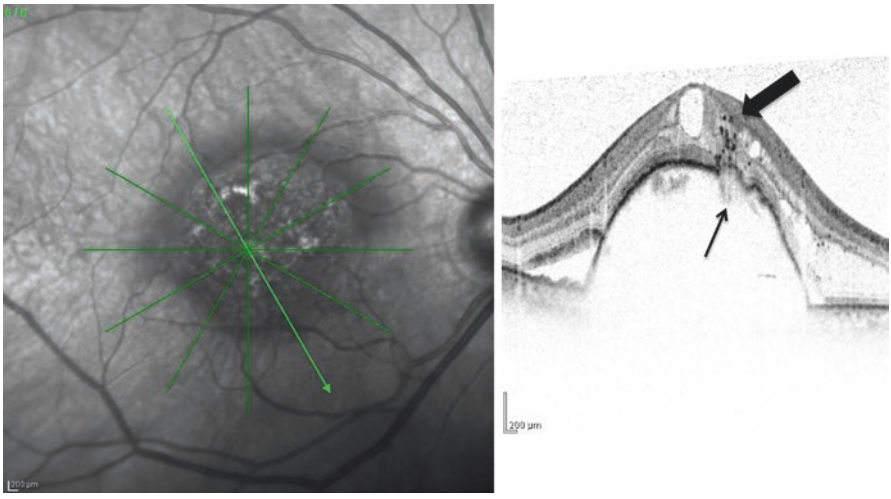

Fig. 5.3 Typical SD-OCT-image of a RAP lesion stage 2: serous PED with accompanying cystoid intraretinal edema. Corresponding to the intraretinal neovascularization, intraretinal hyperreflective spots (*thick arrow*) and interruption of RPE band with medium reflectivity tissue in this gap (*thin arrow*) can be visualized

5.5 Imaging

5.5.1 Fluorescein Angiography

Using FA, RAP lesions can only inconsistently be detected in the very early phases of angiography or in early video sequences [2]. RAP lesions always begin to grow in an extra- or parafoveal location—consistent with their presumed origin from retinal capillaries—and extend towards the foveal center with time [2]. These early signs are rapidly covered by the diffuse leakage from the accompanying cystoid edema or by the pooling of the dye in the serous PED (Figs. 5.4, 5.5, and 5.6). Most RAP lesions are therefore falsely diagnosed as occult or minimal classic CNV, depending on their stage, and coexisting PED is often missed on FA because of the profuse leakage from the extensive cystoid edema [29, 30]. However, indirectly, an early small hyperreflective point at the end of a parafoveal capillary followed by profuse leakage from cystoid edema in late frames in conjunction with the above-mentioned clinical fundoscopic signs, very strongly hints to a possible RAP and should be followed by an ICG-angiography [3].

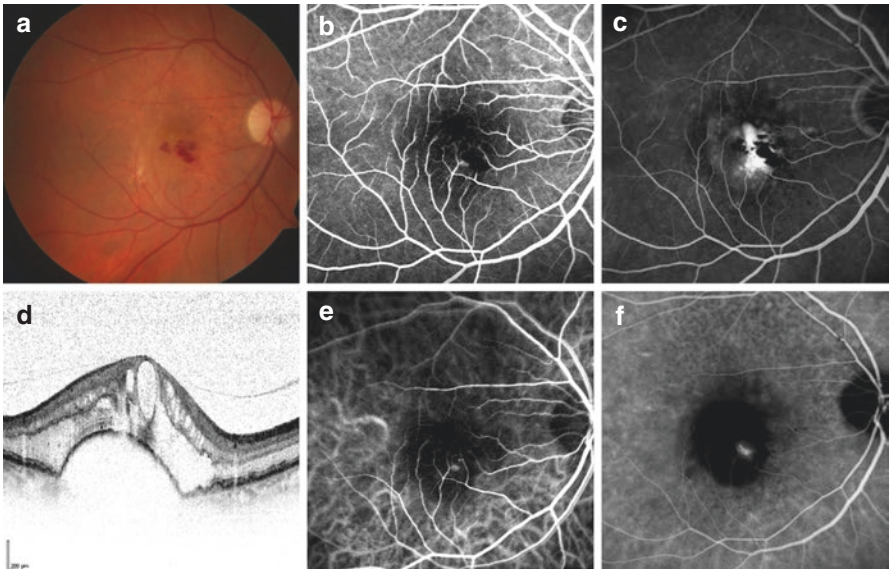

Fig. 5.4 RAP lesion stage 2: (**a**) intra- and subretinal bleeding at the end of a parafoveal capillary, surrounded by retinal thickening. In this case, only drusen but no hard exudates can be seen. (**b**, **c**) Early and late phase FA. Bleeding obscures the intraretinal neovascularization in early phase, while in the late phase profuse leakage from cystoid edema precludes its visualization. (**e**, **f**) In ICGA, spot-like intraretinal neovascularization can be clearly seen in early phase, and it persists as "hot spot" surrounded by the hyporeflective blockage of serous PED in late phase. (**d**) SD-OCT showing serous PED with overlying extensive intraretinal cystoid edema

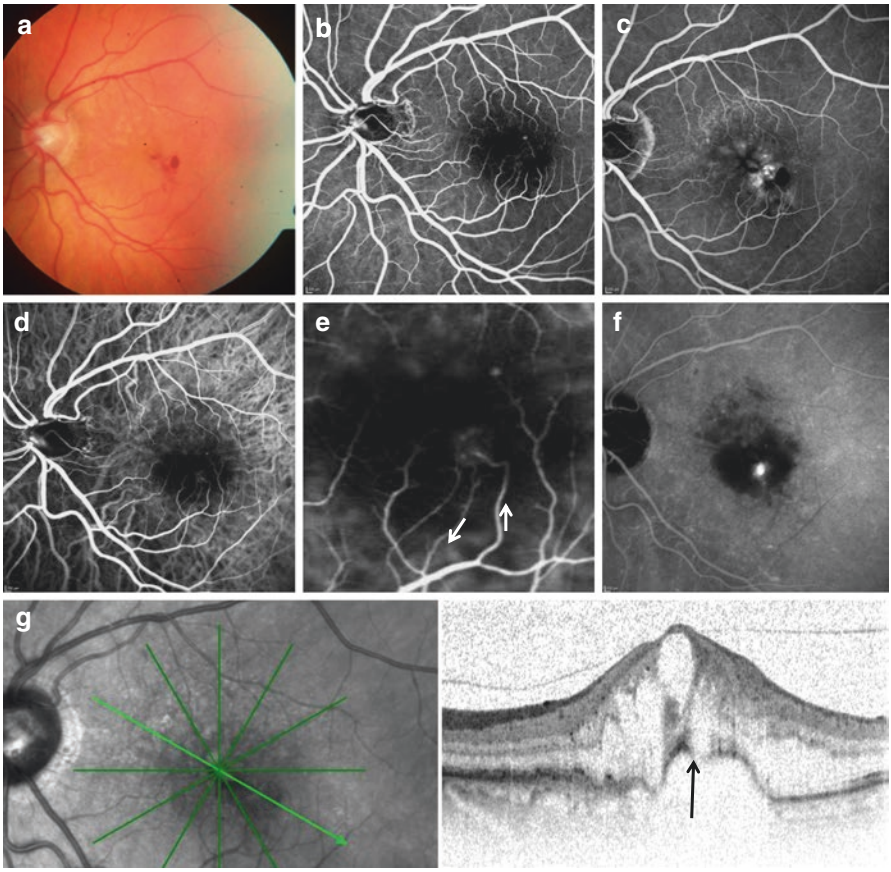

Fig. 5.5 RAP lesion stage 2: (**a**) intraretinal bleeding at the end of a parafoveal capillary, surrounded by retinal thickening. Again, only drusen but no hard exudates can be seen. (**b**, **c**) Early and late phase of FA. Bleeding overlies the intraretinal neovascularization in early phase; a microaneurysm superiorly could be mistaken for the RAP lesion. In late phase, leakage from cystoid edema obscures its visualization. (**d–f**) In ICGA, spot-like intraretinal neovascularization can be clearly seen in early phase with feeding arteriole and draining venule (see magnification in (**e**)), and it persists as "hot spot" surrounded by hyporeflective serous PED in late phase. (**g**) Infrared reflectance and SD-OCT showing serous PED with overlying extensive intraretinal cystoid edema and discontinuity of RPE layer in the region of RAP lesion (*arrow*)

5.5.2 ICGA

Due to its higher molecular weight and its stronger binding to serum proteins (namely, albumin), indocyanine green does not seep into the extravasal space and subsequently cystoid edema and serous PED remain "silent" and hypofluorescent. In this setting, the intraretinal neovascular complex (retinal–retinal anastomosis) and, later, the retino-choroidal anastomosis appears as a small hyperfluorescent "hot

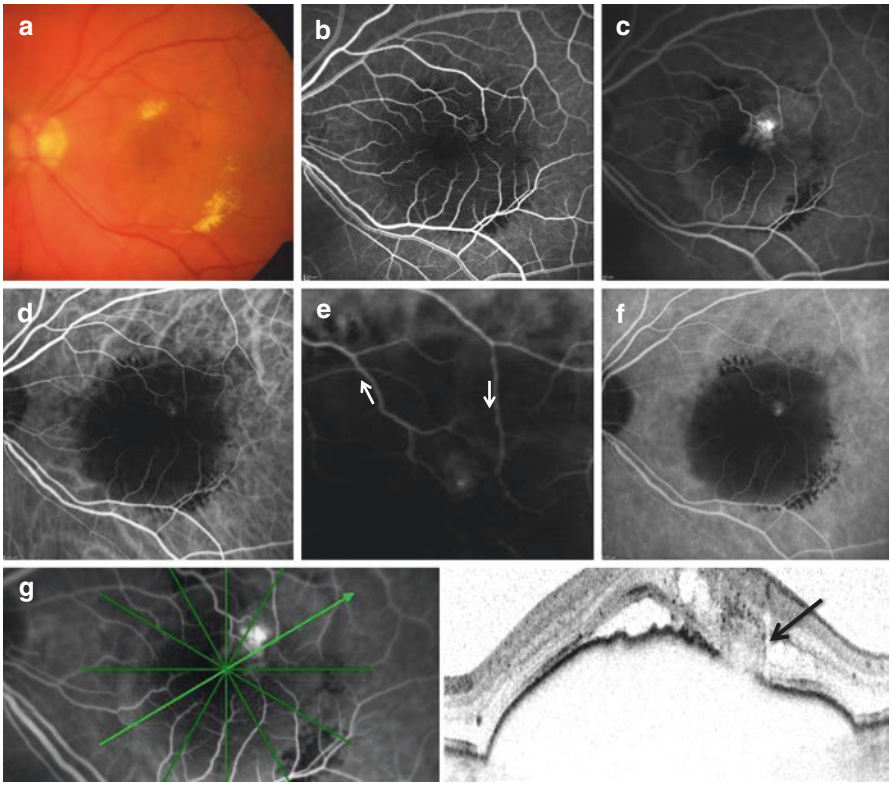

Fig. 5.6 RAP lesion stage 2: (**a**) pinpoint intraretinal bleeding at the end of a parafoveal capillary with surrounding retinal edema and ring-like hard exudates. (**b**, **c**) Early and late phase of FA. Intraretinal neovascularization can be suspected in early phase superior to the fovea, and in the late phase localized hyperfluorescence can be seen in this area, surrounded by a slowly filling and less hyperreflective PED. (**d–f**) ICGA demonstrating clearly better visualization of the spot-like intraretinal neovascularization in early phase, and persisting as "hot spot" surrounded by the dark blockage of the PED in late phase. (**e**) Magnification of (**d**) showing intraretinal neovascularization in ICGA with feeding and draining vessels. (**g**) Infrared reflectance and SD-OCT showing serous PED with overlying intraretinal cystoid edema and subretinal fluid. *Arrow* indicates intraretinal neovascularization in an area of disrupted RPE

spot" in the hypofluorescent surroundings of intraretinal edema or PED (Figs. 5.4, 5.5, 5.6, and 5.7) [2]. Rouvas et al. proposed a classification based on ICGA staining patterns and OCT findings: in their series, ICGA staining patterns were focal (27.2%), irregular (21.8%), circular (21.8%), multifocal (18.2%), and combined (10.9%). The "typical" sign of sudden termination of a retinal vessel and its angulated course dipping down towards the outer retina (Fig. 5.7) was only seen in 25.4% in eyes; all of those eyes had a circular or irregular pattern on ICGA. Eighty-six percent of the eyes had PED that was apparent only in ICGA, not in FA. On OCT, all eyes had intraretinal cystoid spaces [30].

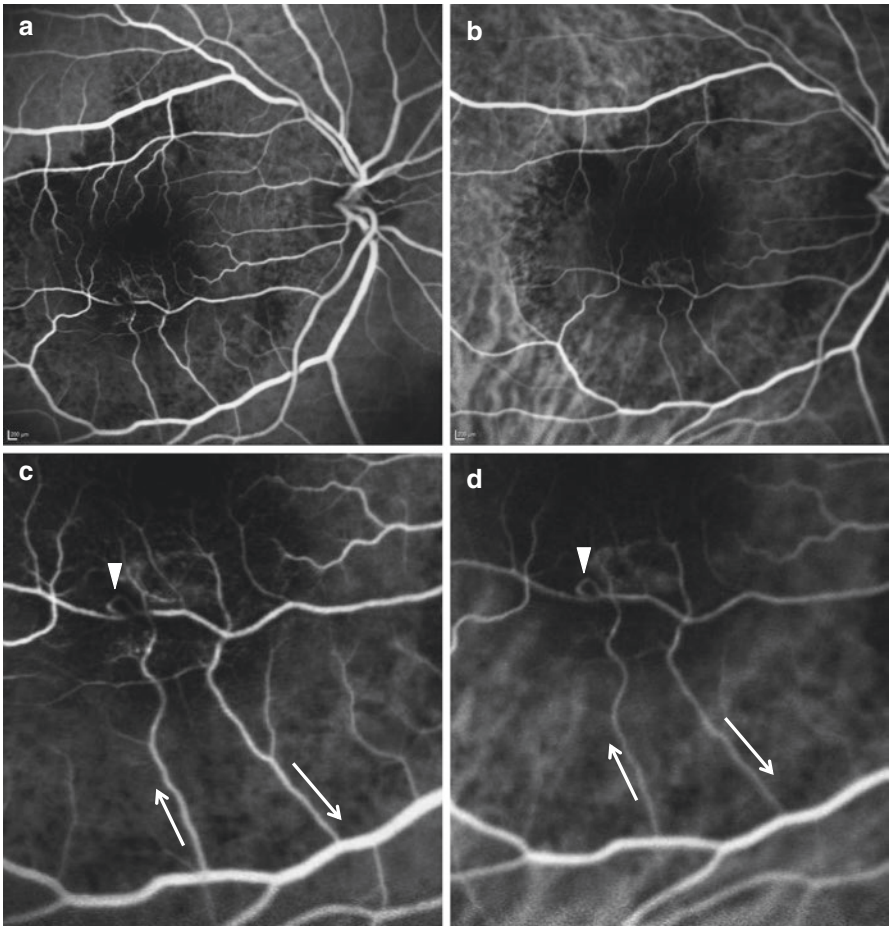

Fig. 5.7 FA (**a**) and ICGA (**b**) of an intraretinal neovascularization with feeding and draining vessels (magnifications (**c**) and (**d**), respectively). *Arrowhead* in (**c**) and (**d**) pointing to the typical angulated vessels dipping down to the choroid

5.5.3 OCT

Nowadays, because of its noninvasive technique, its speed of imaging acquisition and its broad availability, OCT imaging is widely used in macular diagnostics and is often performed even before FA or ICGA.

Stage 1 RAP lesions (intraretinal neovascularization) are often missed but can be visualized as a focal area of higher intraretinal reflectivity, usually situated extrafoveally and not associated with any retinal or RPE-changes or with retinal thickening [29].

With progression to stage 2, the RAP lesions form intraretinal edema and grow towards the subretinal space and the RPE, forming a serous PED. In this stage, specific features are strongly indicative for RAP lesions: the combination of serous PED with pronounced cystoid intraretinal edema (Figs. 5.3, 5.4, 5.5, and 5.6), the

latter of which is not normally found in typical exudative AMD with choroidal neovascularization even if they are associated with RPE detachment. Sometimes, the intraretinal neovascular complex can even be visualized sitting on top of the PED over a discontinuous portion of the RPE line (Figs. 5.3, 5.5, 5.6, and 5.8), sometimes with stratified sub-RPE formations within the PED. This intraretinal neovascular complex co-localizes with the intraretinal feathery bleedings seen on fundoscopy and with the hot spot on ICGA.

However, OCT cannot clearly differentiate the structures below the PED, therefore, further differentiation of the later stages of RAP is difficult in OCT [29].

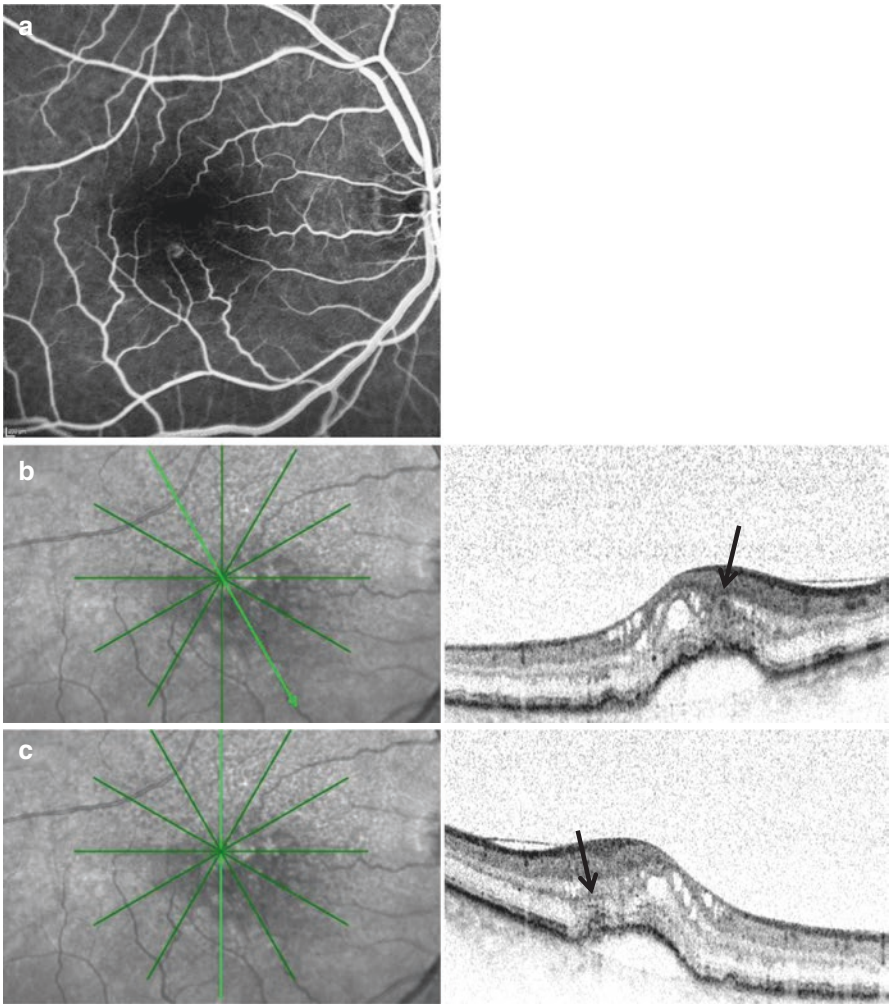

Fig. 5.8 (**a**) FA showing the parafoveal RAP lesion. (**b**, **c**) Corresponding infrared reflectance and SD-OCTs showing intraretinal neovascularization (*arrow*) in an area with cystoid intraretinal edema and accompanying serous PED (**b**) and intraretinal neovascularization attached to the detached RPE (**c**)

5.6 Natural History

The natural course of RAP lesions differs from typical exudative AMD and often shows poor visual outcomes with initial and final visual acuities below 0.1 decimal [9, 31, 32]. RAP lesions are growing fast and aggressive [20, 32] and can lead to extremely large PEDs with risk of RPE-tear and consecutively loss of visual acuity (Figs. 5.9 and 5.10) [33]. Sometimes, serous PEDs become vascularized over time leading to extensive fibrovascular scars [9]. Oftentimes, however, atrophy evolves in the region of former PED, especially in association with RPD and after intravitreal treatment, with incidence rates as high as 50–86% [35–37] (Fig. 5.11).

Monitoring of the second eye is imperative in patients with RAP lesions. Although the rate of 100% bilaterality in 3 years that Gross first published (40% in 1 year, 56% in 2 years, 100% in 3 years) [37] could not be verified in following publications, the incidence of RAP in the second eye of patients with RAP lesions in the first eye seems to be higher than in typical exudative AMD, where 28% of the patients develop exudative AMD lesions in their second eye during a 3-year follow-up. [38]. In patients with RAP lesions in their first eye, incidence rates of 36.4% in

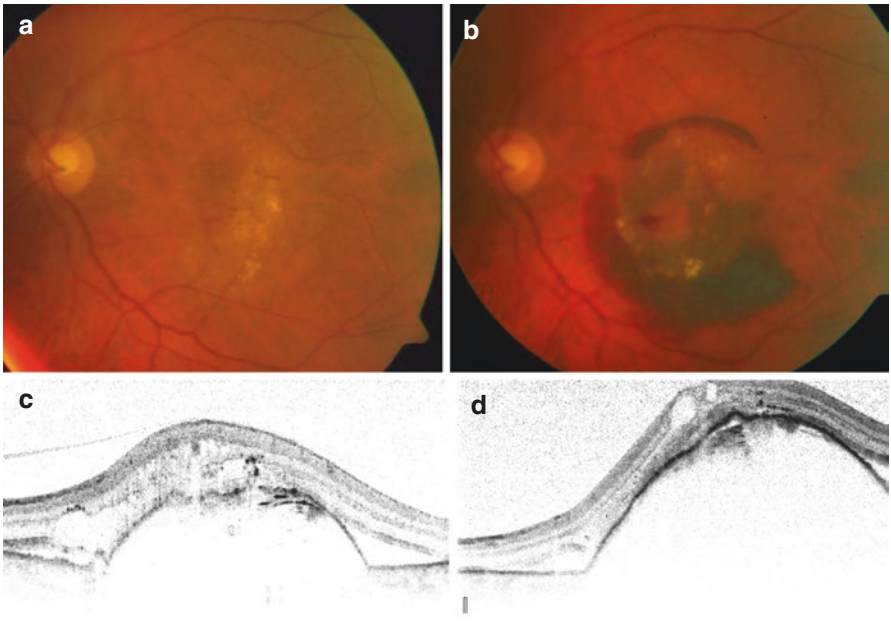

Fig. 5.9 Poor outcome of RAP lesion despite extensive and continuous intravitreal therapy over the course of 8 years: (**a**, **c**) Fundus photo and SD-OCT at initial presentation, (**b**, **d**): after completion of anti-VEGF upload with increased PED and subretinal bleeding, (**e**, **g**) RPE-rip, (**f**, **h**) extensive scarring, still with active parts showing newer subretinal bleeding at the nasal superior border

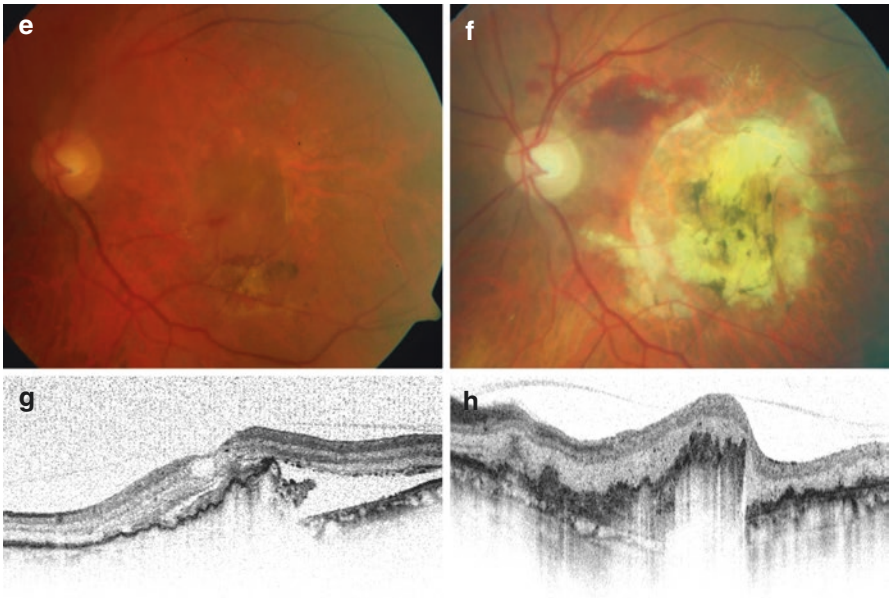

Fig. 5.9 (continued)

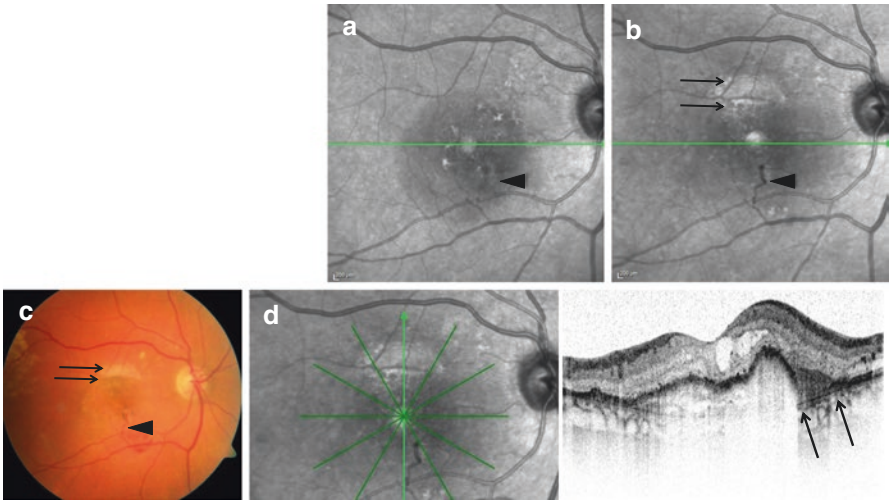

Fig. 5.10 Progression and thickening of the retino-choroidal anastomosis in a RAP lesion over the course of 3 years (**a–c**, *arrowhead*) and the development of a RPE-rip at the superior border of the PED opposite to the RAP lesion itself (**b–d**, *arrows*)

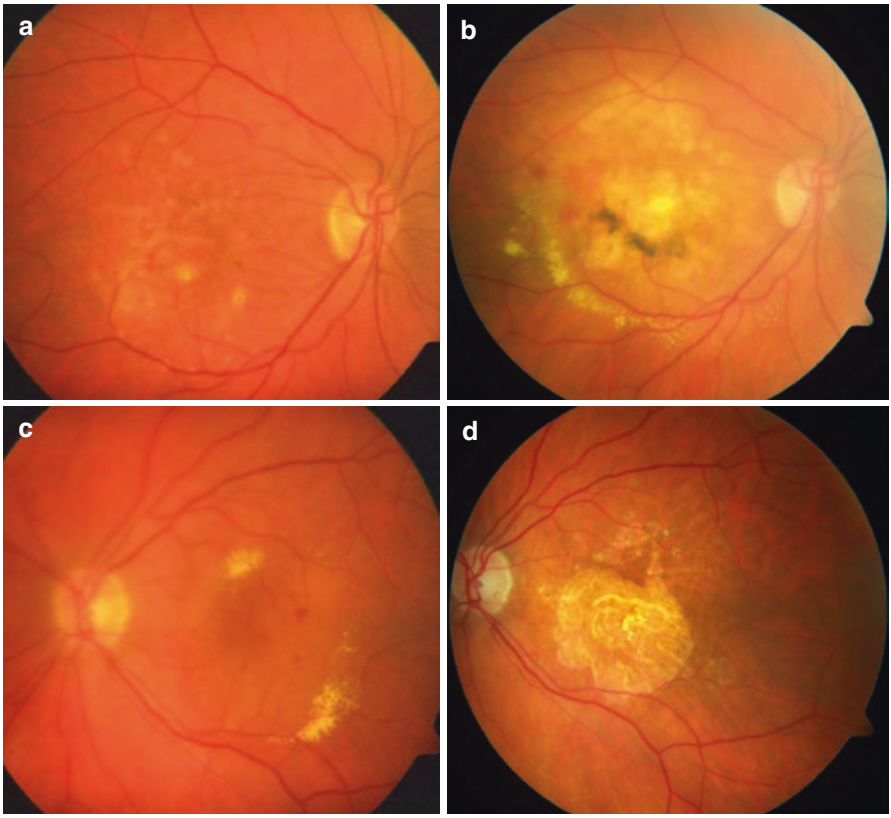

Fig. 5.11 Bilateral RAP lesions in a patient with different course of the disease, 6-year follow-up with multiple intravitreal anti-VEGF treatments: right eye (**a**) progressing to extensive fibrovascular scar (**b**), left eye (**c**) developing subfoveal geographic atrophy (**d**)

3 years [39] and 45% in 4 years have been recently published [25]. The lower incidence in newer publications is discussed to be due to different inclusion criteria (exclusion of patients with scarring in their first eye) or the treatment of the first eye carried out with intravitreal anti-VEGF injections with possible systemic exposure and possible stabilizing effect on the second eye [40].

If the second eye becomes exudative, the lesion in the fellow eye seems to be RAP in almost all cases [37, 39, 41] and 40% seem to be localized in the same area as in the first eye [39]. Risk factors for development of RAP lesions in fellow eyes are focal atrophy and hyperpigmentation [39]. However, only few of those lesions in second eyes have concomitant PED (7%), putatively because of earlier detection [2], making differentiation to occult CNV, especially when performing only FA, more difficult (Fig. 5.12).

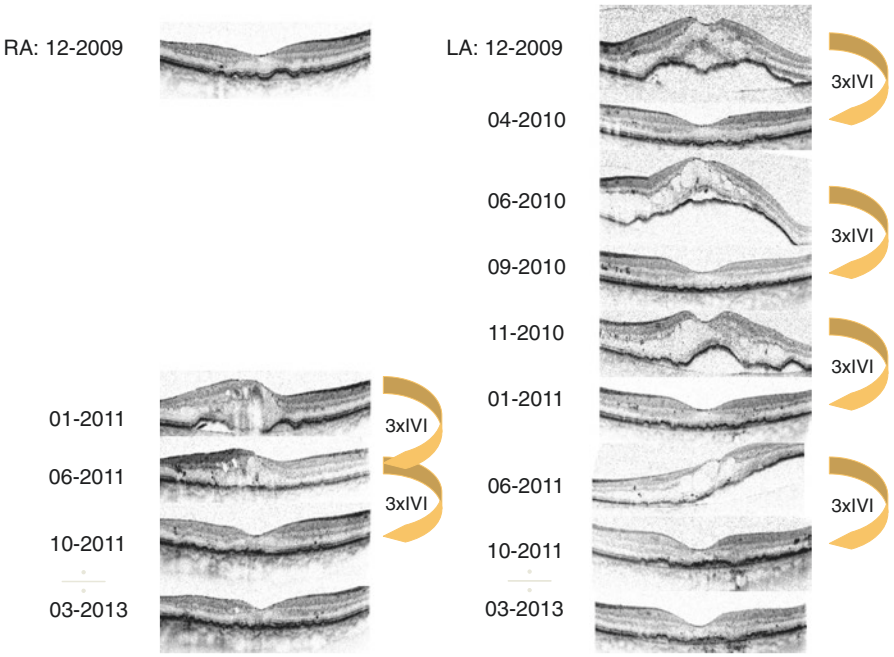

Fig. 5.12 Four-year follow-up of SD-OCT images showing good response to intravitreal anti-VEGF treatment but frequent recurrences of PED and cystoid intraretinal edema (*right side*), as well as the development of RAP lesion in the fellow eye 2 years later (*left side*)

5.7 Therapy

Because of their retinal–retinal or retinal–choroidal anastomosis, RAP lesions show a high blood flow and often have been refractory to many conventional therapies such as conventional laser photocoagulation, monotherapy with verteporfin photodynamic therapy, or even surgical ablation [3, 4, 31]. Recurrent edema, evolving geographic atrophy and associated serous PED with high imminent risk for RPE-tears limited the visual outcome [42]. However, early detection and small lesion size seem to be associated with better outcomes [31, 43].

Nowadays, intravitreal anti-VEGF substances are the gold standard of therapy in exudative age-related macular degeneration, as VEGF-driven edema and exudations respond well to anti-VEGF monotherapy. Under the presumption that RAP lesions are the sequel of increased intraretinal VEGF-levels [17, 18], this type of exudative AMD should also respond well to anti-VEGF (mono)therapy. Indeed, RAP lesions usually show fast and oftentimes complete resolution of intraretinal edema as well as of the accompanying serous PED after treatment with intravitreal anti-VEGF-substances [44]—only rarely seen in typical serous PEDs. However, anti-VEGF

does not seem to occlude the retinal–retinal anastomosis completely, and the remaining flow may cause frequent recurrences (Fig. 5.12). In a paper by Cho et al, anti-VEGF injections showed favorable visual outcome with significant visual improvement during the first year, but this gain could not be maintained after the second year [45]. Therefore, combination treatment of PDT and intravitreal anti-VEGF injections has been proposed. In a paper by Saito et al, combination treatment resulted in a significantly improved visual acuity, significantly decreased central retinal thickness and occlusion of the retinal–retinal anastomosis in 33 of 35 patients with a mean of 2.5 PDT and 5.5 IVT during 24 months [27]. However, subgroup analysis of RAP lesions in the CATT trial with anti-VEGF monotherapy also showed that eyes with RAP were less likely to have fluid on OCT, leakage on FA, and scarring at 1 and 2 years compared to eyes with typical exudative AMD. Visual acuity in RAP eyes had greater improvement from baseline at year 1, but was similar to non-RAP eyes at year 2. Overall, RAP lesions required slightly less intravitreal injections than non-RAP lesion during the 2 years [50]. The same trial, however, showed that RAP eyes were more likely to have geographic atrophy over the follow-up period than non-RAP eyes. The development of geographic atrophy is reported with incidence rates as high as 37–86% [35, 36, 45] especially in eyes with coexistent RPD, here a more cautious anti-VEGF therapy was discussed [33, 34] (Fig. 5.13).

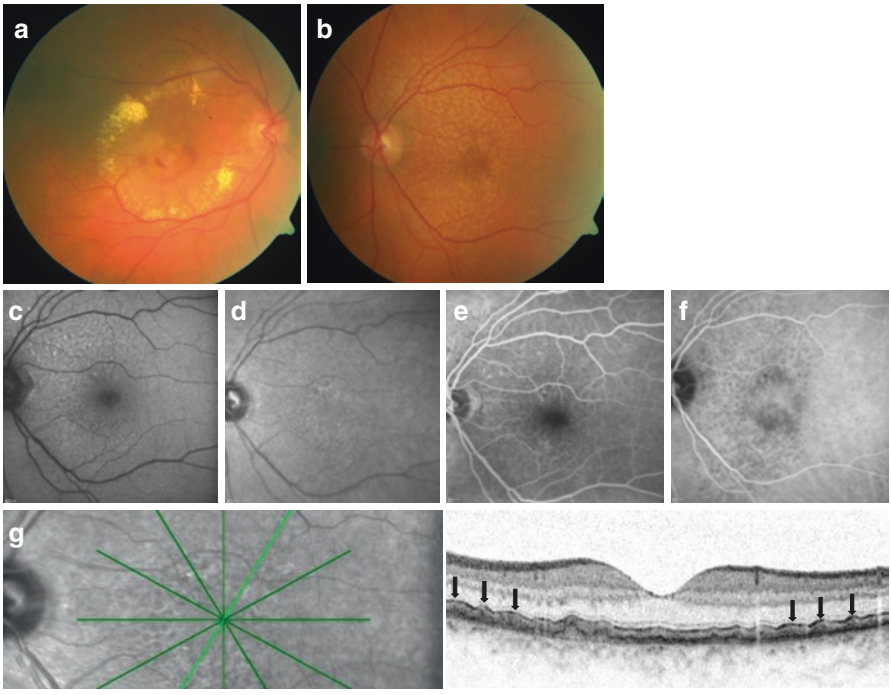

Fig. 5.13 RAP lesion in the right eye (**a**) and reticular pseudodrusen showing a honeycomb pattern in the left eye (**b**) of a patient, demonstrated on blue-light autofluorescence (**c**), infrared fundus reflectance (**d**), FA (**e**), ICGA (**f**), and SD-OCT (**g**)

The difficulty in the treatment of RAP lesions is to find the individual balance for each patient between consequent treatment of active lesions, regular and frequent follow-up examinations of the first but also of the fellow eye, and—maybe—more guarded treatment schemes in eyes with no or low activity and evidence of RPD, in order to minimize atrophy formation and enlargement. Further long-term follow-up studies will hopefully shed light on this in the future.

5.8 Differential Diagnosis

RAP lesions have to be differentiated from type I or type II neovascularization in exudative AMD: as mentioned above, RAP can sometimes be falsely interpreted as minimal classic CNV, especially if only FA is performed and no ICGA and OCT, or if no PED is present in early stages.

Differentiation from advanced polypoidal choroidal vasculopathy (PCV) is sometimes difficult, as both entities can display large PED, retinal bleedings, extensive hard exudates, and intraretinal edema. However, PCV often displays multiple clustered small and steep PED with middle internal reflectance representing the polyps, while RAP lesions in most cases have fewer, smaller bleedings localized mainly intratretinaly and more cystoid macular edema over a single serous PED.

Furthermore, their differentiation from serous or serous-vascularized PEDs is important, as RAP lesions progress much faster and demand a faster treatment, and because oftentimes they respond well to anti-VEGF intravitreal treatment—at least at the beginning—with reduction or resolution of PED.

5.9 Summary

RAP lesions are a distinct neovascular entity causing a very characteristic funduscopic picture and typical signs in imaging. Suspicion of a RAP lesion should always prompt the clinicial to perform additional ICGA. Therapy with intravitreal anti-VEGF compounds seems to be highly effective, however, frequent recurrences, the possible development of geographic atrophy (especially in conjunction with RPD) and the involvment of the second eye in a high percentage of eyes limits visual prognosis.

References

1. Kürzinger GR, Lang GK, Lang GE. Retinal angiomatous proliferation in age-related macular degeneration. Klin Monbl Augenheilkd. 2006;223(8):691–5.
2. Massacesi AL, Sacchi L, Bergamini F, Bottoni F. The prevalence of retinal angiomatous proliferation in age-related macular degeneration with occult choroidal neovascularization. Graefes Arch Clin Exp Ophthalmol. 2008;246:89–92.

3. Slakter JS, Yannuzzi LA, Schneider U, Sorenson JA, Ciardella A, Guyer DR, Spaide RF, Freund KB, Orlock DA. Retinal choroidal anastomoses and occult choroidal neovascularization in age-related macular degeneration. Ophthalmology. 2000;107:742–54.
4. Kuhn D, Meunier I, Soubrane G, Coscas G. Imaging of chorioretinal anastomoses in vascularized retinal pigment epithelium detachments. Arch Ophthalmol. 1995;113(11):1392–8.
5. Jung JJ, Chen CY, Mrejen S, Gallogo-Pinazo R, Xu L, Marsiglia M, Boddu S, Freund KB. The incidence of neovascular subtypes in newly diagnosed neovascular age-related macular degeneration. Am J Ophthalmol. 2014;158:769–79.
6. Axer-Siegel R, Bourla D, Priel E, et al. Angiographic and flow patterns of retinal choroidal anastomoses in age-related macular degeneration with occult choroidal neovascularization. Ophthalmology. 2002;109:1726–36.
7. Song SJ, Youm DJ, Chang Y, Yu HG. Age-related macular degeneration in a screened South Korean population: prevalence, risk factors, and subtypes. Ophthalmic Epidemiol. 2009;16(5):304–10.
8. Maruko I, Iida T, Saito M, Nagayama D, Saito K. Clinical characteristics of exudative age-related macular degeneration in Japanes patients. Am J Ophthalmol. 2007;44:15–22.
9. Hartnett ME, Weiter JJ, Gardts A, Jalkh AE. Classification of retinal pigment epithelial detachments associated with drusen. Graefes Arch Clin Exp Ophthalmol. 1992;230:11–9.
10. Yannuzzi LA, Negrao S, Iida T, et al. Retinal angiomatous proliferation in age-related macular degeneration. Retina. 2001;21:416–34.
11. Gass JDM, AgarwalA LA, et al. Focal inner retinal hemorrhages in patients with drusen: an early sign of occult choroidal neovascularization and chorioretinal anastomosis. Retina. 2003;23:741–51.
12. Brancato R, Introini U, Piero L, et al. Optical coherence tomography (OCT) in retinal angiomatous proliferation (RAP). Eur J Ophthalmol. 2002;12:467–72.
13. Costa RA, Calucci D, Paccola L, et al. Occult chorioretinal anastomosis in age-related macular degeneration: a prospective study by optical coherence tomography. Am J Ophthalmol. 2005;140:107–16.
14. Truong SN, Alam S, Zawadzki RJ, Choi SS, Telander DG, Park SS, Werner JS, Morse LS. High resolution fourier-domain optical coherence tomograph of retinal angiomatous proliferation. Retina. 2007;27:915–25.
15. Lafaut BA, Aisenbrey S, Broecke CV, et al. Clinicopathological correlation of deep retinal vascular anomalous complex in age-related macular degeneration. Br J Ophthalmol. 2000;84:1269–74.
16. Shimada H, Kawamura A, Mori R, Yuzawa M. Clinicopathological findings of retinal angiomatous proliferation. Graefes Arch Clin Exp Ophthalmol. 2007;245:295–300.
17. Monson DM, Smith JR, Klein ML, Wilson DJ. Clinicopathologic correlation of retinal angiomatous proliferation. Arch Ophthalmol. 2008;126:1664–8.
18. Okamoto N, Tobe T, Hackett SF, Ozaki H, Vinores MA, LaRochelle W, et al. Transgenic mice with increased expression of vascular endothelial growth factor in the retina: a new model of intraretinal and subretinal neovascularization. Am J Pathol. 1997;151:281–91.
19. Tobe T, Okamoto N, Vinores MA, Derevjanik NL, Vinores SA, Zack DJ, Campochiaro PA. Evolution of neovascularization in mice with overexpression of vascular endothelial growth factor in photoreceptors. Invest Ophthalmol Vis Sci. 1998;39(1):180–8.
20. Freund KB, Ho IV, Barbazetto IA, Koizumi H, Laud K, et al. Type 3 neovascularization. The expanded spectrum of retinal angiomatous proliferation. Retina. 2008;28:201–11.
21. Yannuzzi LA, Freund KB, Takahashi BS. Review of retinal angiomatous proliferation or type 3 neovascularization. Retina. 2008;28:375–84.
22. Klein R, Davis MD, Magli YL, et al. The Wisconsin age-related maculopathy grading system. Ophthalmology. 1991;98(7):1128–34.
23. Arnold JJ, Sharks SH, Killingsworth MC, et al. Reticular pseudodrusen. A risk factor in age-related maculopathy. Retina. 1995;15(3):183–91.
24. Klein R, Meuer SM, Knudtson MD, Iyengar SK, Klein BEK. The epidemiology of retinal reticular drusen. Am J Ophthalmol. 2008;145(2):317–26.

25. Ueta-Arakawa N, Ooto S, Nakatta I, et al. Prevalence and genomic association of reticular pseudodrusen in age-related macular degeneration. Am J Ophthalmol. 2013;155:260–9.
26. Sawa M, Ueno C, Gomi F, Nishida K. Incidence and characteristics of neovascularization in fellow eyes of Japanese patients with unilateral retinal angiomatous proliferation. Retina. 2014;34:761–7.
27. Cohen SY, Dubois L, Tadayoni R, et al. Prevalence of reticular pseudodrusen in age-related macular degeneration with newly diagnosed choroidal neovascularization. Br J Ophthalmol. 2007;91:354–9.
28. Saito M, Iida T, Kano M, Itagaki K. Two-year results of combined intravitreal ranibizumab and photodynamic therapy for retinal angiomatous proliferation. Jpn J Ophthalmol. 2016;60:42–50.
29. De Bats F, Mathis T, Mauget-Faÿsse M, Joubert F, Denis P, Kodjikian L. Prevalence of reticular pseudodrusen in age-related macular degeneration using multimodal imaging. Retina. 2016;36(1):46–52.
30. Polito A, Napolitano MC, Bandello F, Chiodini RG. The role of optical coherence tomography (OCT) in the diagnosis and management of retinal angiomatous proliferation (RAP) in patients with age-related macular degeneration. Ann Acad Med Singapore. 2006;35:420–4.
31. Rouvas AA, Papakostas TD, Ntouraki A, Douvali M, Vergados I, Ladas ID. Angiographic and OCT features of retinal angiomatous proliferation. Eye. 2010;24:1633–43.
32. Bottoni F, Massacesi A, Cigada M, Viola F, Musicco I, Staurenghi G. Treatment of retinal angiomatous proliferation in age-related macular degeneration: a series of 104 cases of retinal angiomatous proliferation. Arch Ophthalmol. 2005;123:1644–50.
33. Viola F, Massacesi A, Orzalesi N, Ratiglia R, Staurenghi G. Retinal angiomatous proliferation: natural history and progression of visual loss. Retina. 2009;29:732–9.
34. Cho HJ, Kim HS, Yoo SG, Han JI, Lew YJ, Cho SW, Lee TG, Kim JW. Retinal pigment epithelial tear after intravitreal ranibizumab treatment for retinal angiomatous proliferation. Am J Ophthalmol. 2015a;160(5):1000–5.
35. Cho HJ, Yoo SG, Kim HS, Kim JH, Kim CG, Lee TG, et al. Risk factors for geographic atrophy after intravitreal ranibizumab injections for retinal angiomatous proliferation. Am J Ophthalmol. 2015b;159:285–92.
36. Sutter FK, Kurz-Levin MM, Fleischhauer J, Bösch MM, Barthelmes D, Helbig H. Macular atrophy after combined intravitreal triamcinolone acetonide (IVTA) and photodynamic therapy (PDT) for retinal angiomatous proliferation (RAP). Klin Monbl Augenheilkd. 2006;223:376–8.
37. McBain VA, Kumari R, Townend J, Lois N. Geographic atrophy in retinal angiomatous proliferation. Retina. 2011;31:1043–52.
38. Gross NE, Aizman A, Brucker A, Klancnik Jr JM, Yannuzzi LA. Nature and risk of neovascularization in the fellow eye of patients with unilateral retinal angiomatous proliferation. Retina. 2005;25:713–8.
39. Macular Photocoagulation Study Group. Five-year follow-up of fellow eyes of patients with age-related macular degeneration and unilateral extrafoveal choroidal neovascularization. Arch Ophthalmol. 1993;111:1189–99.
40. Campa C, Harding SP, Pearce IA, Beare NAV, Briggs MC, Heimann H. Incidence of neovascularization in the fellow eye of patients with unilateral retinal angiomatous proliferation. Eye. 2010;24:1585–9.
41. Barbazetto IA, Kumar K, Karamchandani H, Rabinowitz D, Takahashi B, Yannuzzi LA. Risk for choroidal neovascularization in the fellow eye of patients on anti-VEGF therapy for age-related macular degeneration. Invest Ophthalmol Vis Sci. 2008;49:2227. E Abstract 256.
42. Bottoni F, Cigada M, Romano M, et al. The incidence of retinal angiomatous proliferation in the fellow eye. Updated findings. IOVS. 2006; ARVO abstract 2177.
43. Marques MF, Marques JP, Gil JQ, Costa J, Almeida E, Cachulo Mda L, Pires I, Figueira J, Silva R. Long-term management of RAP lesions in clinical practice: treatment efficacy and predictors of functional improvement. Ophthalmic Res. 2016;55(3):119–25.

44. Johnson TM, Glaser BM. Focal laser ablation of retinal angiomatous proliferation. Retina. 2006;26(7):765–72.
45. Konstantinidis L, Mameletzi E, Mantel I, Pournaras JA, Zografos L, Ambresin A. Intravitreal ranibizumab (Lucentis) in the treatment of retinal angiomatous proliferation (RAP). Graefes Arch Clin Exp Ophthalmol. 2009;247(9):1165–71.
46. Cho HJ, Lee TG, Han SY, Kim HS, Kim HJ, Han JI, Lew YJ, Kim JW. Long-term visual outcome and prognostic factors of intravitreal anti-vascular endothelial growth factor treatment for retinal angiomatous proliferation. Graefes Arch Clin Exp Ophthalmol. 2016;254(1):23–30.
47. Daniel E, Shaffer J, Ying GS, Grunwald JE, Martin DF, Jaffe GJ, et al. Outcomes in eyes with retinal angiomatous proliferation in the Comparison of Age-Related Macular Degeneration Treatments Trials (CATT). Ophthalmology. 2016;123(3):609–16. doi:10.1016/j.ophtha.2015.10.034.

Chapter 6
Retinal Pigment Epithelial Detachment in Polypoidal Choroidal Vasculopathy

Werner Inhoffen

6.1 Introduction

Formerly described mostly in Asian populations, polypoidal lesions are nowadays detected at a much higher rate also in Caucasians. With up to 17% of nAMD caucasian patients, polypoidal choroidal vasculopathy (PCV) is not a rare disease anymore. Active PCV lesions may be the reason for a developing pigment epithelial detachment (PED) and, as a consequence, these PEDs can be influenced by treating the underlying PCV lesions with laser photocoagulation, photodynamic therapy (PDT), and/or intravitreal anti-VEGF (vascular endothelial growth factor) injections.

In 1982, Yannuzzi was the first to describe a small series of patients with subpigment epithelial neovascularization and massive hemorrhages at a meeting. As a presumed source of theses hemorrhages, patients also showed some choroidal vascular abnormalities in fundus and in fluorescein angiography (FA) at the posterior pole. Thus, he described this disease as "Idiopathic polypoidal choroidal vasculopathy (IPCV)". Multiple names were given to this specific disease including "Multiple recurrent serosangineous retinal pigment epithelial detachments in black women" [1], "Posterior Uveal Bleeding Syndrome" [2], and "Multifocal idiopathic sub-RPE neovascularization occuring in darkly pigmented individuals" [3].

In 1990, Yannuzzi et al. published their description of the disease, again emphasizing the vascular origin as "Idiopathic polypoidal choroidal vasculopathy (IPCV)" [4]. With the assumption of other researchers that this was a rare disease, the high percentage of black women was due to the increased visibility of one of the most important detail besides hemorrhagic PEDs: prominent orange areas seen in funduscopy, identified in FA as small leaky bulbs at the end of some visible abnormal choroidal vessels and thought to be responsible for hemorrhagic PEDs. Thus, Yannuzzi described two

W. Inhoffen
University Eye Hospital Tuebingen, Tuebingen, Germany
e-mail: werner.inhoffen@med.uni-tuebingen.de

M.A. Gamulescu et al. (eds.), *Retinal Pigment Epithelial Detachment*,
DOI 10.1007/978-3-319-56133-2_6

components: (1) dilated and branching inner choroidal vessels and (2) terminal reddish-orange, spheroid aneurysmal-like protrusions which he called “polyp-like.”

In the following years, indocyanine green angiography (ICGA) was introduced for the diagnosis of IPCV (the term idiopathic was dropped later = PCV), which now better showed choroidal aneurysms (polyps) and dilated choroidal vessels, even those not visible in funduscopy. These vessels were described as irregular latticework made up of choroidal vessels that were heterogeneous in size and did not follow the normal choroidal architecture, termed branching vessel network [5]. In the vicinity of the polyps, pulsatile flow could be demonstrated in the abnormal vessels by videoangiography [5]. These distinct features had not been visible in the often used FA due to the absorption of blue light by the pigment epithelium. With the introduction of ICGA, PCV detection increased very fast world-wide [6].

[In the following chapter, data presented inside square brackets represent results of 50 PCV patients from the University Eye Hospital Tuebingen (UEHT).]

6.1.1 Epidemiology

Imamura [7] and Ciardella [8] summarized epidemiological data of patients with PCV: Age: At first presentation, patients diagnosed with PCV were mostly 50 and 65 years old (range 20–80 years, average 60 years), [UEHT: 43–82 years, mean 65 years].

Incidence of PCV in presumed nAMD:

- Japan: 55%, increasing to 70–80% in patients with hemorrhagic PEDs
- China: 9.3%
- USA: 8%
- Caucasian: Up to 17%, mostly patients with poor response to prior ranibizumab treatment (Hatz [9])

Sex:

- Asia: men predominantly affected (69%)
- Europe: men only 25–29% [UEHT: men 50%]

Bilateral involvement:

- Japan: 10–20%
- Europe/USA: 30–60%, [UEHT: 39%]

Location of PCV (BVN + polyps):

- Japan: 90% macular
- Europe/USA: 50% macular [UEHT: macular 69%]

Complications:

- China: subretinal hemorrhage (63.6%), exudative neurosensory detachment (59.1%), hemorrhagic PED (59.1%).
- Other countries: lower frequencies.

- Cumulative incidence of massive subfoveal hemorrhage increases with time reaching 30% in 10 years [10].

These data show the great variability of PCV, which makes it questionable to transfer the prevailing Asian study results to a Caucasian population [7–9].

6.1.2 Pathogenesis

According to Honda et al. [11], the two major AMD susceptibility loci (CFH and ARMS2/HTRA1) can influence the risk of PCV in Asian population. But as single-nucleotide polymorphisms (SNPs) in the CFH region vary among races, this may not be valid in European populations. It is very likely that PCV is not a genetically homogeneous pathology, considering the inhomogeneous response to anti-VEGF therapy. Nevertheless, PCV is classified as a specific form of exudative AMD, accompanied by soft drusen in up to 23%. However, in contrast to nAMD, these soft drusen seem to have no significant effect on the clinical course [12].

6.1.3 Histopathology

Kuroiwa et al. [13] and Yuzawa et al. [14] described features of surgically excised PCV: arterioles had a disrupted inner elastic layer (not seen in CNV), possibly explaining the spontaneous pulsation of polyps sometimes seen. In two cases, large choroidal arterioles and/or venules were found within the nodules, thus some polyps seemed to have an "inner structure." Nakajima et al. [15] demonstrated dilatation of a thin-walled vessel which may explain why polyps fill fast or slow depending on the entrance diameter of the dilatation.

Clinicopathologic findings in PCV demonstrated abnormally dilated vessels beneath the RPE, with thickened and hyalinized walls, often obstructed, the diameter of the most dilated vessel exceeding 250 μm, similar to the measured diameters in ICGA (see chapter "Imaging"). It was hypothesized that vascular hyalinization was followed by massive extravasation of plasma proteins, raising choroidal tissue pressure sufficiently to produce protrusion of choroidal tissues through the weakened or disrupted RPE and Bruch's membrane [16].

6.1.4 Clinical Examination

Patients present with metamorphopsia similar to other neovascular AMD subtypes and mild or severe visual deterioration depending on location, duration, and appearance of PCV. Some of them present with one or multiple serous, small or large

PEDs, with or without sub-RPE hemorrhage, lipid exudation, and subretinal bleeding (Figs. 6.1, 6.2, 6.3, 6.4, 6.5, and 6.6). The lesions may arise in the peripapillary, macular, or mid peripheral region.

PCV lesions can originate from a reactivated hyperpigmented scar as one of the possible end stages of PCV (Fig. 6.1a), near atrophic regions (Fig. 6.1b) or from

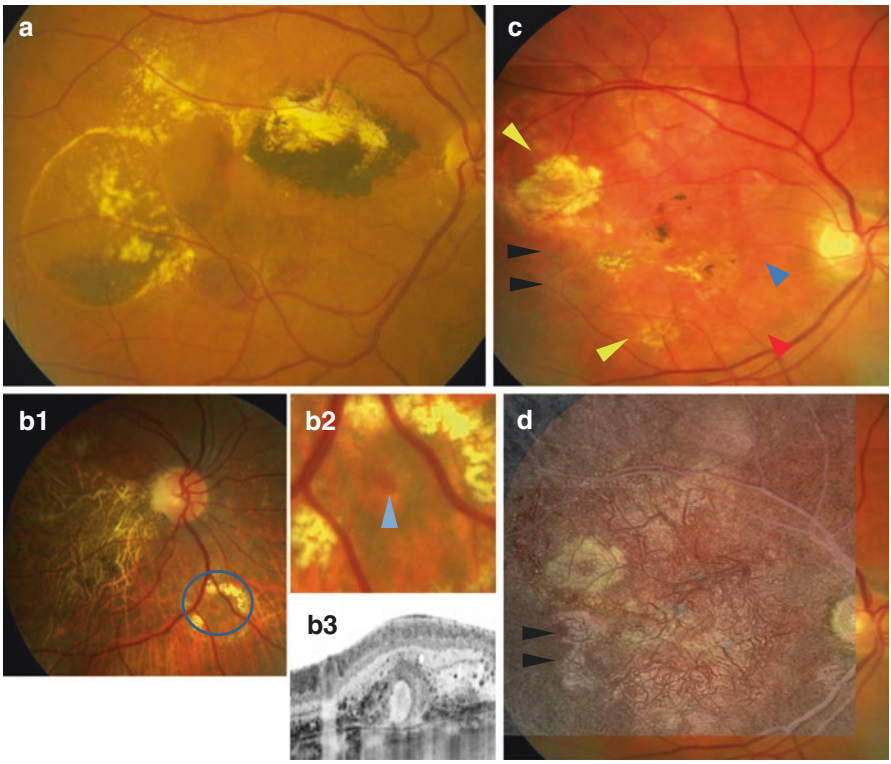

Fig. 6.1 (**a**) Central old hyperpigmented scar near the optic disc of unknown origin, formerly suspected as being induced by uveitis. In many patients with PCV, these scars can be observed. Now, this scar is active: PEDs with sub-RPE hemorrhages, horizontal blood-level in the biggest PED and yellow deposits can be seen in the temporal macular region. (**b1**) Another patient with long standing PCV, now ending in an atrophic scar centrally without nodules in this area. In the periphery hard exudates with reddish noduls (encircled, magnified in (**b2**) with arrowhead), which appear as aneurysmatic dilatations with large hyporeflective lumen seemingly breaking through the RPE layer in OCT (**b3**). Thus, it is highly probable that the atrophic macular scar belongs to a former PCV lesion. In (**c**) fundus photography of another patient with long standing PCV showing two areas as "honey exudates" (*yellow arrowheads*), a few hard exudates centrally, pigmentary hypertrophy nearby and new reddish and creamy PEDs (*black arrowheads*) at the temporal rim of the whole lesion. The whole lesion is visible as reddish atrophic area with distinct borders (*red arrowhead*). Red "streets" (*blue arrowhead*) turned out to be thick choroidal vessels or bundles of choroidal vessels as depicted on the overlay with 50% transparency of OCT-Angiography (**d**). The overlay shows that the whole lesion is vascularized with abnormal vessels (BVN) and the new PEDs overly terminating vascularization, most probable polyps. However, ICGA was not possible in this patient to further confirm this

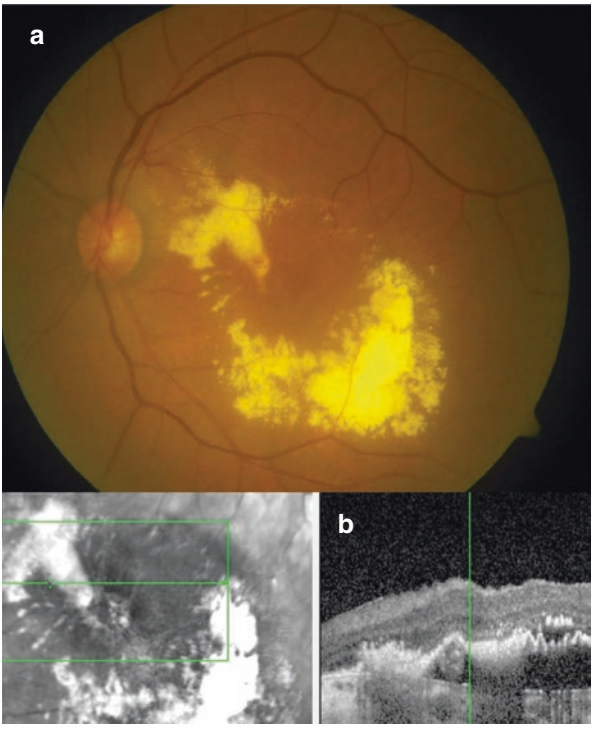

Fig. 6.2 (**a**) Another patient with PED, massive fibrosis, and yellow lipid deposits but no hemorrhage. (**b**) Corresponding B scan of the OCT examination shows directly to the right of the green bar, that the lipid deposit is located below the RPE. One origin of this sub-RPE exudation can be seen on the left of the green bar: a polyp with three different hollow spaces located below the RPE

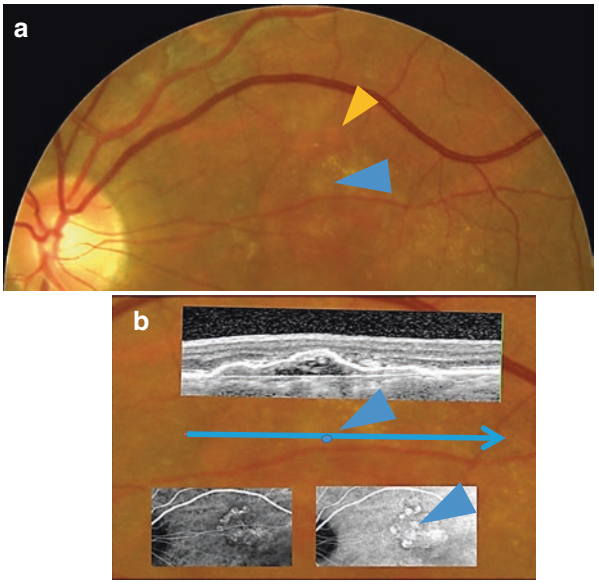

Fig. 6.3 (**a**) Another patient showing orange nodules (*yellow arrowhead*) and one yellow fibrotic nodule (*blue arrowhead*). (**b**) Overlay with OCT shows the yellow nodule (along the blue bar and near blue point) as an arrangement of vessels covered by hyperreflective tissue, explaining ICGA behavior and the color of the nodule (*inset below left*: early ICGA with no central polyp but peripheral polyps, *inset below right*: late ICGA with staining of fibrosis in the center of the lesion, *blue arrowhead*)

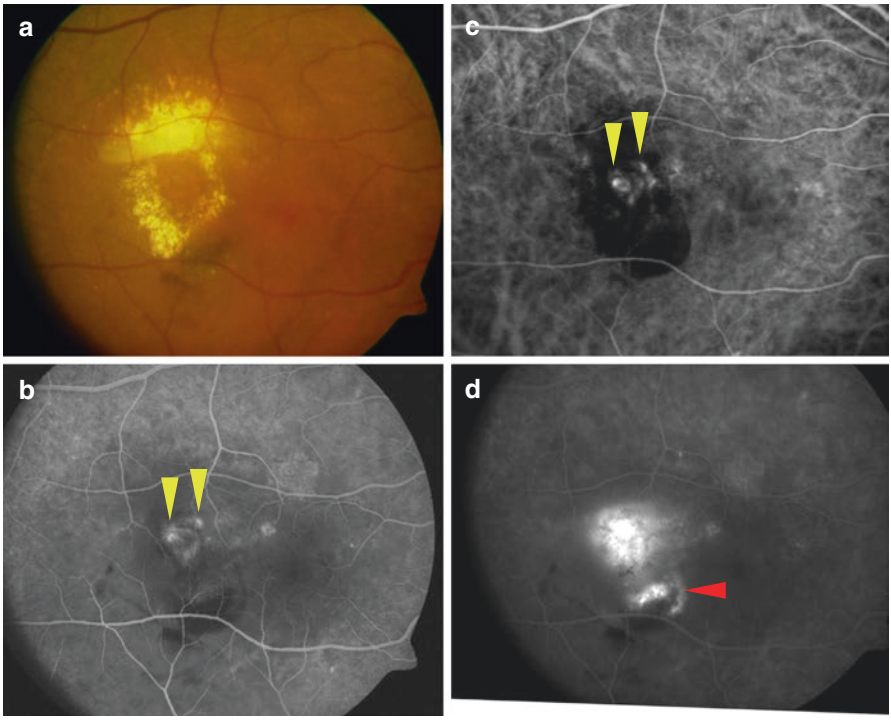

Fig. 6.4 (**a**) Another patient with central PED, yellow lipid deposits, and subretinal hemorrhage. Fibrotic nodule suspected centrally. (**b**) FA early phase with suspected polyps (*yellow arrowheads*), confirmed by ICGA (**c**) at 45 s. (**d**) Late FA shows in addition leakage especially near the hemorrhage, suggestive of active polyps obscured by hemorrhage in ICGA

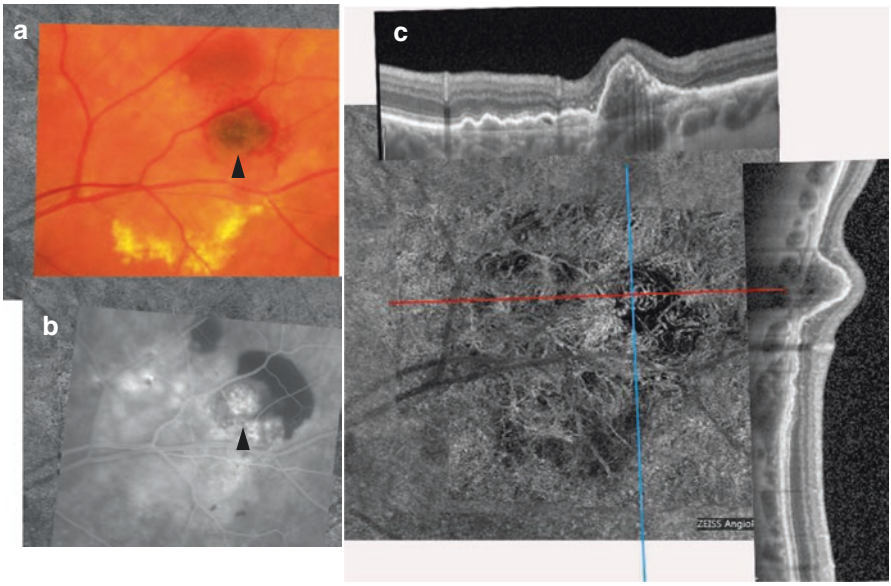

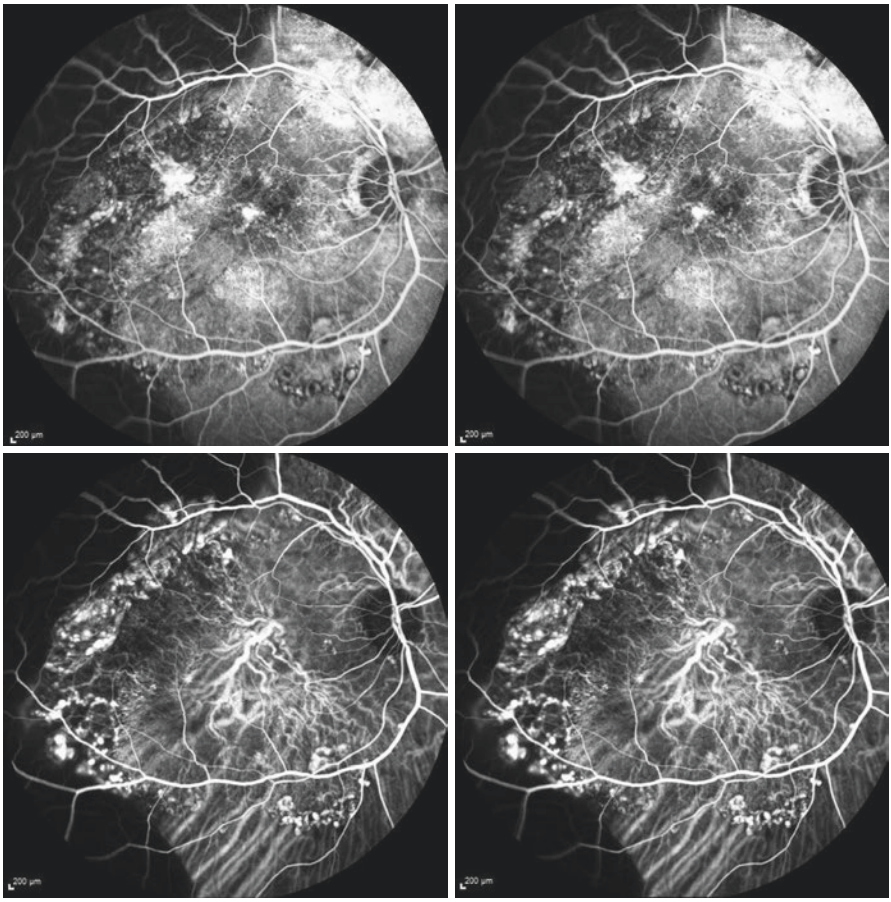

Fig. 6.6 This patient shows large PEDs in the periphery due to peripheral polyps best visualized in stereo ICGA (00:41, lower pictures), FA above (00:48), courtesy: Rumana Hussain and Heinrich Heimann, Royal Liverpool University Hospital, GB

Fig. 6.5 (**a**) Another patient with hemorrhagic PED showing internal structures suggesting polyps inside (*black arrowhead*). (**b**) Late FA (a few days later) is highly suggestive of polyps with leakage (*black arrowhead*) inside the PED. This is confirmed by OCT scans along the two lines (**c**) with small polyps. In addition, the OCTA enface (**c**) shows high density of vessels ("ball of wool") inside the PED area at the crossing of the two lines

pigmentary changes or isolated yellow and flat areas (Fig. 6.1c). However, sometimes PCV can also occur without any obvious visible pigmentary changes (Fig. 6.3a).

PEDs arise from nearby polyps below the RPE, which explains the high rate of sub-RPE hemorrhages and sub-RPE lipid exudates ("honey exudates"). As many forms at the beginning start without striking fundoscopic findings, it is important to actively search for polyps in funduscopy. Sometimes, they can be observed on funduscopy as small and round nodules colored red orange, red, yellow gray or dark.

Lipid exudation can exist above and below the RPE. In Fig. 6.2, isolated yellow and flat areas are not drusen but hyperreflective very flat and small PEDs, most probably with a thin layer of lipid as part of the beginning of a PCV as seen in OCT.

[UEHT: Red orange nodules 48%, drusen 11%, hemorrhages 53%, hard exudates 49%, grayish nodules 17%. After years of disease progression: atrophy 39%, new hemorrhages 51%.]

After therapy, hemorrhages and often the PEDs themselves are reduced or vanish which can be seen even by funduscopy. One reason may be occlusion of dilated choroidal vessels with slow blood velocity. However, this occlusion can only be observed with modern imaging methods as FA, ICGA, Optical Coherence Tomography (OCT), and OCT-angiography (OCTA).

6.2 Imaging

At present, presumed nAMD patients are primarily examined with FA and OCT. Thus, it is important to recognize signs of polyps as multiple small hyperfluorescent spots (PEDs, not drusen!) in FA scattered over the assumed occult CNV, mostly at the rim (Figs. 6.3, 6.4, and 6.6). However, some but not all of the PEDs may correspond to polyps (Figs. 6.4 lower row and 6.6): in FA, both PEDs and polyps appear as hyperfluorescent areas with fast or slow, homogeneous or inhomogeneous filling. In contrast, in ICGA PEDs and thick hemorrhages are hypofluorescent, but polyps are hyperfluorescent. This means that polyps below a thick sub-RPE hemorrhage may be indirectly detected in FA as leakage in late images, especially at the rim of hemorrhages (Fig. 6.4d). BVN can also show leakage (Fig. 6.14).

In our patients, polyps mostly occurred at the rim of the CNV lesion, sometimes even a distance apart. As history of polyps is highly variable, in one eye there may be no nodules nor polyps, but CNV or BVN vessels, whereas in the other eye with a central scar peripheral polyps may be visible in ICGA. Thus, it is highly possible, that the eye under consideration suffers from PCV too, although no polyps/nodules are detected.

A correspondence of more than 70% between FA and ICGA, as far as the diagnosis of PCV with FA is concerned, was found by Tan and Ngo [17] and Coscas et al. [18]. In our patients, if PCV was suspected in FA, 93% of them showed PCV in ICGA.

6.2.1 *Imaging of PCV in ICGA*

Early ICGA:

- pulsation of choroidal vessels filling a polyp (suggesting hyperelasticity of vessels) in the first 30 s. Tan et al. ([19], EVEREST study): 7%, Byeon et al. [20]: 22%, [UEHT: 20%].
- successive filling of different polyp chambers or different polyps (20 s–6 min) (Figs. 6.7 and 6.8).
- abnormal choroidal vessels or BVN, best seen in the very early phase of ICGA or on video angiography (observed in 75% (Everest study, Tan et al. [19]), [UEHT: 74%])

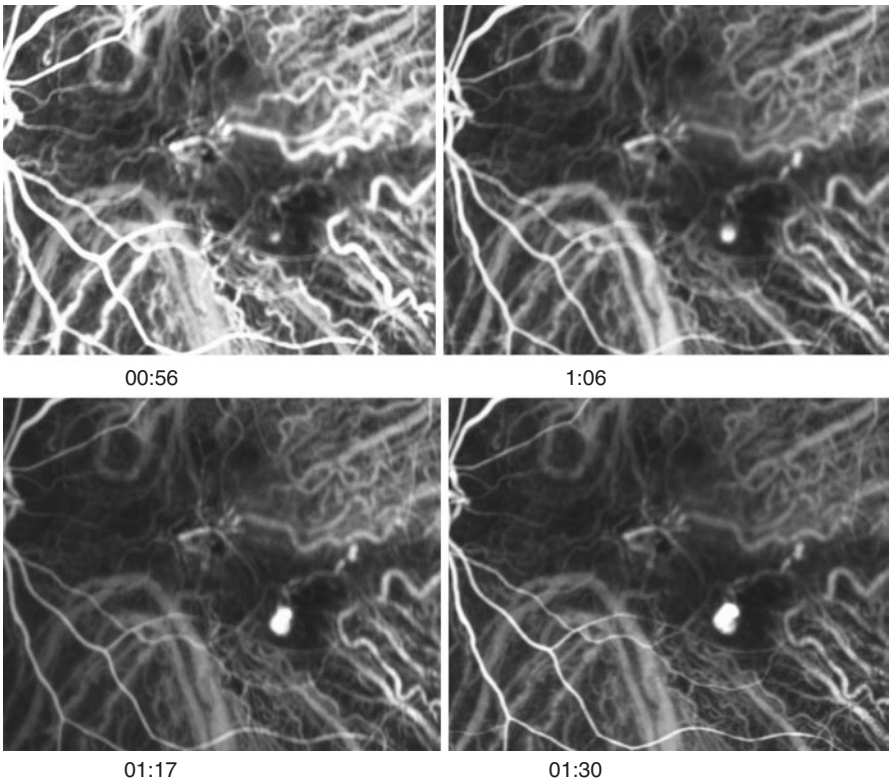

Fig. 6.7 Another patient with a sequence of an ICGA: The polyp fills first at the lower part (00:56 and 1:06), then another compartment is filled at the upper part (1:17) and at the lower right part (1:30). Thus, the polyp complex seems to have internal structures

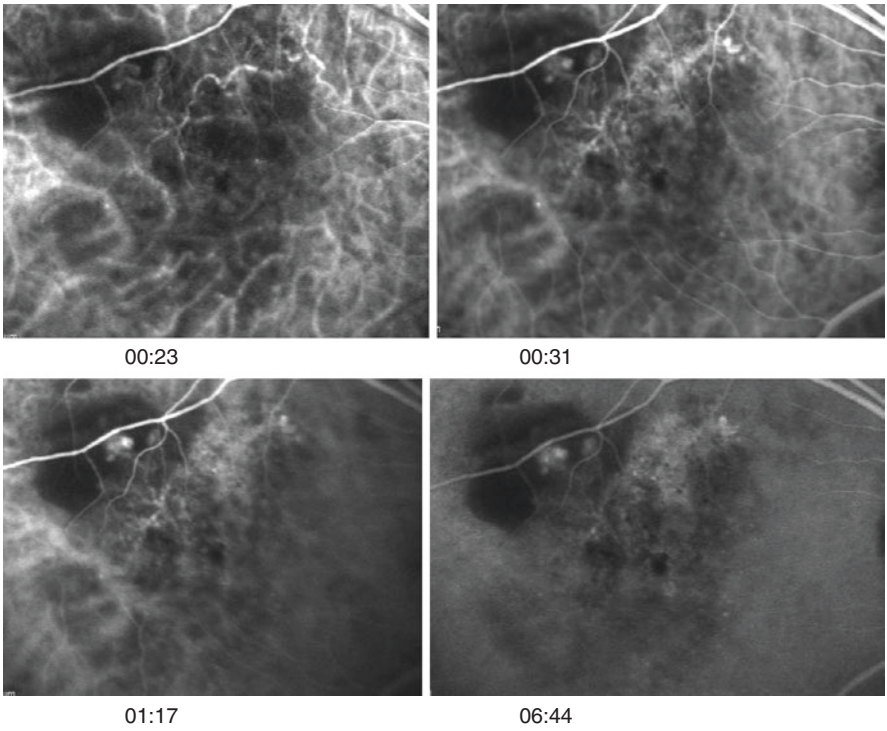

Fig. 6.8 Another patient with a sequence of an ICGA: Three polyps are filled from a long feeder vessel (00:23, 00:31, 1:17, and 6:44), at the end it seems as if they were confluent. Feeding vessels are very long. BVN is visible, most of the BVN also visible as late geographic hyperfluorescence (LGH) (6:44)

Late ICGA:

- dark halo around the filling polyps (69% EVEREST study) [UEHT: dark halo not seen in all cases]
- late geographic hyperfluorescence (LGH, sometimes visible after 10 min) with long feeder vessels (Fig. 6.8) and with polyps at the rim (Fig. 6.9) or inside: rim: 65% and inside: 24% [21] [UEHT: 74% and 26%, respectively].

Other features detected in ICGA are:

- choroidal vessels with dilatations, tortuositas, and 90° wrinkling [UEHT: 63%]
- hyperfluorescent pearls along choroidal vessels, best seen in stereo ICGA [UEHT: 27%] (Fig. 6.10a)

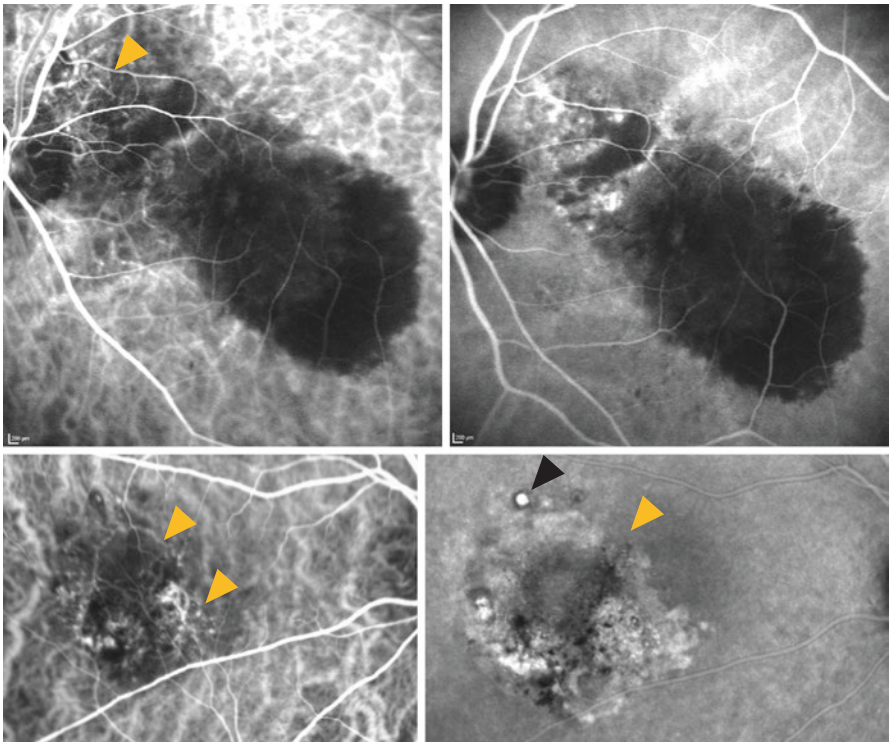

Fig. 6.9 *Upper row:* Same patient as in Fig. 6.2. BVN in ICGA best visible at 00:26 (*yellow arrowhead*), polyps better in later frames (05:09); lower row: another patient with BVN (ICGA 1:04, *yellow arrowheads*), area of late geographic hyperfluorescence bottom right (ICGA 15 min, *yellow arrowhead*) is approximately equal to BVN area including polyps. *Black arrowhead*: active polyp at the rim of LGH

- location of polyps mostly near large PED, sometimes within a notch [UEHT: 15%] (Figs. 6.11, 6.12, and 6.13)
- progression of BVN over long time (Figs. 6.8 vs. 6.14; 6.12 vs. 6.9 upper row; 6.11 vs. 6.10a, b)
- coexisting CNV or conversion into vessels similar to CNV (Fig. 6.10b (OCTA image), Fig. 6.6 (ICGA stereo image) with large extensions and polyps at the rim as a source of peripheral PEDs (Fig. 6.6) [UEHT: 11%]
- remodelling and new locations of polyps (Figs. 6.12 and 6.17).

What to do if ICGA was not possible?

Figure 6.5b, c shows that in some cases diagnosing PCV without ICGA is possible with high probability using OCT.

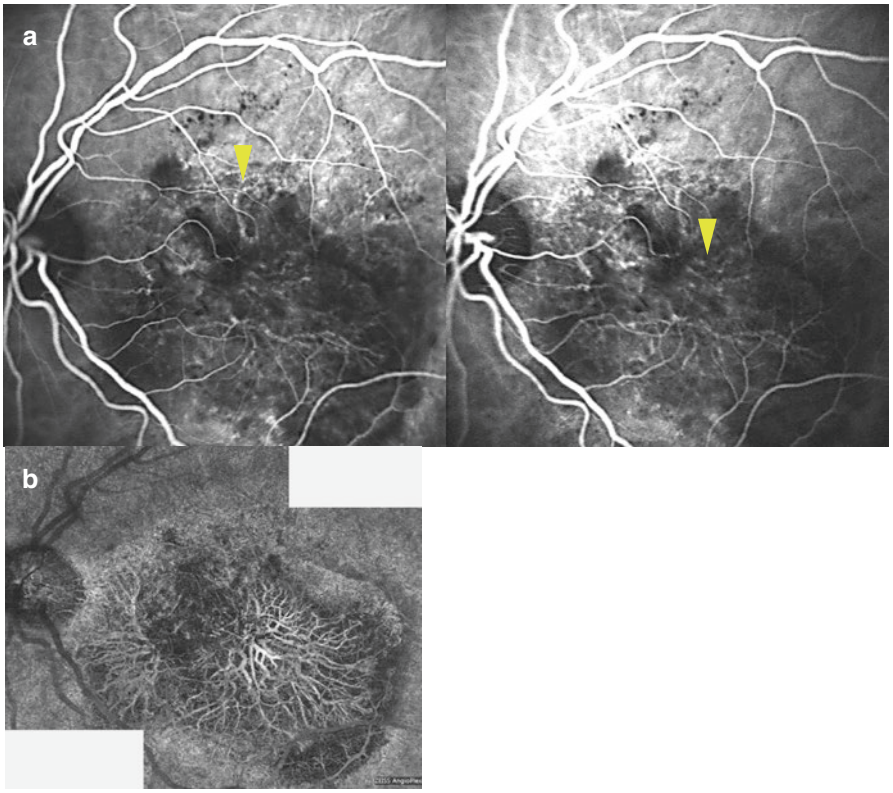

Fig. 6.10 Same patient as in fig. 6.11 but at a later stage: (**a**) Stereo ICGA 01:27 shows slow change of BVN into classic CNV. Also small hyperfluorescent dots lined up at the surface of choridal vessels are visible (*yellow arrowheads*). (**b**) OCT-angiography of the same patient years later depicts now vessels resembling classic CNV

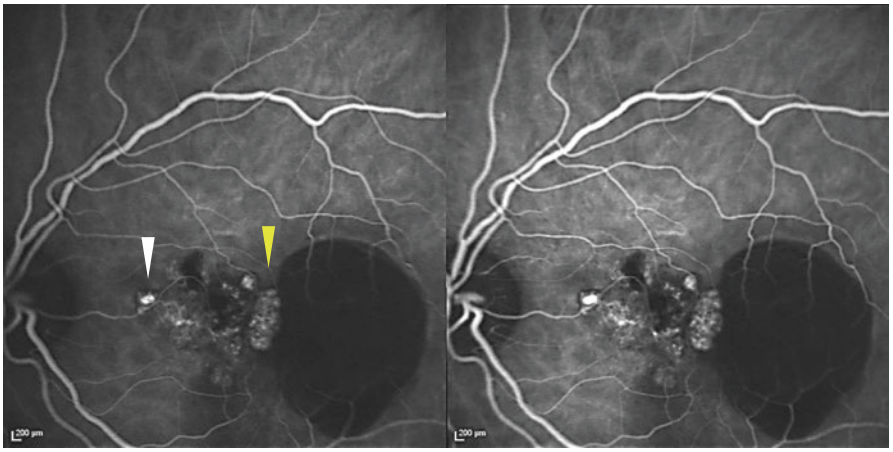

Fig. 6.11 Same patient as in Fig. 6.10a, here at an earlier stage with stereo ICGA (00:51): Notch of hypofluorescent PED with polypoidal lesion inside the notch rising, suggesting to be the source of new PED (*yellow arrowhead*). Other polyp (*white arrowhead*) does not contribute to the PED

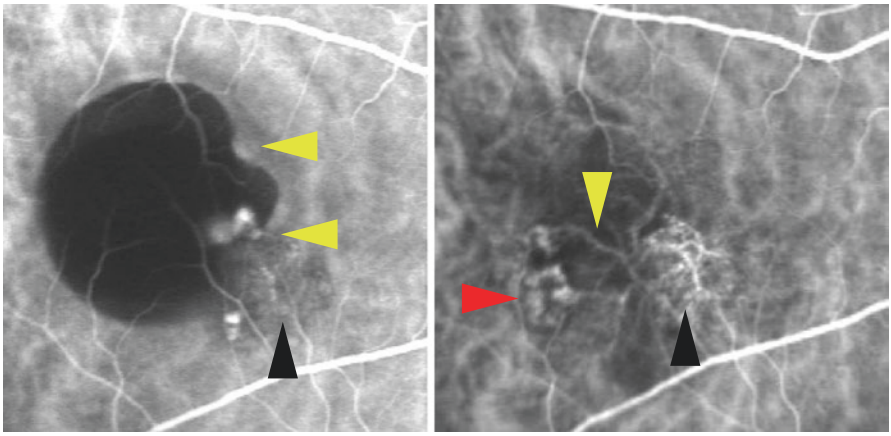

Fig. 6.12 Same patient as in Fig. 6.9 (lower row) but here at an ealier phase. Early phase ICGAs (*right* 1:21, after anti-VEGF therapy): left image shows polyps at the rim of BVN at the location of one of the two PED notches (*yellow arrowhead*) before treatment. The second notch shows a suspected polyp; right image after anti-VEGF therapy with loss of former polyps, but long feeder vessels now crossing the PED (*yellow arrowhead*) to form new polyps (*red arrowhead*) at the rim of the still existing PED (hypofluorescent area), first BVN becomes more visible (*black arrowhead*)

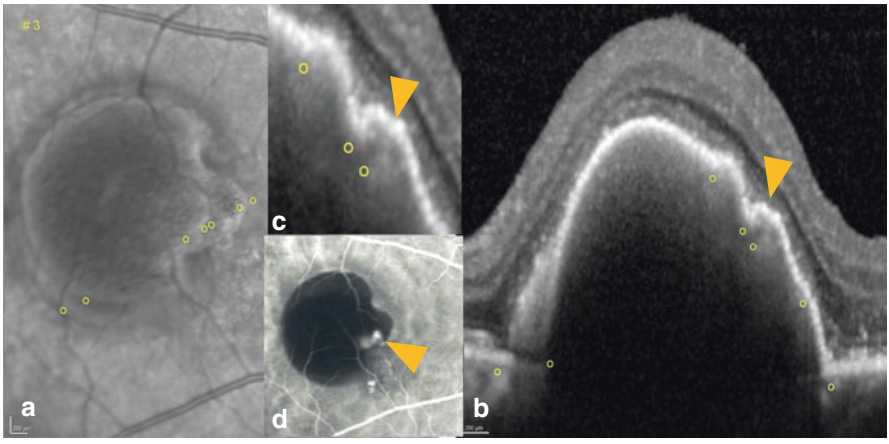

Fig. 6.13 (**a**, **b**) OCT of same patient, yellow circles indicate locations in fundus image and OCT scan. Of the three tomographic notches in OCT (**b**) one clearly shows two hyporeflective spaces as part of the polyp complex (enhanced in **c**). Thus, OCT notch can be a sign of PED vascularization. The location of these vessels in OCT correspond to the location of the polyps (ICGA in **d**)

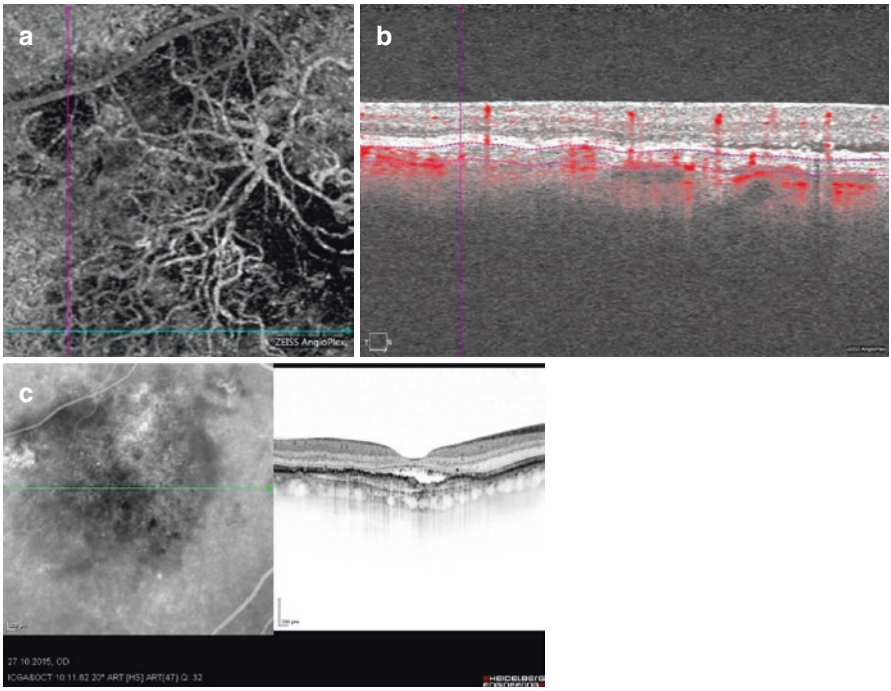

Fig. 6.14 Same patient as in Fig. 6.8, here at a later time: (**a**) OCTA enface and (**b**) corresponding flow B scan (vessels with flow in red) along the green blue line show that progressive BVN does not lead to PED nor NSD automatically. Nevertheless, BVN (OCT at different scan location) can be exudative as depicted in OCT scan (**c**)

6.2.2 Imaging of PCV in OCT

Possible OCT signs are [22]:

- Double layer sign in 58% (= flat detached RPE, separated from Bruch's membrane by hyperreflective tissue and connected to a PED)
- several small and steep PEDs with medium reflectivity or internal structures in close vicinity ("bola sign") in 23% (Fig. 6.17 c)
- needle-shaped PEDs ("needles") mostly contain polyps, may arise directly from choroidal vessels as part of the polyp complex (Figs. 6.16 and 6.17)
- polyps may appear adherent to the inner side of detached PE, pushing the PE upwards more at the region with adherence (this is described as"tomographic notch", not to be confused with the "angiographic notch" visible in ICGA) (Figs. 6.13 and 6.16).
- Connections between PEDs and polyps can be depicted using 3D SD-OCT programs (Figs. 6.17, 6.18, and 6.19)

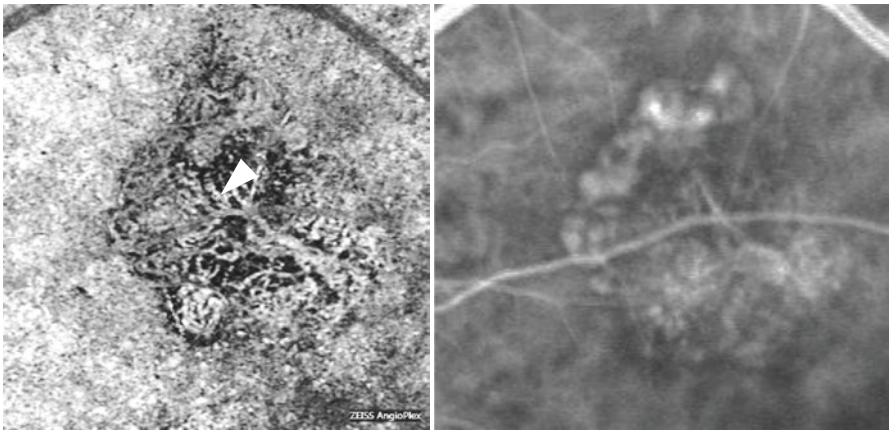

Fig. 6.15 Same patient as in Fig. 6.3: ICGA (00:31, *right*) and OCT-angiography left show internal structure of polyps and interconnecting vessels, polyps with feeder vessels (*white arrowhead*)

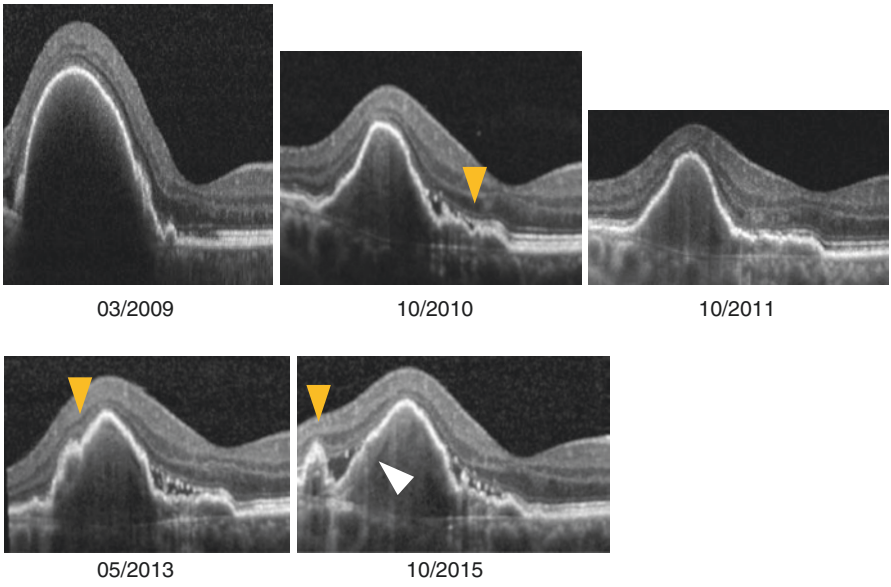

Fig. 6.16 OCT of the patient in fig. 6.12: Behavior of PED after therapy over time: BVN increasing (*first yellow arrowhead*) and notch "moves" to the left (*second yellow arrowhead*, hyperfluorescent area below) crossing the PED and moving thereafter outside the PED to form a needle (*third yellow arrowhead*). The PED has now less height but fibrovascular tissue inside below the RPE (*white arrowhead*) and did not regress totally. The former OCT notch inside the PED has gone (resolved notch)

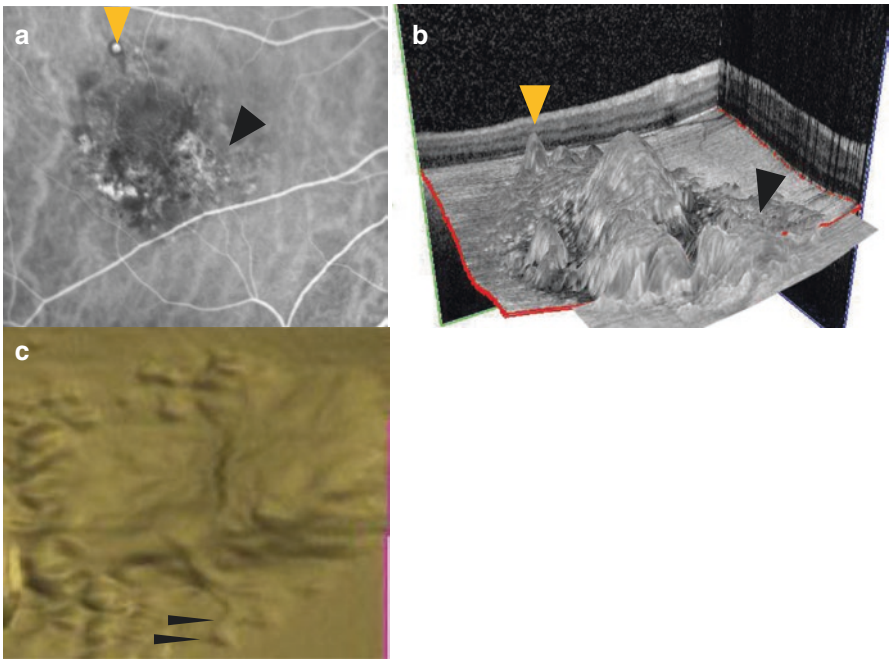

Fig. 6.17 (**a**) ICGA 7:51 of the same patient, later stage: one polyp marked with yellow arrowhead and BVN area (*black arrowhead*). (**b**) A corresponding three-dimensional image (later time) showing needles (*yellow arrowhead*: same polyp as marked in (**a**)) and PEDs can be obtained by using Spectralis OCT volume scan (10 μm separation, manual segmentation, top layer RPE, bottom layer BM). (**c**) Cirrus 5000 OCT cube modus and 3D presentation of RPE protrusion of another patient: the first large PED was formerly on the right of this image, then it lowered and progressed to another PED on the left side of the image; small PEDs around are seen, connected to the main PED ("Bola sign," similar to Boccie game: spheres with a track in the sand, black arrowheads)

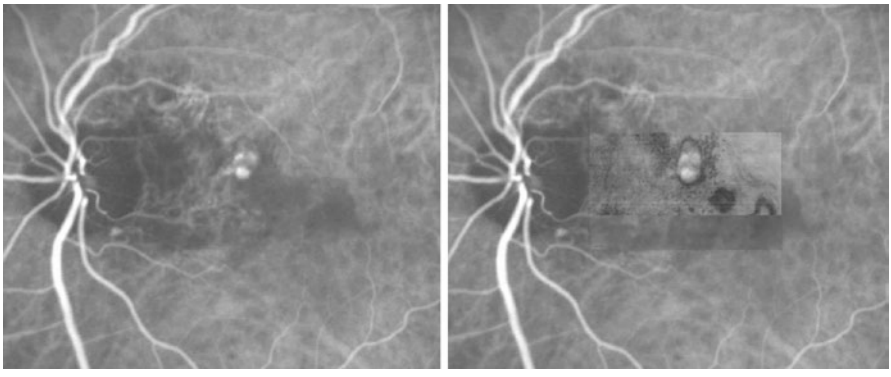

Fig. 6.18 Another patient: Left side with ICGA (01:14): BVN and polyps; right side same image but with 40% Spectralis enface overlay showing the polyps enclosed inside a PED and additional PEDs without polyps ("associated PEDs," see next figure)

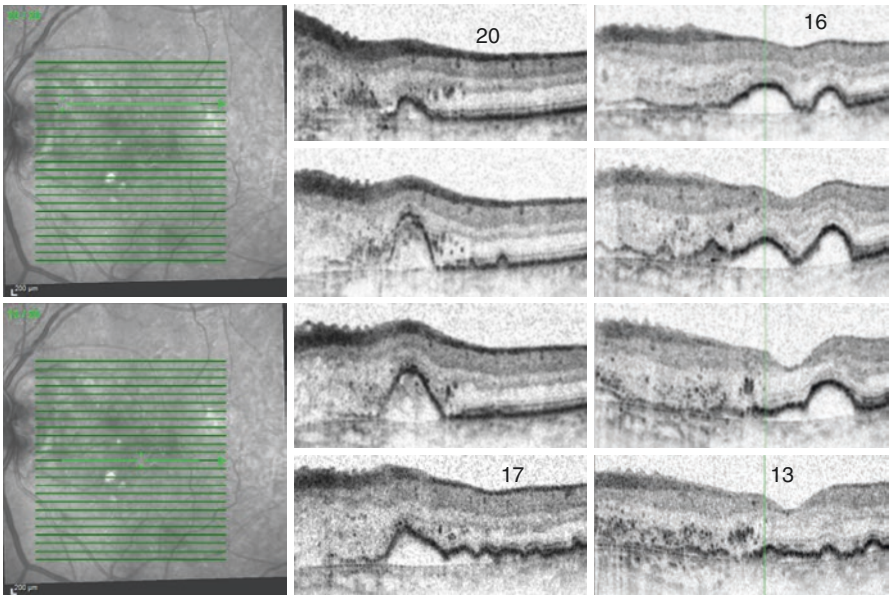

Fig. 6.19 Same patient and Spectralis OCT volume scans number 20 down to 13: polyps (visible in scan 18) seem to be connected to the temporal PED near the fovea (scan 14) as there is continuous PED starting from the polyps. Thus, if activity of these polyps can be stopped, the associated PED near the fovea should vanish. This was indeed the case after PDT treatment.

de Salvo et al. [23] recommends the diagnosis of PCV to be based on the presence of at least 3 different of 4 OCT signs:

- multiple PEDs
- sharp PED peak (needle)
- PED tomographic notch
- rounded hyporeflective area representing the polyp lumen within the hyperreflective lesions adherent to the underside of the RPE

Imaging of PCV in OCT-angiography (OCTA):

The latest imaging technology is OCTA, detecting a vessel if reflectivity changes at repeated measurements at the same fundus location are high enough. We used the AngioPlex Cirrus 5000 (Carl Zeiss Meditec, Germany), which gave excellent images of BVN in enface technique. OCTA may also help in detecting BVN and polyp changes spontaneously or after therapy, especially when remodelling of the polyp area occurs. However, detection of low flow in polyps turned out to be uncertain: the polyps were not as bright as in ICGA (Fig. 6.20), or they remained "dark" and hereby undetectable. Only 13% of polyps were better visualized by OCTA compared to ICGA, sometimes they could be detected on OCTA as hypo-flow structures contrasting with hyper-flow BVN [24]. Compared to

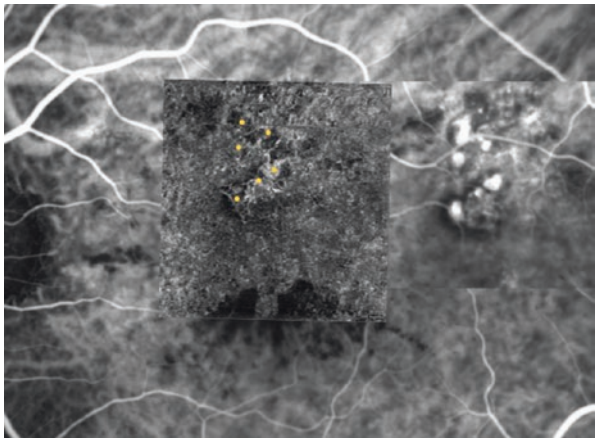

Fig. 6.20 Another patient: Inset shows an OCTA enface image with additional yellow points indicating the locations of polyps detected from the underlying ICGA (*inset right side*). Thus, not all polyps are shown in OCTA and they are mostly not recognizable as such even when compared with ICGA findings. Some polyps show in OCTA as dark (=hypo-flow) areas

OCTA, detection of polyps using conventional B scans from SD-OCTs was easier (Fig. 6.1b3).

Interestingly, OCTA shows that BVN vessel can sprout directly from big choroidal vessels below Bruch's membrane as small caliber vessels, explaining why in big lesions the BVN has more than one source [UEHT].

Possible OCTA signs are:

- polyps can be surrounded (wrapped) by BVN vessels (Fig. 6.15)
- in contrast to CNV, vascularization of PEDs induced by PCV progresses along the detached PE (Figs. 6.14, 6.16 and 6.21).

6.3 Natural History

Yannuzzi first described a prolonged, relapsing and recurring course. Uyama et al. [25] reported that 50% of untreated eyes with PCV remained stable and maintained vision of 20/30 or better for at least 2 years. Sho et al. [26] compared PCV with neovascular AMD and reported that eyes with PCV may manifest clinically more slowly than AMD.

Cheung et al. [27] studied the time course of 32 eyes with active and symptomatic PCV. At month 12, visual acuity improved in 22%, remained unchanged in 31%, and worsened in 47%.

Reasons for poor vision over time were retinal or subretinal hemorrhage, PE atrophy, or scarring.

Our own observations with untreated eyes are somewhat similar to anti-VEGF-treated eyes: polyps may bleed, grow or leak, regress, and a CNV may appear. After regression of a polyp, a new BVN may progress with new polyps forming further away. The BVN itself may also leak and cause subretinal fluid accumulation or

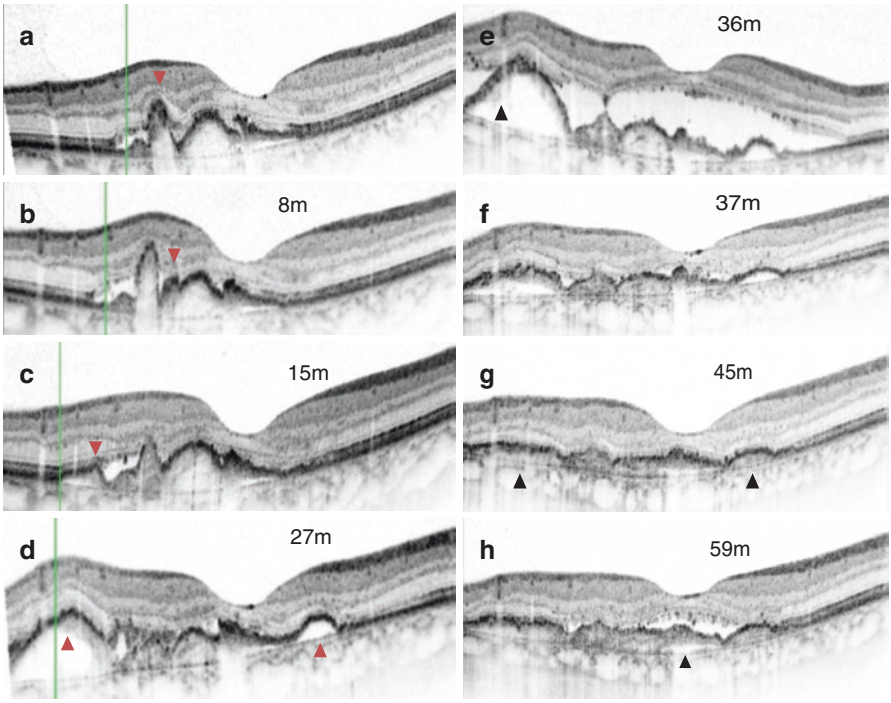

Fig. 6.21 Patient in fig. 6.8 with OCT findings after anti-VEGF therapy: (**a**) "Needle" (steep PED, *first red arrowhead*) grows upwards after 8 months and a second tomographic notch arises (**b**) (*red arrowhead*). (**c**) and (**d**) After 15 and 27 months new PEDs to the right (with sub-PE material) and to the left arise (*red arrowheads*) indicating further growth of BVN. (**e**)After 36 months, macular NSD and growing PED/sub-PE material at the left (*black arrowhead*) were visible while the PED at the right remained stable. (**f**, **g**) After change to aflibercept, the PED at the left gradually decreased (*black arrowhead*), but NSD was still persistent after 59 months (**h**) with increasing sub-PE material (*black arrowhead*).

intraretinal edema. Development of RPE atrophy and its progression to late-stage disease can be related to resolution of PED or flattening of the lesion, chronic leakage through the RPE and cystic intraretinal degeneration.

6.4 Therapy

Therapeutic options for PCV are:

- Laser Treatment (Photocoagulation)
- vPDT = Photodymanic treatment with verteporfin
- anti-VEGF therapy with:
  - ranibizumab
  - aflibercept
  - bevacizumab

6.4.1 Laser Treatment (Photocoagulation):

Yuzawa described laser photocoagulation in 47 PCV eyes [28]. The percentages of increased or stable vision after 1–3 years was 90% when BVN and polyps were treated and reduced to 75% when only polyps were treated. Thus, laser photocoagulation of both BNV and polyps was recommended.Vision deterioration was due to recurrent serosanguineous detachment and development of classic CNV.

Shiraga et al. [29] described laser treatment of extrafoveal peripapillary PCV. BVN and polyps were coagulated using a 689 nm wavelength laser and the beam focussed on the RPE beneath the detachment until a grayish-white lesion was attained. Follow-up was 27 months (mean), mean visual acuity did not change significantly, subretinal fluid resolved 1 month after laser treatment.

Drawbacks of laser treatment are scotomas induced by laser scars, risk of RPE-rip, partially obscured polyps beneath hemorrhagic areas and the lacking possibility to treat hemorrhagic areas directly. However, laser photocoagulation may be an option in eccentric active PCV areas without hemorrhagic PEDs.

6.4.2 PDT

When performing PDT, the whole lesion of BVN and polyps has to be treated. However, there is no consensus on optimal disease management, and PDT dosing including possible combination therapy with anti-VEGF compounds are still under investigation [30].

PDT treatment of PEDs induced by PCV is a challenge: it is easy when PEDs are small, polyps/BVN are clearly visible (Figs. 6.4, 6.18), and PDT laser area can cover BVN as well as polyps. However, PDT treatment is impossible if polyps are obscured by hemorrhage/PED or if the whole lesion is very large (Figs. 6.1c, d, 6.6, 6.9 upper row, 6.11, and 6.12). Treating only visible polyps and BVN of the patient in Fig. 6.12, left side, (Fig. 6.13 with OCT) would include most parts of the inhomogeneously vascularized PED inducing a high risk of RPE tear and hemorrhage. The same holds true after progression as shown in Fig. 6.17a-c: PDT would then have to include all PEDs and needles.

6.4.3 Anti-VEGF Treatment

Ueno et al. [31] examined PCV lesions treated with ranibizumab alone, using ICGA and OCT. At 3 months, 35% (26 eyes) resolved on ICGA, but 67% (33 eyes) had persistent lesions on ICGA and OCT.

Kang and Koh [32] reported a more than 3-year follow-up study with ranibizumab alone. BCVA was significantly improved by 1 month and could be maintained

up to 12 months, then deteriorated. Mean number of injections were 11.45 ± 7.81 during the mean follow-up of 43 months, mean CRT decreased from 368 to 294 μm, but 67% of eyes showed recurrence of PCV.

Doubling the dose of ranibizumab (2.0 mg instead of 1 mg) lead to higher rates of polyp closure (79% vs. 38%) and better resolution of subretinal fluid (82% vs. 66%) over 12 months; however, BVN persisted and visual results did not reflect these anatomic results (Kokame, PEARL-study [33], Kokame, PEARL-2-study [34]).

Comparing monotherapy of ranibizumab based on PrONTO OCT criteria versus monotherapy vPDT, the LAPTOP-study, a phase IV, 24-month study showed that VA improvement was significantly greater with ranibizumab compared to vPDT. Complete resolution of polyps in ICGA, however, was achieved in 77% with vPDT and in 61% with ranibizumab, growth of PCV after PDT was seen in 9%, and in 6% after ranibizumab [35].

Another anti-VEGF compound, aflibercept, is being used increasingly for PCV and PCV-associated PED. In a short-term efficacy study (16 eyes, 6 months) of aflibercept monotherapy (Inoue et al. [36], initially three times aflibercept followed by aflibercept every 2 months) 75% of the polyps were closed in ICGA but only 13% showed a decrease in size. Of the nine eyes with PED, five had complete resolution, while four exhibited only a partial decrease. 14 of 15 eyes with subretinal fluid showed complete resolution (93.3%). Similar results were obtained in another 6 months study by Hosokawa et al. [37]. However, in contrast to the polyps, BVN was resistant to aflibercept.

6.4.4 Combination Treatment (vPDT and anti-VEGF)

Kang et al. [38] reported the long-term outcome of vPDT with or without additional anti-VEGF treatment of PCV after 5 years. vPDT was administered when polypoidal lesions with exudative changes were observed by ICGA, and intravitreal anti-VEGF was given when exudative changes were observed with no definite polypoidal lesions.

Recurrence was noted in 33 eyes (78.6%) during follow-up. After 60 months, mean BCVA was improved in 33.3%, stable in 54.8%, and decreased 11.9%, with mean VA improving from 0.16 to 0.2. Mean recurrence interval after first remission was 25.2 months. The extent of abnormal branching vascular network was stable in 5 eyes and enlarged in 28/36 eyes at the 60-month follow-up with respect to baseline observations. Among the 28 eyes showing an expanded abnormal branching vascular network, 25 of them had new polypoidal lesions in the periphery of their abnormal vascular networks. The authors considered vPDT (with additional anti-VEGF as needed) an effective treatment for PCV despite the high recurrence rate.

Wong et al. [39] treated patients starting with half-dose vPDT to avoid atrophy. vPDT was given within 7 days after intravitreal ranibizumab. If disease activity was seen on OCT, ranibizumab was further given after a certain therapeutic algorithm.

After 1 year, there was no closure but regression of polyps in ICGA, increase in VA and decrease in CRT, achieved with 1–3 PDTs and 1–7 ranibizumab injections, with best results for lesions with only one polyp.

The EVEREST study started in 2008 with Asian patients is the first multicenter, double-masked, randomized, controlled trial with an angiographic (not OCT defined) treatment outcome designed to assess the effect of Verteporfin PDT alone (vPDT, treatment of the whole lesion: BVN plus polyps) or in combination with ranibizumab (vPDT-R) compared to ranibizumab alone (R) in patients with symptomatic macular PCV [40, 41]. It was shown that a complete polyp regression (=no flow in ICGA) was achieved in 78% (vPDT-R), 72% (vPDT) and 29% (R), respectively. Ranibizumab alone was nevertheless effective in the absorption of subretinal fluid. VA improved after 6 months by an average of 11 letters (vPDT-R), 8 letters (vPDT), and 9 letters (R) from baseline. Thus, complete polyp closure does not seem to be necessary to gain vision. The authors therefore recommended vPDT therapy in the initial treatment phase in all active lesions. Combination therapy with ranibizumab was advocated if there was:

– leakage from BVN and polyps
– large exudation associated with PED
– ICGA features ambiguous between PCV and CNV
– lesions were a combination of PCV and typical CNV.

Monthly reexamination should be performed in the first 3 months, with repeated FA, ICGA, and OCT every 3 months. vPDT retreatment was recommended if there was incomplete regression of polyps in ICGA. In case of leakage on FA or OCT signs of activity (subretinal fluid, PED) or significant decrease in visual acuity (5 letters), retreatment with ranibizumab was recommended.

Classification of different PCV types in the same study showed that therapy outcome was best in PCV with polyps showing only interconnecting vessels, followed by PCV with BVN without leakage and was worst in PCV with BVN and leakage [42].

Anti-VEGF therapy may influence activity of the polyps with following resolution of associated PED, but often the polyps themselves cannot be resolved (Fig. 6.16) even after repeated vPDT in combination with anti-VEGF: ICGA showed no flow in the polyps of Fig. 6.18 after vPDT, but in OCT the polyps were still present, although slowly regressing in height. The behavior of the lesions over time in Fig. 6.21 shows how PCV progresses from the middle of the scan to the left side, although treated with anti-VEGF: the needle on the left is growing upward first (b) as a second presumed polyp nearby arises to the right. The next PEDs arise to the left (c-d) and the original needle is collapsing (d) indicating progress of BVN and resolved polyps. Vascularisation of the highest PED progresses to the left (e) and this PED was reduced after therapy switch (f-h), but after 5 years the BVN in the middle of the scan is leaking persistently (h). The appearance of “walking needles into the periphery” in Figs. 6.16 and 6.21 seems to be a typical behavior of PCV lesions.

Kokame [33] recommends concerning therapy:

– Patient asymptomatic and without visual loss: wait

Otherwise,

– VA equal or better than 20/50: anti-VEGF therapy alone (risk of hemorrhage after vPDT)
– VA equal or worse than 20/60: vPDT or vPDT plus anti-VEGF
– persistent leakage despite resolution of polyps after vPDT: continue with anti-VEGF in between the potential 3-monthly vPDT.

Thus, anti-VEGF on an "as needed" basis may be a good choice and needs only simple fundus/OCT criteria (hemorrhage, fluid, PED height). ICGA can be performed from time to time, but not based on a rigid 3-monthly basis. As an example: Hemorrhages at the rim of the lesions were treatable with anti-VEGF alone (Fig. 6.1a).

After therapy:

– exudation (neurosensory detachment, cysts) may vanish with or without resolved PED
– PED may be unchanged or regresses in part or totally down to the height of BVN tissue
– vascularization of PED may progress radially
– new PEDs or needles with or without connection to the old PED, may be seen, which in turn may regress with time partially or completely ("walking PEDs") (Figs. 6.16, 6.21)
– BVN may remain unchanged
– even old PCV lesions may change to activity at their rim with massive hemorrhage (same as in disciforme scars)

Individualized treatment plans are necessary as the disease course can vary in many aspects over time. One possibility seems to be a Treat and Extend regimen [43]. Most probably, other or additional agents will help to optimize PCV treatment, e.g., longer lasting anti-VEGF agents in combination with other antibodies.

Our own experience is that visual acuity decreased from 0.4 to 0.33 during a mean time of observation after first therapy of 72 months. In maintenance phase, we treated our patients with vPDT and/or anti-VEGF (ranibizumab, aflibercept) based mainly on OCT and fundus criteria reducing the burden of many invasive examinations (FA/ICG): retreatment if PED progresses or hemorrhages and exudation in OCT occur. Patients received a mean of 1.9 vPDT treatments in total and 3.5 anti-VEGF treatments/year. Switching between aflibercept and ranibizumab showed no consistent outcome. In five patients, there was spontaneous absorption of persistent subretinal fluid. Poor outcome of visual acuity may be due to increased examination intervals. This emphasizes again the need for a strict regimen with monthly examinations.

6.5 Differential Diagnosis

The differentiation from CNV may be very difficult (Fig. 6.22). Often, patients are diagnosed as occult CNV in AMD if only FA is performed. But even if ICGA is additionally performed, PCV diagnosis may be missed if only leaking BVN with small protrusions along choroidal vessels below Bruch's membrane is found at the beginning. When polyps appear in later ICGA examinations, diagnosis is changed to PCV.

Chronic CSCR can be confused with PCV as some PEDs or atrophic areas may be round and bright in FA/ICGA. But ICGA does not show a BVN in chronic CSCR. Nevertheless, secondary PCV may arise.

An RPE tear may also lead to massive hemorrhage subretinal, but there are no polyps in FA/ICGA.

The hot spot in early stages RAP-lesion showing a small hyperfluorescence in FA and ICGA may be mistaken for a PCV lesion, but mostly a visible anastomosis can be shown in ICGA.

At first sight in Fig. 6.23, there may be a macroaneurysm at the upper arcade, but OCT clearly depicts two polyps covered by PE.

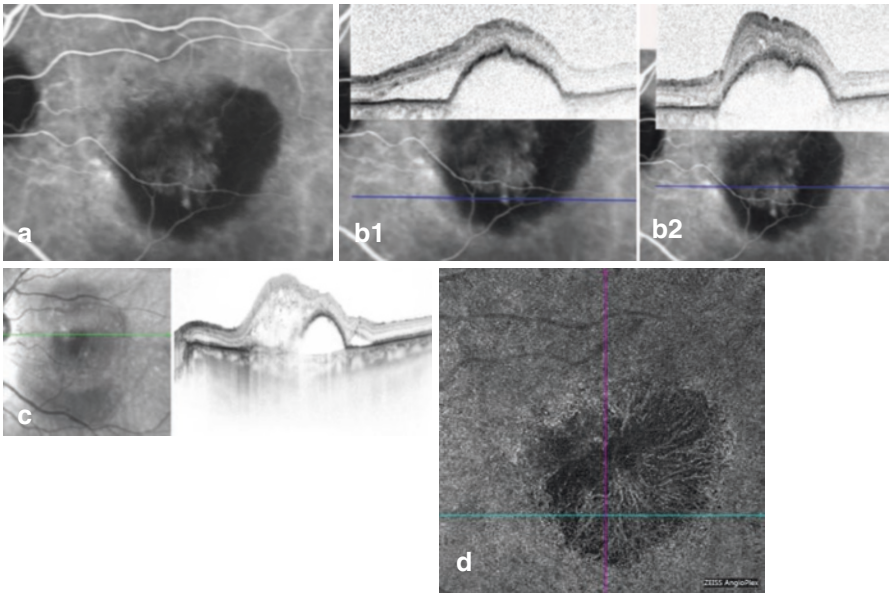

Fig. 6.22 Another patient with PED and suspected PCV due to ICGA findings (time 03:53, (**a**)). (**b**) ICGA 07:53 as before (*left*) and overlays with OCT (**b1**, **b2**): Protrusion/OCT notch at the top of PED where the suggested polyp is located (*upper middle*) and OCT notch at the right edge of CNV (material below PE of PED, *right*). Also, the double layer sign is present (OCT, **c**). Thus, a PCV was assumed and vPDT was applied, but 2 months later the lesion has grown with CNV appearance reaching the boundaries of the PED ((**d**), OCTA). In conclusion, the lesion before vPDT was not a PCV (with polyp) but a CNV (or PCV without polyp) instead, not responding to vPDT

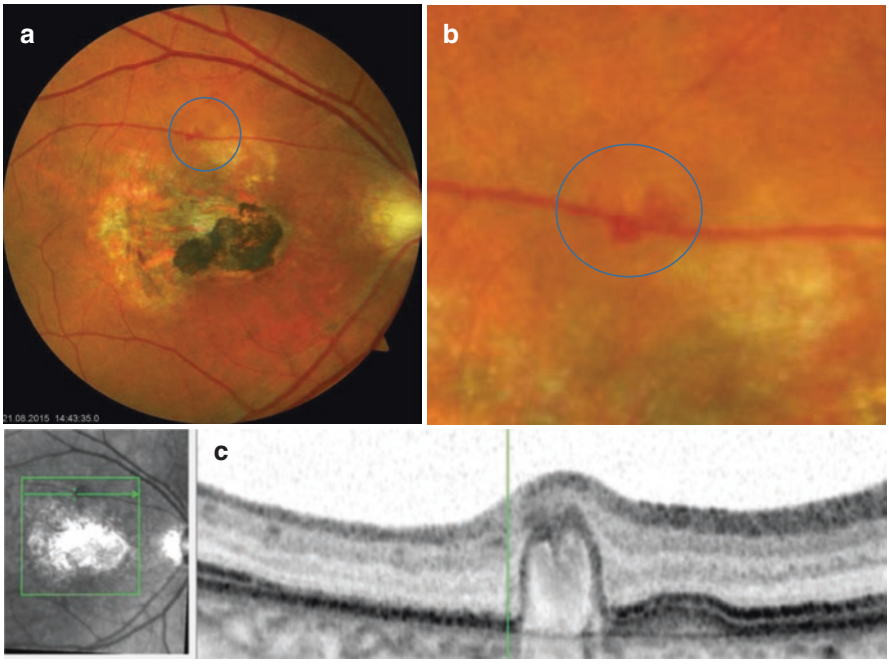

Fig. 6.23 Another patient: Above the central scar, two reddish lesions (encircled, **a**, **b**, nodules) near a retinal vessel are not macroaneurysms as the OCT scan below (**c**) shows polyps (with 2 notches), enclosed by PE, which excludes the possibility of retinal macroaneurysms.6.6

6.6 Natural History

Summary PCV is a very inhomogenous sub-division of exudative maculopathies with features ranging from only slight disturbances as in occult CNV to devastating and extensive exudative and hemorrhagic lesions comprising the whole posterior pole. The suspicion of possible PCV should always be raised in patients with multiple different features (edema, hemorrhages, hard exudates) and in patients not showing the expected results under anti-VEGF-therapy alone. Supplementary ICGA should then always be performed

References

1. Stern RM, Zakov AN, Zegarra N, et al. Multiple recurrent serosanguineous retinal pigment epithelial detachments in black women. Am J Ophthalmol. 1985;10:560–9.
2. Kleiner RC, Brucker AJ, Johnston RL. The posterior uveal bleeding syndrome. Retina. 1990;10:9–17.
3. Gass JDM. Diseases causing choroidal exsudative and hemorrhagic localized (disciform) detachment of the retina and retinal pigment epithelium. In:Stereoscopic atlas of macular diseases, vol. 1. 4th ed. London: Mosby; 1997. p. 250–1.

4. Yannuzzi LA, Sorenson J, Spaide RF, et al. Idiopathic polypoidal choroidal vasculopathy (IPCV). Retina. 1990;10:1–8.
5. Spaide RF, Yannuzzi LA, Slakter JS, et al. Indocyanine green videoangiography of idiopathic polypoidal choroidal vasculopathy. Retina. 1995;15:100–10.
6. Yannuzzi LA, Ciardella A, Spaide RF, et al. The expanding clinical spectrum of idiopathic polypoidal vasculopathy. Arch Ophthalmol. 1997;115:478–85.
7. Imamura Y, Engelbert M, Iida T, et al. Polypoidal choroidal vasculopathy. Surv Ophthalmol. 2010;55:501–15.
8. Ciardella AP, Donsoff IM, Huang SJ, et al. Polypoidal choroidal vasculopathy. Surv Ophthalmol. 2004;49:25–37.
9. Hatz K, Prünte C. Polypoidal choroidal vasculopythy in Caucasian patients with presumed neovascular age-related macular degneration and poor ranibizumab response. Br J Ophthalmol. 2014;98:188–94.
10. Cho JH, Ryod NK, Cho KH, et al. Incidence rate of massive submacular hemorrhage and its risk factors in polypidal vasculopathy. In: Abstract, ARVO 2016; 2016.
11. Honda S, Matsumiya W, Negi A. Polypoidal choroidal vasculopathy: clinical features and genetic predisposition. Ophthalmologica. 2014;231:59–74.
12. Iwama D, Tsujikawa A, Sasahara M, et al. Polypoidal choroidal vasculopathy with drusen. Jpn J Ophthalmol. 2008;52:116–21.
13. Kuroiwa S, Tateiwa H, Hisatomi T, et al. Pathologic features of surgically excised polypoidal choroidal vasculopathy membranes. Clin Exp Ophthalmol. 2004;32:297–302.
14. Yuzawa M, Mori R, Kawamura A. The origins of polypoidal choroidal vasculopathy. Br J Ophthalmol. 2005;89:602–7.
15. Nakajima M, Yuzawa M, Shimada H, et al. Correlation between indocyanine green angiographic findings and histopathology of polypoidal choroidal vasculopathy. Jpn J Ophthalmol. 2004;48:249–55.
16. Nakashizuka H, Mitsumata M, Okisaka S, et al. Clinicopathologic findings in polypoidal choroidal vasculopathy. IOVS. 2008;49:4729–37.
17. Tan CS, Ngo WK. Predictive features of polypoidal choroidal vasculopathy detected using fluorescein angiography. In: Abstract from ASCRS, ASOA Sympoium and Congress; 2015 Apr 17–21; San Diego.
18. Coscas G, Yamashiro K, Coscas F, et al. Comparison of exudative age-related macular degeneration subtypes in Japanese and French patients: Mulicenter diagnosis with multimodal imaging. Am J Ophthalmol. 2014;158:309–18.
19. Tan CS, Ngo WK, Chen JP, et al. EVEREST study report 2: imaging and grading protocol, and baseline characteristics of a randomised controlled trial of polypoidal choroidal vasculopathy. Br J Ophthalmol. 2015;99(5):624–8. doi:10.1136/bjophthalmol-2014-305674.
20. Byeon SH, Lee SC, HS O, et al. Incidence and clinical patterns of polypoidal choroidal vasculopathy in Korean patients. Jpn J Ophthalmol. 2008;52:57–62.
21. Tsujikawa A, Sasahara M, Otani A, et al. Pigment epithelial Detchment in polypoidal choroidal vasculopathy. Am J Ophthalmol. 2007;143:102–11.
22. Shaimov T, Panova I. Diagnostic capabilities of polypoidal choroidal vasculopathy in the absence of indocyanine green angiography. Poster presented at 14th EURETINA Congress; 2014; London.
23. de Salvo G, Vaz-Pereira S, Keane PA, et al. Sensitivity and specificity of spectral-domain optical coherence tomography in detecting idiopathic polypoidal choroidal vasculopathy. Am J Ophthalmol. 2014;158:1228–38.
24. Lim LW, Tan CS, Chay IW, et al. Optical coherence tomography angiography features of polypoidal vasculopathy and its correlation with indocyanine green angiography. In: Abstract, ARVO 2016; 2016.
25. Uyama M, Wada M, Nagai Y, et al. Polypoidal choroidal vasculopythy: natural history. Am J Ophthalmol. 2002;133:639–48.
26. Sho K, Takahashi K, Yamada H, et al. Polypoidal choroidal vasculopathy: incidence, demographic features, and clinical characteristics. Arch Ophthalmol. 2003;121:1392–6.

27. Cheung CMG, Yang E, Lee WK, et al. The natural history of polypoidal choroidal vasculopathy: a multi-center series of untreated Asian patients. Graefes Arch Clin Exp Ophthalmol. 2015;253:2075–85.
28. Yuzawa M, Mori R, Haruyama M. A study of laser photocoagulation for polypoidal vasculopathy. Jpn J Ophthalmol. 2003;47:379–84.
29. Shiraga F, Shirakata Y, Shiragami C, et al. Laser photocoagulation sparing the Papillomacular bundle for peripapillary polypoidal choroidal vasculopathy lesions. Austin J Clin Ophthalmol. 2014;1:1015–3.
30. Wong CW, Wong TY, Cheung CMG. Polypoidal choroidal vasculopathy in Asians. J Clin Med. 2015b;4:782–821.
31. Ueno C, Gomi F, Sawa M, et al. Correlation of indocyanine green angiography and optical coherence tomography findings after intravitreal ranibizumab for polypoidal choroidal vasculopathy. Retina. 2012;32:2006–13.
32. Kang HM, Koh HJ. Long-term visual outcome and prognostic factors after intravitreal ranibizumab injections for polypoidal choroidal vasculoparthy. Am J Ophthalmol. 2013;156:652–60.
33. Kokame GT, Yeung L, Teramoto K, et al. Polypoidal choroidal vasculopathy, exudation and hemorrhage: results of monthly ranibizumab therapy at one year. Ophthalmologica. 2014;231:94–102.
34. Kokame GT. Prospective evaluation of subretinal vessel location in polypoidal choroidal vasculopathy and response of hemorrhagic and exudative PCV to high-dose Antiangiogenic therapy. Trans Am Ophthalmol Soc. 2014;112:74–93.
35. Oishi A, Kojima KH, Mandai M, et al. Comparison of the effect of ranibizumab and verteporfin for polypoidal choroidal vasculopathy: 12-month LAPTOP study results. Am J Opthalmol. 2014;156:644–51.
36. Inoue M, Arakawa A, Yamane S. Short-term efficacy of intravitreal aflibercept in treatment-naïve patients with polypoidal choroidal vasculopathy. Retina. 2014;34:2178–84.
37. Hosokawa M, Shiraga F, Yamashita A, et al. Six-month results of intravitreal aflibercept injections for patients with polypoidal choroidal vasculopathy. Br J Ophthalmol. 2015; doi:10.1136/bjophthalmol-2014-305275.
38. Kang HM, Kim YM, Koh HJ. Five-year follow-up results of photodynamic therapy for polypoidal choroidal vasculopathy. Am J Ophthalmol. 2013;155:438–47.
39. Wong IY, Shi X, Gangwani R, et al. 1-year results of combined half-dose photodynamic therapy and ranibizumab for polypoidal choroidal vasculopathy. BMC Ophthalmol. 2015;15:66–72.
40. Koh AHC, Lee WK, Chen LJ, et al. EVEREST study: efficacy and safety of verteporfin photodynamic therapy in combination with ranibizumab or alone versus ranibizumab monotherapy in patients with symptomatic macular polypoidal choroidal vasculopathy. Retina. 2012;32:1453–64.
41. Koh AHC, Chen LJ, Chen SJ, et al. Polypoidal vasculopathy: evidence-based guidelines for clinical diagnosis and treatment. Retina. 2013;33:686–716.
42. Tan CS, Lim LW, Ngo WK. Comparison of treatment outcomes among subtypes of polypoidal choroidal vasculopathy in a multicenter randomized controlled study (EVEREST study). In: Abstract, ARVO 2016; 2016.
43. Lee SJ, Pak KY, Byon IS. Treat-and-extend regimen using ranibizumab for polypoidal choroidal vasculopathy: one year results. In: Abstract, ARVO 2016; 2016.

Chapter 7
Retinal Pigment Epithelial Tears: Clinical Review and Update

Christoph Roman Clemens and Nicole Eter

7.1 Introduction

Retinal pigment epithelium (RPE) tears are known to occur as a natural result in the course of retinal pigment epithelial detachment (PED) because of underlying choroidal neovascularization (CNV), retinal angiomatous proliferation, or polypoidal choroidal vasculopathy. They represent a rare complication in exudative AMD; however, they frequently result in a devastating loss of visual acuity [1–3]. Since the beginning of intravitreal anti-VEGF therapies in patients with PED due to exudative AMD, the incidence of RPE tears has increasingly been reported as a complication after injection. Meanwhile, the evolution of retinal imaging has significantly contributed to a better understanding of RPE tear development. In the light of an increasing number of intravitreal injections, clinicians face more frequently the question of RPE tear prevention as well as the treatment after tear formation. Thus, this chapter shall highlight current aspects on RPE tear development, predictive factors, and treatment strategies before and after RPE tear formation.

7.2 Epidemiology

In 1981, Hoskin and coworkers firstly identified RPE tears as a complication in patients with PED due to AMD [4]. RPE tears can be either part of the natural course of a vascularized PED (vPED) or they can occur in association with various treatments such as photodynamic therapy, laser photocoagulation, or

C.R. Clemens, M.D. (✉) • N. Eter
Department of Ophthalmology, University of Münster Medical Centre,
Domagkstrasse 15, 48149 Münster, Germany
e-mail: Christoph.Clemens@ukmuenster.de; Nicole.Eter@ukmuenster.de

M.A. Gamulescu et al. (eds.), *Retinal Pigment Epithelial Detachment*,
DOI 10.1007/978-3-319-56133-2_7

transpupillary thermotherapy [5–7]. The incidence for RPE tears is reported to be between 5 and 27% in the elderly during different observation periods [1–21]. Casswell reported a spontaneous tear rate of vPED of 10% during a follow-up of 1 year or more [1]. In today's clinical routine, most RPE tears seem to be closely associated with anti-VEGF treatments and have been reported for the substances pegaptanib, bevacizumab, ranibizumab, and aflibercept [8–11]. A broad variety of RPE tear incidences are reported under different treatment agents and various treatment regimens [12–22]. For instance, a large retrospective 1-year study of 1280 eyes treated with bevacizumab included 125 eyes with a vPED showing a RPE tear rate of 16.8% [12]. In a case series with 22 patients with vPED treated with pegaptanib, six patients developed RPE tears during the first injections [13]. Clemens and coworkers reported a tear incidence of 25% in a prospective 1-year study of a monthly ranibizumab regimen in 40 patients with vPED [14]. Recently, Sarraf et al. presented results from a prospective randomized study on 0.5 or 2.0 mg ranibizumab therapy based on a monthly or pro re nata regimen in eyes with vPED that showed an incidence of 14% (5/37 patients). Interestingly, four out of the five reported RPE tears occurred in the high-dosage group [15]. Up to date, there is no prospective data available on the RPE tear rate in vPED patients under a treatment of aflibercept [11].

Notably, reported incidences of RPE tears in the literature must be interpreted cautiously as underlying patient collectives, treatment regimen as well as nomenclature of morphologic lesions tend to be very heterogeneous. Although there is no comparative study between natural course and therapy, it appears likely that risk of RPE tears is increased under anti-VEGF therapy.

7.3 Imaging

7.3.1 Color Fundus Photography

Sarraf and coworkers introduced an RPE tear grading system including color fundus photography (CFP) [22]. Grade 1 tears were defined as <200 μm. Grade 2 tears were between 200 μm and 1-disk diameter. Grade 3 tears were >1-disk diameter. Grade 4 tears were defined as Grade 3 tears that involved the center of the fovea.

An RPE tear may be suspected based on an often well-defined hyperpigmented line at the site of the rolled RPE, and a depigmented area corresponding to the exposed choroid (Fig. 7.1a) [4]. Compared to other modalities, CFP allows to clearly differentiate retinal or subretinal hemorrhages from RPE tear areas. In contrast, in fundus autofluorescence (FAF), hemorrhages block the autofluorescent properties of the retina, which often interferes with a distinct RPE tear area detection. This makes CFP indispensable in this entity.

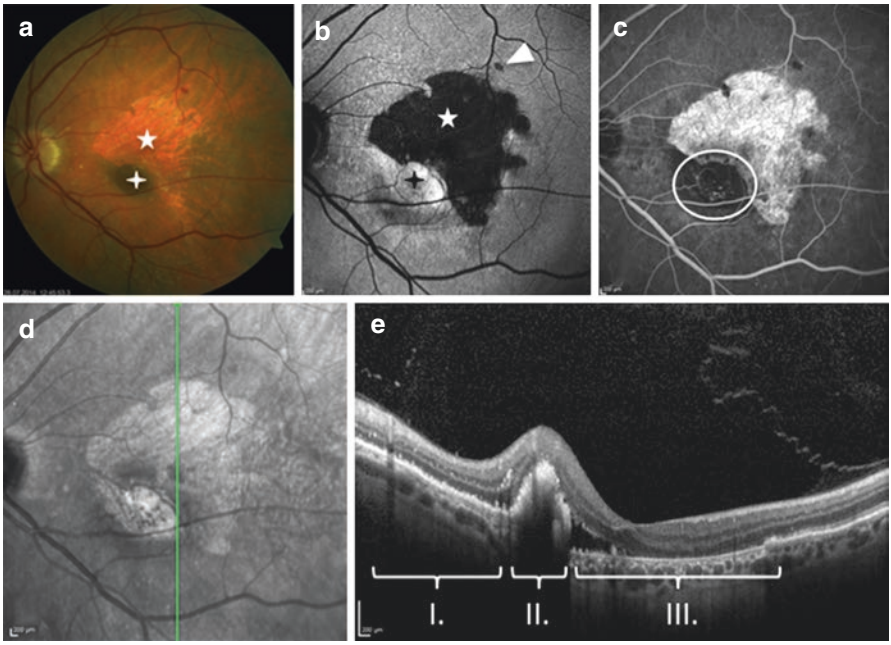

Fig. 7.1 Multimodal imaging of an exemplary patient with vascularized pigment epithelial detachment (vPED) due to age-related macular degeneration after retinal pigment epithelium (RPE) tear development. (**a**) Color fundus photography shows a depigmented area corresponding to the exposed choroid (*star*) and a hyperpigmented area corresponding to the enrolled RPE (*diamond*). (**b**) Confocal scanning laser ophthalmoscopy (cSLO) fundus autofluorescence (FAF) image shows a large sharply delineated, hypoautofluorescent signal in the RPE tear area (*star*) as well as a hyperautofluorescent area corresponding to the enrolled RPE (*diamond*). (**c**) Late phase fluorescein angiography reveals choroidal neovascularization (CNV) in the inferior part of the lesion (*circle*) and a hyperfluorescent signal in the tear area. Notably, RPE tear has occurred at the opposite side of CNV localization. (**d**, **e**) Combined cSLO near-infrared image and spectral-domain optical coherence tomography (SD-OCT) scan showing a normal architecture of the outer retinal bands in the first part. In the second part, the free edge of torn RPE is being retracted towards the CNV. Note the missing RPE band in the RPE tear area representing the third part

7.3.2 Fundus Autofluorescence

In FAF imaging, areas of RPE tears exhibit a markedly reduced autofluorescent signal because RPE cells with fluorescent lipofuscin are lost in the tear area [23]. Small RPE tears are more evident in FAF and are easier to detect than in CFP—in cases without associated hemorrhage. The high contrast of these reduced autofluorescent areas, compared with the intact RPE, allows for an easy and accurate determination of lesion boundaries, especially in recent tears (Fig. 7.1b). The configuration of RPE tears is classified as unilobular if RPE areas are homogeneously formed and as multilobular if RPE defects consist of two or more lobes separated by a piece of

intact RPE [24]. Over time, edges of reduced autofluorescence become hazier and less demarcated in FAF imaging. Remodeling processes at the border zone do not seem to be detectable by FAF imaging during the first few months [25]. Reduced autofluorescent areas in FAF due to RPE tear formation do not show patterns of abnormally increased FAF in the junctional zone of atrophy as it was previously described in geographic atrophy (GA) due to AMD [26].

7.3.3 Fluorescein Angiography

In 2010, Sarraf et al. described a thin defect at the margin of the PED with a subtle ring sign of hyperfluorescence in fluorescein angiography (FA). This observation was found in RPE tears grade one and represents a microscopic RPE defect detectable in corresponding OCT scans. Lesions >200 μm present angiographically as small oval hyperfluorescent defects at the edge of PED with early transmission and late staining and a subtle inner edge of hypofluorescent blockage. Larger RPE tears show a large crescentic area of early transmission hyperfluorescence with an adjacent patch of hypofluorescent blockage at the site of the rolled RPE (Fig. 7.1c) [22].

7.3.4 SD-OCT

Looking at an SD-OCT scan, three parts of an RPE tear can be distinguished. In the first one, the outer retinal bands show a normal architecture. In the second part, the retina forms a dome-shaped detachment from the choroid. In this elevated zone, SD-OCT shows the free edge of a wavy, contracted RPE being retracted towards the CNV. The rolled RPE causes a hyperreflectivity and an intense back-shadowing, which completely masks the choroid. In the third part, the RPE is completely absent and the neurosensory retina appears thinned. SD-OCT demonstrates an increased depth signal due to the absent RPE monolayer (Fig. 7.1d). In some cases, an exudative reaction between the neurosensory retina and the choroid can be visualized in the follow-up after the acute event. In other cases, the neurosensory retina remains directly on the choroid [27].

7.4 Mechanism of RPE Tear Formation

For many years, numerous authors have postulated a RPE tear mechanism based on contraction of fibrovascular membranes [28–31]. Arevalo firstly described an increase in fibrovascular traction under anti-VEGF treatment in patients with proliferative diabetic retinopathy [32]. Later on in the anti-VEGF era, an increase in the RPE tear incidence in AMD patients was interpreted as a confirmation of the

established theory of traction forces causing the tear event. Contraction of CNV membranes induces shrinkage of the RPE, which may cause an increased tension on the surface of the cavity. During this process, two opposite forces are acting on the marginal RPE: traction forces from CNV contraction and adhesive forces from the RPE that is still attached. The increase in contraction eventually results in the anatomic failure of the RPE at the junction of attached and detached RPE [27, 33].

Contracture of this CNV adherent to the undersurface of the RPE applies the maximum traction at the junction of the attached and detached RPE representing the "locus minoris resistentiae" and lying perpendicular to the CNV's contraction force. The contracted RPE monolayer comes to rest on the side of the CNV, the origin of contraction, which becomes evident in SD-OCT or as increased autofluorescence in FAF.

RPE tear formation in fibrovascular PED, in which the lesion cavity is entirely filled by the CNV membrane, is less frequent presumably as contraction forces in response to an anti-VEGF therapy may spread evenly over the entire PED lesion exposing the RPE monolayer to less mechanical stress. Interestingly, RPE tears in patients under anti-VEGF therapy tend to occur within 1–3 months of the beginning of intravitreal treatment whereas late onset RPE tears tend to occur in treatment-naive patients or in patients treated with PDT [16].

7.5 Predicting Factors

The identification of reliable risk factors of RPE tears is of great clinical importance. So far, several prognostic markers for an impending RPE tear have been described: (a) PED lesion's height and diameter, (b) a small ratio of CNV size to PED size, (c) hyperreflective lines in near-infrared images, (d) subretinal clefts, (e) microrips, and (f) duration of PED.

(a) Chan and coworkers postulated PED height to represent a predictor of RPE tears. They reported an increased prevalence of RPE tears in PED lesions higher than 400 μm [12]. Several other authors addressed the issue of at what cutoff point PED height becomes a risk factor. Doguizi et al. statistically determined that 580 μm may be regarded as the cutoff point of PED height for the risk of an RPE tear [18]. Similarly, Sarraf et al. described a height of 550 μm as a high-risk factor for the subsequent development of an RPE tear. Leitritz and coworkers additionally described an increasing probability of RPE tears particularly beyond the height of 400 μm [15, 34]. Chiang et al. hypothesized that an increased surface area and a large linear diameter of a subfoveal PED both represent predisposing factors for RPE tear development (Fig. 7.2a) [19].
(b) Chan et al. reported a stronger tendency to tear development in those PED lesions that show a smaller ratio of CNV size to PED size (Fig. 7.2b) [21].
(c) Confocal scanning laser ophthalmoscopy (cSLO) near-infrared reflectance (NIR) images often reveal another predictive marker for an impending RPE

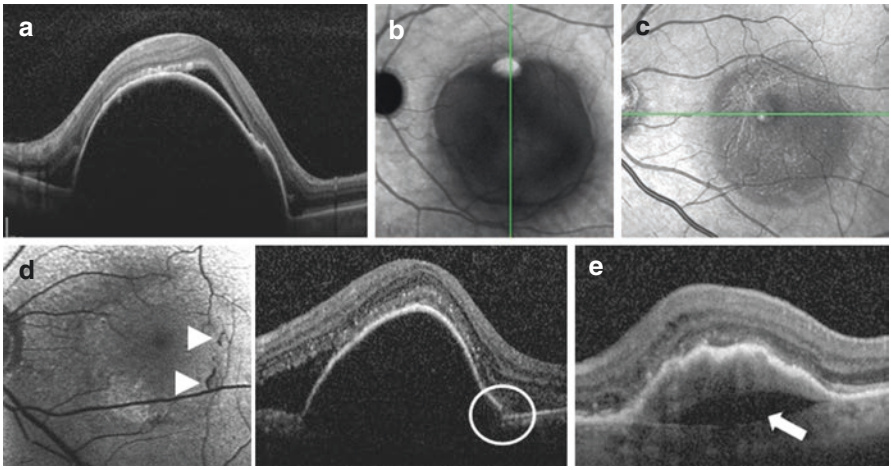

Fig. 7.2 Retinal pigment epithelium (RPE) tear risk factors in patients with vascularized pigment epithelial detachment (vPED) due to age-related macular degeneration. (**a**) Spectral-domain optical coherence tomography (SD-OCT) scan of a vPED lesion with both a large diameter and a large height. (**b**) Indocyanine green angiography image illustrating the concept of a small CNV/PED ratio. Hyperfluorescence superiorly represents a small choroidal neovascularization (CNV) while the round hypofluorescence represents the large dimensions of the vPED resulting in a small ratio. (**c**) Confocal scanning laser ophthalmoscopy (cSLO) near-infrared image of another vPED lesion shows hyperreflective lines originating from the edge of vPED that spread like a funnel across the lesion. (**d**) Combined cSLO fundus autofluorescence and SD-OCT of another patient depicting small hypoautofluorescences at the edge of a vPED indicating areas of microrips (*arrow heads*) that correspond to microscopic RPE defects detectable in the SD-OCT scan aside (*circle*). (**e**) Enhanced depth imaging SD-OCT scan showing a subretinal cleft. Arrow points to hyporeflective space underneath the sub-RPE neovascular tissue

tear. Hyperreflective lines that originate from the edge of PED lesions correspond to the CNV localization observed in angiography (Fig. 7.2c). Additionally, these hyperreflective lines in NIR correlate with folds in the RPE as detectable in corresponding SD-OCT scans [33]. These imaging findings illustrate the mechanical stress that the RPE is exposed to and that is caused by both CNV contraction and CNV relaxation.

(d) Another sign of increasing mechanic stress in the sub-RPE space is the subretinal cleft recently described by Mukai and colleagues as a hyporeflective space between choroidal neovascularization and Bruch's membrane under the PED. They reported the formation of this characteristic morphology prior to RPE tear development in three patients suggesting this SD-OCT characteristic as a potential risk factor (Fig. 7.2e) [35].

(e) Microrips of the RPE were firstly described as a leak at the edge of the RPE detachment with passage of fluorescein into the subretinal space [36]. Clemens et al. recently postulated to regard microrips as a RPE tear risk factor presenting a patient with microrips that developed a foveal RPE tear after one anti-VEGF injection. Microrips supposedly lower the threshold of RPE resistance and an

increase in contraction after anti-VEGF therapy may eventually result in the anatomic failure of the RPE (Fig. 7.2d) [37].

(f) Doguizi and coworkers reported an inverse relationship between the duration of PED and RPE tear formation. Based on their research, they postulate that a short duration of PED means that the neovascular process is fresh featuring immature vessels which are more susceptible to anti-VEGF agents resulting in more dramatic responses to anti-VEGF therapy [18]. Most RPE tears occur during the first three injections which additionally suggests that one should consider a pro re nata regimen with careful observation particularly during the uploading phase in high-risk PED patients.

In patients at risk for a RPE tear, it is recommended to perform a thorough examination including SD-OCT and FAF after each injection. If several predicting factors accumulate or single risk factors significantly grow during an anti-VEGF treatment, we postulate to pause the injection therapy, to re-evaluate the vPED lesion 1–2 weeks later, and to re-inject if signs of CNV contraction have declined, for instance, if RPE folds decline or hyperreflective lines disappear. Such an adapted regimen may make anti-VEGF therapy safer with regard to RPE tear development in vPED patients at high risk. Besides the issue of the most appropriate anti-VEGF agents for high-risk RPE tear patients, another unanswered question is whether a certain treatment regimen may be beneficial to adhere to regarding tear development in this patient group. Particularly patients that show predisposing factors must be informed about the chance of tear development during anti-VEGF treatment.

7.6 Therapy After Tear Formation

Controversy exists among clinicians regarding treatment criteria after formation of RPE tears.

Doguizi et al. found stable visual acuity results in 28 patients with continued anti-VEGF therapy after the formation of RPE tears within a mean follow-up period of 20.6 months. The mean number of anti-VEGF injections was 4.1 during this period. Final visual acuity was worse for the larger RPE tears (Grades 3 and 4) when compared with the smaller tears (Grades 1 and 2) which is in accordance with Sarraf and coworkers [18, 22]. A retrospective analysis of data from three phase III randomized, multicenter clinical trials of ranibizumab for the treatment of neovascular AMD showed that among patients who had an RPE tear, those treated with ranibizumab tended to have better improvements in visual acuity [38]. Similar functional results were reported by Coco and colleagues [39]. Improvements in visual acuity have also been reported in patients with spontaneous RPE tears who were subsequently treated with anti-VEGF therapy [40]. Recently, Bartels et al. reported a case of significant functional improvement in microperimetry and morphology after continuation of anti-VEGF therapy over 3 years because of persistent subretinal and intraretinal fluid after tear formation [41].

At present, an interventional multicenter trial is currently recruiting patients and investigates the effect of fixed monthly intravitreal injections of ranibizumab on visual acuity and retinal morphology over a study period of 12 months in 30 patients with an RPE tear due to neovascular AMD (ClinicalTrials.gov Identifier: NCT01914159). Reinjection after RPE tear has to be carefully evaluated as RPE tear area may increase significantly under anti-VEGF therapy. Asao and coworkers evaluated the effects of additional anti-VEGF therapy in ten eyes with a RPE tear after anti-VEGF therapy over 12 months. They observed an increase in RPE tear area size >20% in half of the included eyes [42]. Clemens et al. presented three patients initially presenting with a multilobular RPE tear revealing a significant enlargement of RPE tear with foveal involvement after another anti-VEGF injection (Fig. 7.3) [24].

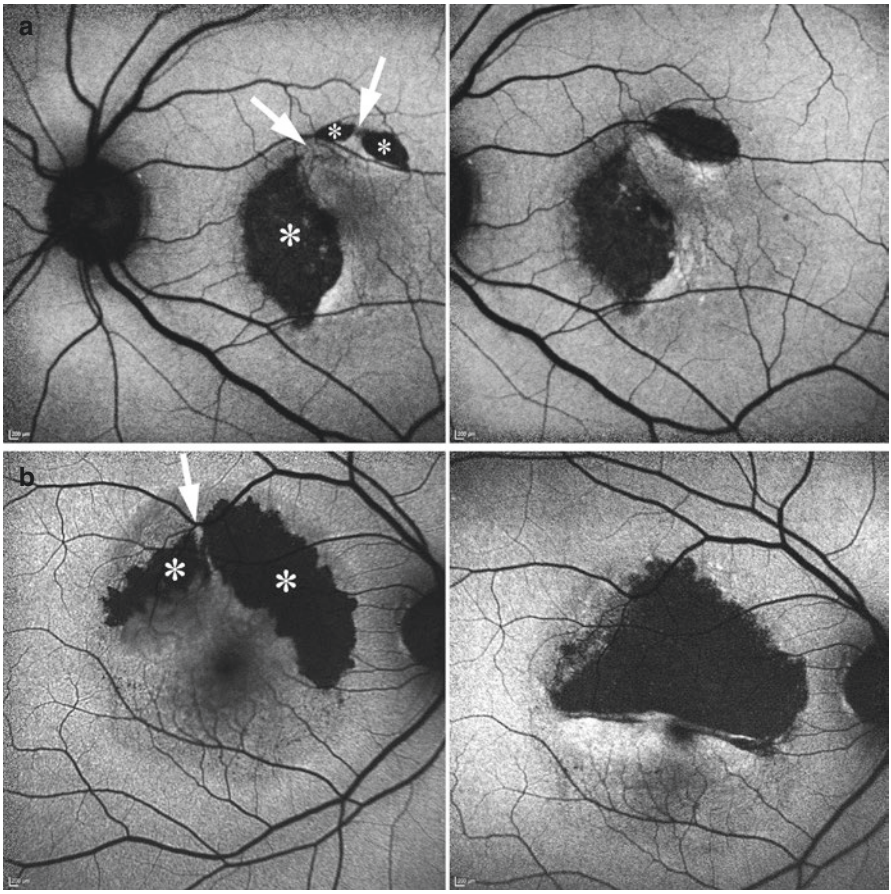

Fig. 7.3 Representative examples for a multilobular RPE tear area increasing under intravitreal therapy. (**a**) Fundus autofluorescence demonstrates an RPE tear consisting of three lobes (*stars*) with two RPE strands in between (*arrows*) and (**b**) shows an RPE tear consisting of two lobes (*stars*) with one RPE strand in between (*arrow*). Follow-up images on the right show a clear increase in RPE tear area, respectively

On the other hand, the same study showed that unilobular RPE tear defects remained stable during a 6-month follow-up period. Measuring RPE tear areas in these patients may have therapeutic consequences. If RPE tear area in multilobular lesions increases, intravitreal anti-VEGF therapy should be postponed and re-treatment should only be considered if signs of disease activity further increase. Currently, most retina experts recommend continuing anti-VEGF treatment after RPE tear development based on the presence of disease activity such as intra- or subretinal fluid.

Mukai et al. observed two types of repair processes after RPE tear development in a small imaging study of ten patients [43]. Firstly, persistent subretinal fluid after the tear event seems to lead to subsequent repair with a thickened proliferative tissue in the area where the RPE was lost. Secondly, if an early and complete resolution of subretinal fluid after RPE tear development is achieved, the outer retina appears to be directly attached to Bruch's membrane without an ingrowth of proliferative tissue along Bruch's membrane. These observations suggest a beneficial effect on macular morphology of a continuative anti-VEGF therapy after RPE tear development. Yet, whether the two repair mechanisms result in diverging functional results remains to be shown. Caramoy et al. analyzed RPE tissue remodeling in RPE tears based on FAF and SD-OCT imaging and observed evidence of resurfacing in small RPE tears, whereas RPE migration and proliferation may not occur in the right plane in large tears [44]. Transplantation of the RPE using human embryonic stem cells and induced pluripotent stem cell derived RPE is being developed and evaluated as a cell-replacement therapy for AMD. Further studies are needed to assess its potential to restore some of the lost RPE function in patients suffering from an RPE tear [45].

7.7 Summary

Due to a growing number of intravitreal anti-VEGF injections in AMD patients, the incidence of RPE tear formation has increased. Thus, clinicians must be aware of strategies to prevent RPE tear development during anti-VEGF therapy and to treat patients after RPE tear formation. After RPE tear formation, anti-VEGF treatment is recommended as long as activity signs are present. Multimodal imaging during anti-VEGF therapy in high-risk patients represents the key tool to detect risk factors and to make antiangiogenic treatment safer. Future studies must address several issues, such as, which anti-VEGF agent is most appropriate in high-risk vPED patients, which treatment regimen is most beneficial after RPE tear development, and in how far can retinal imaging be improved to visualize RPE tear risk factors as early as possible and to identify new characteristics indicating an impending RPE tear.

References

1. Casswell AG, Kohen D, Bird AC. Retinal pigment epithelial detachments in the elderly: classification and outcome. Br J Ophthalmol. 1985;69:397–403.
2. Yeo JH, Marcus S, Murphy RP. Retinal pigment epithelial tears. Patterns and prognosis. Ophthalmology. 1988;95:8–13.
3. Pauleikhoff D, Löffert D, Spital G, et al. Pigment epithelial detachment in the elderly. Clinical differentiation, natural course and pathogenetic implications. Graefes Arch Clin Exp Ophthalmol. 2002;240:533–8.
4. Hoskin A, Bird AC, Sehmi K. Tears of detached retinal pigment epithelium. Br J Ophthalmol. 1981;65:417–22.
5. Gelisken F, Inhoffen W, Partsch M, et al. Retinal pigment epithelial tear after photodynamic therapy for choroidal neovascularization. Am J Ophthalmol. 2001;131:518–20.
6. Gass JD. Retinal pigment epithelial rip during krypton red laser photocoagulation. Am J Ophthalmol. 1984;98:700–6.
7. Thompson JT. Retinal pigment epithelial tear after transpupillary thermotherapy for choroidal neovascularization. Am J Ophthalmol. 2001;131:662–4.
8. Singh RP, Sears JE. Retinal pigment epithelial tears after pegaptanib injection for exudative age-related macular degeneration. Am J Ophthalmol. 2006;142:160–2.
9. Shah CP, Hsu J, Garg SJ, et al. Retinal pigment epithelial tear after intravitreal bevacizumab injection. Am J Ophthalmol. 2006;142:1070–2.
10. Carvounis PE, Kopel AC, Benz MS. Retinal pigment epithelium tears following ranibizumab for exudative age-related macular degeneration. Am J Ophthalmol. 2007;143:504–5.
11. Saito M, Kano M, Itagaki K, et al. Retinal pigment epithelium tear after intravitreal aflibercept injection. Clin Ophthalmol. 2013;7:1287–9.
12. Chan CK, Abraham P, Meyer CH, et al. Optical coherence tomography-measured pigment epithelial detachment height as a predictor for retinal pigment epithelial tears associated with intravitreal bevacizumab injections. Retina. 2010;30:203–11.
13. Chang LK, Flaxel CJ, Lauer AK, et al. RPE tears after pegaptanib treatment in age-related macular degeneration. Retina. 2007;27:857–63.
14. Clemens CR, Wolf A, Alten F, et al. Monthly treatment of ranibizumab in vascular pigment epithelium detachment due to age-related macular degeneration. ARVO. 2015; Poster Number: 2838–C0066.
15. Sarraf D, Chan C, Rahimy E, et al. Prospective evaluation of the incidence and risk factors for the development of RPE tears after high- and low-dose ranibizumab therapy. Retina. 2013;33:1551–7.
16. Guber J, Praveen A, Saeed MU. Higher incidence of retinal pigment epithelium tears after ranibizumab in neovascular age-related macular degeneration with increasing pigment epithelium detachment height. Br J Ophthalmol. 2013;97:1486–7.
17. Smith BT, Kraus CL, Apte RS. Retinal pigment epithelial tears in ranibizumab-treated eyes. Retina. 2009;29:335–9.
18. Doguizi S, Ozdek S. Pigment epithelial tears associated with anti-VEGF therapy: incidence, long-term visual outcome, and relationship with pigment epithelial detachment in age-related macular degeneration. Retina. 2014;34:1156–62.
19. Chiang A, Chang LK, Yu F, et al. Predictors of anti-VEGF-associated retinal pigment epithelial tear using FA and OCT analysis. Retina. 2008;28:1265–9.
20. Wong LJ, Desai RU, Jain A, et al. Surveillance for potential adverse events associated with the use of intravitreal bevacizumab for retinal and choroidal vascular disease. Retina. 2008;28:1151–8.
21. Chan CK, Meyer CH, Gross JG, et al. Retinal pigment epithelial tears after intravitreal bevacizumab injection for neovascular age-related macular degeneration. Retina. 2007;27:541–51.

22. Sarraf D, Reddy S, Chiang A, et al. A new grading system for retinal pigment epithelial tears. Retina. 2010;30:1039–45.
23. von Rückmann A, Fitzke FW, Bird AC. Distribution of fundus autofluorescence with a scanning laser ophthalmoscope. Br J Ophthalmol. 1995;79:407–12.
24. Clemens CR, Alten F, Baumgart C, et al. Quantification of retinal pigment epithelium tear area in age-related macular degeneration. Retina. 2014;34:24–31.
25. Caramoy A, Fauser S, Kirchhof B. Fundus autofluorescence and spectral domain optical coherence tomography findings suggesting tissue remodelling in retinal pigment epithelium tear. Br J Ophthalmol. 2010;96:1211–6.
26. Bindewald A, Schmitz-Valckenberg S, Jorzik JJ, et al. Classification of abnormal fundus autofluorescence patterns in the junctional zone of geographic atrophy in patients with age related macular degeneration. Br J Ophthalmol. 2005;89:874–8.
27. Nagiel A, Freund KB, Spaide RF, et al. Mechanism of retinal pigment epithelium tear formation following intravitreal anti-vascular endothelial growth factor therapy revealed by spectral-domain optical coherence tomography. Am J Ophthalmol. 2013;156:981–8.
28. Chuang EL, Bird AC. The pathogenesis of tears of the retinal pigment epithelium. Am J Ophthalmol. 1988;105:285–90.
29. Gass JDM. Pathogenesis of tears of the retinal pigment epithelium. Br J Ophthalmol. 1984;68:513–9.
30. Toth CA, Pasquale III AC, Graichen DF. Clinicopathologic correlation of spontaneous retinal pigment epithelial tears with choroidal neovascular membranes in age-related macular degeneration. Ophthalmology. 1995;102:272–7.
31. Lafaut BA, Aisenbrey S, Vanden Broecke C, et al. Clinicopathological correlation of retinal pigment epithelial tears in exudative age-related macular degeneration: pretear, tear, and scarred tear. Br J Ophthalmol. 2001;85:454–60.
32. Arevalo JF, Maia M, Flynn Jr HW, et al. Tractional retinal detachment following intravitreal bevacizumab (Avastin) in patients with severe proliferative diabetic retinopathy. Br J Ophthalmol. 2008;92:213–6.
33. Clemens CR, Bastian N, Alten F, et al. Prediction of retinal pigment epithelial tear in serous vascularized pigment epithelium detachment. Acta Ophthalmol. 2014;92:50–6.
34. Leitritz M, Gelisken F, Inhoffen W, et al. Can the risk of retinal pigment epithelium tears after bevacizumab treatment be predicted? An optical coherence tomography study. Eye. 2008;22:1504–7.
35. Mukai R, Sato T, Kishi S. Precursor stage of retinal pigment epithelial tear in age-related macular degeneration. Acta Ophthalmol. 2014;92:407–8.
36. Ie D, Yannuzzi LA, Spaide RF, et al. Microrips of the retinal pigment epithelium. Arch Ophthalmol. 1992;110:1443–9.
37. Clemens CR, Alten F, Eter N. Reading the signs: microrips as a prognostic sign for impending RPE tear development. Acta Ophthalmol. 2015;93(7):e600–2.
38. Cunningham Jr ET, Feiner L, Chung C, et al. Incidence of retinal pigment epithelial tears after intravitreal ranibizumab injection for neovascular age-related macular degeneration. Ophthalmology. 2011;118:2447–52.
39. Coco RM, Sanabria MR, Hernandez AG, et al. Retinal pigment epithelium tears in age-related macular degeneration treated with antiangiogenic drugs: a controlled study with long follow-up. Ophthalmologica. 2012;228:78–83.
40. Lesniak SP, Fine HF, Prenner JL, et al. Long-term follow-up of spontaneous retinal pigment epithelium tears in age-related macular degeneration treated with anti-VEGF therapy. Eur J Ophthalmol. 2011;21:73–6.
41. Bartels S, Barrelmann A, Book B, et al. Tear in retinal pigment epithelium under anti-VEGF therapy for exudative age-related macular degeneration: function recovery under intensive therapy. Ophthalmologe. 2014;111:460–4.

42. Asao K, Gomi F, Sawa M, et al. Additional anti-vascular endothelial growth factor therapy for eyes with a retinal pigment epithelial tear after the initial therapy. Retina. 2014;34: 512–8.
43. Mukai R, Sato T, Kishi S. Repair mechanism of retinal pigment epithelial tears in age-related macular degeneration. Retina. 2015;35:473–80.
44. Caramoy A, Kirchhof B, Fauser S. Morphological versus functional photoreceptor viability of retinal pigment epithelium tears. Acta Ophthalmol. 2012;90:328–9.
45. Stanzel BV, Liu Z, Somboonthanakij S, et al. Human RPE stem cells grown into polarized RPE monolayers on a polyester matrix are maintained after grafting into rabbit subretinal space. Stem Cell Reports. 2014;2:64–77.

Chapter 8
Retinal Pigment Epithelial Detachment in Central Serous Chorioretinopathy

Mathias Maier

8.1 Introduction

In 1866, Albrecht von Graefe described a disease, which he called "recurrent central retinitis" [1]. Patients suffering from this condition showed a circumscribed serous retinal detachment typically affecting the posterior pole [1–3]. Since then, several publications with further definitions and terminologies of this disease followed.

In 1965, Maumenee was the first to describe his observation of leakage at the level of the retinal pigment epithelium (RPE) during fluorescein angiography (FA), suggesting an involvement of both the RPE and the choroid [4].

More detailed observations and further understanding of the condition finally led to the term "idiopathic central serous choroidopathy" by Donald Gass, which over time has been adjusted to "central serous chorioretinopathy" (CSCR) owing to the knowledge about the hyperpermeability of the RPE [3, 5, 6].

In the 1960s and 1970s, Gass and Klein et al. described three angiographic subclasses of CSCR. The most frequent, type 1 (94%), showing subretinal fluid (SRF) and one or more leakage points. Type 2 (3%) showing one or more PEDs without SRF and type 3 (3%) as hybrid form of type 1 and type 2 [2, 5, 7], (Fig. 8.1).

Today, however, high resolution spectral domain OCT (SD-OCT) demonstrates that a PED of variable size is detectable under the SRF in most cases (Figs. 8.2, 8.3, 8.4, and 8.5). Based on these findings, the abovementioned classification is unsustainable nowadays [2, 8]. The different forms may rather represent sequential manifestations of the same disease [2, 8–10].

M. Maier
Leitender Oberarzt und stellv. Direktor, Klinik und Poliklinik für Augenheilkunde,
Klinikum rechts der Isar, Technische Universität München,
Ismaningerstraße 22, D-81675 München, Germany
e-mail: Mathias.Maier@mri.tum.de

M.A. Gamulescu et al. (eds.), *Retinal Pigment Epithelial Detachment*,
DOI 10.1007/978-3-319-56133-2_8

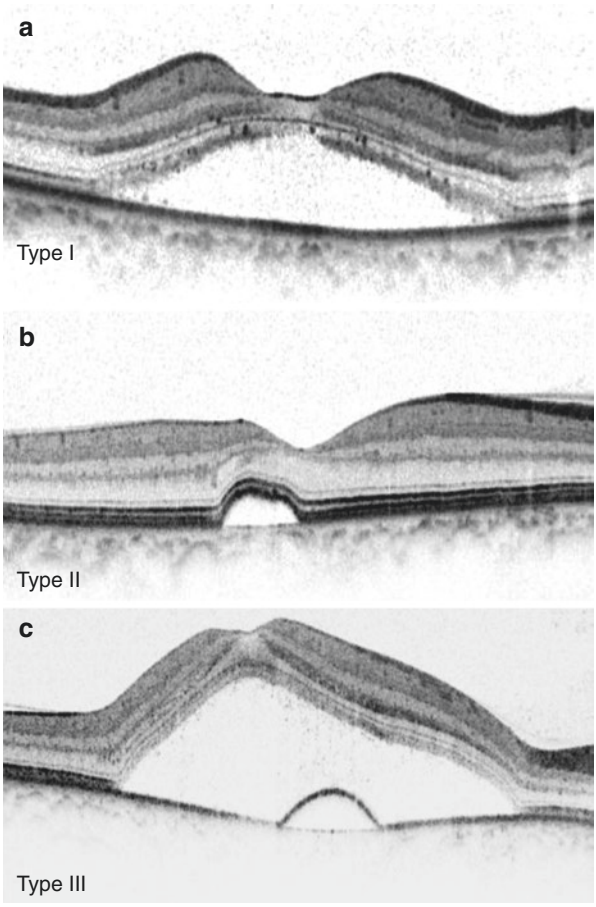

Fig. 8.1 CSCR: Former morphologic classification. (**a**) Type I: only subretinal fluid, (**b**) Type II: only PED, (**c**) Type III: combined subretinal fluid and PED

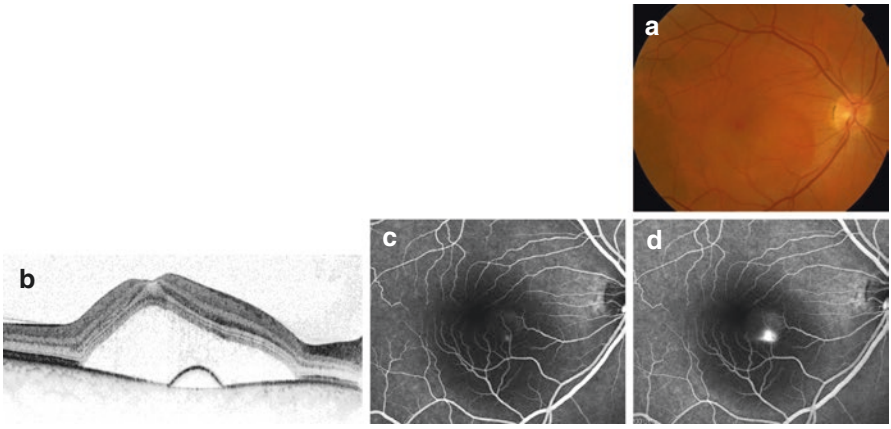

Fig. 8.2 (**a**) Color fundus photograph of a patient with CSCR and circumscribed serous retinal detachment. (**b**) SD-OCT: subretinal fluid (SRF) and pigment epithelial detachment (PED), (**c**) FA early phase: pinpoint leakage. (**d**) FA late phase "inkblot leakage" and pooling

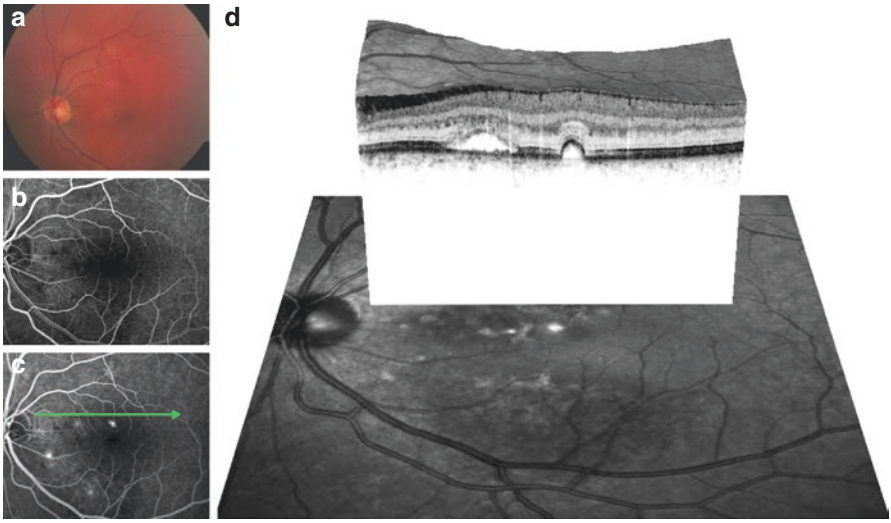

Fig. 8.3 Multifocal CSCR. (**a**) Color fundus photograph of a patient with CSCR. (**b**) FA early phase. (**c**) FA late phase showing multiple leakage points scattered over the macular region. (**d**) SD-OCT: SRF und PED coexist in this patient

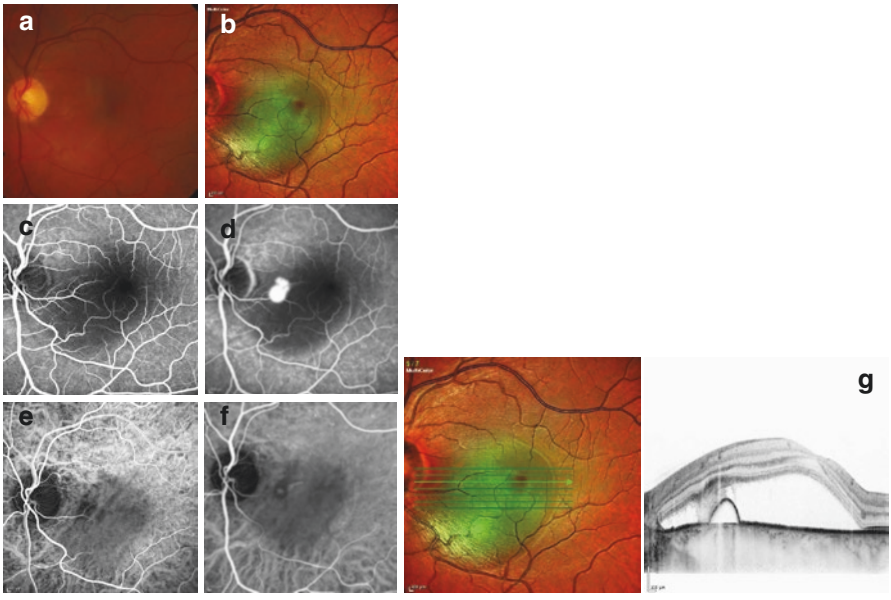

Fig. 8.4 Acute CSCR: (**a**) Color fundus photograph, (**b**) Multicolor image, (**c**) FA early phase, (**d**) FA late phase with "inkblot leak," (**e**) ICGA early phase, (**f**) ICGA late phase showing choroidal vascular dilatation and vascular hyperpermeability, (**g**) Multicolor image combined with SD-OCT: circumscribed area of serous retinal detachment in the multicolor image (*left*). PED and SRF on SD-OCT (*right*)

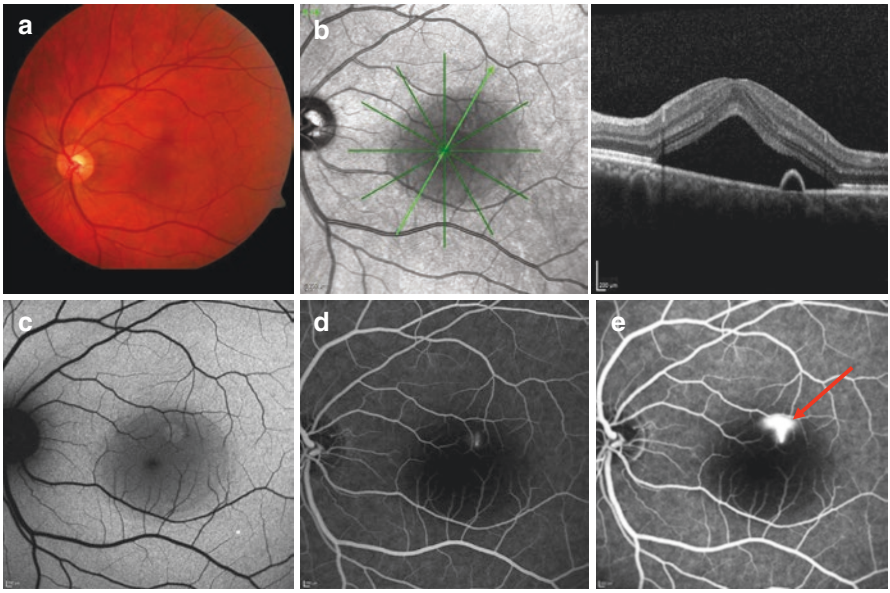

Fig. 8.5 (**a**) Color fundus photograph of a patient with CSCR and circumscribed serous retinal detachment, (**b**) SD-OCT: subretinal fluid (SRF) and pigment epithelial detachment (PED), (**c**) reduced FAF in the area of SRF, (**d**) FA early phase shows leakage point, (**e**) FA late phase: leakage ("smoke stack") (*red arrow*)

8.2 Epidemiology

CSCR is supposed to be the fourth most common nonsurgical retinopathy after age-related macular degeneration, diabetic retinopathy, and branch retinal vein occlusion [6]. Although only one population-based study and no systemic epidemiologic survey of CSCR has been carried out, a large number of single studies support the finding of men (72–88%) being more often affected than women [2, 3, 11–16]. CSCR usually affects middle-aged individuals with a peak at around 40–45 years in men although some studies suggest even higher mean ages for men and particularly for women and patients with chronic CSCR [2, 3, 17]. It has been associated with the so-called "type A" personality, or those who are experiencing psychological stress [6, 18]. It has also been linked to use of sympathomimetic agents, corticosteroid use in any form, and endogenous high levels of corticosteroids [2, 18]. CSCR often shows bilateral involvement, and in a study of Gupta high-definition OCT showed bilateral changes in 94% of the cases [2, 19].

8.3 Pathogenesis

In the past, CSCR has been thought to arise primarily from an abnormality of the RPE [20]. With indocyanine green angiography (ICGA), however, areas of choroidal vascular hyperpermeability in patients with CSCR have been reported [21–25] (Fig. 8.4f).

Although the exact pathomechanism of CSCR is not yet completely understood, the primary pathology is thought to begin with disruption of the choroidal circulation [26]. FA, ICGA, and enhanced depth imaging spectral domain-optical coherence tomography (EDI SD-OCT) have provided evidence suggesting hyperpermeability and increased hydrostatic pressure within the choroidal circulation [8, 21–23, 27, 28] (Figs. 8.4e, f and 8.6), leading to the formation of pigment epithelial detachments (PEDs). PED is a condition in which the retinal pigment epithelium is detached from its basement Bruch's membrane due to pathological accumulation of fluid. This in turn results in discontinuity of the RPE barrier, leading to various degrees of pinpoint areas of leakage in FA, often referred to as "microrips" or "blowouts" [3, 9, 19, 29] (Figs. 8.2, 8.3, 8.4, 8.7, and 8.8). In addition, the damage of the RPE is thought to lead to an aggravation of this condition since the RPE may be restricted in its ability to pump fluid out of the subretinal space.

The mechanistic hypothesis proposing that fluid coming from hyperpermeable vessels leads to increased tissue hydrostatic pressure—which results in RPE damage—may explain different extents of RPE alterations; however, it does not explain the hyperpermeability of the choroidal vascular system in the first place [3].

This might be explained by overactivation of mineralocorticoid receptors in the choroid, potentially triggered by endogenous and exogenous glucocorticoids [30–32]. Experimental studies showed that overactivation of mineralocorticoid receptors in the endothelial cell of the choroid induces increased permeability. In a pilot study,

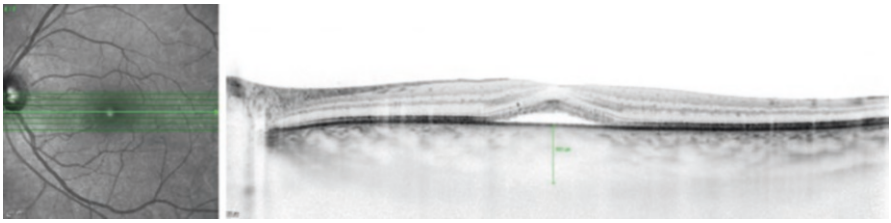

Fig. 8.6 Enhanced depth imaging (EDI) SD-OCT showing the thickened choroid (503 μm) in acute CSCR

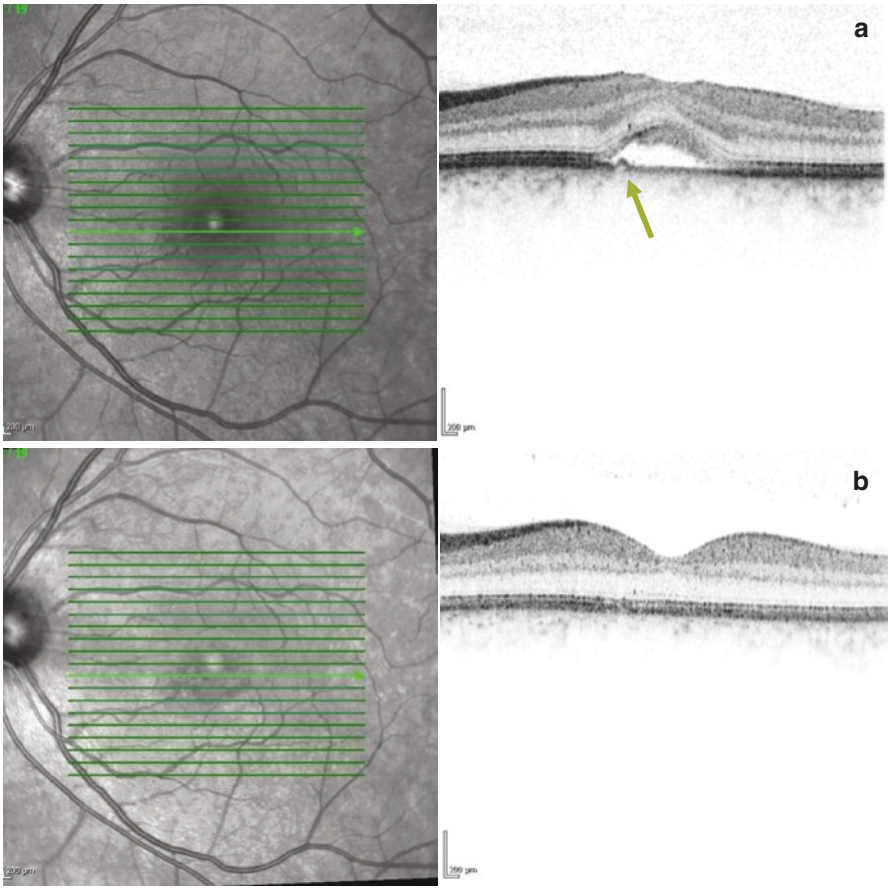

Fig. 8.7 Patient with chronic CSCR, VA 0.8: case study of therapy. (**a**) Baseline: subretinal fluid (SRF), elongation of the photoreceptor outer segments and small PED (*arrow*). (**b**) 1 month after aldosterone antagonist therapy VA: 1.0, SRF and PED resolved

blocking of mineralocorticoid receptors was successful in treating CSCR [30, 32]. However, the primary trigger for these choroidal abnormalities and the precise sequence of events involved in CSCR remain unclear.

Recently, an association between CSCR and common Complement Factor H (CFH) polymorphisms was identified, hinting to an involvement of CFH in the pathogenesis of CSCR [33]. The CFH polymorphisms are some of the best-established susceptibility loci for AMD; however, the exact functional basis of these associations for CSCR is currently unclear [33].

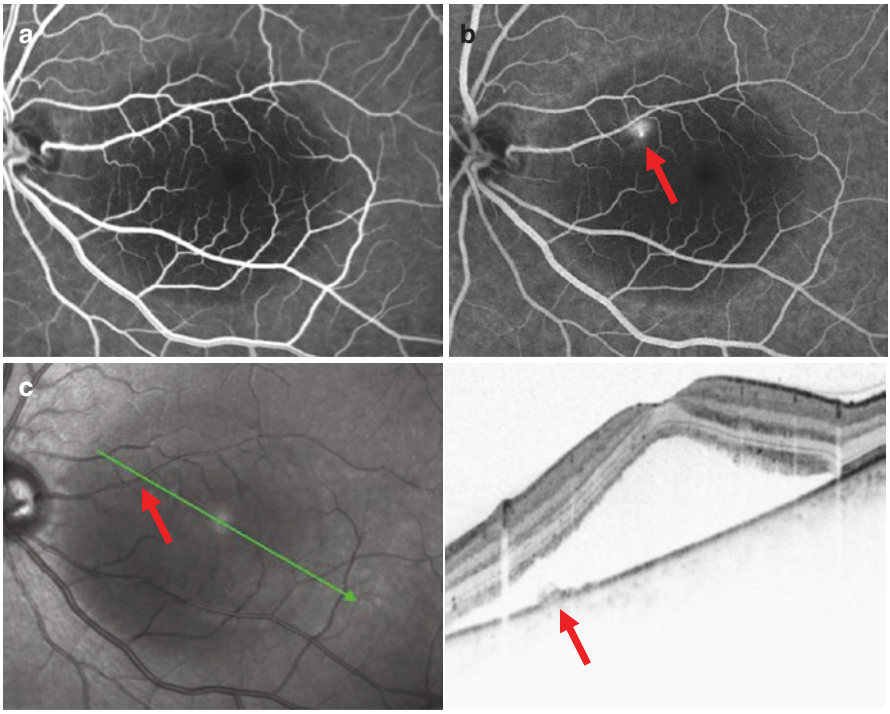

Fig. 8.8 FA and SD-OCT in acute CSCR: (**a**) FA early phase, (**b**) FA late phase showing leakage with focal pinpoint (*red arrow*), (**c**) SD-OCT: *Green arrow*: direction of the OCT-Scan. *Red arrow*: small RPE bulges exactly at the leakage area on FA, increased retinal thickness, and photoreceptor elongation

8.4 Clinical Examination

CSCR predominantly affects middle-aged males. Symptoms are blurred vision, metamorphopsia, micropsia, and disturbed contrast and color sensitivity.

Typical signs on fundus examination include a roundish, well-demarcated detachment of the neurosensory retina at the macula (Figs. 8.2, 8.4, and 8.5). Pigment epithelial detachment (PED) of variable size can also occur and can be single or multiple. The subretinal fluid (SRF) can be clear or turbid/fibrinous.

In chronic CSCR or in patients with old resolved disease, RPE mottling, atrophy, and clumping might be observed (Fig. 8.9). Other atypical CSCR presentations include bullous neurosensory retinal detachment and multifocal CSCR [2, 6, 8, 18] (Figs. 8.3 and 8.4).

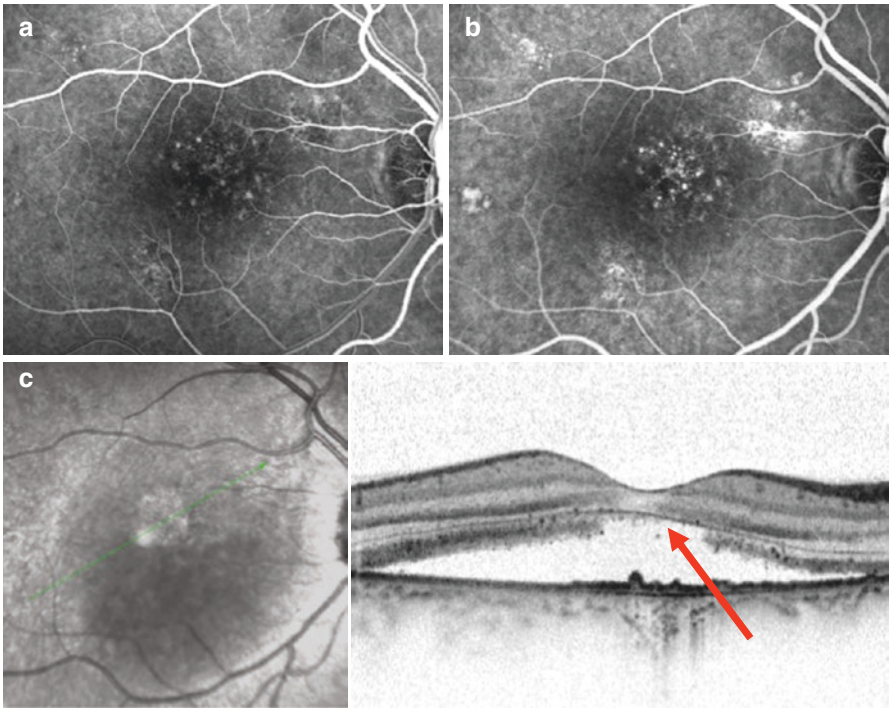

Fig. 8.9 FA and SD-OCT in a patient with chronic CSCR since 19 months (VA 0.05). (**a**) FA early phase and (**b**) FA late phase show RPE atrophy and diffuse leakage, (**c**) SD-OCT showing subretinal granular deposits, defects of the photoreceptor layer and photoreceptor atrophy (*red arrow*), and granular alterations of the RPE

8.5 Imaging

Further investigations for CSCR include fluorescein angiography (FA) which may show "ink blot" pattern of leakage (Fig. 8.2c, d) or the less common "smoke stack" (Fig. 8.5e) appearance. In addition, dye pooling in the sub-RPE space can be seen in cases of PED. Diffuse leakage or multiple leaking points can be seen in recurrent, chronic (Fig. 8.9), or multifocal CSCR (Figs. 8.3 and 8.10).

Indocyanine green angiography (ICGA) may demonstrate dilated choroidal vasculature corresponding to the site of CSCR with choroidal hyperpermeability in the late phase [2, 6, 8, 18] (Fig. 8.4e, f). Exsudative changes within the choroid are considered to be the primary event in the disease and the subsequent changes at the RPE allow the fluid to enter the subretinal space, resulting in neurosensory retinal detachment (RD) [25] (Fig. 8.4g). Abnormal ICGA hyperfluorescene in the symptomatic eye and in clinically asymptomatic fellow eyes is well known. No RPE abnormalities were found in areas without ICG hyperfluorescene. It has been shown that the leakage area at the level of RPE on FA was contiguous with the areas of choroidal vascular hyperpermeability on ICGA [21] (Fig. 8.4).

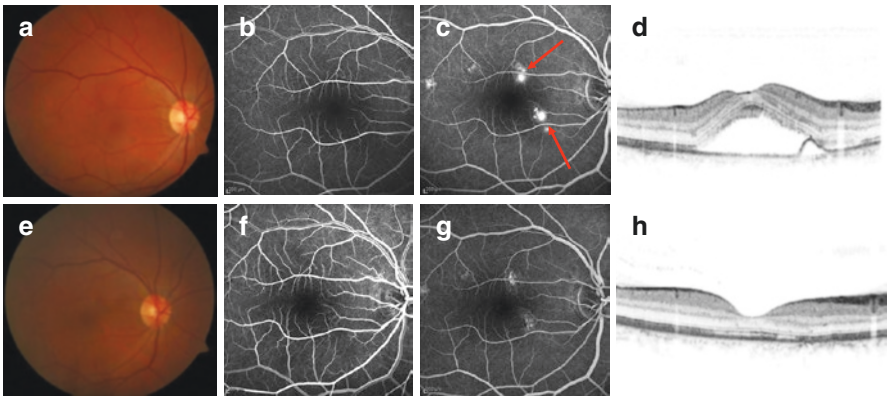

Fig. 8.10 Chronic CSCR: (**a**, **e**) fundus photograph, (**b**, **f**) FA early phase, (**c**, **g**) FA late phase, and (**d**, **h**) SD-OCT. Late phase FA shows two extrafoveal leakage points with leakage before (**c**, *red arrows*) and without leakage after focal laser treatment. SD-OCT shows subretinal fluid and PED before treatment (**d**) and resolution after treatment (**h**). VA improved from 0.3 to 0.7 after treatment

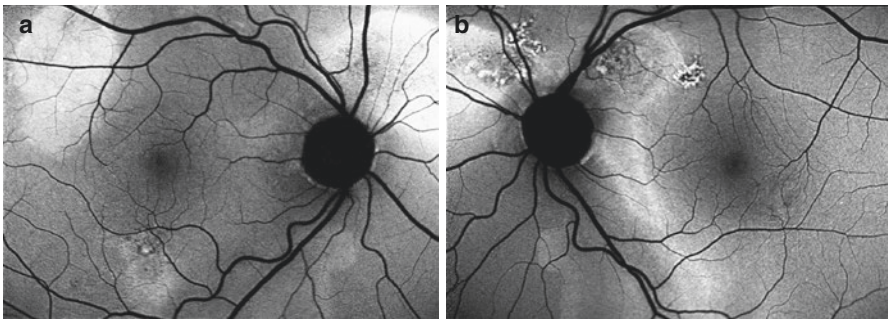

Fig. 8.11 Fundus autofluorescence (FAF) in CSCR: (**a**) right eye, (**b**) left eye: FAF with areas of increased autofluorescence and patchy irregular granular reduced autofluorescence

Fundus autofluorescence shows a reduced signal in acute CSCR because of the accumulation of subretinal fluid (Fig. 8.5c) and granular hyper-autofluorescence in chronic CSCR or in areas of former episodes of CSCR (Fig. 8.11b). In long-standing chronic CSCR with RPE atrophy, hypoautofluorescence is detectable [2, 15].

High resolution OCT (SD-OCT) allows detailed imaging of the macular microstructures. The typical appearance in CSCR shows detachment of the neurosensory retina and elongation of the photoreceptor outer segments accompanied by a circumscribed PED of various extents (Figs. 8.5b and 8.8c). Sometimes, discrete RPE alterations are found in the fellow eye [2, 19].

In chronic stages, subretinal fibrinous depositions and, seldom, cystic changes within the retina can be visualized [2, 8, 16, 27, 34–37].

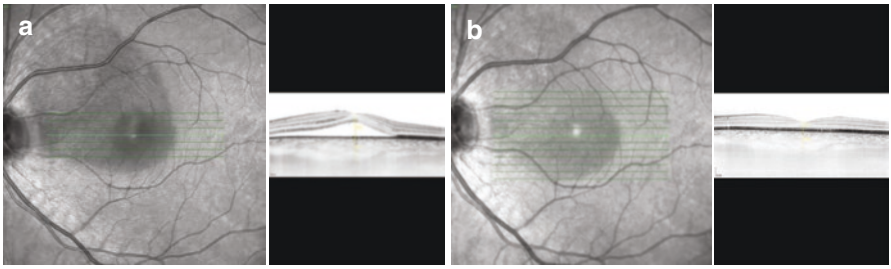

Fig. 8.12 EDI SD-OCT: patient (35 years, male), acute CSCR, VA: 0.7. (**a**) Baseline: retinal thickness: 571 µm, choroidal thickness: 489 µm, subretinal fluid (SRF): 448 µm. (**b**) 1 month after 50 mg Spironolactone/day: VA: 1.0: retinal thickness: 203 µm, choroidal thickness: 434 µm, no SRF

Enhanced depth imaging (EDI) OCT shows a thickened choroid in patients suffering from active CSCR in both the affected eye—especially in the areas corresponding to the neurosensory detachment—and the fellow eye compared with normal controls (Fig. 8.6). The choroidal thickness diminishes with therapy, however not reaching normal values [27, 38, 39] (Fig. 8.12).

The exact pathophysiology of RPE bumps in the asymptomatic fellow eyes of patients with CSCR is not well defined. It was speculated that a combination of choroidal vascular hyperpermeability and impaired RPE function leads to pooling of fluid in the sub-RPE space, which results in RPE bumps [8, 9, 37]. These bumps might represent a preclinical or subclinical state of the disease. Kim et al. support the belief that CSCR is essentially a bilateral asymmetric disease that causes morphologic alterations of the RPE in both eyes: they found RPE abnormalities corresponding to the leakage sites in all patients, SD-OCT images showing PED in 22 of 69 (31.9%), and a small lump of the RPE layers in 47 of 69 leakage sites (68.1%) [9]. In previous reports, PED was even found in 61–71% of leakage sites [10, 16]. Montero et al. described small RPE bulges, observed with time-domain OCT (TD-OCT), and related to angiographic leakage sites in 35 of 36 eyes [37]. This difference in PED incidence might be explained by a difference in nomenclature: some authors considered small or atypical PEDs as RPE abnormalities, others as PED.

8.6 Differential Diagnosis

Usually acute CSCR can be diagnosed based on fundoscopy, SD-OCT, and FA. In multifocal and chronic CSCR, classification sometimes may be difficult. Several differential diagnoses should be considered:

Age-related Macular Degeneration (AMD) with choroidal neovasular degeneration: In older patients, differentiation between CSCR and neovascular (n)AMD can be difficult. Oftentimes, shallow RPE detachments and shallow subretinal fluid

accumulation with or without intraretinal cystoid spaces display a patchy hyperfluorescence in FA with only little leakage. Differentiation from occult CNV is not always possible. However, if there are no drusen visible at the posterior pole of the affected or the fellow eye, AMD seems unlikely [2].

Further differential diagnoses are idiopathic isolated PED, infectious and inflammatory diseases (e.g., presumed ocular histoplasmosis syndrome, choroiditis, posterior scleritis, and Vogt Koyanagi Harada syndrome, see also chapter 9), and tumors (e.g., choroidal hemangioma) [2].

8.7 Natural History

CSCR is usually a self-limiting disease with spontaneous resolution within 3–4 months with overall good visual outcome. However, CSCR can show an acute relapsing, a chronic, or a multifocal form. Recurrent CSCR forms are frequent and may be seen in more than 50% of patients suffering from CSCR [2, 40, 41].

Chronic CSCR on the other hand, with long-standing detachment of the neurosensoric retina, can result in significant visual loss. Some patients may develop diffuse retinal pigmentepitheliopathy, which is characterized by widespread RPE damage and destruction, often with consecutive atrophy of the photoreceptors [2, 18, 42] (Fig. 8.9c).

Patients with chronic CSCR are at increased risk to develop secondary CNV (risk for a single patient: 0.3–2% per year). Therefore, in elderly patients presenting with unilateral CNV without drusen, CNV in chronic CSCR should be considered [2].

8.8 Therapy

Acute CSCR is in most cases self-limiting with spontaneous resolution of the SRF and therefore initially observation is recommended [2, 7, 18, 25]. Risk factors should be addressed to increase the chance of spontaneous resolution. This includes discontinuing exogenous corticosteroids intake and lifestyle modification for patients with type A personality traits [2, 18].

If SRF is persisting over 3 months, initiation of therapy is recommended to avoid irreversible loss of visual acuity and RPE and/or photoreceptor atrophy [2, 3, 17, 31, 43]. There is no uniform definition of chronic CSCR (durations differ between 3–6 months), most authors defining chronic CSCR if symptoms last longer than 3 months [2, 3, 31].

Although there are no evidence-based guidelines, treatment options based on case series consist of systemic carbonic anhydrase, inhibitors of the mineralocorticoid receptor, mild laser photocoagulation, selective retina therapy (SRT), diode micropulse laser (DMPL) photocoagulation, half dose/half fluence photodynamic therapy (PDT), and intravitreal injection of VEGF inhibitors [11–13, 31, 40, 43–47].

Transpupillary thermotherapy (TTT), anti-corticosteroids, antiandrogens, adrenergic blockers, rifampicin, aspirin, and antimetabolite drugs have also been described [14, 17, 18, 31, 48].

8.8.1 Anti-corticosteroids

Observations of corticosteroid use and the development of CSCR have led to the suggestion of anti-corticosteroids as a treatment. This has led to clinical trials to assess the effect of such treatment. Ketoconazole is a synthetic imidazole which, in addition to its antifungal properties, has anti-glucocorticoid effects by blocking the conversion of cholesterol to androgenic glucocorticoid end-products. However, Meyerle et al. did not note any change in visual acuity, median lesion height on OCT, and linear dimensions through an 8-week follow-up period for five chronic CSCR patients who received oral ketoconazole 600 mg per day for 4 weeks in spite of documented decrease in endogenous cortisol levels [42].

8.8.2 Inhibitors of the Mineralocorticoid Receptor

Spironolactone and eplerenone are both aldosterone antagonist agents. Spironolactone possesses additional antiandrogenic properties. Few case series documented a reduction or complete resolution of SRF level and significant CMT reduction under oral therapy [18, 30, 31, 49] (Figs. 8.7 and 8.12).

8.8.3 Systemic Carbonic Anhydrase Inhibitors (CAIs)

CAIs are thought to mediate their action by inhibiting carbonic anhydrase enzyme in RPE, which supposedly aids in SRF absorption. Pikkel et al. reported on a prospective non-randomized trial on 15 CAI-treated patients against seven controls. They found that oral acetazolamide shortens the time to subjective and clinical improvement, but there was no difference in final visual acuity or recurrence rate between the two groups [18, 46].

8.8.4 Laser Photocoagulation

Focal laser photocoagulation to the leaking RPE guided by FA has been shown to hasten resolution of the neurosensory detachment in CSCR. Studies have demonstrated faster resolution of SRF in patients who underwent laser photocoagulation

compared to control eyes [50]. Nevertheless, laser photocoagulation does not influence the final visual outcome or rate of recurrence. Therefore, laser photocoagulation is an effective treatment for acute CSCR with clearly defined focal leakage point as seen on FA given that the leakage point is not sub- or juxtafoveal (Fig. 8.10). Still, side effects such as permanent scotoma, laser scar enlargement, and laser-induced CNV can occur [2, 18, 51].

8.8.5 Diode Micropulse Laser (DMPL) Photocoagulation

This method of treatment uses subthreshold diode laser energy in order to minimize damage to the neurosensory retina. It is similarly effective as conventional laser treatment in CSCR with point source leakage but not in eyes with diffuse leakage, and leaves no clinically detectable laser-induced damage [18, 41, 52]. A randomized clinical trial assessed DMPL versus argon laser photocoagulation in acute CSCR [41]. Patients in both groups had complete resolution of SRF at 12 weeks follow-up. No patients in the DMPL group had scotoma compared to 3 out of 15 patients in the argon laser group who had persistent scotoma. Contrast sensitivity was also significantly better in the DMPL group [41].

8.8.6 Selective Retina Therapy

Selective retina therapy (SRT) selectively treats RPE without damaging the photoreceptors. In small clinical trials, SRT was effective without clinically detectable laser-induced damage [13, 53].

8.8.7 Photodynamic Therapy

Photodynamic therapy (PDT) with verteporfin has been employed to treat both chronic and acute CSCR. It is believed that PDT works in CSCR by inducing choroidal hypoperfusion and choroidal remodelling [17, 25, 45]. It was also proposed that PDT can tighten the blood retina barrier [18].

Standard PDT

Chan et al. reported the first case series of full dose, full fluence PDT (50 J/cm^2) in six patients with persistent or chronic CSCR with subfoveal leakage [45]. Ruiz-Moreno treated 82 eyes with standard PDT for chronic CSCR and showed that it can improve visual acuity and reduce central macular thickness (CMT). SRF has

disappeared in all cases [54]. Morphological and functional chorioretinal changes such as RPE atrophy, external limiting membrane and inner/outer segment junction line discontinuity have been observed after standard PDT treatment for CSCR [18]. To enhance safety, dose or power (fluence) of PDT was reduced.

Reduced Dose PDT

Chan et al. showed that half dose PDT was effective both anatomically and functionally in treating acute symptomatic CSCR [11]. A comparative case series by Lim et al. showed that half dose PDT facilitated earlier resolution of SRF and earlier recovery of visual function when compared to focal laser. No difference in final functional and anatomical results was noted at 6 months follow-up [55].

Reduced-Fluence PDT

Reduction of the fluence by decreasing laser time or power was also attempted. Reibaldi et al. compared full fluence (50 J/cm^2) to half fluence PDT (25 J/cm^2) in chronic CSCR. Both treatments achieved similar results in terms of visual outcome and SRF resolution, but choriocapillaris ischemia was significantly more in the full fluence group [56].

8.8.8 Intravitreal Antivascular Endothelial Growth Factor (VEGF)

Attempts to treat acute and chronic CSCR with intravitreal bevacizumab are based on the hypothesis that choroidal hyperpermeability is associated with increased expression of VEGF although high VEGF levels were not detected in the aqueous humor [57]. Uncontrolled case series suggest efficacy of anti-VEGF intravitreal injections for CSCR both functionally and anatomically [18, 43]. However, Bae et al. demonstrated that reduced-fluence PDT was superior to 3 monthly doses of intravitreal ranibizumab [44].

On the other hand, in CNV secondary to CSCR, anti-VEGF treatment is the established therapy [2, 3, 18].

8.8.9 Treatment Recommendation

According to the above mentioned, a stepwise approach according to the stage is recommended (Table 8.1) [2, 31]:

Table 8.1 Proposed escalation algorithm in CSCR

Stage	Duration	Medication
I	Up to 3 months	Clinical control, Eplerenone 50 mg, Acetazolamide 2 × 250 mg
II	3–6 months no resorption of SRF reduced VA	Eplerenone 50 mg, Acetazolamide 2 × 250 mg, photocoagulation of leakage point (50 µm, 100 mW, 100 ms, up to discrete white color), leakage point sub- or juxtafoveal: low-dose/fluence PDT, (SRT, DMPL, anti-VEGF therapy)
	3–6 months partial res. of SRF VA better or stable	Clinical control, Eplerenone 50 mg, Acetazolamide 2 × 250 mg
III	>6 months and/or diff. leakage on FA	Low-dose/fluence PDT (± anti-VEGF therapy)
IV	>6 months and/or sec. CNV	anti-VEGF therapy

Eplerenone 50 mg (Inspra) (25 mg during 1 week), alternative: Spironolactone 50 mg, (important: K^+ – control)
SRT Selective retina therapy, *DMPL* Micropulse diode laser photocoagulation, *res.* resorption, *diff.* diffuse, *sec.* secondary. Modified after Baraki et al. Chorioretinopathia centralis serosa (CSCR) Ophthalmologe 2010 [3]

Stage 1 (up to 3 months):

Observation is recommended. In cases where the fellow eye showed VA loss from CSCR and the patient suffers from massive symptoms, and has a strong willingness to be treated earlier, treatment can be initiated.

Stage 2 (3–6 months):

If no resorption of SRF and reduced VA is seen: Eplerenone 50 mg/day (starting with 25 mg/day in the first week), Acetazolamide 2 × 250 mg/day, or photocoagulation of the leakage point. If the leakage point is located sub- or juxtafoveal: Low-dose/fluence PDT is recommnended, alternative (SRT, DMPL, anti-VEGF therapy).

With resorption of SRF and stable or better VA: clinical control, Eplerenone 50 mg, Acetazolamide 2 × 250 mg.

Stage 3 (>6 months):

If diffuse leakage is seen on FA: Photodynamic therapy with reduced dose/fluence or combination therapy PDT and anti-VEGF.

Stage 4 (>Stage III with secondary CNV):

Intravitreal anti-VEGF therapy (Ranibizumab/Bevacizumab/Aflibercept).

8.9 Summary

In the acute stage, central serous chorioretinopathy (CSCR) is characterized by serous retinal detachment and RPE alterations. Structural changes of the retinal pigment epithelium (RPE) layer can be monofocal or multifocal. Spectral domain OCT (SD-OCT) shows diagnostic details of the choroidea, RPE, and retinal

microstructure and allows a better understanding of the pathophysiology and detailed monitoring.

RPE abnormalities are presumably found in all CSCR patients and consist of PED, RPE bulges or RPE "microrips" in acute CSCR and in retinal pigmentepitheliopathy and RPE atrophy in chronic CSCR.

Spontaneously acute CSCR usually has a good prognosis. Recurrent and chronic CSCR with long-standing detachment of the neurosensoric retina leads to atrophy of the RPE and the photoreceptors and causes irreversible reduction of the visual acuity and therefore an escalating stepwise therapy is recommended.

References

1. Graefe A. Über die zentrale rezidivierende retinitis. Graefes Arch Ophthalmol. 1866;12:211–5.
2. Baraki H, Feltgen N, Roider J, Hoerauf H, Klatt C. Central serous chorioretinopathy (CSC). Ophthalmologe. 2010;107:479–92.
3. Liegl R, Ulbig MW. Central serous chorioretinopathy. Ophthalmologica. 2014;232(2):65–76.
4. Maumenee AE. Macular diseases: clinical manifestations. Trans Am Acad Ophthalmol Otolaryngol. 1965;69:605–13.
5. Gass JD. Pathogenesis of disciform detachment of the neuroepithelium. Am J Ophthalmol. 1967;63(3):Suppl:1–139.
6. Wang M, Munch IC, Hasler PW, Prünte C, Larsen M. Central serous chorioretinopathy. Acta Ophthalmol. 2008;86:126–45.
7. Klein ML, Van Buskirk EM, Friedman E, Gragoudas E, Chandra S. Experience with nontreatment of central serous choroidopathy. Arch Ophthalmol. 1974;91(4):247–50.
8. Valet V, Lohmann CP, Maier M. Spectral domain OCT in central serous chorioretinopathy: description of retinal changes. Ophthalmologe. 2012;109(9):879–87.
9. Kim HC, Cho WB, Chung H. Morphologic changes in acute central serous chorioretinopathy using spectral domain optical coherence tomography. Korean J Ophthalmol. 2012;26(5): 347–54.
10. Shinojima A, Hirose T, Mori R, et al. Morphologic findings in acute central serous chorioretinopathy using spectral domain-optical coherence tomography with simultaneous angiography. Retina. 2010;30:193–202.
11. Chan WM, et al. Half-dose verteporfin photodynamic therapy for acute central serous chorioretinopathy: one-year results of a randomized controlled trial. Ophthalmology. 2008;115:1756–65.
12. Chen SN, et al. Subthreshold diode micropulse photocoagulation for the treatment of chronic central serous chorioretinopathy with juxtafoveal leakage. Ophthalmology. 2008;115:2229–34.
13. Elsner H, et al. Selective retina therapy in patients with central serous chorioretinopathy. Graefes Arch Clin Exp Ophthalmol. 2006;244:1638–45.
14. Forooghian F, Meleth AD, Cukras C, Chew EY, Wong WT, Meyerle CB. Finasteride for chronic central serous chorioretinopathy. Retina. 2011;31(4):766–71.
15. Framme C, et al. Fundus autofluorescence in acute and chronic-recurrent central serous chorioretinopathy. Acta Ophthalmol Scand. 2005;83:161–7.
16. Fujimoto H, Gomi F, Wakabayashi T, et al. Morphologic changes in acute central serous chorioretinopathy evaluated by fourier-domain optical coherence tomography. Ophthalmology. 2008;115:1494–500, 1500.e1–2.
17. Maier M, Valet V, Feucht N, Lohmann CP. Therapy options for chronic central serous chorioretinopathy. Photodynamic therapy combined with bevacizumab—a case series. Ophthalmologe. 2011;108(11):1027–31.

18. Abouammoh MA. Advances in the treatment of central serous chorioretinopathy. Saudi J Ophthalmol. 2015;29:278–86.
19. Gupta P, et al. Morphological changes in the retinal pigment epithelium on spectral-domain OCT in the unaffected eyes with idiopathic central serous chorioretinopathy. Int Ophthalmol. 2010;30:175–81.
20. Kamppeter B, Jonas JB. Central serous chorioretinopathy imaged by optical coherence tomography. Arch Ophthalmol. 2003;121:742–3.
21. Piccolino FC, Borgia L. Central serous chorioretinopathy and indocyanine green angiography. Retina. 1994;14(3):231–42.
22. Prünte C, Flammer J. Choroidal capillary and venous congestion in central serous chorioretinopathy. Am J Ophthalmol. 1996;121(1):26–34.
23. Spaide RF, Hall L, Haas A, Campeas L, Yannuzzi LA, Fisher YL, Guyer DR, Slakter JS, Sorenson JA. Indocyanine green videoangiography of older patients with central serous chorioretinopathy. Retina. 1996;16:203–13.
24. Yannuzzi LA, Slakter JS, Gross NE, Spaide RF, Costa DL, Huang SJ, Klancnik Jr JM, Aizman A. Indocyanine green angiography-guided photodynamic therapy for treatment of chronic central serous chorioretinopathy: a pilot study. Retina. 2003;23:288–98.
25. Yannuzzi LA. Central serous chorioretinopathy: a personal perspective. Am J Ophthalmol. 2010;149:361–3.
26. Kitaya N, Nagaoka T, Hikichi T, Sugawara R, Kukui K, Ishiko S, Yoshida A. Features of abnormal choroidal circulation in central serous chorioretinopathy. Br J Ophthalmol. 2003;87:709–12.
27. Imamura Y, Fujuwara T, Margolis R, Spaide RF. Enhanced depth imaging optical coherence tomography of the choroid in central serous chorioretinopathy. Retina. 2009;29:1469–73.
28. Spaide RF, Campeas L, Haas A, et al. Central serous chorioretinopathy in younger and older adults. Ophthalmology. 1996;103:2070–80.
29. Goldstein BG, Pavan PR. 'Blow-outs' in the retinal pigment epithelium. Br J Ophthalmol. 1987;71(9):676–81.
30. Bousquet E, Beydoun T, Zhao M, Hassan L, Offret O, Behar-Cohen F. Mineralocorticoid receptor antagonism in the treatment of chronic central serous chorioretinopathy. A pilot study. Retina. 2013;33(10):2096–102.
31. Maier M, Stumpfe S, Feucht N, Strobl P, Rath V, Lohmann CP. Mineralocorticoid receptor antagonists as treatment option for acute and chronic central serous chorioretinopathy. Ophthalmologe. 2014;111(2):173–80.
32. Zhao M, Célérier I, Bousquet E, Jeanny JC, Jonet L, Savoldelli M, Offret O, Curan A, Farman N, Jaisser F, Behar-Cohen F. Mineralocorticoid receptor is involved in rat and human ocular chorioretinopathy. J Clin Invest. 2012;122(7):2672–9.
33. Miki A, Kondo N, Yanagisawa S, Bessho H, Honda S, Negi A. Common variants in the complement factor h gene confer genetic susceptibility to central serous chorioretinopathy. Ophthalmology. 2014;121(5):1067–72.
34. Matsumoto H, Kishi S, Otani T, Sato T. Elongation of photoreceptor outer segment in central serous chorioretinopathy. Am J Ophthalmol. 2008;145:162–8.
35. Matsumoto H, Sato T, Kishi S. Outer nuclear layer thickness at the fovea determines visual outcomes in resolved central serous chorioretinopathy. Am J Ophthalmol. 2009;148:105–10.e1.
36. Mitarai K, Gomi F, Tano Y. Three-dimensional optical coherence tomographic findings in central serous chorioretinopathy. Graefes Arch Clin Exp Ophthalmol. 2006;244:1415–20.
37. Montero JA, Ruiz-Moreno JM. Optical coherence tomography characterisation of idiopathic central serous chorioretinopathy. Br J Ophthalmol. 2005;89:562–4.
38. Brandl C, Helbig H, Gamulescu MA. Choroidal thickness measurements during central serous chorioretinopathy treatment. Int Ophthalmol. 2014;34(1):7–13.
39. Maruko I, Iida T, Sugano Y, Ojima A, Ogawawara M, Spaide RF. Subfoveal choroidal thickness after treatment of central serous chorioretinopathy. Ophthalmology. 2010;117:1792–9.
40. Lai TYY, Chan W-M, Li H, Lai RYK, Liu DTL, Lam DSC. Safety enhanced photodynamic therapy with half dose verteporfin for chronic central serous chorioretinopathy: a short term pilot study. Br J Ophthalmol. 2006;90(7):869–74.

41. Verma L, Sinha R, Venkatesh P, Tewari HK. Comparative evaluation of diode laser versus argon laser photocoagulation in patients with central serous retinopathy: a pilot, randomized controlled trial ISRCTN84128484. BMC Ophthalmol. 2004;4:15.
42. Meyerle CB, Freund KB, Bhatnagar P, Shah V, Yannuzzi LA. Ketoconazole in the treatment of chronic idiopathic central serous chorioretinopathy. Retina. 2007;27:943–6.
43. Schaal KB, Hoeh AE, Scheuerle A, Schuett F, Dithmar S. Intravitreal bevacizumab for treatment of chronic central serous chorioretinopathy. Eur J Ophthalmol. 2009;19:613–7.
44. Bae SH, Heo J, Kim C, et al. Low-fluence photodynamic therapy versus ranibizumab for chronic central serous chorioretinopathy: one-year results of a randomized trial. Ophthalmology. 2014;121(2):558–65.
45. Chan WM, et al. Choroidal vascular remodelling in central serous chorioretinopathy after indocyanine green guided photodynamic therapy with verteporfin: a novel treatment at the primary disease level. Br J Ophthalmol. 2003;87:1453–8.
46. Pikkel J, Beiran I, Ophir A, et al. Acetazolamide for central serous retinopathy. Ophthalmology. 2002;109:1723–5.
47. Shibata A, Ohkuma Y, Hayashi T, Tsuneoka H. Efficacy of reduced-fluence photodynamic therapy for serous retinal pigment epithelial detachment with choroidal hyperpermeability. Clin Ophthalmol. 2013;7:2123–6.
48. Shukla D, Kolluru C, Vignesh TP, Karthikprakash S, Kim R. Transpupillary thermotherapy for subfoveal leaks in central serous chorioretinopathy. Eye (Lond). 2008;22(1):100–6.
49. Bouzas EA, Karadimas P, Pournaras CJ. Central serous chorioretinopathy and glucocorticoids. Surv Ophthalmol. 2002;47:431–48.
50. Novak MA, Singerman LJ, Rice TA. Krypton and argon laser photocoagulation for central serous chorioretinopathy. Retina. 1987;7(3):162–9.
51. Robertson DM, Ilstrup D. Direct, indirect, and sham laser photocoagulation in the management of central serous chorioretinopathy. Am J Ophthalmol. 1983;95(4):457–66.
52. Gupta B, Elagouz M, McHugh D, Chong V, Sivaprasad S. Micropulse diode laser photocoagulation for central serous chorio-retinopathy. Clin Experiment Ophthalmol. 2009;37(8):801–5.
53. Brinkmann R, Schule G, Neumann J, et al. Selektive Retinatherapie: Methodik, Technik und Online-Dosimetrie. Ophthalmologe. 2006;103:839–49.
54. Ruiz-Moreno JM, Lugo FL, Armadá F, et al. Photodynamic therapy for chronic central serous chorioretinopathy. Acta Ophthalmol. 2010;88(3):371–6.
55. Lim JW, Kang SW, Kim Y-T, Chung SE, Lee SW. Comparative study of patients with central serous chorioretinopathy undergoing focal laser photocoagulation or photodynamic therapy. Br J Ophthalmol. 2011;95(4):514–7.
56. Reibaldi M, Cardascia N, Longo A, et al. Standard-fluence versus low-fluence photodynamic therapy in chronic central serous chorioretinopathy: a nonrandomized clinical trial. Am J Ophthalmol. 2010;149(2):307–15.
57. Shin MC, Lim JW. Concentration of cytokines in the aqueous humor of patients with central serous chorioretinopathy. Retina. 2011;31(9):1937–43.

Chapter 9
Retinal Pigment Epithelial Detachment in Systemic Disease

Horst Helbig

9.1 Introduction

Retinal pigment epithelial (RPE) detachment is in most cases associated with ocular disease such as age-related macular degeneration (AMD), central serous chorioretinopathy (CSCR), and others. In rare cases, it may be caused by systemic changes primarily manifesting themselves in the choroid. It is important to recognize these systemic diseases correctly, since therapeutic strategies have to focus not only on ocular manifestations but also have to include the systemic changes.

9.2 Pathophysiology

Pathophysiologically, diseases that involve the choroid and induce hyperpermeability of the choriocapillaris are prone to cause detachments of the RPE. As long as the outer blood retina barrier with the tight junctions between the RPE cells is intact, fluid will accumulate under the RPE and RPE detachment is seen. If however the damage to the RPE is so severe that the outer blood retinal barrier collapses, fluid from the diseased choroidal vessels will cross the leaky RPE and rather cause exudative detachments of the neuroretina. In systemic diseases, the damage to the choroid and the RPE appears to be so severe in most cases that we rather see exudative neuroretinal detachment than RPE detachments. Occurrence of RPE detachment is therefore a hint for an at least partially functioning outer blood retinal barrier being able to retain fluid from the choroid under the RPE. Serous retinal detachment primarily originating from choroidal involvement

H. Helbig, M.D.
Department Ophthalmology, University Hospital Regensburg,
Franz-Josef-Strauss-Allee 11, 93042 Regensburg, Germany
e-mail: horst.helbig@ukr.de

M.A. Gamulescu et al. (eds.), *Retinal Pigment Epithelial Detachment*,
DOI 10.1007/978-3-319-56133-2_9

requires breakdown of the outer blood retinal barrier and is therefore a sign of more severe damage. In addition, as described in the chapter 1 “Anatomy and Pathophysiology of Retinal Pigment epithelial Detachments” by Olaf Strauss, degenerative changes in Bruch’s membrane appear to play a role in certain cases of RPE detachment. Such changes are not to be expected in systemic diseases, especially in those which have an acute course of the disease such as eclampsia or Vogt Koyanagi Harada disease.

9.3 Systemic Diseases Associated with PED

Isolated PED in systemic disease in general is rare. In the literature, it is mostly described together with serous detachment of the neuroretina. A comprehensive overview is given by Wolfensberger and Tufail [1]. The diagnosis of RPE detachment has been mostly made clinically or with fluorescein angiography in the pre-OCT era. With OCT, however, RPE detachment can be more reliably differentiated from other manifestations. Early descriptions of PED detachments without OCT should therefore be judged carefully. Even those being confirmed by OCT—see below—show in many cases relatively flat and minor RPE detachments.

9.4 Inflammatory Diseases

Vogt Koyanagi Harada disease (VKH) is a common cause of panuveitis in darkly pigmented populations, but also occurs in Caucasians. Uveitis in VKH is only one manifestation of a systemic disease involving the central nervous system, the inner ear, and the skin. It is suggested that the common patho-immunological mechanism of VKH is an autoimmune reaction directed against melanocytes. Primary manifestation of ocular VKH is a stromal choroiditis. The inflammation may then spread to the neighboring RPE and neuroretina. Hyperpermeability of the choroicapillaris as well as malnutrition due to impaired microcirculation may contribute to involvement of the structures adjacent to the choriocapillaris. Typical clinical manifestations are papilledema with exudative detachment(s) of the neuroretina and choroidal folds (Fig. 9.1), and in late stages depigmentation with a “sunset glow” appearance may occur. VKH may also involve the anterior segment and cause iridocyclitis with supraciliar effusion and shallow anterior chamber. On fluorescein angiography (FA), delayed filling of the choriocapillaris may be seen with pinpoint leakage at the posterior pole and pooling of the dye in the late frames in the areas of exsudative subretinal fluid. Choroidal folds may be seen as hypofluorescent lines radiation from the optic disc to the mid-periphery (Figs. 9.1 and 9.2). Indocyaninegreen angiography (ICGA) shows early leakage of choroidal vessels, the choroid and

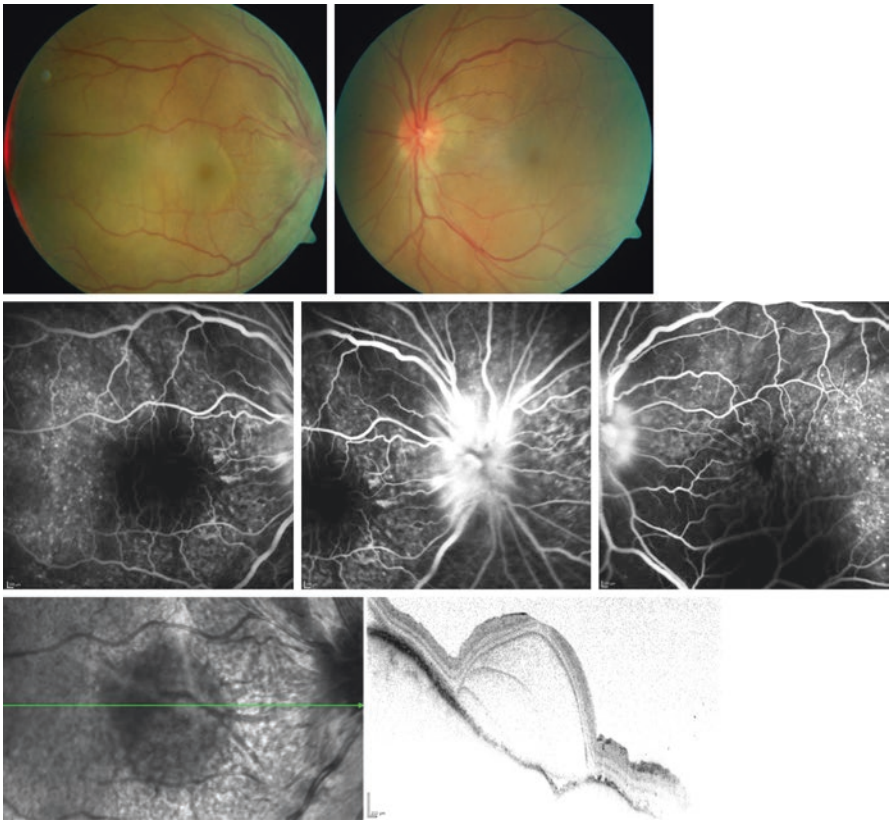

Fig. 9.1 VKH before therapy. On fundoscopy, papilledema and subretinal fluid involving the macula are seen right > left eye. FA shows prominent leakage from papilledema and pinpoint leakage throughout the posterior pole. Macular OCT scan of the right eye shows typical lobulated intraretinal fluid with septae and choroidal folds

choriocapillaris having a blurred appearance. Dark hypofluorescent spots may represent areas of hypoperfusion/ischemia or prominent inflammation of the choriocapillaris (Fig. 9.2). OCT shows more detailed changes. While the inner retina shows less change, multiple multilobular cystic spaces may be seen in the outer retina (Figs. 9.1 and 9.2). It appears that they represent separation of inner and outer segments of the photoreceptors. The basal and lateral spaces of these "cysts" appear to be formed by pseudomembranes containing outer segments and fibrin. RPE detachment is a rare manifestation of VKH. However, folds of the RPE (Fig. 9.3) and even RPE rips can be found [2]. Rather than serous PED, inward bulging of the thickened choroid and undulations of the overlying RPE are typically found in VKH (Figs. 9.1 and 9.3) [3]. By these features, OCT can differentiate between VKH and

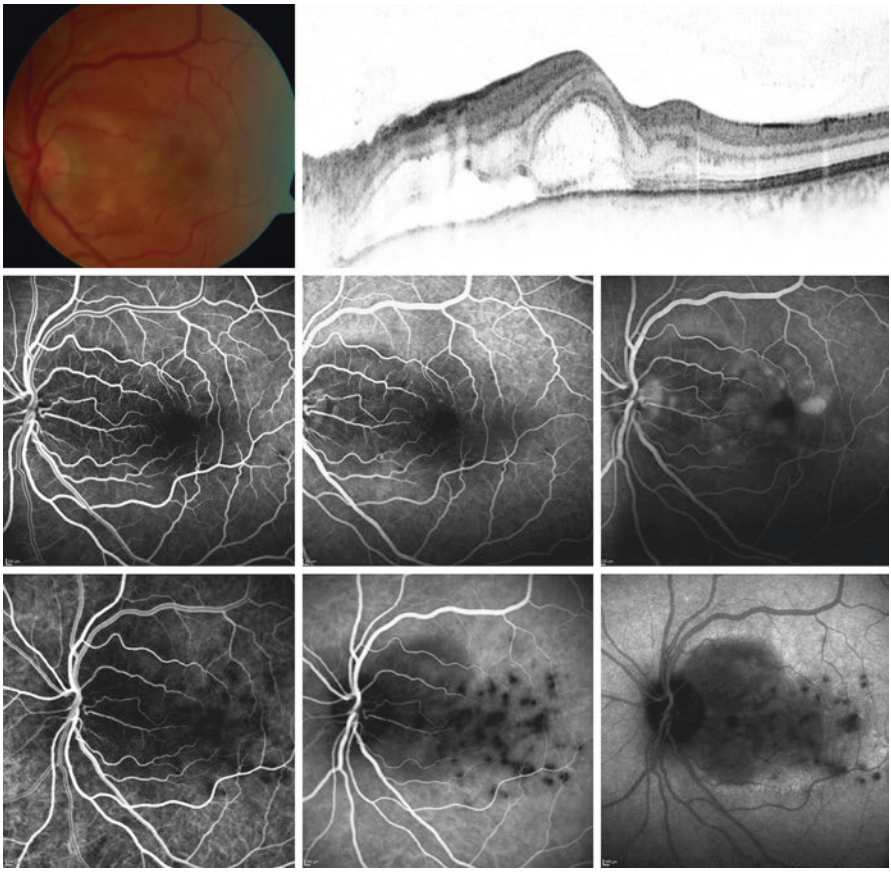

Fig. 9.2 VKH in the left eye of a patient showing slight hyperemia of the optic disc, yellowish areas at the posterior pole and typical intraretinal cystoid spaces with septae, as well as subretinal fluid. FA shows pooling of the dye in the intraretinal fluid spaces in the late frames, ICGA shows shadowing of the fluorescence in the area of subretinal fluid and multiple dark spots, presumably corresponding to areas of active inflammation or hypoperfusion of the choriocapillaris

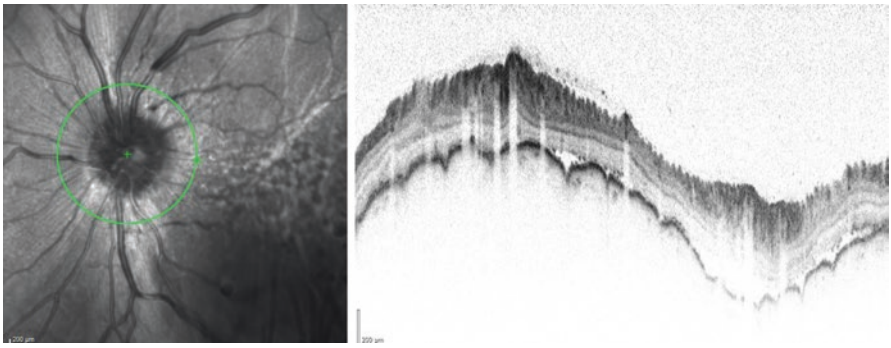

Fig. 9.3 Multiple choroidal folds around the optic disc as depicted on circular peripapillary OCT

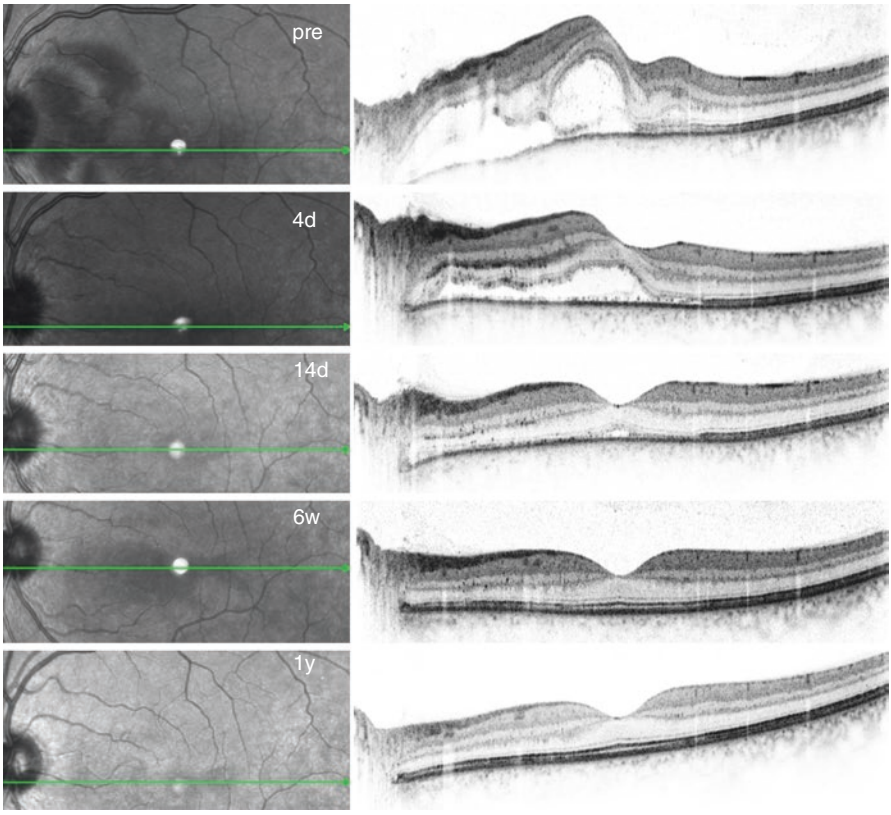

Fig. 9.4 Evolution of intra- and subretinal fluid over time (1 year) after initiation of systemic steroid treatment as monitored by serial OCT scans

CSCR, both diseases causing exudative detachment of the neuroretina. Differential diagnosis is important since treatment of both diseases is opposite. VKH requires high dose steroid treatment (Figs. 9.4. and 9.5), while in CSCR steroids are contra-indicated [4].

PED has also been described in sarcoidosis with and without granulomatous involvement of the choroid [5, 6]. With very few cases in the literature, PED is a very unusual manifestation of sarcoidosis.

Inflammatory bowel disease may also be associated with posterior uveitis including exudative retinal detachment and RPE disturbances [7, 8].

Any other systemic inflammatory disease involving the choroid (e.g., systemic vasculitis) may also lead to exudation of fluid under the RPE and therefore PED and/or RPE pigment disturbances.

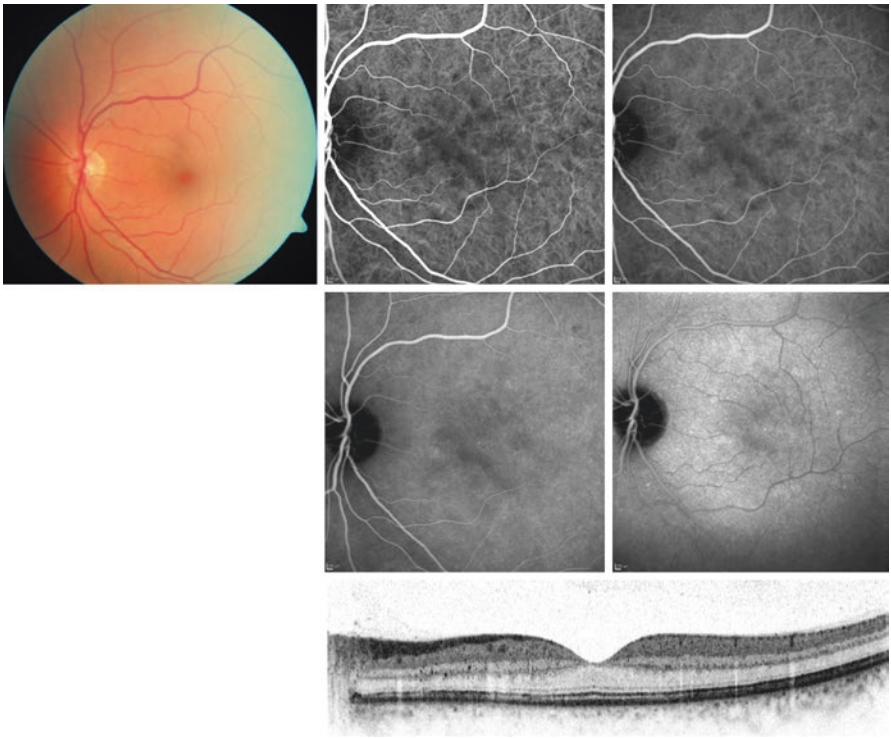

Fig. 9.5 After therapy, papilledema and intra- and subretinal fluid have resolved; however, FA and ICGA show persistent hypofluorescent spots centrally

9.5 Systemic Disease Causing Choroidal Ischemia

Ocular involvement in severe systemic arterial hypertension has long been recognized. It was Albrecht von Graefe in 1855 who first observed exudative retinal detachment in toxemia of pregnancy [9].

Siegrist streaks have been described as a fundus lesion in hypertension in 1899 [10]. They represent chains of pigmented spots overlying occluded choroidal vessels.

Elschnig described, in 1904, severe nephritis with albuminuria and choroidal lesions which were named after him [11]. Clinical studies have shown such spots nearly invariably in malignant hypertension. They represent focal ischemic infarcts due to acute occlusion of the choriocapillaris and/or small choroidal vessels. In the center of the Elschnig spot, the RPE is necrotic; towards the periphery the RPE appears edematous. OCT studies on Elschnig spots have shown focal RPE elevations in the resolution stage [12].

Clinicians have focussed for a long time mainly on the retinal changes, being visible in ophthalmoscopy. Pathologists very early have found even more pronounced changes in the choroidal vessels.

Fundus lesions and pathological studies in experimental induced malignant arterial hypertension showed impaired choroidal circulation and extensive occlusive and ischemic changes. Hypertensive choroidopathy and retinopathy were classified as two independent and unrelated manifestations of renovasular hypertension. Hypertensive choroidopathy showed an acute phase which was characterized by constriction of choroidal vessels leading to focal necrosis of the choriocapillaris and the overlying RPE with serous retinal detachment. In the chronic phase, extensive RPE-degenerative lesions due to choroidal ischemia develop [13, 14].

Song et al. described OCT images in hypertensive choroidopathy with eclampsia [15]. In addition to detachments of the neuroretina, a waveform of the RPE caused by multiple flat confluent RPE detachments was visible. RPE and outer segments of photoreceptors appeared swollen and reflectivity was reduced, features probably caused by choroidal ischemia.

9.6 Blood Disorders

Blood disorders such as hyperviscosity syndrome or paraproteinemia were also associated with PED and serous macular detachment in very few published cases. Subretinal fluid is more common than RPE detachment. Reduced choroidal circulation due to hyperviscosity has been implicated in the pathophysiology of these changes [16, 17].

9.7 Kidney Disease

In renal failure and hemodialysis, RPE detachment and serous retinal detachment have repeatedly been reported. Possible pathophysiological mechanisms are toxic uremic effects, with effects on vascular permeability, changes in hemodynamics, and fluid osmolarity [18–20].

Patients with Type II mesangiocapillary or membrano proliferative glomerulonephritis (type II MCGN or type II MPGN) may develop drusen-like depositions in the macula. Interestingly, they may have C3 nephritic factor (C3NeF), an autoantibody against C3 convertase of the alternate pathway, resulting in loss of complement regulation systemically. Affected patients may develop features similar to AMD including PED [21, 22].

9.8 Hypercortisolism

Systemic diseases associated with endogenous hypercortisolism are well known to cause CSCR. In these cases, the systemic hypercortisolism has to be treated rather than the local manifestation in the eye.

Iatrogenic, exogenic hypercortisolism is found in systemic steroid therapy. Most systemic inflammatory diseases are primarily treated with systemic steroids. This is especially true for sarcoid inflammatory bowels disease, organ transplant, and others. If RPE detachment or serous detachments of the neuroretina occur in these circumstances, the primary inflammatory disease may not be the only cause for the ocular changes. A side effect of the therapeutic systemic steroids inducing CSCR may be a more likely explanation. Therefore, PED described in the literature in some of the systemic inflammatory diseases might be rather a complication of steroid treatment.

9.9 Summary

Several systemic diseases may cause PED. Although rather rare, it is important to recognize these diseases because they require different treatment. Malignant arterial hypertension especially in pregnancy is a life threatening condition which may have visual disturbances as symptom. Other possible systemic diseases include inflammatory, endocrine, and blood or kidney disorde rs. The ophthalmologist has to be aware of these rare conditions to guide diagnostic measures and adequate therapy.

References

1. Wolfensberger TJ, Tufail A. Systemic disorders associated with detachment of the neurosensory retina and retinal pigment epithelium. Curr Opin Ophthalmol. 2000;11(6):455–61.
2. Mili-Boussen I, Letaief I, Dridi H, Ouertani A. Bilateral retinal pigment epithelium tears in acute Vogt-Koyanagi-Harada disease. Retin Cases Brief Rep. 2013;7(4):350–4. doi:10.1097/ICB.0b013e3182964f68.
3. Hosoda Y, Uji A, Hangai M, Morooka S, Nishijima K, Yoshimura N. Relationship between retinal lesions and inward choroidal bulging in Vogt-Koyanagi-Harada disease. Am J Ophthalmol. 2014;157(5):1056–63. doi:10.1016/j.ajo.2014.01.015.
4. Lin D, Chen W, Zhang G, Huang H, Zhou Z, Cen L, Chen H. Comparison of the optical coherence tomographic characters between acute Vogt-Koyanagi-Harada disease and acute central serous chorioretinopathy. BMC Ophthalmol. 2014;14:87. doi:10.1186/1471-2415-14-87.
5. Bourcier T, Lumbroso L, Cassoux N, Fardeau C, Lehoang P. Retinal pigment epithelial detachment: an unusual presentation in ocular sarcoidosis. Br J Ophthalmol. 1998;82(5):585.
6. Salchow DJ, Weiss MJ. Retinal pigment epithelial detachment in sarcoidosis. Ocul Immunol Inflamm. 2006;14(4):245–8. doi:10.1080/09273940600826489.
7. Ernst BB, Lowder CY, Meisler DM, Gutman FA. Posterior segment manifestations of inflammatory bowel disease. Ophthalmology. 1991;98(8):1272–80.

8. Felekis T, Katsanos K, Kitsanou M, Trakos N, Theopistos V, Christodoulou D, et al. Spectrum and frequency of ophthalmologic manifestations in patients with inflammatory bowel disease: a prospective single-center study. Inflamm Bowel Dis. 2009;15(1):29–34. doi:10.1002/ibd.20584.
9. von Graefe A. Mitteilungen vermischten Inhalts: Beobachtungen über Akkomodation bei Linsendefekt, Muskelkrankheiten und Anomalien der iris. Albrecht Von Graefes Arch Ophthalmol. 1855;2:187–94.
10. Siegrist A. Beitrag zur Kenntnis der Arteriosklerose der Augengefässe. Z Augenheilkunde. 1899;2(Suppl):36–7.
11. Elschnig A. Die diagnostische und prognostische Bedeutung der Netzhauterkrankungen bei nephritis. Wien Med Wochenschr. 1904;54:446–50.
12. AlTalbishi A, Khateb S, Amer R. Elschnig's spots in the acute and remission stages in pre-eclampsia. Spectral-domain optical coherence tomographic features. Eur J Ophthalmol. 2015;25(5):e84–7. doi:10.5301/ejo.5000586.
13. Hayreh SS, Servais GE, Virdi PS. Fundus lesions in malignant hypertension. VI. Hypertensive choroidopathy. Ophthalmology. 1986;93(11):1383–400.
14. Kishi S, Tso MO, Hayreh SS. Fundus lesions in malignant hypertension. I. A pathologic study of experimental hypertensive choroidopathy. Arch Ophthalmol. 1985;103(8):1189–97.
15. Song Y-s, Kinouchi R, Ishiko S, Fukui K, Yoshida A. Hypertensive choroidopathy with eclampsia viewed on spectral-domain optical coherence tomography. Graefes Arch Clin Exp Ophthalmol. 2013;251(11):2647–50. doi:10.1007/s00417-013-2462-9.
16. Baker PS, Garg SJ, Fineman MS, Chiang A, Alshareef RA, Belmont J, Brown GC. Serous macular detachment in Waldenström macroglobulinemia: a report of four cases. Am J Ophthalmol. 2013;155(3):448–55. doi:10.1016/j.ajo.2012.09.018.
17. Ogata N, Ida H, Takahashi K, Fukuchi T, Uyama M. Occult retinal pigment epithelial detachment in hyperviscosity syndrome. Ophthalmic Surg Lasers. 2000;31(3):248–52.
18. Basu S, Das T, Padhi TR. Serous retinal detachment and multiple retinal pigment epithelial detachments, following hemodialysis for multi-organ failure. Indian J Ophthalmol. 2010;58(3):261–2. doi:10.4103/0301-4738.62670.
19. Gass JD. Bullous retinal detachment and multiple retinal pigment epithelial detachments in patients receiving hemodialysis. Graefes Arch Clin Exp Ophthalmol. 1992;230(5):454–8.
20. Troiano P, Buccianti G. Bilateral symmetric retinal detachment and multiple retinal pigment epithelial detachments during haemodialysis. Nephrol Dial Transplant. 1998;13(8):2135–7.
21. Awan MA, Grierson DJ, Walker S. Bilateral macular sub-retinal fluid and retinal pigment epithelial detachment associated with type 2 membrano-proliferative glomerulonephritis. Clin Exp Optom. 2008;91(5):476–9. doi:10.1111/j.1444-0938.2008.00268.x.
22. D'souza Y, Short CD, McLeod D, Bonshek RE. Long-term follow-up of drusen-like lesions in patients with type II mesangiocapillary glomerulonephritis. Br J Ophthalmol. 2008;92(7):950–3. doi:10.1136/bjo.2007.130138.